UNIVERSITY OF SOUTHAMPTON

RESPONSE OF SHINGLE BARRIER BEACHES, TO EXTREME HYDRODYNAMIC CONDITIONS

Andrew P. Bradbury, BSc

Submitted in fulfillment for the degree of

Doctor of Philosophy

SCHOOL OF OCEAN AND EARTH SCIENCE

FACULTY OF SCIENCE

November 1998

UNIVERSITY OF SOUTHAMPTON

ABSTRACT

FACULTY OF SCIENCE

OCEANOGRAPHY

Doctor of Philosophy

RESPONSE OF SHINGLE BARRIER BEACHES TO EXTREME HYDRODYNAMIC CONDITIONS

Andrew P. Bradbury

The cross-shore profile response of shingle barrier beaches to storm waves are investigated with the aid of: random wave studies in a 3-dimensional mobile bed physical model; and by full-scale field measurements of shingle beaches to storm action. The investigations focus upon crest evolution of barrier beach profiles and conditions giving rise to overwashing and overtopping of the unconfined beach crest.

The influence of a wide range of hydraulic variables and beach geometry are examined, in a dimensionless framework, on the development of the dynamic equilibrium profiles of shingle barriers. A dimensionless barrier inertia parameter is presented and a parametric threshold equation is proposed, to describe the onset of barrier beach overwashing; this is combined with a list of governing variables and their range of validity. Hypotheses postulated previously for profile response of shingle beaches are examined. Such studies define the limits of the validity of the empirical framework, developed by Powell (1990); they suggest modifications to the predictive formulae for the crest elevation parameter. Overtopping and crest elevation build-up can be described by these predictive formulae, within the limits of the barrier inertia parameter overwashing threshold. Process studies attribute both overtopping, by run-up and foreshore widening by undermining of the barrier crest, to overwashing.

Physical model data are validated and predictive methods verified for a limited range of conditions, using field measurements made during and following extreme events on Hurst Spit. Model studies are used, to provide the basis of design of a large-scale beach recharge scheme for Hurst Spit, this was implemented in 1996. An extensive regional field monitoring programme and SANDS database has been established, comprising measurement of water levels, barrier response, wind and wave conditions.

LIST OF CONTENTS

List of Figures

Chapter 1

Chapter 2

Chapter 3

Chapter 4

Chapter 5

Chapter 6

Chapter 7

Chapter 8

List of Tables

List of Plates

List of Appendices

Acknowledgements

Professor Michael Collins has provided invaluable guidance on the direction of the research and preparation of this thesis and John Cross of the University of Southampton, School of Ocean and Earth Science has provided tireless field support and valuable practical advice. The research discussed in this thesis was supported financially by New Forest District Council; particular thanks are due to John Rainbow and Doug Wright.

Technical support and advice has been afforded by HR Wallingford, who have provided both facilities and technical support (under contract to NFDC). Advice and discussions with Dr Keith Powell, together with the technical assistance provided on the physical model by Adrian Channell, have been crucial to the smooth progress of the physical modelling programme. Technical input to parts of the numerical modelling, carried out and analysed by Dr. Peter Hawkes and Carol Jelliman, (specifically the HINDWAVE and INRAY modelling) have provided valuable data.

Many of my old colleagues from HR Wallingford have also offered invaluable advice on the hydraulic model studies and analysis, in particular; Dr Alan Brampton; Michael Owen; George Motyka; Dr Duncan Herbert; Dr Jane Smallman and Professor William Allsop.

Additional technical support has also been given by Rose Hawker, Catherine Eastick, Matt. Hosey, Andy Colenutt and Graham Toms (all NFDC). Valuable discussions with Dr Travis Mason, Dr George Voulgaris and Dr Adonis Velekrakis (University of Southampton) have all inspired and encouraged progress.

Finally, I should like to thank my wife, Lyndsey, for her encouragement and patience during preparation of this thesis.

Notation

B	Barrier height
B_a	Supra-tidal barrier cross section area
B_i	dimensionless barrier inertia parameter
C_f	critical freeboard factor
d	diameter of the particle in millimetres
d_o	near-bed orbital diameter
D_z	diameter of sediment which exceeds the z% value of the sieve curve
D_w	water depth, at the structure toe
g	acceleration due to gravity
h	water depth
h_b	elevation of the wave base
h_{bb}	elevation of back barrier toe
h_c	elevation of the beach crest
hr	hours
h_t	position of the beach step
H	wave height
H_o	offshore wave height
H_{rms}	root mean square wave height
H_s	significant wave height (the average of highest one-third wave heights)
H_{sb}	significant wave height at breaking
J	percolation slope
K	permeability coefficient
L	wave length
L_m	wave length of mean T_m period
L_o	deep water wave length
L_{om}	offshore wave length of mean T_m period
m	beach slope (= cotan α)
m	metres
min	minutes
m_o	zeroth spectral moment
N	number of waves in a storm event
p_b	position of the wave base
p_{bb}	position of back barrier toe
p_c	position of the beach crest
p_r	position of the maximum run-up
p_t	position of the beach step
$P(X<x)$	Probability less than a given value
Qw	Overwashing volume
R	Run-up

R_{Bc} relative barrier elevation
R_{Bw} relative barrier width
R_{ba} relative barrier cross section
R_c crest freeboard, level of crest relative to still water level
Re_v voids Reynolds number
s wave steepness or seconds
SWL_s barrier width at static water level
T wave period
T_m mean wave period
T_p spectral peak period
U depth averaged current speed
U_m peak value of the near-bed wave orbital velocity at the threshold of motion
v velocity through voids
yr years

α angle between the plane of the beach and the horizontal plane
Δ relative bouyant density
κ Spectral shape and wave grouping
λ Froude scale ratio
μ graphic mean,
ν kinematic viscosity
ξ surf similarity parameter
θ wave direction
ρ mass density
ρ_s density of sediment
ρ_r density of fluid
σ inclusive graphic sorting,
ϕ dimensionless sediment size
ψ angle between wave orthogonal and beach normal

Acronyms

CD	Chart datum
CSA	Cross sectional area
GPS	Global positioning system
MHW	mean high water
MHWN	mean high water of Neap tides
MHWS	mean high water of Spring tides
MSL	mean sea level
NFDC	New Forest District Council
ODN	Ordnance Datum Newlyn
PSD	Particle size distribution
RTK	Real time kinematic
SWL	Static water level

CHAPTER 1: INTRODUCTION

1.1 BACKGROUND

Beaches can be defined, broadly, as accumulations of unconsolidated material at the shoreline, limited by the landward and seaward extents of wave action. Beach composition may vary widely: shingle or gravel beaches are one of a number of generic types. Varied definitions of shingle have generated some confusion throughout the established literature. Definitions of shingle have varied from material with a D_{50} grain size in excess of 10mm (Muir Wood, 1970), to partially rounded marine worked material in the size range 4mm-256mm (Carr, 1974). Alternative definitions have been used by other researchers. Shingle is defined here in accordance with the Udden-Wentworth scheme (Krumbein, 1934; McManus, 1963) for gravel, pebbles and cobbles, which lie within the range -2ϕ to -6ϕ, (4-64mm) for the purposes of this research.

Shingle beaches occur widely around the coastline of the British Isles and at many locations elsewhere, although on a world-wide scale they are relatively scarce. Composition, size and form of the beaches varies widely; some being rich in sand on the lower foreshore or in interstices between the pebbles; others consisting totally of coarse grained shingle. Shingle beaches are composed usually and primarily of flint and chert, together with varying proportions of quartzite, although other materials may occasionally be present. A typical example is of Chesil Beach which comprises 98.5% pebbles of flint and chert, whilst 1.2% are of quartzite (Carr and Blackley, 1969).

1.1.1 Geomorphology of shingle beaches

The incidence of shingle beaches is strongly dependent upon a supply of suitable material; this may be supplied by erosion of land-based sources of material from cliffs, or from fluvial or marine deposits. The southern coast-line of England incorporates a

number of potential sources of shingle; much material is a relict, relating to glacial reworking of river gravels or deposition of gravel river terraces (Powell, 1986). Extensive deposits of shingle occur on the bed of the English Channel and the North Sea; many of these have migrated inshore, as sea level has risen following the most recent glaciations. The landward migration of these relict shorelines and erosion of the existing shoreline provides the sediment budget responsible for the formation and natural maintenance of the shingle beaches.

The morphological definition of the beach is generally given in terms of the limits of wave action; this is the definition used in this study. The seaward limit, or depth of closure, can extend into relatively deep water to the point at which waves are first able to "feel" the bed, resulting in a net movement of bed material. Such movement depends upon the wavelength, depth of water and bed sediment size. The landward limit of the beach is defined as the upper limit of the accumulation of loose material , as used in this study. In some instances the upper beach may be a relict or fossil deposit, which has resulted from progradation of the beach, or is due to lowering of mean sea level.

In general, the landward extent of the beach is controlled and restricted, either by natural cliffs or by a seawall, for example Hordle Beach, Hampshire. The process of profile formation in these circumstances is necessarily different to a barrier beach which has no fixed landward control, and the beach is free to migrate landwards, as "roll back" under storm action (Carter, 1988). Barriers migrate when the beach is overtopped, causing overwash deposits to form on the lee face of the beach; these may take the form of simple barriers backed by a lagoon, such as Chesil Beach, Dorset. Alternatively, the barrier beach may take the form of a spit at the mouth of a tidal inlet, such as Hurst Spit, Hampshire, which is backed by saltmarsh. Spits tend to be unstable features and are usually reliant upon a supply of material at their updrift end (Horn *et al*, 1996). Breaching of these features may occur, if such a supply of material is interrupted.

1.1.2 Hydrodynamics

The shape and form of a shingle beach is controlled by the prevailing hydrodynamic regime, in combination with the solid geology and sediment characteristics. Although shingle beaches may be diverse in shape and structure, their morphology is controlled by processes with two main components; longshore movement and cross-shore movement. These movements are controlled, in turn, by varying combinations of water levels, wave conditions and currents, in combination with the beach particles.

Wind-generated waves are the main driving mechanism for the modification of the shingle beach profile. Wave energy dissipation at the shoreline arises as a result of the continuity requirements of energy, mass and momentum (Bowen, 1969). Waves may reliably be described numerically, in terms of variables of measured intensity such as significant wave height, wave period, spectral shape and angle of incidence. Wave conditions vary both spatially and temporally. The complex spatial variation of wave conditions results from varied fetch lengths, bathymetry, wind direction, duration and intensity. These spatial variations combine with equally complex patterns of temporal changes in conditions which compound the complexity of beach response. Temporal variations can be considered at many scales; these may vary from periods of an individual wave of several seconds duration, through storms and tidal cycles with a duration of several hours (Powell, 1990), to much longer temporal variations of thousands of years (Orford *et al*, 1991). Relatively slow movements of mean sea level changes occur during the latter. The wide ranging combinations of conditions result in constantly changing shoreline responses and migration of the beach profile and plan shape. The present study focuses on the relatively short-term effects of storm events - over periods of several hours, which can result in significant modification to both the beach profile and the plan shape of the system.

The complex nature of the beach profile response is well illustrated by an examination of the principle responses of a shingle barrier beach to storm wave activity. Water may cross the barrier beach either by wave run-up exceeding the crest level, or by seepage through the permeable barrier. When unconfined wave run-up is small, sediment deposition is restricted to the crest and the deposits form a thin veneer

(Orford and Carter, 1982) at the crest of the beach. This type of overtop deposit builds up the crest level of the beach: crest level increases of up to 0.5m have been measured on Hurst Spit, due to this process (Nicholls, 1985). More substantial shingle movement occurs as a result of overwashing, when the unconfined wave run-up is higher. Washover flats (Schwartz, 1975) may result due to severe overtopping. Throat-confined overwash fans (Nicholls, 1984; Andrews, 1970; Schwartz, 1975; Leatherman, 1976a,b; Leatherman and Williams 1977, 1983, and Suter *et al.* 1982) are associated frequently with barrier beaches. Turbulent flow at the crest of the beach may occur, resulting in scour and fan-shaped deposition on to the lee side of the beach. Washover surge velocities of 0.5-3ms^{-1} have been measured, in the field, by Fisher *et al.* (1974) and Leatherman (1977) on sand barriers. Such processes are very sensitive to changes in wave and water level conditions, although combinations of these variables, (together with the shingle barrier geometry) have not previously been investigated by reference to clearly quantified hydrodynamic and geometric variables and their responses.

Similar processes connected with barrier beaches, but related to seepage through the mound, have been studied also in the field. The permeability of shingle beaches is significantly greater than that of sandy beaches: Darcy's permeability coefficient for gravel is in the range 2.5-5cms^{-1}, whilst it is only 0.0001-0.01cms^{-1} for sand. This difference results in the formation of interesting seepage features on shingle barrier beaches. Seepage has been observed by Nicholls (1985) on Hurst Spit, and by Arkell (1955) on Chesil beach. Whilst this process results generally only in the formation of small seepage hollows and cans, due often to a differential head from one side of the barrier to the other, it can be the precursor to large-scale breaching by fluidisation of the barrier (Viscocky, 1977).

1.1.3 Management of shingle beaches

The highly permeable form of shingle beaches provides excellent energy dissipation characteristics; consequently, they provide a valuable natural coast protection function at many sites. Although a number of beach recharge schemes have been constructed using shingle, there is extremely limited guidance available for the design or

management of these schemes - particularly for barrier beaches. The inadequate design of many seawalls and coastal structures, for the control of sediment transport and erosion, has resulted in the denudation of beaches, in response to wave reflection from the structures. Consequently, serious coastal erosion and flooding problems have occurred at many locations. The understanding of the interaction of beaches with these structures is poor generally; it needs to be more clearly understood, to allow more cost-effective and hydraulically-effective shoreline management.

The rapidly advancing techniques for the analyses of wave climates, together with their prediction and transformation in shallow water, have provided the engineer and scientist with better detailed information about the nearshore wave conditions. However, these have rarely been examined with respect to the shoreline response of either restrained shingle beaches or shingle barrier beaches. Although recent efforts have been made to improve the quantification of profile response of restrained shingle beaches to storm waves (Powell, 1990), no quantitative work has previously been undertaken for barrier beaches.

Whilst many regular-wave laboratory studies have been carried out on sandy beaches, few attempts have been made to identify (or quantify) the hydraulic performance of shingle beaches to random wave attack. This omission represents perhaps the difficulties in scaling beach material, to provide the appropriate profile response in the model.

The need to provide energy-dissipating coast protection structures, instead of reflecting seawalls, combined with the pressures to use more natural forms of flexible (or soft) coastal defence, has prompted recent research into the hydraulic performance of shingle beaches (van der Meer, 1988; Powell, 1990). The influence of beach permeability on energy dissipation, together with the formation of the beach profile, has been demonstrated by numerous attempts to reproduce physical scale models of shingle beaches, (using simple Froudian scaling to model the sediment). This approach results in a beach of incorrectly-scaled permeability and, consequently, the model beach does not reproduce correctly the profile performance of the full-scale shingle beach. Recent advances in physical modelling techniques have overcome many of the early problems, that have beset the laboratory study of shingle beaches (Powell, 1990). Significant advances have been made in

the quantification of the shingle beach profile response to random waves (Powell, 1990; van der Meer, 1988), but these are restricted to 2-dimensional flume studies of restrained shingle beaches. Laboratory testing has not previously been undertaken to examine and quantify the profile response of barrier or unrestrained shingle beaches, under random wave attack. However, several extensive field studies have been carried out to examine these types of beaches (Nicholls, 1985; Carter and Orford, 1981).

1.2 OBJECTIVES OF THE PRESENT STUDY

The main objective of this investigation is to identify and examine the variables controlling the short-term profile performance of shingle barrier beaches under storm wave attack. The study methodology seeks to develop a quantitative approach to the parametric description of the short-term profile response of shingle beaches to storms using numerical profile descriptors. Particular emphasis is placed upon shingle barrier beaches.

The following aspects of profile response are examined:

(a) modification of the unconfined shingle crest by wave overtopping;

(b) investigation of a range of hydrodynamic and geometric controls on the development of the beach profile;

(c) the development and spatial variation of the plan shape of a shingle barrier beach due to the combined influence of longshore transport and overtopping;

(d) the identification and quantification of the first-order hydrodynamic and geometric threshold conditions, which give rise to crest level raising by wave run-up and crest level lowering by overtopping; and

(e) preliminary development of a widely applicable method for the prediction of the short-term shingle beach response of barrier beaches to normally incident wave attack;

The study has provided an opportunity for the validation of earlier investigations into the profile response of normally-incident waves on restrained beaches, (Powell, 1990; van der Meer, 1988). It also provided the opportunity to extend the validity of the hypotheses presented by these researchers, to include the influence of oblique wave approach, depth limited foreshores and the applicability of the parametric framework to shingle barrier beaches.

Christchurch Bay, located on the south coast of England has been selected as the study area for the fieldwork element of the studies. Its exposure to long fetches to the south and south-west provided a reasonable expectancy that suitably severe wave conditions would occur during the study period, to provide statistically-valid results. Exposure of both restrained and barrier shingle beaches, within the embayment, provided an appropriate contrast in beach morphology within the study area. Two shingle beaches, the Hurst Spit barrier beach and the Hordle cliff beach, provided the two control sites. The beaches lie under the control of the New Forest District Council, who were seeking to develop beach management techniques within the bay at the time of the study. Funding of instrumentation, through this beach management programme, provided significant commercial and practical advantages to the selection of this study area - in addition to the scientific interest.

A parallel study was undertaken to design a major beach renourishment scheme for Hurst Spit (on behalf of New Forest District Council): consequently, the scientific and site specific management studies have been developed together. Hence, the present investigation seeks to: (a) provide site specific guidance on beach management of Hurst Spit following implementation of the beach recharge scheme; (b) undertake scientific studies of the beach processes; and (c) develop a generalised parametric model, of the response of the shingle beaches to storm waves.

This study will examine hydrodynamic and geometric variables through a complementary programme of fieldwork, laboratory experiments and numerical modelling (Figure 1.1). The beach morphology and response of beaches to storm conditions will be undertaken by field measurements of waves, tides, currents and beach profiles. A regional wave climate will be developed with the aid of numerical models of wave hindcasting, wave refraction, shoaling and bed friction. An extensive series of 3-dimensional large scale physical model studies will be used to investigate the influence of varied hydrodynamic and geometric variables through a controlled programme of tests.

The physical modelling techniques used to develop the empirical model of beach profile response have not previously been used to investigate the development of barrier beaches. Thus, a further important objective is to validate the laboratory test methodology: this will be undertaken by comparison of the response of the physical model, with full-scale natural beaches, to severe wave action (prior to the main phase of investigation). In this particular case reference is made to the development and maintenance of Hurst Spit.

1.3 THESIS STRUCTURE

An introduction to shingle beach processes and an assessment of recent developments in the numerical description of beach profiles is discussed in Chapter 2. Morphodynamics of the study area are discussed in Chapter 3. The study methodology is described in Chapter 4. The results of the numerical modelling of wave climate, field studies, and the physical model studies are presented in Chapters 5-7. Finally, an analysis of the test results, synthesis and testing of hypotheses developed during the investigations are discussed together with the limitations of the study findings and recommendations for further studies in Chapter 8.

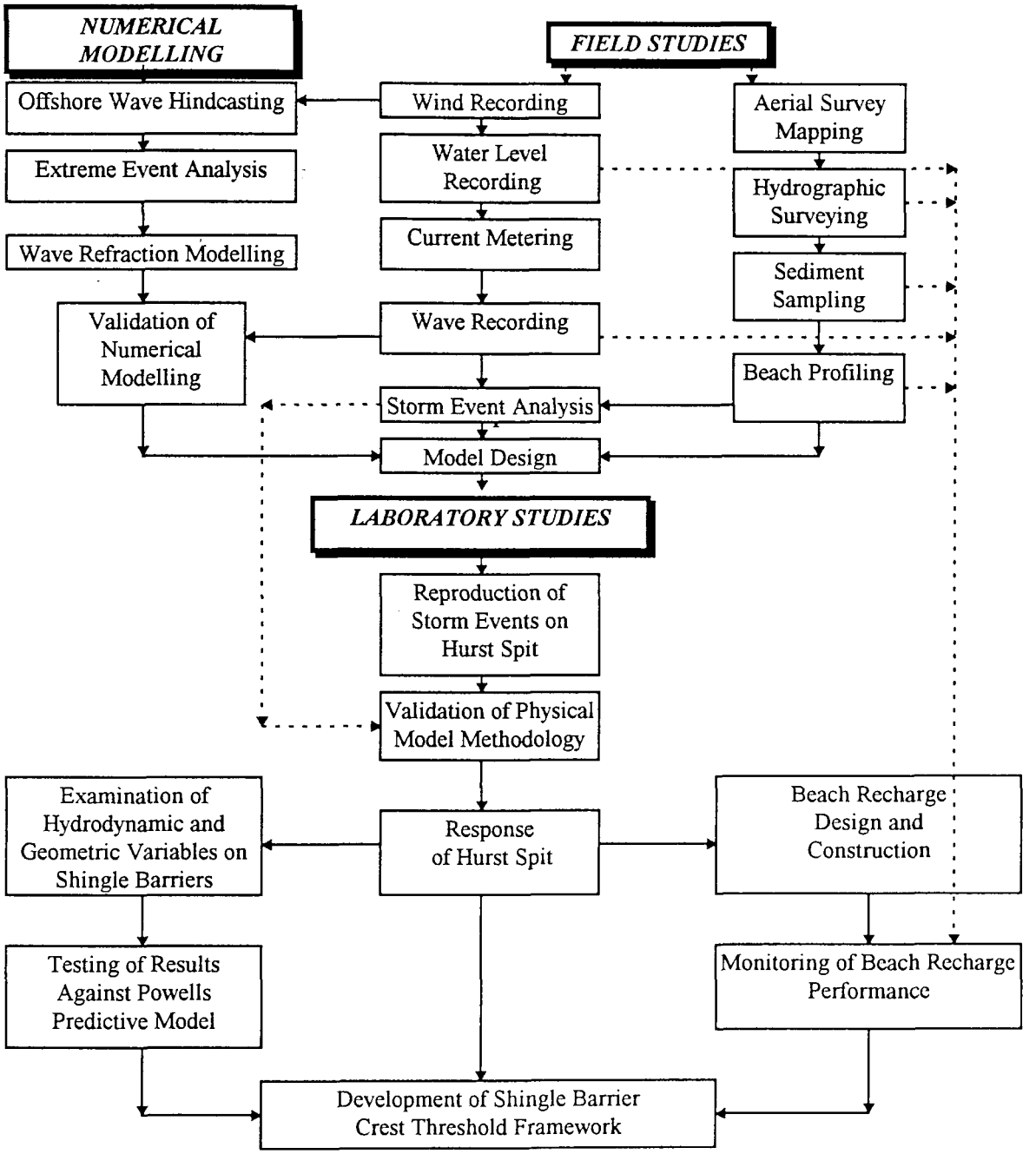

Figure 1.1 Investigation Flow Chart

CHAPTER 2: SHINGLE BEACH DYNAMICS- PREVIOUS INVESTIGATIONS

2.1 SHINGLE BEACH DYNAMICS

Shingle beaches are characterised by both sediment size and hydrodynamic response characteristics. Their morphological development is controlled primarily by wave action: it has been suggested, for example, that the beach responds critically to the proportion of the wave energy dissipated (Wright and Short, 1984). Movement of shingle is less influenced by tidal currents, than sand, as shingle moves primarily in bed load as opposed to suspension (Velegrakis, 1994).

Shingle beaches are often reflective, with steep upper faces, dominated by plunging wave conditions over a narrow surf zone (Carter, 1988). A series of stages of beach form, ranging from 'totally reflective' to 'dissipative' conditions, have been recognised (Short, 1979). Reflective shingle beaches show a characteristic highly reflective form under storm wave conditions (Kirk, 1980; Carter and Orford, 1984): these are characterised by a shallow gradient offshore profile, a steep linear beach face and a high crest berm. Bars may develop during storm conditions (Kemp, 1963), particularly when the lower foreshore comprises a finer sand fraction (Short, 1979). Shingle beach profiles are often described as stepped, due to the distinctive inflexions on the profile. Formation of a step-berm at the breaker point on the cross shore profile is reported to induce premature wave breaking; this results in partially reformed spilling breakers running high up the beach, to form ramp and overtop deposits (Orford and Carter, 1985).

McLean and Kirk (1969) suggest a linear relationship between grain size sorting and foreshore slope. Kirk, (1980) extended this work to identify the zonation of barrier profiles. Distinctive cross-shore shape sorting is sometimes apparent (Bluck, 1967; Orford, 1975) with spherical material concentrated over the lower segment of the profile. Large clasts can be stranded preferentially at the berm crest (Carr, 1969). Working and sorting of sediments is possible only within a confined zone on a simple beach backed by cliffs; energy absorption is confined to reflection and dissipation within the voids. In contrast, flow can pass over the crest of a barrier beach, causing

modification of the crest and the lee slope profiles of the beach, creating a new depositional regime (Carter, 1988). A cross-shore correlation between sediment size and cross-shore elevation has been proposed for gravel barriers in Washington State, (U.S.A) (McKay and Terich, 1992). The nature of overwash deposits results often in the deposition of a mixture of the finer and coarser sediments; consequently the permeability of the beach is reduced due to this layering effect. Similarly, beach recharge operations may influence the sorting of the beach, often resulting in much reduced permeability (McFarland *et al*, 1996). Hydraulic or mechanical processes used for placement of beach recharge materials results in artificial mixing of beach material; semi-cohesive recharge deposits may "cliff", forming nearly vertical supratidal slopes under these circumstances.

2.2 BARRIER BEACHES

2.2.1 Definition and distribution

Barriers may be subdivided into swash- or drift-aligned structures (Orford and Carter, 1991, Orford *et al* 1995), depending upon their orientation relative to the incident wave climate: the essential feature which defines a barrier is a well-developed back slope and barrier depression. Barriers may take a number of forms, including recurved ridges which form adjacent to tidal inlets; alternatively, they may be attached to solid geology at either end, protecting brackish lagoons. Whitten (1972) defined a spit connecting two sides of a bay as a bar: such a feature is termed a barrier beach in this study. The definition of a spit adopted by Horn *et al* (1996) is " a detached beach that is tied to the coast at one end and free at the other, with a free end that often terminates in a hook".

Classification of spits and barriers has been addressed in a number of ways. Zenkovitch (1967) defined coastal depositional features on the basis of morphology and sediment sources, whilst King (1972) adopted a purely morphological approach to classification. King (*op. cit*) differentiated between spits and barriers, by defining the latter as being attached at both ends, whilst Zenkovitch (*op. cit*) categorised both into a single grouping. Swift (1976) and Carter and Orford (1991) have suggested similar

definitions of beach-and-barrier coasts, by subdividing according to their plan shape: drift coasts have a straight plan form (Swift, 1976), whilst swash coasts are cuspate in plan shape. Carter and Orford (1991) suggest that drift-aligned coasts form when longshore processes dominate over cross-shore processes: swash-aligned beaches, in contrast, undergo little longshore development.

Coarse clastic barriers are distributed widely on a global basis, but are especially common in formerly glaciated areas (Forbes and Taylor, 1987; Forbes *et al*, 1993, 1995). Amongst regional studies which have examined the morphology of spits, Steers (1948) examined the form of many spits around the coast of England and Wales. Similarly, Kidson (1963) examined the form of a number spits in the south-west of England. The spits of Dingle Bay on the west coast of Ireland were studied by Guilcher and King (1961) and analysed by King (1972): it is suggested that realignment of the spits due to the orientation of incident wave conditions, which are dominantly swell waves, has resulted in narrowing of the spits close to their point of attachment. King (1973) examined a long-term beach profile analysis of the spit at Gibralter Point, near Skegness and postulated cyclical lengthening and shortening of the spit due to swash processes, together with progradation. Similar cyclic elongation and breaching was observed by Carr (1965) in studies of progradation of North Weir Point, Orfordness over a period of 30 years. Extension of the spit varied annually between 0-80m. The cause of breaching was attributed to a combination of beach thinning due to shoreface erosion, storm action and differential hydraulic gradients. Spurn Head has been extensively studied by many researchers. DeBoer (1981) and De Boer and Carr (1969) examined historical records and linked erosion of the Holderness coast with breaching of the spit. Geomorphological evolution has been controlled by engineering works (Stevens, 1992; Thomas, 1996), with the natural washover cycle now being partially artificially-controlled.

Early coastal geomorphological studies on spits were largely descriptive in character; (Evans, 1942; Zenkovitch, 1959). Lewis, (1938) suggested that Hurst Spit was developed due to oblique wave attack and that the recurves resulted from the combined effects of wave refraction and waves from within the adjacent Solent waters. Steers (1948) also focused on the alignment and development of spits relative to the normally incident wave direction. Robinson (1955) suggested that spits on two sides of an estuary could develop from a breach in a spit formed within a single dominant drift

direction. In contrast, Kidson (1963) has reviewed several features which have drifted towards each other. Yasso (1964) presented a numerical description of a recurved spit, but did not discuss the processes which might support this theory. Hayes (1979) related the type of coastline to tidal range and characterised wave-dominated coasts as generally long smooth barrier coasts, with inlets on which washover features are prominent.

Scolt Head Island (Norfolk), has a history of extension of 1.5km during the past 100 years (Steers, 1960; Allison and Morley, 1989). Changes are episodic, with periods of erosion between the dominant depositional process. Davis (1991) used aerial photography to examine changes between 1965-1990 at Far Point (Norfolk). Cyclic extension due to longshore transport was demonstrated followed by onshore migration and formation of recurves. Raper *et al* (1996) have suggested a similar cyclic process in the evolution of recurved spits at Far Point: washover is considered to be of minor importance, limited only to extreme events. Tidal currents at the end of the spit are considered to be the dominant process leading to shaping of the end of the recurve spits. Bristow *et al* (1992,1993) examined the structure of Scolt Head through coring; this indicated that the structure of the spits is largely of coarse gravel. Evidence of overwash processes is seen in the lee of the spits.

Outside of the British Isles relatively few studies have been made of spits, particularly in terms of their morphodynamics. Sevon (1966) has examined the effects of wind processes on Farewell sand spit, (New Zealand). Plan shape changes at Chilka Lake Spit (India) have been attributed to offshore bathymetry (Venkatarathnam, 1970). Studies using aerial photographs examined erosion and accretion of spits at Price Inlet, South Carolina, (U.S.A) (Fitzgerald, 1976); similar studies by Galichon (1985) presented evidence of a reduction in the rate of lengthening of the Pointe d'Arcay, (France). This latter researcher postulated that the decline in rate of growth from 25m per year to 10m per year is due to sediment starvation, resulting from up-drift coastal protection works.

The studies discussed above have focused upon the development of the plan form of spits and barriers. Investigators consistently attribute shoreward migration of the features to washover processes; at the same time, some quantify the rate of progradation. However, none of the studies have attempted to quantify the forces they

discuss in support of their hypotheses to describe the rollback of the barriers. Process studies of barrier evolution are much more restricted.

2.2.2 Barrier structure

The geological record presents a confused interpretation of barrier and spit preservation, primarily because of the difficulty in differentiating between the various types of beach on the basis of the analysis of the internal sedimentary structure (Nielson *et al*, 1988). Spits and barriers can both be characterised by large-scale landward-dipping sedimentary structures which form as a result of progradation. Structures demonstrating a coarsening upwards sequence, with washover deposits at the crest, could be argued to fit into the category of beach, barrier or spit. The most obvious characteristic of these structures is their plan shape, which can rarely be seen within a geological exposure. Kraft *et al* (1979) have presented sedimentary models for coastal environments which differentiate "ocean-estuarine systems" from "estuarine barrier washover systems", using type combinations of sedimentary sequence. Similarly, geophysical methods have been used to examine spit migration (Siringan and Anderson, 1993; Smith and Jol 1992 and Jol *et al,* 1994). Description of the washover processes has been examined on the basis of vibracore studies (Hequette *et al*, 1995). Back barrier stratification has presented evidence for overwashing through landward-dipping wedge-shaped , intertidal sub-beach structures, with upward coarsening sediments at Carnsore, (Ireland) (Orford and Carter, 1982, 1984): here, washover processes are suggested as the main migratory process. Hurst Spit is similar in broad terms, but there are some significant differences. Such differences include the shingle/sand ratio, and the mean shingle fraction of the beach size distribution which are both higher at Hurst Spit (Nicholls, 1985), than at Carnsore. Similar circumstantial evidence of overwashing is provided by Carr and Blackley (1973) at Chesil Beach, and by Leatherman and Williams (1977, 1983) in sand barriers, on the basis of the description of the barrier stratification.

2.2.3 Cross-shore processes

Berm formation is the most frequently-occurring process, which reshapes the supratidal section of the beach; it occurs close to the limit of wave run-up, when the swash fails to reach the crest. Beach deposits arising from this process are ephemeral and berms may only exist for a single tidal cycle, depending upon the prevailing wave conditions (Nicholls, 1985). Berm deposits are virtually always composed of the coarser fraction of the beach; these may be preserved occasionally, if the beach progrades.

Evolution of swash ramps, associated with run-up that cannot reach the barrier crest has been examined by Orford and Carter (1984); it is suggested that their formation results from the development of supratidal terraces by spilling wave conditions during storm surges. Hypothetical wave conditions have been examined to hindcast ramp-forming conditions based upon empirical relationships between run-up and wave height and the basic analysis of local breaking wave conditions (Carter and Orford, 1981).

The crest level of a shingle barrier beach is one of its most critical parameters in defining its stability (Nicholls, 1985) and is dependent upon wave run-up and sediment availability. Landwards recession occurs when wave conditions exceed the unconfined crest: this can occur on barriers which lie many metres above mean sea level. For example, the maximum crest height of Chesil Beach was 14.7m OD (Carr, 1969); this was reduced to 13.7m OD due to overwashing (Carr, 1982). Orford (1977) examined hypotheses proposed by Palmer (1834) and Lewis, (1931), which suggested that shingle beach crests were deposited by plunging breakers, but concluded that spilling breakers in combination with a storm surge were a more likely mechanism. Orford and Carter(1984) suggest that edge waves may form a significant role in the crestal and overwash processes on drift-aligned barriers.

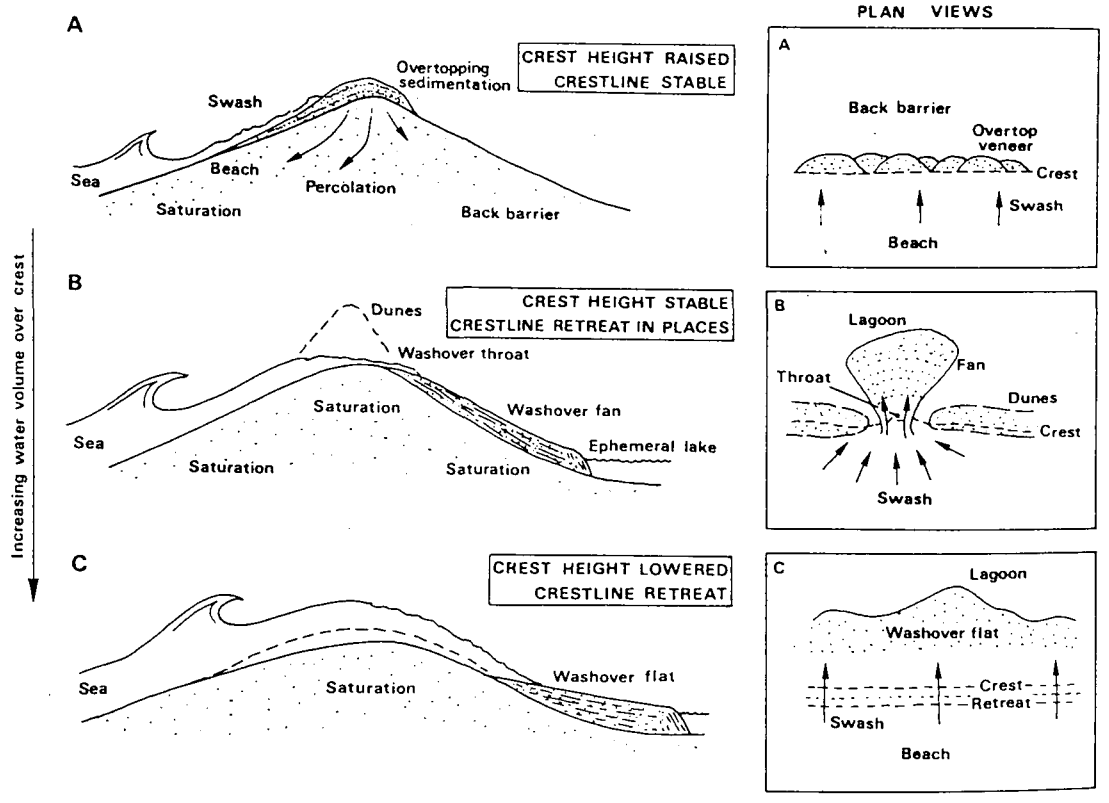

Figure 2.1 Contemporary barrier beach processes - the continuum of overtop-washover sedimentation as a function of the increasing volume of water passing over a barrier crest during a severe storm (from Orford and Carter, 1982)

Overtopping occurs in response to appropriate combinations of wave and water level conditions, and beach geometry (Figure 2.1). Orford and Carter (1982) and Orford *et al* (1991a), suggest that where the volume of unconstrained run-up is small, sediment deposition tends to be confined to thin veneer overtop deposits; this results in vertical crestal accretion, when wave energy is inadequate to pass over the crest. Such deposits occur as virtually horizontal open-work shingle. Swash returns to seawards by percolation through the permeable shingle. Nicholls (1985) has identified maximum accretion of the beach crest of 0.45m due to this process; this is primarily during storm surges, suggesting that this process occurs more frequently than overwashing. Shingle overtopping, without overwashing, has also been recorded at Chesil Beach (Dorset) and Llanrhystyd (Wales) (Orford, 1979). Landward thinning deposits predominate at

Carnsore, demonstrating a preference for barrier crest build-up (Orford and Carter 1982).

Overwashing takes place when swash continues over the unconfined crest, onto the back crest of the beach. Differentiation between the processes on sand and shingle barriers relates to the higher permeability of shingle beaches (Nicholls, 1985). Whilst coarse clastic barriers exhibit high permeability, the nature of overwash often results in the mixing of coarse- and fine-grained materials in the washover deposits (Carter and Orford, 1993). Hayes and Kana (1976) suggest that overwashing is associated only with topographic lows, in sand barriers. Carter and Orford, (1981) and Orford and Carter, (1982, 1984) suggest a similar control on the coarse clastic barriers of SE Ireland. Leatherman *et al*, (1977) suggests a barrier elevation overwashing threshold of 2.5m above sea level on a sand barrier system at Assateague Bay (U.S.A), but does not reference this to wave conditions. Overtopping gives way to discrete overwash and the formation of throat-confined washovers, often at topographic lows, when run-up exceeds crest height; this can develop further, as wave intensity increases, leading to sluicing overwash (Orford *et al* 1991a). The entire barrier crest may be displaced in surge-like swash flow, under such circumstances (Figure 2.2).

Orford and Carter (1982) have discussed the possibility of simultaneous overtopping and overwashing at various locations, under the same hydrodynamic conditions; it is suggested that throat-confined overwash fan formation may result. A periodicity of spacing of throats has been observed by Carter *et al* (1990) at a spacing of 15-25m on the drift aligned barrier at Story Head, (Canada).

Nicholls (1985) identified two types of overwashing:

(i) Type 1 Overwashing - without a reduction in crestal height;

(ii) Type 2 Overwashing - with a reduction in crestal height.

Type 1 Overwashing is characterised by the deposition of open-work shingle, on the lee crest of the barrier. Such deposits consist of thin layers, of approximately 0.1m

with a dip similar to the leeward face of the beach; this is typically at a slope of 5-13^{O}, but also reaching steepnesses of 19^{O} in places on Hurst Spit (Nicholls, 1985). The deposits are characterised also by steep fronts, probably resulting from sudden cessation of the flow, due to percolation.

Type 2 Overwashing occurs less frequently; it results when the combination of wave and water level conditions are severe, relative to the beach geometry. A range of features may result from this process; these include throat confined overwash fans , or more wide-spread sluicing overwash. Examples of both of these processes were observed and documented during the course of the present study (Chapter 6).

Development of such features can be quite rapid. Once the crest level has been reduced the wave energy required to overtop the crest is reduced; hence, the frequency of overtopping events increases. This process is the most significant in terms of the volumetric movement of material onto the back crest of the barrier. Nicholls (*op. cit*) observed Type 2 Overwashing on at least 13 occasions, between 1980-1982, at Hurst Spit. Washover fans and flats generated during these events were up to 1.5 m thick; one extended up to 100m to landwards of the crest. Fans are characterised generally by a steep face at their landward end, where the fan intersects the lagoon. The composition of sediments within the fans can be highly variable, and they may comprise of a mixture of open-work shingle, sandy open-work and sandy-shingle: landward dips vary at between 3 - 6^{O} at Hurst Spit (Nicholls, *op. cit*). The maximum reduction recorded by Nicholls (*op. cit*) was 2.5m. A 30m wide throat formed on 10/4/83; this widened to 100m on 2/9/83. Beach face erosion accompanied overwashing, resulting in crest elevation reduction of 0.5-1m over a 100m length of the beach. The landward dip of the washover deposits were typically at a slope angle of 6-10^{O}.

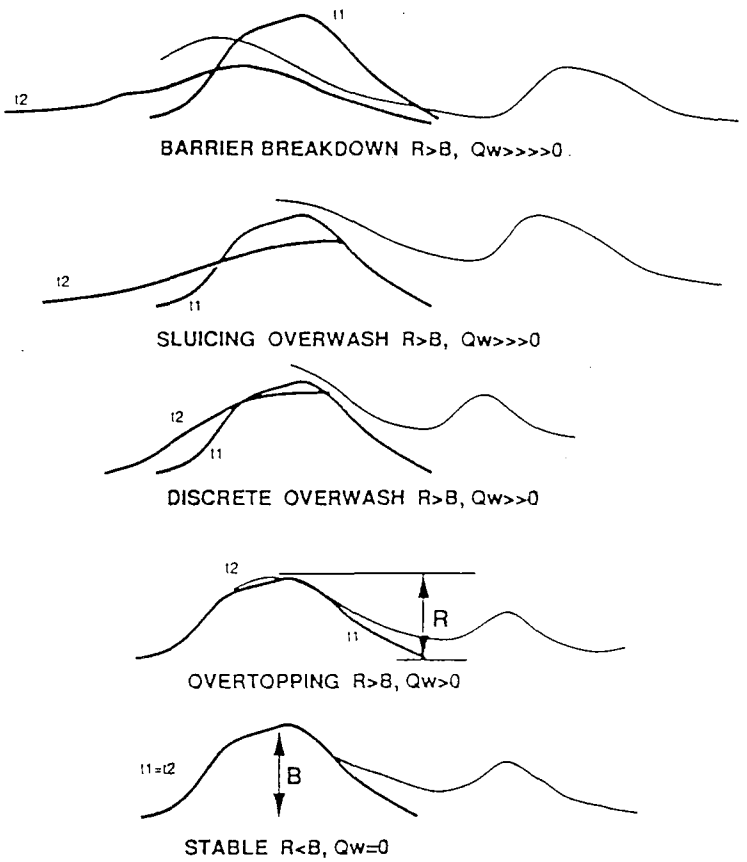

Figure 2.2 The continuum of overtopping and overwashing modes by which gravel barrier crest migration may occur: crestal profiles before and after storm generated overtopping and/ or overwashing run-up (from Orford et al 1991)

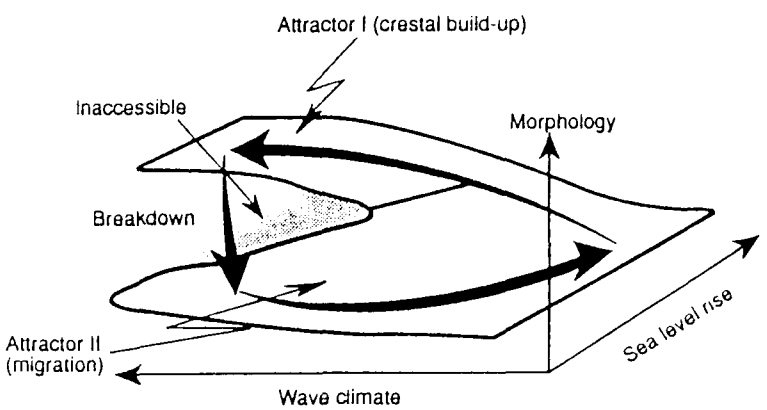

Figure 2.3 The two attractors for gravel barriers under the influence of rising sea level (after Carter and Orford, 1993)

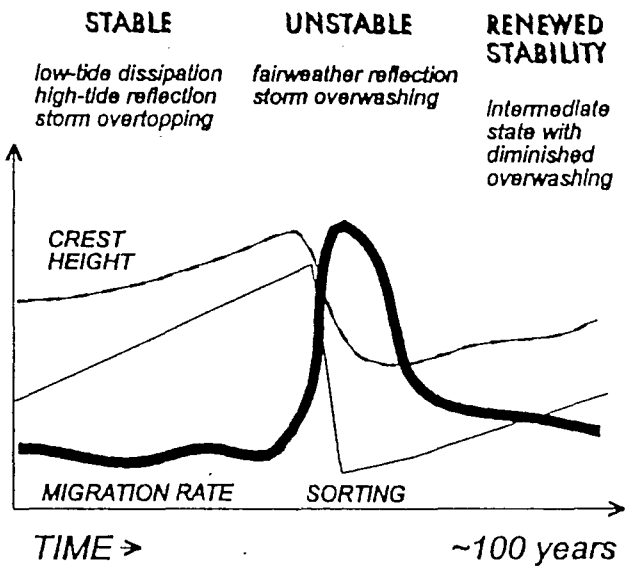

Figure 2.4 Schematic representation of catastrophic transition from stable to unstable hydrodynamic states (attractors I and II of Carter and Orford, 1993) for swash-aligned single-ridge gravel structures.

The jump from crestal build-up to barrier breakdown may involve little additional forcing (Carter and Orford, 1993) (Figure 2.3). Transitional zones may occur between these triggers, when a certain mode of development persists; the sorting and stability of the structure improves during these periods (Figure 2.4) (Carter *et al*, 1993).

Despite numerous field-based studies which have examine cross-shore response processes, none have quantified crest evolution with respect to hydrodynamic forces.

Seepage is also noted as a significant process. This may result in the formation of wash out cans or channels as discussed for sites at Slapton Ley (Devon) (van Vlymen, 1979), Chesil Beach Arkell, (1955); Carr and Blackley, (1974) at Dungeness (Eddison, 1983) and at Hurst Spit (Dobbie and Partners, 1984; Nicholls, 1985). Carter *et al* (1984) quantified stream seepage through coarse clastic barriers in SE Ireland, identifying a relationship between maximum potential head, discharge and barrier

geometry. Barrier seepage throughflow is suggested to occur in the range 0.25-1.8 x 10^{-3} m^3s^{-1}, assuming seepage velocities calculated by reference to Darcy's formula:

$v = k\Delta h / \Delta \ell$, where

k is the permeability coefficient and $\Delta h / \Delta \ell$ is the hydraulic energy loss per unit length. Differential water levels often occur on either side of the barrier, resulting in varied hydraulic gradients. Cross barrier differential water levels of 1.5m were observed at Padre Island, (U.S.A) during hurricane Allen (Suter *et al* 1982); these may have encouraged breaching to occur.

2.2.4 Hydrodynamic conditions

Whilst the influence of wave conditions is recognised by many authors: (Boyd *et al*, 1987; Forbes and Taylor, 1987; and Carter *et al* 1990); none provide local measurements of shallow water conditions. Orford *et al* (1991a), Forbes and Drapeau (1989), Orford and Carter (1982, 1984) and Fitzgerald *et al*, (1994); all provide information on the magnitude of offshore conditions but no details of nearshore storm-specific conditions. Carter *et al* (1990) have recognised the significance of these limitations. Carter and Orford (1993) emphasise the importance of wave conditions in the change of the morphodynamical status of the barrier, as the critical wave height to depth (H_s/d) and depth to wave length (d/L_o) change; this suggests that morphodynamic shifts occur at abrupt thresholds.

The tendency for crest elevation to build is greater under spilling waves (Orford, 1977), which are characteristic of dissipative shorelines. Edge wave development in the nearshore zone is considered to be an important factor in the development of drift-aligned barriers, when the predominant wave train is not normally incident to the beach (Carter and Orford, 1993). Refraction and diffraction have both been postulated, as important factors in the evolution of spits (Carter, 1988); however, their role is unclear.

2.2.5 Evolutionary timescales

Holocene developments within the North Sea have resulted in net sea level changes of about 20m over the past 8000 years (Shennan, 1987). This rapid change in sea level has enabled spits and barriers to evolve rapidly, through erosion of the shoreface and increasing washover (Hequette and Ruz, 1991; and Hequette *et al*, 1995). A number of features around the coast of the UK are attributed to formation at approximately 5000-6000BP. For example, Larcombe and Jago (1994) have suggested that the formation of the Mawddach estuary bar (Wales) was by sediment rolling landwards in response to sea level change: Nicholls (1985) suggests a similar evolution for Hurst Spit. The effects of sediment supply on the evolution of Orford Ness (Suffolk), were examined by Carr (1970); a correlation with both sediment supply and changes in water level was demonstrated. Borrego *et al* (1993) examined evolution of the spit at the mouth of the Piedras River (Spain), on the basis of geophysical profiling. These investigators demonstrated the effects of episodic overwashing and changes to the sediment supply over the course of 4000 years. Boyd *et al* (1987) present a six stage evolutionary model for barriers; the first two of these phases relate to geological and oceanographical conditions for the initial formation; the latter stages conform broadly with evolutionary processes discussed by Orford and Carter (1982, 1991).

The balance between barrier crest build up due to overtopping, and crest breakdown by overwashing, dictates the rate of barrier migration (Orford *et al*, 1991). Differential response of the barrier crest and back barrier limit provides an indication of the evolutionary phase (Figure 2.5). If the seaward shoreline retreats faster than the back barrier, then the crest must be building. The opposite response suggests a falling crest elevation. These inferences suppose that net sediment transport is in balance and that the cross section of the barrier is maintained. The balance between overtopping and overwashing is controlled by the frequency and magnitude of storms and storm surges, which are independent of water level. The theory that barrier migration is partially a function of sea-level rise is supported by Dillon (1971), who postulated that an increasing volume of material is required to maintain a stable barrier under sea level rise. Unless there is a longshore or offshore supply, this balance is unlikely to be maintained. It is suggested that barrier rollover will be spasmodic when sea-level is static: however, this theory does not allow for the effects of increased 'storminess'.

Orford *et al* (1991) suggest that barrier migration must cease with time in a static sea level situation as the fetch limiting storm event approaches asymptotically: it is suggested that the large gravel barriers of SE Ireland fall into this category. This hypothesis could be applicable to fetch-limited situations, but does not allow for the influence of storm surges.

Carter and Orford (1993) suggest that the study of the short-term morphodynamics associated with coarse clastic barriers has been neglected; this reflects the difficulty of measurement within a high energy zone. As a result information of a near instantaneous-scale dynamics of such barriers is rare. Horn *et al* (1996) confirms that detailed short-term process studies on spits are virtually non-existent.

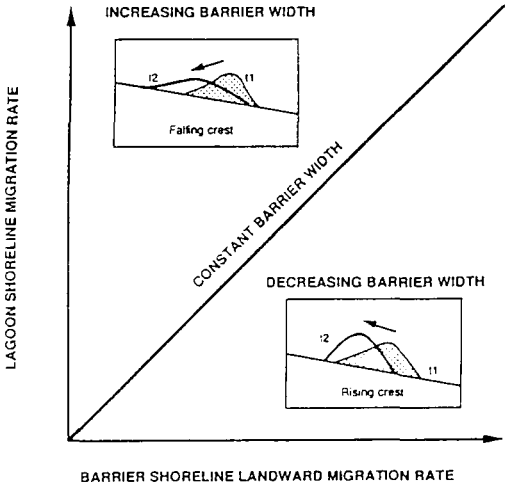

Figure 2.5 Schematic view of barrier crestal stability domains as a function of seaward and back-barrier shoreline migration. (from Orford et al 1991a)

The geometric variability of the structure shape and size has a significant effect on barrier response, in addition to the hydrodynamic conditions. A summary of geometric variables considered by various investigations is presented in Table 2.1. Data does not consistently relate barrier geometry to clearly defined tidal elevations.

Location	*Width (m)*	*Height (m)*	*Investigator*
Story Head (Nova Scotia, Canada)	40-60	4	Orford et al (1991)
Olympic National park (Washington, USA)	20-30	5-6	McKay & Terich (1992)
Louisburg (W.Ireland)	80	4-5	Carter & Orford (1993)
New Harbour (Nova Scotia)	30-40	4	Carter & Orford (1993)
Ballantree (Ireland)	80	10-12	Carter & Orford (1993)
Porlock (Devon)	40-60	10	Carter & Orford (1993)
Carrs Pond, (Nova Scotia)	40-50	4	Carter & Orford (1993)
Hurst Spit (Hampshire)	30-50	4-5	Nicholls (1985)

Table 2.1 Typical coarse clastic barrier geometry

2.2.6 Methods of study

Aerial photography provided the basis for investigations by Regnauld *et al* (1993) at Sillon du Talbert (France); and Suter *et al* (1982) and Penland and Suter (1984) on sand barrier islands of the Gulf Coast (U.S.A). Similar techniques have been used by Orford *et al* (1991a), to determine the rates of barrier migration at Story Head, (Nova Scotia), in parallel with long-term time-series of tidal records, (over periods of several decades) (Orford *et al* 1993). The relationship between back barrier and sea level margins has been used to infer phases of crest lowering and build up (Orford *et al*, 1991). Beach profiling and sediment analysis has been used to investigate the profile

response of gravel barriers in Olympic Park, Washington (McKay and Terich, 1992). Observations of the response of an artificial breach and natural closure of a shingle ridge to tidal currents and waves were made using tracers, topographical surveys and by reference to offshore waves by Walker *et al* (1991), at Batiquitos, San Diego.

Leatherman (1977) presents details of current measurements of overwash surge velocities, using electro-magnetic current meters and pressure transducers located in a throat on a sand barrier at Assateague Island (U.S.A). Velocities of 8ft/second were recorded. Similar overwash bore velocities were recorded by Holland *et al* (1991) on a sand barrier in Louisiana, using a video system and a series of capacitance wave staffs located in an overwash throat. Maximum storm event erosion depths have been analysed using plugs of dyed sand, by Fisher *et al* (1974); these investigations identified wave conditions resulting in profile and throat development on Assateague Island. Extensive throat-confined overwash-fans formed on the sand barrier: fans extending 100m, with a 30m wide head and 12m wide throat were recorded.

2.2.7 Conceptual models of morphodynamic forcing

Although Bruun (1962) suggests a relationship between sea level rise and shoreline migration which is applicable to all grain sizes, the validity of the 'Bruun Rule' is unproven for coarse clastic barriers. Orford *et al* (1991a) have provided qualified evidence in support of the Bruun Rule, for coarse grained systems, recognising the importance of wave activity but questioning the representativeness of barrier type used in their investigation.

Carter and Orford (1993) discuss a conceptual model describing medium-term changes on coarse clastic barriers, linking wave climate, morphology and sea level rise to crestal build up and barrier migration. As the relative width of the seaward slope increases, the slope becomes increasingly dissipative, even to the point where the crest ridge may become abandoned; this is especially significant if accompanied by a fall in sea level (Carter and Wilson, 1992). If the barrier progressively loses material, migration is likely to increase and it may ultimately breach (Carter, *et al* 1987).

Whilst sea level is a passive plane, it forms the basis for dynamic mechanisms such as wave activity. Evidence for the landward migration of gravel barriers in response to sea-level rise has been provided for Loe in Cornwall (Hardy, 1964), Chesil Beach (Carr and Blackley, 1974); and in Ireland (Carter and Orford, 1981). These hypotheses are developed by inference, but Orford *et al* (1993, 1993a) has presented evidence, at a decadal time scale of relationships between sea level rise and barrier migration in Nova Scotia.

Much research on the evolution of shingle barrier beaches has focused upon the effects of sea level rise on the transgression of the beach (Orford *et al*, 1995). Whilst recognising that barriers are influenced by the effects of storm waves, few researchers have attempted to quantify these effects. Changes in mean sea level are seen as the primary driving mechanism for the evolution of barriers (Hardy, 1964; Carr and Hails, 1972); this must assume a non-varying wave climate over the period of sea level change. The effects of relative sea level rise, on the geomorphological response of swash-aligned gravel barriers, have been examined over a range of temporal scales by Orford *et al* (1995); McKenna *et al* (1993); and Carter *et al* (1993). Evidence is presented for a linear relationship between sea-level rise, barrier inertia, (specified in terms of height and cross section geometry) and barrier migration; this was based upon three gravel barriers, over the period 1837-1986 . The importance of barrier cross section and elevation is emphasised and it was suggested that the smaller the cross-sectional area, the more rapid the retreat regardless of sea-level rise (Figure 2.6). Importantly, reference was made to the assumption that wave climate remains constant over this period.

The studies discussed above provide evidence for the evolution of shingle barriers over periods ranging from several thousand years to the sub-decadal scale. Whilst the evolutionary processes have been discussed, by inference, no near-instantaneous measurements have been made of the response of shingle barriers to extreme storm-events with simultaneous measurement of wave, water level and geometric conditions. These short-term processes may be particularly important where the barriers provide a coastal defence function. Barriers which provide this function have been discussed for a number of locations, including Chesil Beach (Babtie, 1997; Bray, 1997) and Hurst Spit (Nicholls, 1985; Bradbury and Powell, 1992; and Bradbury and Kidd, 1998).

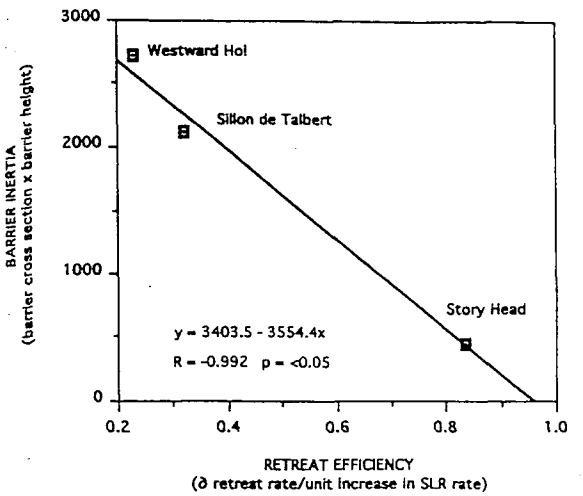

Figure 2.6 Barrier inertia against the efficiency of barrier retreat for Story Head, Sillon de Talbert and Wetsward Ho! barriers. (from Orford et al 1995)

2.3 BEACH PROFILE ANALYSIS

The profile and form of a shingle beach can be considered as part of a general morphodynamic model. It has been suggested by many researchers that two main types of beach profile exist: a step or swell profile formed by waves of low steepness and associated with beach accretion; and, bar or storm profiles formed by waves of high steepness and associated with beach erosion. These two forms of profile (Figure 2.7) have been identified largely through regular wave model testing and have focused upon the shape of sand beach profiles (Powell, 1990). Profile evolution is significantly more complex however, than these regular wave studies would suggest.

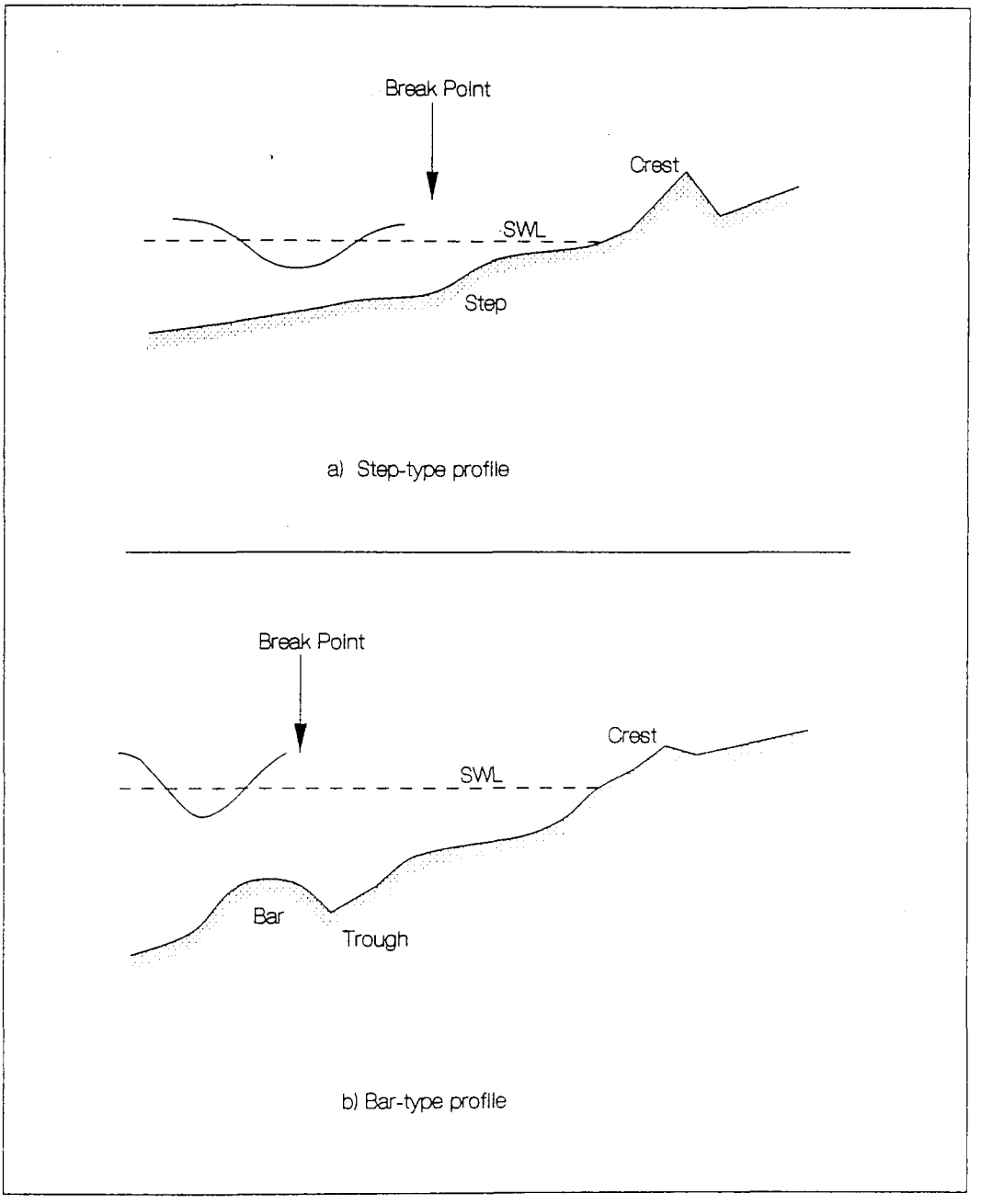

Figure 2.7 Idealised beach profiles (after Powell, 1990)

Whilst the concave profile of a shingle beach has been commented upon by many investigators, few have attempted a mathematical description of this curve. Where

sandy beach profiles have been described mathematically, it has generally been concluded that the profile can be described by a hyperbolic curve of the form:

$$y = Ax^n \qquad [2.1]$$

A and n are functions of the beach material and the incident wave conditions, whilst x and y are the horizontal and vertical distances, respectively.

Similarly, a general form of the equation has been used by Keulegan and Krumbein (1949), to describe the curve of a beach profile:

$$y^{7/4} = \frac{x}{4.86(v^{2/9})^{0.25}} \qquad [2.2]$$

Where v is the kinematic viscosity of water (9.7×10^{-6} ft^2 /s) and x and y (feet), are expressed in Imperial Units.

Keulegan and Krumbein (*op.cit*) derived this equation from the solitary wave theories of Boussinesq and Russell, in combination with laboratory tests of energy loss within a solitary wave. Assumptions made in the theoretical derivation do not appear however, to represent the experimental conditions used for their laboratory tests.

A theoretical expression for the equilibrium profile of a sandy beach was derived by Bruun (1954), based upon the following assumptions:

a) the beach profile is formed only by the onshore /offshore component of the shear stress, due to wave action;

b) the shear stress per unit area of sea-bed is constant, in both time and along the onshore axis; and

c) the wave energy loss is uniform, as the wave approaches the shoreline.

The general form of equation derived by Bruun (1954) based upon these assumptions is given below as:

$$y = Ax^{2/3} \qquad [2.3]$$

Comparisons have been made between this formula and field data derived from Denmark and from Mission Bay, California. This comparison indicates that A is dependant partly upon wave steepness, suggesting that A increases with a reduction in wave steepness.

Studies by Dean (1977) have suggested three models to describe the equilibrium profiles of sandy beaches, in the zone between the wave break point and the shoreline. The models are limited to spilling breaker conditions, since the ratio of breaker height to water depth must be constant to landward of the first breaker point. Whilst this may be appropriate for many sandy beaches which are relatively flat, it is clearly unsuitable for typically steep shingle beaches where spilling breakers occur only rarely.

Dean's (*op. cit*) first model assumes that the beach profile is created in response to a uniform long-shore shear stress. The second model suggests that the profile results from uniform dissipation of energy per unit surface area of sea-bed; it assumes that energy is transferred into turbulence and then through viscous action, into heat. The resulting equation was derived as follows:

$$d_n = Ax^{2/5} \qquad [2.4]$$

where d_n is the depth below mean sea level

x is the horizontal range

and A is a function of grain size

Deans (1977) third model was derived in a similar way, but assumed that the profile resulted from uniform energy dissipation (per unit of volume of water) within the surf zone. The following equation was derived:

$$d_n = Ax^{2/3} \qquad [2.5]$$

with the constant A being derived from the following equation:

$$A = \frac{(4.8D(d))^{2/3}}{\gamma K^2 g^{1/2}} \qquad [2.6]$$

where

K is a constant H_n / d_n

H_n is wave height within the surf zone

g is density of water

and $D(d)$ is rate of wave energy dissipation per unit volume as a function of grain size.

The constant A appears therefore to be a function only of grain size: this does not appear to be appropriate for the description of shingle beaches, since they are rarely subject to spilling waves. Consequently, the constant used in the formula must include an appropriate function to describe wider ranging wave conditions, if it is to be applicable to shingle beaches.

The above equations were evaluated by Hughes and Chiu (1978) who tested them by fitting measured beach profiles. These investigations found that equation [2.5] provided the best fit to the data, in the majority of cases; this implied that the best approximation for sand beach profile formation in the surf zone is described in terms of a uniform energy dissipation model (per unit volume).

Hughes and Chiu (1981) analysis of sandy beach profiles (with a median size of approximately 0.27mm) from the Florida coast and the Lake Michigan shoreline provided an equation of the form:

$$y = 0.1x^{2/3} \qquad [2.7]$$

This relationship suggests that the constant A in Dean's formula is given by:

$$A = 0.1m^{1/3}$$

Further work by Hughes and Chiu (1981) was undertaken, on the formation of sandy beach profiles in laboratory experiments. The material in these studies had a grain size (D_{50}) of 0.15mm. These studies confirmed the general form of Dean's equation [2.5] for spilling breaker conditions, providing a new coefficient for the constant (A) of;

$$A = 0.132m^{1/3}$$

These authors tested the coefficient as a function of both wave height and wave period, finding that neither had any significant effect. It was suggested instead that the extra surf zone volume necessary to dissipate greater incident wave energy was achieved by a lengthening of the surf zone, rather than a change in the beach profile. As the incident wave energy increased, the position of the bar trough moved farther offshore and into deeper water. The curve $y = Ax^{2/3}$ can be extended seawards, therefore, to intersect the bar trough, without changing the value of the coefficient A. The increased energy is then dissipated within the increased surf zone volume.

Vellinga (1984) carried out studies on the scale factors affecting the laboratory modelling of sand dune erosion, under storm surges. An empirical scale factor was derived, by the curve-fitting of dune erosion profiles and volumes:

$$\frac{y_p}{y_m} = \frac{x_p^{0.78}}{x_m} \qquad [2.8]$$

where the subscripts p and m refer to prototype and model, respectively.

Assuming that beach profiles can be described by a power curve of the form:

$y = Ax^n$, then substitution of equation [2.8] into this form give

$$y = Ax^{0.78} \qquad [2.9]$$

For sandy beaches with a $D_{50} = 0.225mm$ and $H_o / L_o = 0.034$, equation [2.9] can be given by

$$y = 0.08x^{0.78} \qquad [2.10]$$

The curve described by this equation is very similar to that derived by Bruun (1954). Comparison with Hughes and Chius formula (1978) (equation [2.7]) does not show however, such good agreement; their profiles are much more gentle than those described by Vellinga (1984) and Bruun (*op. cit.*). It is suggested that this discrepancy is due to the differences in the wave climates between the two study areas and that, on this basis, there appears to be an effect of wave steepness.

Vellinga (1984) attempted to establish the form of this steepness effect by assuming that it was described solely by the coefficient, not by the exponent. From a rather limited set of model test results, run at a constant wave steepness of 0.034, the following equations were derived;

$$y = A_1(H_o / L_o)^{0.17} x^{0.78} \qquad [2.11]$$

or

$$A = A_1 (H_o / L_o)^{0.17} \qquad [2.12]$$

The same model studies were used to incorporate the influence of sediment size into the coefficient A. An erosion profile was derived of the form:

$$y = 0.7 (H_o / L_o)^{0.17} V_s^{0.44} x^{0.78} \qquad [2.13]$$

while V_s is the fall velocity of a sediment particle of size D_{50}

When compared with full-scale field measurements, equation [2.13] gives reasonable results for the ranges:

$$0.025 < H_o / L_o < 0.04$$

and

$$0.16mm < D_{50} < 0.4mm$$

Comparison of these equations with the results of profiles measured by Powell (1990) for shingle beaches is poor, however, and equation [2.13] gives much shallower beach profiles than those measured on shingle beaches.

All of the equations discussed previously are only valid below the static water level. Similarly, they have all been derived and validated against sandy beach profiles, formed by waves with relatively low steepnesses of the order of (0.034).

Similar techniques have been applied also to the analysis of shingle beach profiles. Van Hijum and Pilarczyk (1982) and Powell (1986) carried out physical model studies, designed to develop profile descriptors for shingle beaches. A similar approach to the profile description was adopted in both sets of investigations. Profiles were schematised as two hyperbolic curves: one from the beach crest to the step; the other from the step to the lower profile limit. Empirical equations relating these curves to the wave and sediment characteristics were determined. Whilst both of these studies provided a useful first attempt at describing the beach

profiles, most of the tests were carried out using monochromatic waves: they do not provide, consequently, a good representation of natural conditions.
Van der Meer (1988) extended his earlier work on the dynamic stability of rock slopes to natural gravel beaches. Beach profiles were schematised by sub-division into three separate curves: from crest to static water level (SWL); from SWL to transition; and from transition to the lower profile limit. An extensive series of random wave tests provided relationships between the profile parameters and either of two dimensionless terms:

(i) Wave Steepness, H_s / L_m

and

(ii) Combined Wave Height and Wave Period $\frac{H_s T_m g^{1/2}}{\Delta D_{50}^{3/2}}$

where d is relative (mass) density $\frac{(\rho_s - \rho_r)}{\rho_r}$

ρ_s is the density of sediment

and ρ_r is the density of fluid

Length parameters were best described by the combined wave height and wave period function, with the elevation parameters by the wave steepness parameter. Correction factors for shallow foreshores and oblique wave attack were also derived. An important omission from these studies was allowance for the scale effects, when working with sediments of shingle size (typically with grain size, D_{50} > 5mm). Failure to compensate for the effects of reduced permeability in the model, when compared with full-scale shingle beaches, has resulted in incorrect reproduction of the profile response of the model. Since the materials in van der Meer's tests were scaled on the basis of simple geometric scaling, the effective permeability in the model was reduced, relative to full-scale. Consequently, the beach slopes produced in the model tests will respond in a different manner and will tend to be flatter than would be expected.

Powell (1990) has provided the most recent and most relevant series of formulae to describe the shape of a shingle beach; these relate to an extensive series of random wave tests, undertaken in a 2-dimensional random wave flume. Material used to represent the shingle beaches was a graded anthracite, scaled to reproduce both the correct beach permeability and the threshold and direction of sediment motion. The tests examined a wide range of conditions, including beaches with depth-limited foreshores, and those overlying impermeable sloping seawalls. The majority of tests were carried out with deep water at the toe of the beach - a condition which does not represent most shingle beaches.

In a similar manner to van der Meer (1988), Powell (*op. cit.*) has described the beach profile by three hyperbolic curves: from beach crest to the static water level and shoreline intersection; static water level to the top edge of the step; and the top edge of the step to the lower limit of profile deformation. Figure 2.8 illustrates the schematisation of the beach profile and defines the co-ordinate descriptors for the three curves. These parameters have formed the basis of the profile analysis used in the present study (Chapters 6 and 7). The resulting schematisation is characterised by the following parameters relative to the still water and shoreline axes:

	p_r	-	the position of the maximum run-up	(-ve);
	h_c	-	the elevation of the beach crest	(+ve);
	p_c	-	the position of the beach crest	(-ve);
	h_t	-	the position of the beach step	(+ve);
	p_t	-	the elevation of the beach step	(-ve);
	h_b	-	the elevation of the wave base	(-ve);
and	p_b	-	the position of the wave base	(+ve)

Powell (1990) derived a series of functional relationships for the profile descriptors and, on the basis of dimensional analysis, produced three dimensionless parameter groupings:

a) H_s / D_{50}, the ratio of wave height to sediment size

b) H_s / L_m, wave steepness

and c) $H_s T_m g^{1/2} / D_{50}^{3/2}$, the ratio of wave power to sediment size (equivalent also to van der Meers dimensionless parameter, H_o / T_o)

A suite of empirical equations were derived, allowing wave run-up distribution, wave reflection coefficients and the beach profile response to be described. Development of a parametric profile model allows the quantification of shingle beach profile changes, due to onshore/offshore sediment transport. Profile equations have been derived by regression analysis of the model data and are summarised in Table 2.2.

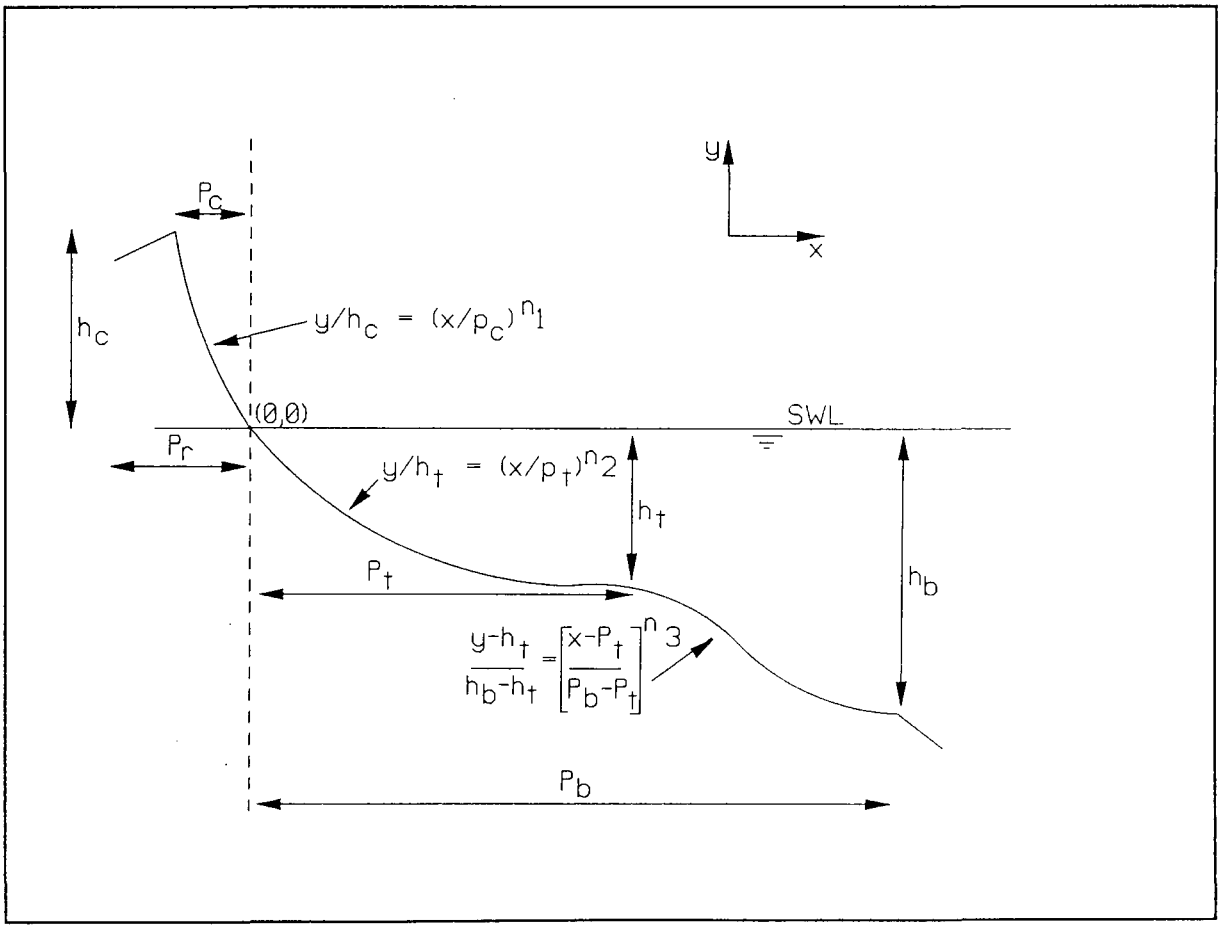

Figure 2.8 Schematised beach profile

Functional Relationship	*Limit of Applicability*
$p_r/H_s = 6.38 + 3.25\ln(H_s/L_m)$	$0.01 < H_s/L_m < 0.06$
$p_c D_{50}/H_s L_m = -0.23\left(H_s T_m g^{1/2} / D_{50}^{3/2}\right)^{-0.588}$	$0.01 < H_s/L_m < 0.06$
$h_c/H_s = 2.86 - 62.69(H_s/L_m) + 443.29(H_s/L_m)^2$	$0.01 < H_s/L_m < 0.06$
$p_t D_{50}/H_s L_m = 1.73\left(H_s T_m g^{1/2} / D_{50}^{3/2}\right)^{-0.81}$	$0.01 < H_s/L_m < 0.03$
$p_t/D_{50} = 55.26 + 41.24\left(H_s^2/L_m D_{50}\right) + 4.90\left(H_s^2/L_m D_{50}\right)^2$	$0.03 < H_s/L_m < 0.06$
$h_t/H_s = -1.12 + 0.65\left(H_s^2/L_m D_{50}\right) - 0.11\left(H_s^2/L_m D_{50}\right)^2$	$0.01 < H_s/L_m < 0.03$
$h_t/D_{50} = -10.41 - 0.025\left(H_s^2/L_m^{1/2} D_{50}^{3/2}\right) - 7.5x10^{-5}\left(H_s^2/L_m^{1/2} D_{50}^{3/2}\right)^2$	$0.03 < H_s/L_m < 0.06$
$p_b/D_{50} = 28.77(H_s/D_{50})^{0.92}$	$0.01 < H_s/L_m < 0.06$
$h_b/L_m = -0.87(H_s/L_m)^{0.64}$	$0.01 < H_s/L_m < 0.06$

Table 2.2 Summary of functional relationships for use as beach profile descriptors (from Powell, 1990)

These equations have formed the basis of the design criteria for the present investigation; they have provided an outline framework for the design of the test programme, comparison of the results, and the development of the numeric models to include new variables. Previous studies discussed in this Chapter have identified a number of variables which may influence the development of a beach profile, including:

wave height
wave period
wave duration
beach material size
beach material grading
effective depth of beach material
foreshore level
water level
angle of wave attack
spectral shape
initial beach profile

These variables, which formed the basis of the design of the experimental work for these studies, are considered in more detail below.

Powell (1990) has demonstrated the effects of wave height and period on beach profile formation. Variations in either of these parameters have a significant effect on the shape of the beach profile. The influence of the wave height parameter is most significant on the upper beach (Figure 2.9). Width of the surf zone is increased in response to increased wave height, and the corresponding increase in wave energy. In general, Powell's (*op. cit.*) results show general agreement with the earlier theories of Hughes and Chiu (1981), who postulated that the extra surf zone volume required to dissipate increased wave energy is provided by lengthening of the surf zone (as opposed to a change in the profile).

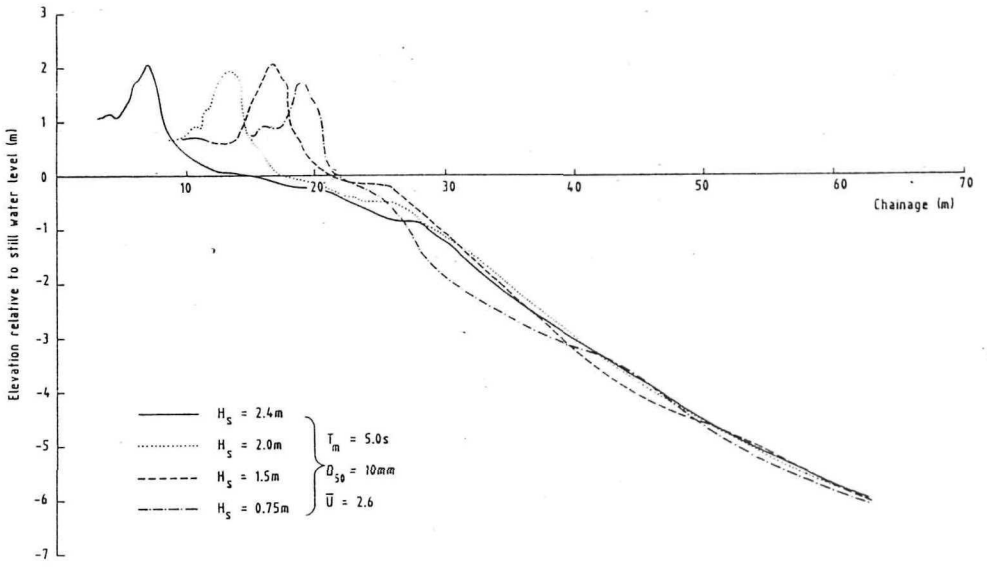

Figure 2.9 Influence of wave height on profile development (from Powell, 1990)

Wave period appears to have a greater effect upon the vertical dimensions of the profile than on the horizontal. The resultant effect of an increase in wave period appears to be increased crest level and a corresponding increase in the volume of material at the top of the beach. A corresponding seaward displacement of the lower limit of profile deformation also occurs, together with erosion of the beach below the step position (Figure 2.10).

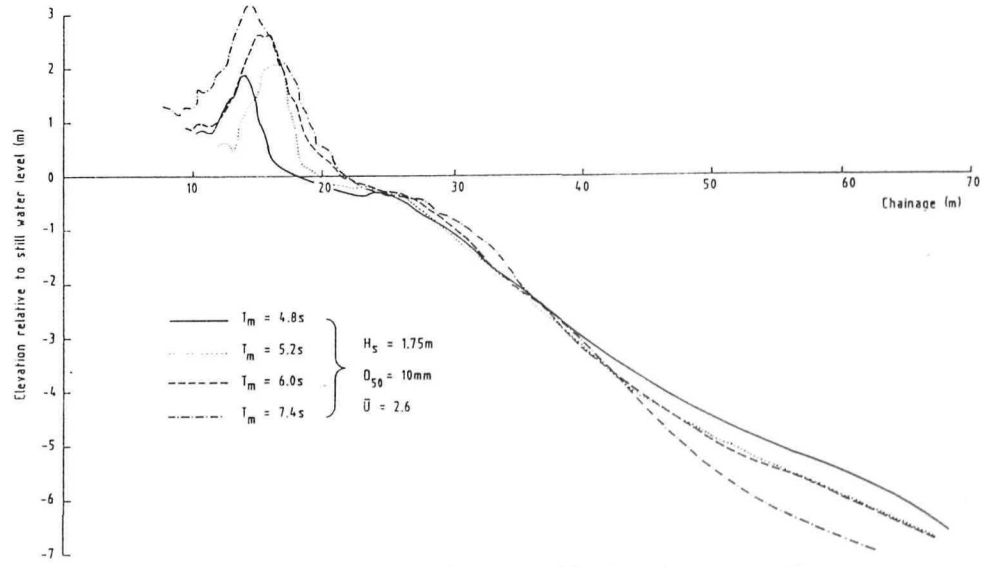

Figure 2.10 Influence of wave period on profile development (from Powell, 1990)

Powell (1990) has investigated the effects of wave duration on the beach profile development. Profile evolution is very rapid in the early stages of wave attack and an equilibrium profile was seen to develop within the first 500 waves at any given water level (Figure 2.11). Whilst the beach profile may be modified by subsequent wave action, the primary features of the profile have evolved by this time. Consequently, minor modifications due to grouping of waves occurs after this time; this has the most significant effect at the step of the beach profile. By contrast van der Meer (1988) suggests that duration is a significant variable, with changes to the profile still occurring after several thousand waves.

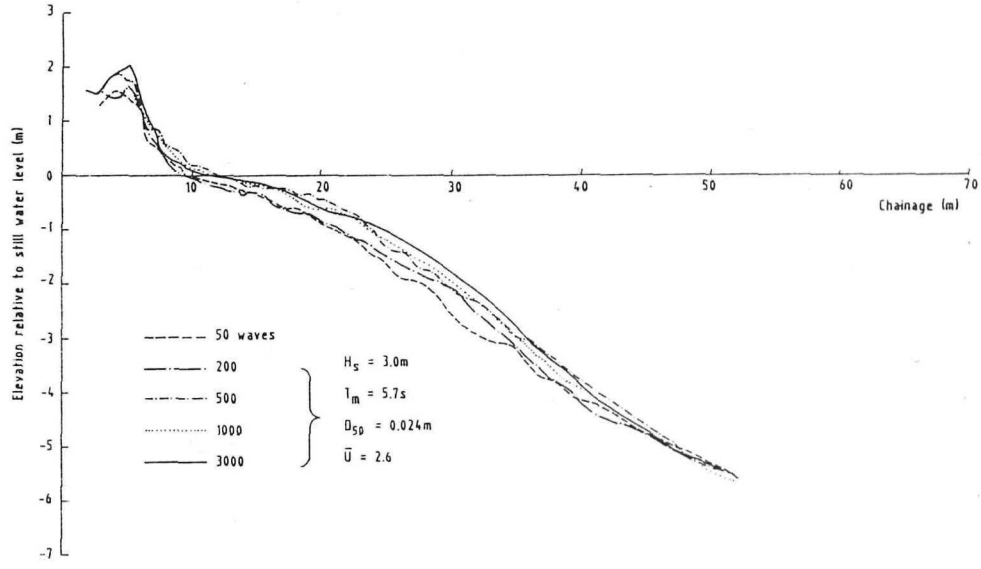

Figure 2.11 Influence of wave duration on profile development (from Powell, 1990)

All of the investigations discussed above have been developed on simple constrained beaches, which have been unable to overtop under the test conditions. There are no documented studies of the profile response of shingle barriers, (to the writers knowledge).

The influence of the depth of impermeable membranes, which affect the flow fields within the beach structure have also been investigated (Powell, *op. cit*). The

significance of the impermeable membrane has not been quantified in detail. Nevertheless, the results of the model tests indicated clearly that the depth of the impermeable membrane, beneath the beach surface, affects the horizontal beach profile displacements. This observation confirms the results of field-work reported by Longuet-Higgins and Parkin (1962), who found that an impermeable layer buried within the beach encouraged erosion of the overlying beach.

The importance of sediment characteristics such as grain size and grading has been examined in earlier studies, (Powell, (1990); van der Meer, (1988)). Sediment grain size appears to have more effect than does grading. It is suggested, however, that there is a strong correlation between the characteristic wave steepness and the mean grain size, when analysing the profile response.

Both of the above studies have indicated that there is little variation in the beach profile response, due to sediment grading. This effect appears to be consistent throughout the results. Since only two grades of material were tested, however, this area of understanding needs further research before wide-ranging conclusions can be drawn. Subsequent research (Powell, 1993) has examined the effects of a wider range of sediment sizes and gradings. Regrettably, the results cannot be related back to the original profile prediction methods, as a much simpler form of analysis, (based upon the mean beach slope) was adopted.

The influence of the foreshore level, relative to the toe of the beach, is significant in influencing the development and change in beach profiles - particularly below static water level. The water depth at the toe of most beaches is shallow, in contrast to the deep water at the toe of the beaches modelled by Powell (1990). There are a few exceptions, notably Chesil Beach and Dungeness; these have relatively deep water at the toe of the beach, under certain tidal conditions. However, the studies undertaken focus largely upon deep water conditions. Consequently, there is considerable scope for an improvement of the profile prediction methods for shallow water conditions; these are much more typical of beaches around the UK. Wave breaking in shallow water complicates the evolutionary processes, but little work has been carried out into such conditions, particularly under random waves. The location of wave breaking clearly has a significant impact on the distribution of energy dissipation and the consequent profile response. As the water becomes shallower,

the waves break farther offshore; consequently, they have a smaller impact on the upper beach profile. Assuming that the waves offshore follow a Raleigh distribution, then depth-limiting is assumed to occur when $H_s/D_w > 0.55$. Van der Meer (1988) suggests that the effect of a reduction in the foreshore depth resulted in a shortening of the beach profile below still water level, over the range $0.56 < H_s / D_w < 0.74$. Similarly, the results of a series of random wave flume studies undertaken at HR, Wallingford (unpublished), on beaches with a shallow foreshore, have indicated that the profiles formed above the depth-limited foreshore do not show the distinctive step feature below the still water line. This observation is perhaps not surprising, in view of the fact that the step part of the profile normally forms directly beneath the breaker point.

Powell's (1990) and van der Meer's (1988) results contradict each other when comparing the profile response above water level, in shallow water conditions. The former results, which suggest a reduction in the profile dimensions at the shoreline in shallow water, seem more credible than those of the latter, who postulates that there is no significant change above static water level. Since the crest dimensions are governed largely by wave run-up, which itself is a function of energy, it seems more likely that the increased energy loss due to wave breaking in shallow water will result in reduced profile dimensions. In view of the very limited amount of previous work on the profile response of shingle beaches with a depth-limited foreshore combined with the fact that beaches occur most commonly under these conditions, this area of research has formed a major focus for the present investigation.

The dependence of the profile development on the initial slope profile, prior to wave action, has been discussed widely. Dalyrmple and Thompson (1976) investigated the profile response of sandy beaches (0.4mm) and found that initial slopes within the range 1:5 to 1:10 had no effect on the development of the beach profile. Nichollson (1968) also examined similar sandy beaches, with slopes of 1:5 to 1:20 and a mean sand size of 2mm. Van Hijum (1974) studied a range of material of sizes up to 16.5mm and at slope angles of 1:5 and 1:10. Both authors established similar results, suggesting that the initial gradient did not have a significant effect on the final profile. Similarly the results of studies undertaken by Rector (1954) have suggested that the initial profile of sandy beaches, in the size range 0.21mm - 3.44mm, had no effect on the post-storm profile, other than to determine whether the upper

beach was formed by erosion or accretion. These tests were carried out across a range of initial slope angles ranging from 1:15 to 1:30. Van der Meer's (1988) investigations on coarse-grained sediments, with random waves, have suggested that most of the slope profile was unaffected by the initial slope; however, that the mode of profile formation was affected by the direction of the material transport.

In contrast to the observations discussed above, several researchers have suggested that profile response is affected by the initial profile slope. Chesnutt (1975) found that profiles formed in 0.2mm sand were affected by the initial slope angle, by examination of slopes of 1:10 and 1:20. Elsewhere, Sunumara and Horikawa (1974) observed that initial slopes of 1:10, 1:20 and 1:30 influenced the final profile formed in 0.2mm and 0.7mm sands. Subsequent work undertaken by Gourlay (1980) has suggested that the initial profile of the slope was only a significant control if the initial beach profile was steep.

The early studies (Powell, 1990) have highlighted a number of shortcomings in the research undertaken to date. In particular, the study of the effects of oblique wave attack and the influence of longshore sediment transport on the profile response of a beach has been recommended. Subsequently, a limited experimental programme was carried out to examine the effects of oblique wave attack on profile response (Coates and Lowe, 1993); on the basis of this modifications to the original predictive formulae were suggested. The influence of beach grading and a depth-limiting foreshore on profile modification has not been addressed fully. High quality field data is needed to validate the results of laboratory studies, in order that numerical models may be of direct use in beach design and management. Limited field investigations have been carried out to test the validity of the numerical methods (Coates and Bona, 1997), but further validation is still required. Likewise, the profile development and characteristics of an overtopping barrier beach, or spit, have not been previously studied. In particular the need for a detailed physical model study to examine, in detail, the hydraulic response of a shingle barrier beach to wave attack has been identified (Nicholls, 1985).

CHAPTER 3: THE STUDY AREA

3.1 GEOMORPHOLOGICAL SETTING

Christchurch Bay is a shallow coastal embayment bounded by Hengistbury Head to the west and by the Needles promontory to the east. The bathymetry of the embayment is dominated by the bedrock outcrop of the Christchurch ledge to the west and the offshore sand and shingle banks system, which extends across the whole of the embayment (Figure 3.1).

Both transgressional and regressional beaches occur within the embayment, which can be divided into a number of distinct geomorphological units. The northern coastline of Christchurch Bay is characterised by rapidly eroding cliffs (Lacey, 1985; Bray *et al* 1991). The coast around the tidal inlets of Christchurch Harbour and the Western Solent are characterised by sand and shingle barrier beaches. Belknap and Kraft (1985) suggest that the antecedent topography of the embayment has probably controlled the differentiation of the embayment into these geomorphological units. Submergence of the area since the last glaciation has provided a supply of sediment from erosion of the cliffs and older coastal lithosomes, to produce a series of beaches. Sediments are generally coarse grained, comprising sand and gravel. Christchurch Bay exhibits a log-spiral curve plan form; as such it has been suggested that the bay has not yet achieved an equilibrium plan shape (Wright, 1982), on the basis of an extended analysis of studies by Silvester (1970). Such analyses were based upon the relationship of the plan shape of the Bay and the prevailing wave direction.

Hurst Spit has evolved as a barrier spit at the entrance to the Western Solent (Figure 3.2); it is composed largely of shingle and is approximately 3.5km long. Shingle recurves at the distal end of the spit confirm, its presence over the past (at least) 500 years. Contemporary beach processes have dominated the structure of Hurst Beach over the study period; this is demonstrated by cartographic evidence which indicates the change in plan position of the beach in response to storm-induced processes (Nicholls, 1985). These observations suggest five main depositional processes on the backshore.

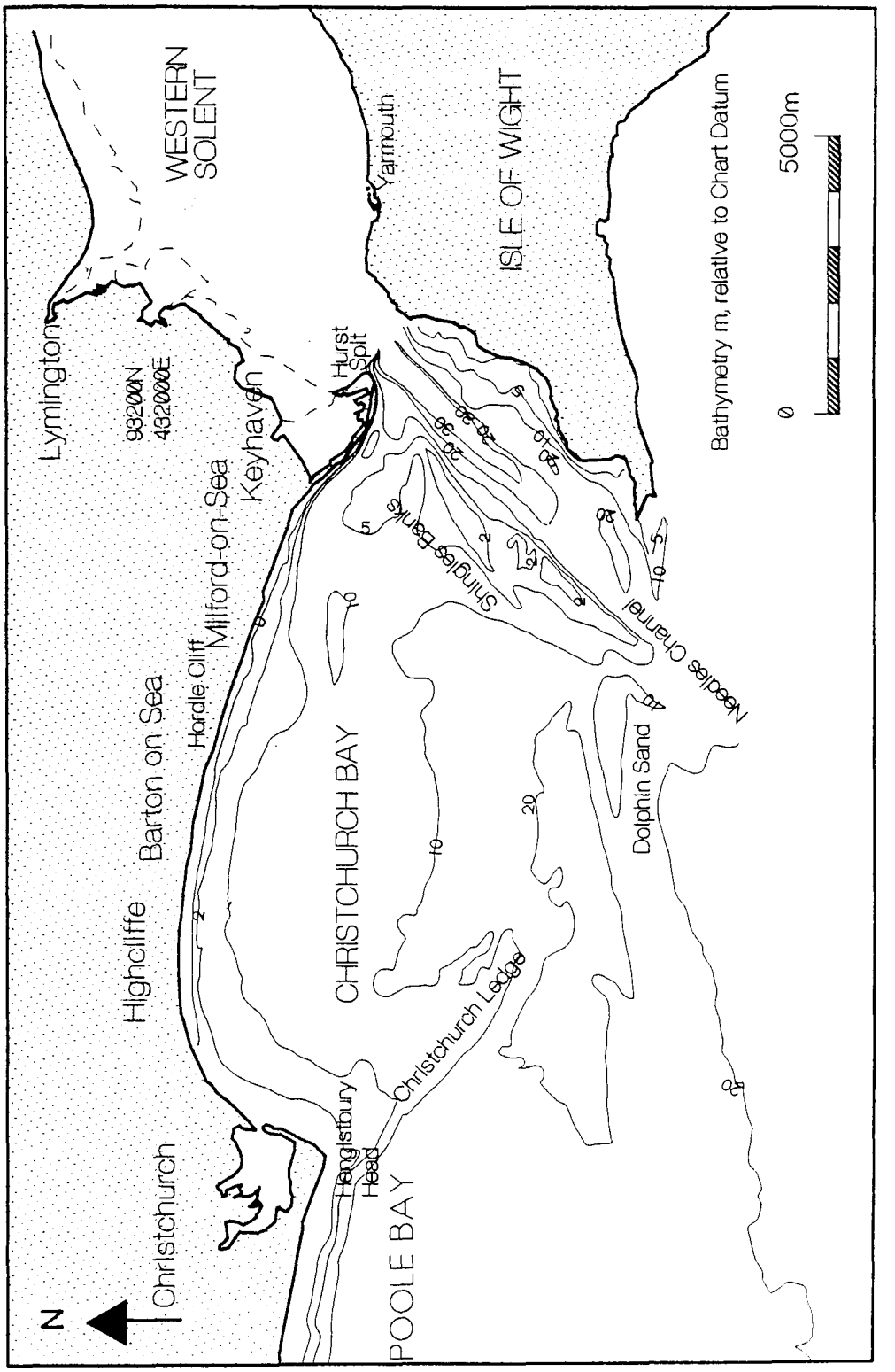

Figure 3.1 Christchurch Bay, showing location and bathymetry of study area.

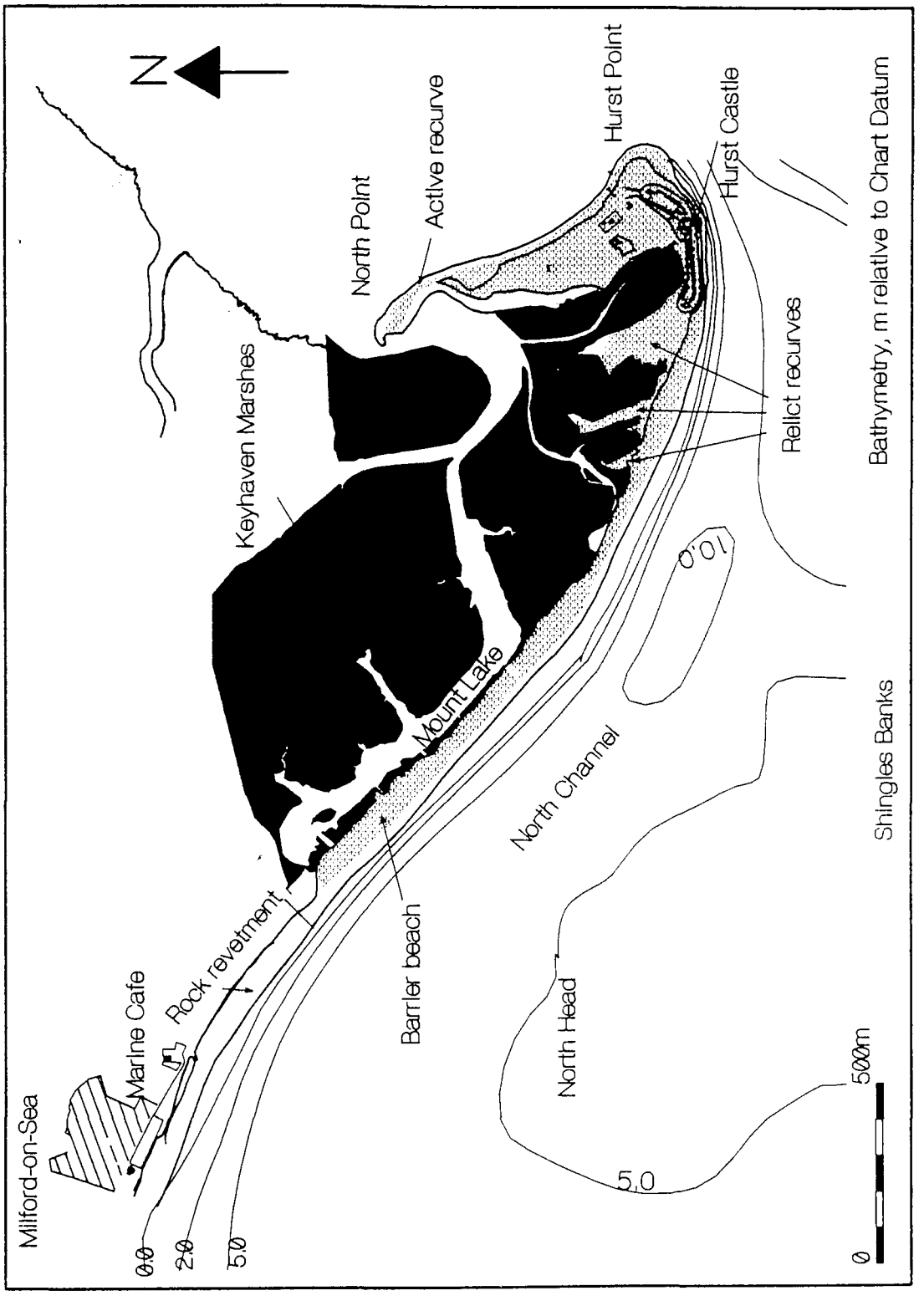

Figure 3.2 Hurst Spit, showing nearshore bathymetry and topographic features

(a) berm formation;

(b) overtopping;

(c) overwashing without reduction of the crest height;

(d) overwashing with reduction of the crest height; and

(e) seepage

The first four of the above processes are dominated by the combination of vertical swash run-up, water level and crest height. Berm formation occurs when the swash is limited to the seaward side of the crest. The distinction between the types of overwashing is dependant upon (a) the volume of swash reaching the crest of the beach; and (b) the geometry of the beach crest.

Hurst Spit has been the subject of a number of investigations (Nicholls, 1985; 1990, and Nicholls and Webber, 1987a,b); its structure is complicated by the varied sorting of the beach sediments which can range from open-work shingle with no sand; through sandy open-work shingle with up to 20% sand; to sandy shingle which leaves only pore spaces within the sand component. The nature of the overwash deposits results often in the deposition of a mixture of the finer- and coarser-grained sediments; consequently, the permeability of the beach is reduced due to this layering effect.

3.2 HYDRODYNAMICAL SETTING

3.2.1 Tides and surges

The tidal regime of the English Channel is characterised by semi-diurnal tides. The study area lies close to the amphidromic point; consequently it is characterised by a relatively low tidal range (2.2m on mean spring tides) and relatively low tidal currents. A double high water occurs, due to the relatively weak local amplitude of the M_2 constituent in combination with a strong shallow water constituent (Tyehurst, 1978). Hence, the tidal characteristics of the area are very complex. The shallow topography

and proliferation of offshore banks and tidal inlets complicates the tidally induced flow (Velegrakis, 1994).

Crestal changes to Hurst Spit occur usually only over high water spring tides, in combination with storm surges (Nicholls, 1985). Surges greater than 1m can occur in Christchurch Bay; these can have a profound effect on the beach response, extending the tidal range by more than 50%. Storm surges are frequently associated with low pressure systems and severe wave activity (Henderson and Webber, 1977, 1979). Large storm surges in 1981 and 1983 resulted in peak water levels of 1.52mODN and 1.65mODN respectively (Nicholls, 1985). The significance of the surge component is twofold. Firstly, the point of attack on the barrier is moved to landwards by the ratio of beach slope to surge: a 1m surge on a beach with a mean slope of 1:7 will move the point of attack landwards by 7m; this is highly significant on a barrier which is only 30m wide at MHW. Secondly, the increased water depth at the beach toe allows higher and longer period waves to attack the beach, prior to breaking.

3.2.2 Wave climate

Wave activity is a major factor controlling the geomorphology and distribution of sediments within the study area. The wave climate of the area has been addressed previously in a number of earlier studies (see below). Whilst the most reliable studies of wave climate can be made by extensive periods of direct measurement of wave conditions, regional wave climates can be derived reasonably reliably from long time-series of appropriately-located wind recording. Synthetic wave climates have been derived successfully at many sites elsewhere, by establishing an empirical relationship between wind stress and waves. Calibration of such hindcasting methods has been carried out with some degree of success against measured wave data at a number of sites (Hydraulics Research, 1989d).

Earlier studies have derived regional wave climates at a number of locations within Christchurch Bay, using wind data from meteorological stations at Portland and Calshot. Despite its distance from the Hurst Spit, Henderson (1979) has suggested that Portland provides the most appropriate site for wind-wave studies within the study area; this has been confirmed by studies undertaken by HR Wallingford (1989b). An

offshore wave climate has been compiled for Christchurch Bay using hindcasting techniques, based upon a series of 15 years of wind data. (Hydraulics Research 1989a, 1989b). A prevailing WSW wind direction was identified within this study (Figure 3.3): waves with a significant wave height >1m were predicted for 31% of the time whilst significant wave heights >3m occur for 2.6% of the time. Extreme values, forecast from the data-set suggest an offshore significant wave height with a 1:1 year return period of 5.8m and 7.9m for a 1:100 year return period.

Whilst the prediction of a spectral wave climate at an offshore location is a reasonably straightforward and reliable process, empirical hindcasting methods are confined to deep water locations: this is when the wave length to water depth relationship is such that the waves are unaffected by the sea bed. Derivation of a nearshore wave climate is a significantly more complex process, as variables such as refraction, diffraction, shoaling and bed friction become important. Further transformation of the data is required to provide a nearshore wave climate, if the data are to be of use for the analysis of wave-forces at the shoreline.

The influence of some of the above variables has been addressed in earlier regional studies, with varying degrees of success. For example, Henderson and Webber (1979) carried out a series of calibrations of a predicted wave regime, on the basis of measurements made from a four year deployment of a waverider buoy, to the east of Boscombe. Focusing of wave energy was observed in the area of Hengistbury head and in central Christchurch Bay. Refraction studies using a monochromatic forward-tracking ray model based on a coarse grid resolution, were used also to examine wave transformations at the eastern end of Christchurch Bay (Henderson, 1979). These studies demonstrated the difficulties in the mathematical modelling of wave processes over a complex sea bed area; their apparent lack of success may be attributed to the coarse resolution of the model grid, which was unable to represent fully the complexity of the nearshore bathymetry. The results of these studies provide useful background information, but the wave refraction modelling results need to be viewed with extreme caution: indeed, they have not been deemed to be suitably robust for input into the present investigation.

Similar problems have arisen with the wave analysis carried out elsewhere (Halcrow, 1982). Wave hindcasting techniques and refraction studies were used to derive a local wave climate for Hurst Castle. A 1:1 year significant wave height of 3 m was suggested, rising to 3.4 m for a 1:20 year period. As outlined previously, this latter study was limited also by the complexity of the nearshore bathymetry. The large differences between extremes wave conditions at the offshore boundary compared with the inshore prediction points demonstrates the dramatic impact of the offshore Shingles Banks as a mechanism for energy dissipation. Nicholls, (1985) and Bray *et al* (1991) suggest, with reason, that the local wave climate at Hurst Castle is affected by the long-term evolution of the Shingles Banks. This evolutionary process is discussed and developed by Velegrakis (1994) which confirms the views of Nicholls and Bray (*op. cit*).

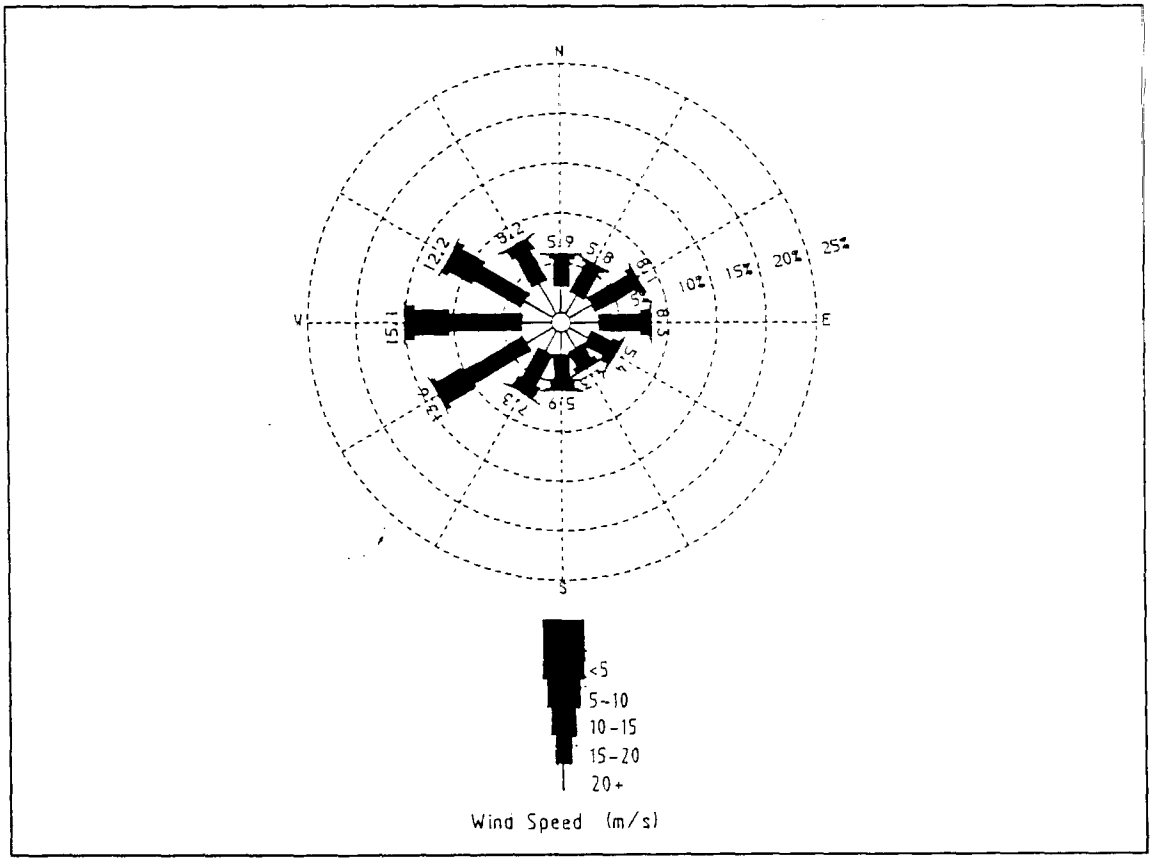

Figure 3.3 Wind direction rose diagram, for Portland (1974-1989) - used for hindcasting waves within the offshore area of Christchurch Bay. (from Hydraulics Research, 1989a)

3.3 COASTAL PROTECTION WORKS

The predominantly easterly littoral drift in Christchurch Bay and the complex pattern of offshore banks and ridges (Figure 3.1) has influenced the alignment and the form of Hurst Spit. The development of Christchurch Bay has also played a significant role in the evolution of Hurst Spit. Activities at the western end of Christchurch Bay, such as dredging of ironstone off the Christchurch Ledge, have resulted in localised increased deepening and wave energy close to the shoreline and, as a consequence, extensive areas of coastal protection have been required at Highcliffe and Barton. Construction of these defences, since the middle of the 19th century, has resulted in a reduced supply of sediment from the west.

The primary supply of shingle to Hurst Spit was derived largely, however, from the Pleistocene gravel terraces in the cliffs at Milford-on-Sea; these dip below the surface at Hurst Spit. Until construction of the defences at Milford-on-Sea, the system remained in balance, with demands for sediment supply being met by erosion of the gravel terraces. Following construction of the concrete sea defences and groyne systems in the 1960s, erosion of the cliffs was halted and the supply of shingle was reduced greatly. Consequently the sediment transport system became unbalanced and the rate of erosion at Hurst Spit has increased. It is estimated that the main body of Hurst Spit is declining in volume, by approximately 7000-8000 m^3 per year (Nicholls, 1985). In comparison, the littoral transport rate has been estimated at 15000m^3 per year. Much of the material is lost from the system at Hurst Point and is removed offshore in the ebb currents; it is recycled onto the Shingles Banks, which are accreting (Velegrakis, 1991). The material remaining in the shoreline system is transported around Hurst Castle and is deposited on the active shingle recurve, known as North Point.

The Spit is a transgressive feature and is moving landwards, due to the processes of overtopping and overwashing. The rate of transgression has increased from approximately 1.5m per year (1867-1968), to 3.5m per year (1968-1982) (Nicholls and Webber, 1987b). Since 1982, the Spit has been subject to more frequent overwashing and crest lowering during storm action, as a consequence of the declining volume of shingle. Extensive throat and overwash fan systems have formed. Similarly, the volume of the barrier above low water has declined further due to displacement

of the shingle into Mount Lake, (in the lee of the spit). (Figure 3.2). The overwash events, which were once sufficiently small to permit the crest to reform have grown in frequency and size to such an extent that the shingle barrier could only recover naturally after very long periods of calm weather, by 1989.

Several extreme storm events have resulted in extensive damage to Hurst Spit, following storm action. In particular, the storms of October and December 1989 have caused dramatic lowering of the crest and roll-back of the spit, across the salt marshes (Figure 3.4); these outflanked the rock armouring at the western end of the spit. Crest lowering (by in excess of 2.5m), roll-back of the seaward toe (of up to 60m) and roll-back of the lee toe (by up to 80m) resulted in displacement of more than 100,000 m^3 shingle overnight. The performance of Hurst Spit during recent winters and the concerns of New Forest District Council, the local Coast Protection Authority, has led to the establishment of a research and monitoring programme: this has formed the nucleus of these studies, described in the subsequent text.

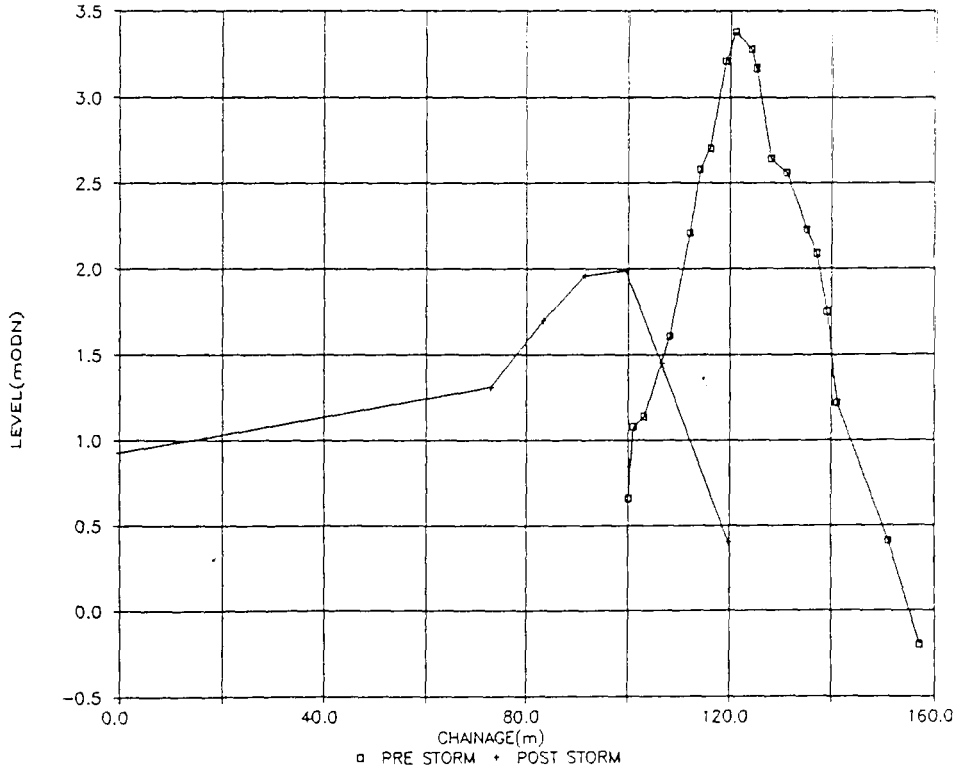

Figure 3.4 Typical cross section response of Hurst Spit (after Bradbury and Powell, 1992)

CHAPTER 4: STUDY METHODOLOGY

4.1 INTRODUCTION

The study objectives (Section 1.2) provide a range of problems for consideration prior to designing the study programme. Suitably instrumented field studies and an extensive fieldwork programme, with a duration of many years would provide the most realistic method of developing a prediction model for the profile performance of a shingle barrier beach. However, this method of study is fraught with practical disadvantages and limitations.

The main difficulty of a field-based investigation is that of control of a complex interacting system which comprises many variables. An understanding of the influence of storms, of varying intensity and at different extreme water levels, is needed to develop a predictive model of the profile performance of barrier beaches. Although such storm conditions might reasonably be expected to occur during a study period of 3-4 years, there could be no guarantee that conditions would be sufficiently severe to cause the destructive overtopping events; these result in either crestal deposition or crest lowering on a barrier beach. For example, the probability of exceedence of a storm event with a joint probability extreme return period of wave and water level of 1:100 years, within a study period of 4 years, is only 0.04 (CIRIA, 1996). The problem is compounded by the need to examine the sensitivity of events which have a similar joint probability of occurrence, but with varying combinations of wave and water level conditions.

Whilst an experimental programme, based solely upon field measurements, provides the most realistic method of examining beach profile response, the lack of control of hydrodynamic variables presents significant limitations. In particular, it is not possible to isolate and investigate the relative influence of certain variables in a controlled manner, i.e. longshore currents or tides.

Development of a generalised predictive model for barrier beaches could also be a problem, if the analytical framework were based solely on the geometric and hydrodynamic conditions at a single site, this may not be generally representative of similar features at other locations. The effects of near-shore bathymetry, local tidal currents and sediment grading could all limit the applicability of field studies at a single site, to a wider framework. Whilst there are obvious advantages to be gained by investigation of a number of field sites with differing characteristics, the majority of the fieldwork was carried out on the shingle beaches of Christchurch Bay in order to optimise resources. Hurst Spit has provided a suitable study area for a detailed evaluation of the response of shingle barrier beaches to storm wave attack: likewise, the beaches at Hordle Cliff (Figure 4.1) have provided a comparison with restrained shingle beaches, subject to similar wave climate. A series of long-term field measurements were planned, to examine hydrodynamic forces and responses of the beach; these included wave conditions, water levels, beach profiles and sediment size. Additional, but somewhat limited, supporting field data has been provided from studies at other sites elsewhere by other researchers.

Simultaneous measurement of all of the key forces and responses is extremely difficult in the field. The nature of conditions immediately following significant storm events presents a series of practical measurement problems: the period immediately following a severe storm is often too rough to allow safe measurement of the beach profile by land survey; or accurate measurement of the lower part of the profile by hydrographic survey. Likewise, further practical limitations may arise due to the tidal conditions in combination with daylight: these may limit access to the beach at suitable times for surveying. In summary, the field measurements cannot be controlled either in terms of intensity or frequency of storms, or in terms of provision of suitable post-storm measurement conditions.

An appropriate programme of laboratory studies could provide the controlled conditions necessary to evaluate the effects of a suitably wide range of hydrodynamic and geometric variables. The ability to control conditions in the laboratory is countered by the difficulties in reproducing sufficient variables, which have the correct relationship with each other at a smaller scale. Thus, laboratory studies are limited by scale effects and the possibility of an oversimplified reproduction of conditions.

Developments in the reliability of mobile bed physical modelling techniques for shingle beaches and calibration of these methods against full-scale measurements (Powell, 1990) have suggested the appropriateness of this method of study. Such an approach would allow reproduction of various combinations of waves and water levels, together with the wide range of beach geometries: such data would permit an extensive empirical framework of barrier beach response to be developed. However, such a programme requires extensive calibration and validation.

The preliminary field-data provided the basis of the design of the laboratory test validation programme; these related to typical beach geometry and the response of shingle beaches to storm waves (and less severe conditions).

A regional wave climate study, based upon a series of mathematical modelling techniques, formed part of the investigation; this simulated a range of extreme conditions, providing a probabilistic framework of incidence and frequency of wave conditions at Hurst Spit. The physical model studies provided an opportunity to reproduce conditions measured in the field and, as such, appropriate validation of the modelling methodology: it also allowed a considerably wider range of conditions, including extreme events, to be tested than could be measured in-situ.

Much of the site-specific data and the results of laboratory physical model studies of Hurst Spit were used also in the design of a major shingle beach renourishment scheme. The beach renourishment scheme provided a practical application of the empirical methods derived from the study, together with an opportunity to validate the laboratory-derived methods, in the field.

The main phases of the investigation are outlined below.

(a) Field studies of the response of shingle beaches to wave attack, within Christchurch Bay.

(b) Wave climate studies to investigate the regional conditions within Christchurch Bay.

(c) Laboratory studies of shingle beach response, to storm waves.

Further fieldwork, following the completion of the laboratory studies provided additional support for the investigation methodology. Every opportunity to monitor the field response of extreme events was taken, to increase the validity of the (limited) fieldwork programme. Further, it should be noted that an integrated approach was adopted throughout the study.

4.2 FIELD STUDIES

The fieldwork programme included measurement of both forcing and response variables. For comparison, earlier studies (Nicholls, 1983b, 1983c,1985) at Hurst Spit focused on the measurement of geomorphological and geological variables. The present investigation has drawn upon these experiences together with the background data framework developed by the NFDC Coastal Monitoring Programme, but has focused upon the response of the beach to storm events.

4.2.1 Topographic surveys

The shoreline response to wave and tidal action was recorded throughout the study period. Several complementary land surveying techniques were used, to record beach profiles and the plan shape of the study area. Most beach profiles were surveyed by levelling, from co-ordinated stations. Profiles were measured also with a total station theodolite and with kinematic differential GPS. Much data was collected as part of the NFDC Coastal Monitoring Programme. Fifty-two survey control stations were established along the coastline of Christchurch Bay (Figure 4.1): profiles were surveyed at each of these. The survey methods are discussed in Appendix 1.

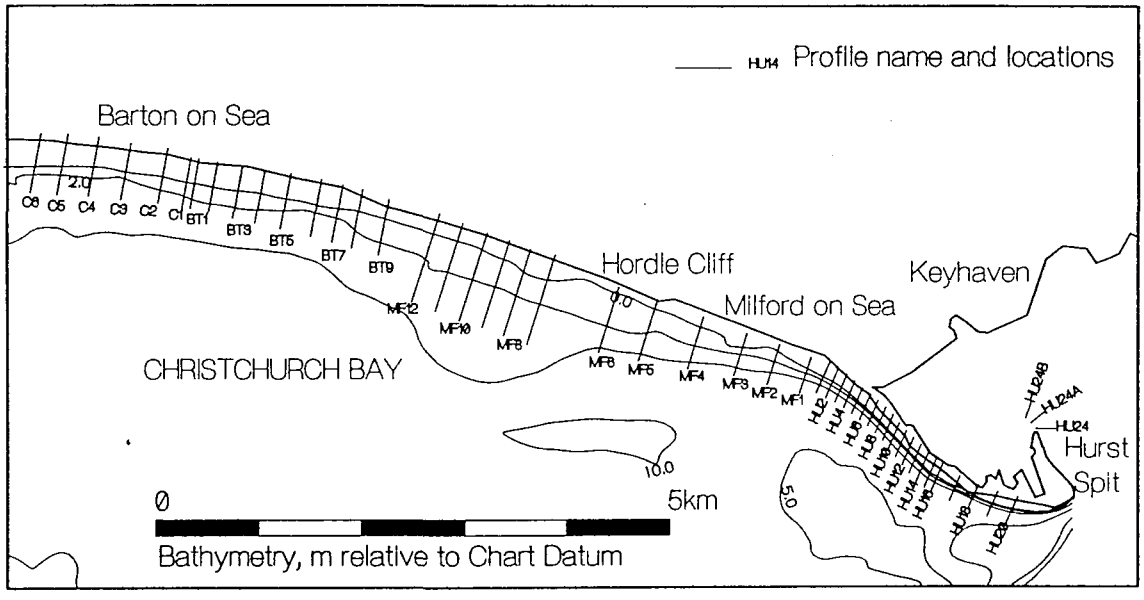

Figure 4.1 Location of topographic and hydrographic survey profiles in Christchurch Bay. (bathymetry in mCD)

(a) Beach profile surveys

The survey profiles extended from co-ordinated control positions as far seawards as a chainman in a dry suit could reach safely. Many of the profiles were measured using standard levelling techniques, surveyed with an automatic level. Chainages were recorded by laying an incremented survey rope across the beach profile. Where possible, the surveys were carried out over low water spring tidal conditions. The survey method contains an inherent error, because the measured chainages are slope chainages i.e. not true horizontal chainages. However, the errors are small, typically less than 0.05m per horizontal metre, due to the generally shallow angles of the beach slope; for comparative purposes, they provide an adequate description of the profile and changes. Most of the surveys undertaken prior to 1994 were carried out using this particular method.

The survey method was updated subsequently to utilise 3-dimensional measurements, gridded to the Ordnance Survey National Grid and recorded using a kinematic differential global positioning system: this provided undistorted profiles with true chainages relative to the control point. The survey initialisation process has an inbuilt quality control system; this prevents the survey from being initiated if the baseline vector between the baseline receiver antenna and the mobile control antenna varies from a known defined baseline vector (outside of a defined range). This approach eliminates problems of station subsidence, or movement, from reducing the survey accuracy: this is significant on Hurst Spit, where the site overlies saltmarsh deposits.

Each profile line was surveyed at least four times per year, since 1989. Certain of the survey lines on Hurst Spit were also surveyed twice yearly, between 1987-1988, this was prior to the commencement of this study (Cross, *pers comm*). Wherever possible, the profile lines were established to correspond with locations of surveys used in earlier studies, thereby extending old data sets (Nicholls, 1985a and NFDC, unpublished). In many cases however, the survey data has not been continuous. New profile lines were established at appropriate locations in those areas which were not previously surveyed, - this has enabled suitable coverage of all of the beaches in eastern Christchurch Bay on :

a) historical regional changes in beach morphology;

b) profile performance of open, but restrained, beaches;

c) profile performance of a shingle barrier beach; and

d) profile performance of beaches affected by coastal protection structures.

In addition to regular monitoring surveys of the beaches, surveys were also carried out following storms. Measurements undertaken during the early stages of the study have provided design information for calibration of the physical model studies. The profiles were measured together with waves, wind and tidal characteristics (Section 4.2.4).

(b) Data quality

The survey data was gathered in a number of formats; regular checks were made on these throughout the fieldwork programme. The control data have consistently been of a high quality; this is despite the regular loss of control points through storm conditions. Simple comparison of the profiles, by overlaying, has identified spurious data points (due to errors in the reduction of the levelling surveys); similar comparisons can be made for survey accuracy by examination of the lee slope of the barrier, which is altered only following overwashing events.

4.2.2 Hydrographic surveys

The topographic surveys extend to a level of approximately -1m ODN; however, the active beach profile extends into much deeper water. Consequently, a programme of (overlapping) hydrographic surveys was carried out twice per year. Initially, the surveys were carried out along 600m extensions of the topographic survey profile lines (Figure 4.1). Subsequently, the survey programme was altered (in 1995), to provide better spatial coverage of the study area, but at a lower (annual) survey frequency. The modified survey programme provided a spatial coverage of 600 m long lines running perpendicular to the shoreline, at an interval of 30 m, and into a water depth of 10-15 m. The modified survey programme allowed volumetric changes to be determined for the North Channel area, adjacent to Hurst Spit.

The offshore surveys were carried out during the summer months, to permit accuracy to be optimised. Nonetheless, time and cost constraints limited the frequency of the hydrographic surveys and no surveys were carried out immediately after storm events (primarily due to the absence of suitable survey conditions). Consequently, the submerged post-storm beach profile has not been measured. The timing of the surveys and the interval between them was subject to variations in weather and tidal conditions. Wherever possible, hydrographic surveys overlapped the topographic surveys, being carried out over high water spring tide periods. The hydrographic and topographic raw data and processed data were archived in an extensive database (Appendix 2). It should be noted that the hydrographic surveys were carried out as part of the long-term regional beach monitoring and research programme set up by NFDC.

Surveys were carried out from a small dory (Coastal Research, SUDO). Soundings were logged from a Raytheon DE719B echosounder, via a digitiser to a portable computer (measuring depths to within +/- 0.1m). Surveys were processed to Ordnance Datum (OD), to allow the data to be merged with the topographic surveys. Tidal corrections were provided from temporary tide gauges; established as near to the survey site as possible. A permanent recording tide gauge was installed in the newly- constructed breakwater, adjacent to Hurst Spit, towards the end of the study programme (1997).

Positioning (to within +/- 5m) was carried out initially by transects fixed by a shore based EDM theodolite: this method was confined to the surveys carried out during the first phase of the fieldwork programme, when surveys were confined to the 20 profile lines along Hurst Spit. Position fixing was improved significantly for the latter stages of the study when a Trimble 4000se differential global positioning system (DGPS), with a real-time position fixing accuracy of better than + / - 2m in the horizontal plane, was used. Surveys carried out since 1994 all used this system, to pre-determined grids, using HYPACK navigation and hydrographic surveying software, to execute and post process the surveys. The results were then processed using the same ground modelling and analysis techniques as the topographic surveys.

(a) Data quality

Surveys carried out during the early stages of the programme are not particularly well controlled (see above). In fact, level positions could potentially be as far as 5 m off line. Nonetheless, comparison of surveys, by overlaying, shows a remarkable consistency in the bathymetry; this may reflect the consistency of the nearshore contours, along the length of the spit. Surveys carried out using DGPS are better controlled. The data are significantly more dense, whilst the line spacing of 30 m allows interpolation of contours with a high degree of confidence.

Further errors may have been introduced by the tidal control: this was carried out by observation at the site and using a Hydrotide (portable) recording tide gauge, during the latter part of the study (i.e. 1997 only). Comparison between shore parallel tracks

and shore normal tracks suggests that tidal control is not a significant problem, along the length of Hurst Spit.

4.2.3 Sediment sampling

Sediment grain size and distribution control the porosity and permeability of the beaches; these affect their hydrodynamic response. Powell (1990) has provided details of the relative response of two sediment gradings, suggesting a tentative relationship between sediment grading and beach profile response. These studies suggest that grading has a more significant effect on profile response than sediment grain size; this is inconsistent with the conclusions of Van der Meer (1988), however. Undistorted sediment scaling may have had adverse effects on the beach profile in these studies. Changes in sediment size and sorting also permit the interpretation of sediment sources and direction of sediment movement (Nicholls, 1985; Velegrakis, 1994). Size distributions of the beach material in the study area were determined, to provide design information for the physical model studies: they were used also as site specific variables for testing the validity of profile response hypotheses (Powell, 1990, 1993; and van der Meer, 1988).

Sediment sampling of the beach was carried out on several occasions, to examine temporal changes. Initial sampling took place in 1990 and the data generated was used to provide design information for the physical model studies. Further sampling took place during the beach recharge programme (at Hurst Spit in 1996); this provided information on the grading of beach recharge materials. The results of this part of the study have been compared with similar data gathered by Nicholls (1985), to assess medium-term temporal changes in the sediment distribution.

Samples were collected at positions adjacent to the selected beach profile survey lines; in four sampling zones (Figure 4.2). Cross-shore sampling locations were consistent with those adopted by Nicholls (1985). The samples were collected at the surface at low water, high water and at the beach crest; they were taken at 1m depth, beneath the surface at each of the crest and high water locations. Sampling was carried out over low water spring tidal conditions.

Various grain size classifications were considered; however, the study has adopted the logarithmic transformation of the Udden-Wentworth scale - the phi (ϕ)scale. This classification was proposed originally by Krumbein (1934) and revised later by McManus (1963). The phi values are dimensionless numbers.

$$\phi = -\log_2 \frac{d}{d_o}$$

where d is the diameter of the particle in mm,

and d_o is the standard grain diameter (1mm).

The sampling strategy adopted was based upon that discussed by Krumbein (1954). Previous research upon the sampling and statistical validity of particle size distribution analysis, in coarse fluvial environments (Kellerhals and Bray, 1971) has identified problems which could also occur on shingle beaches. Large (volumetric) samples were collected at each site (approximately 50-60kg) to ensure that they were representative of beach sediments which were often extremely coarse. A substantial proportion of cobble size sediment (larger than -6ϕ) occurred at some locations, whilst other areas comprised substantial proportions of sand. Samples collected at depth were taken with the aid of a tracked excavator; this enabled the large excavations to be undertaken rapidly, to provide undisturbed samples from an appropriate level.

Samples were oven dried for a minimum of 24 hours, then the sand and shingle fractions were separated at -1ϕ. Shingle samples were sieved across a nest of sieves at 0.5ϕ intervals. Sand-sub samples were also dry sieved, using sieves at the same interval between -1ϕ and 4ϕ. The residual proportion of the mud-sized materials was not sieved; this was consistently < 1% of the sample. Statistical analyses were undertaken. as recommended by Folk (1966); these include the mean, median and sorting (as defined by McGammon (1962)) and the skewness and kurtosis (described by Folk and Ward (1957)). Problems encountered by Dyer (1970) in relation to the determination of extreme percentiles did not present a problem: the samples were sufficiently large to permit statistically-valid distributions.

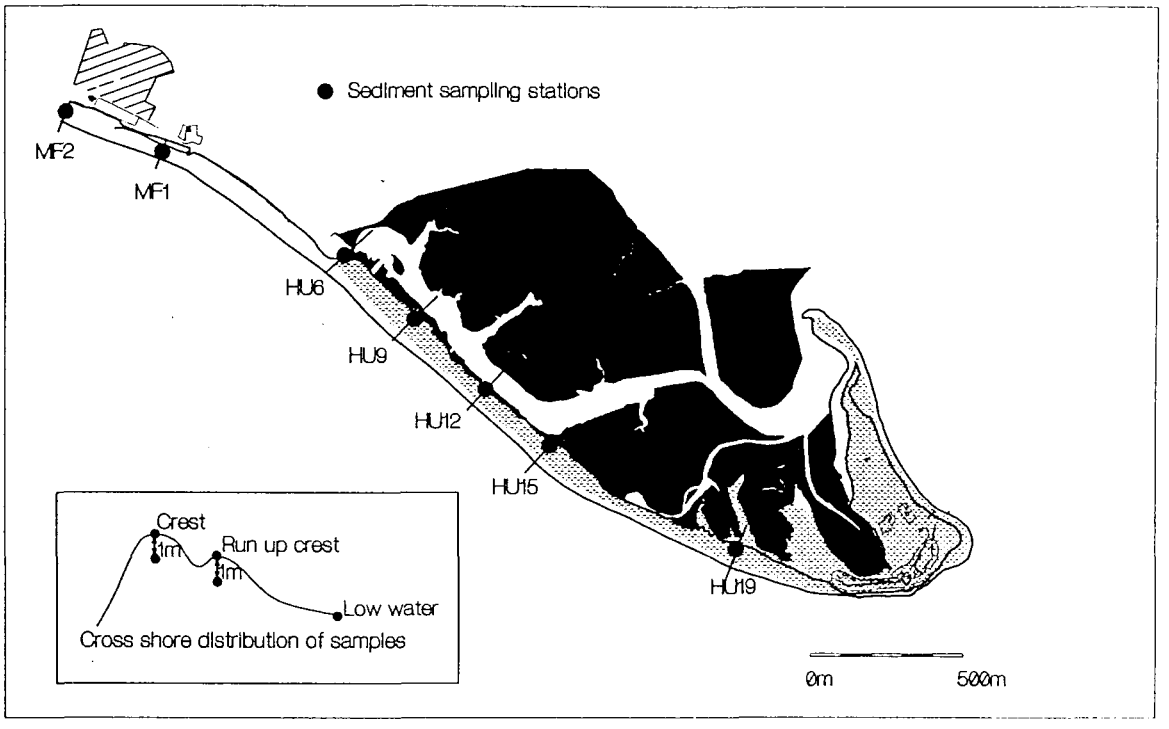

Figure 4.2 Location of sediment sampling positions on Hurst Spit

4.2.4 Hydrodynamic measurement programme

A study of the regional hydrodynamics was necessary, to complement shoreline response investigations. Hydrodynamic variables controlling the response of shingle beaches are wave conditions and water levels; these have been examined in earlier studies (Powell, 1990 and van der Meer, 1988) and are considered further here in this study.

The hydrodynamic phase of the study presented a range of problems; ideally concurrent measurements of hydrodynamic variables should be made together with shoreline responses. Key variables selected for examination included: wave conditions; tidal currents; wind speed and direction; barometric pressure; and water levels. The measurement locations and prediction points for the hydrodynamic variables are shown in Figure 4.3.

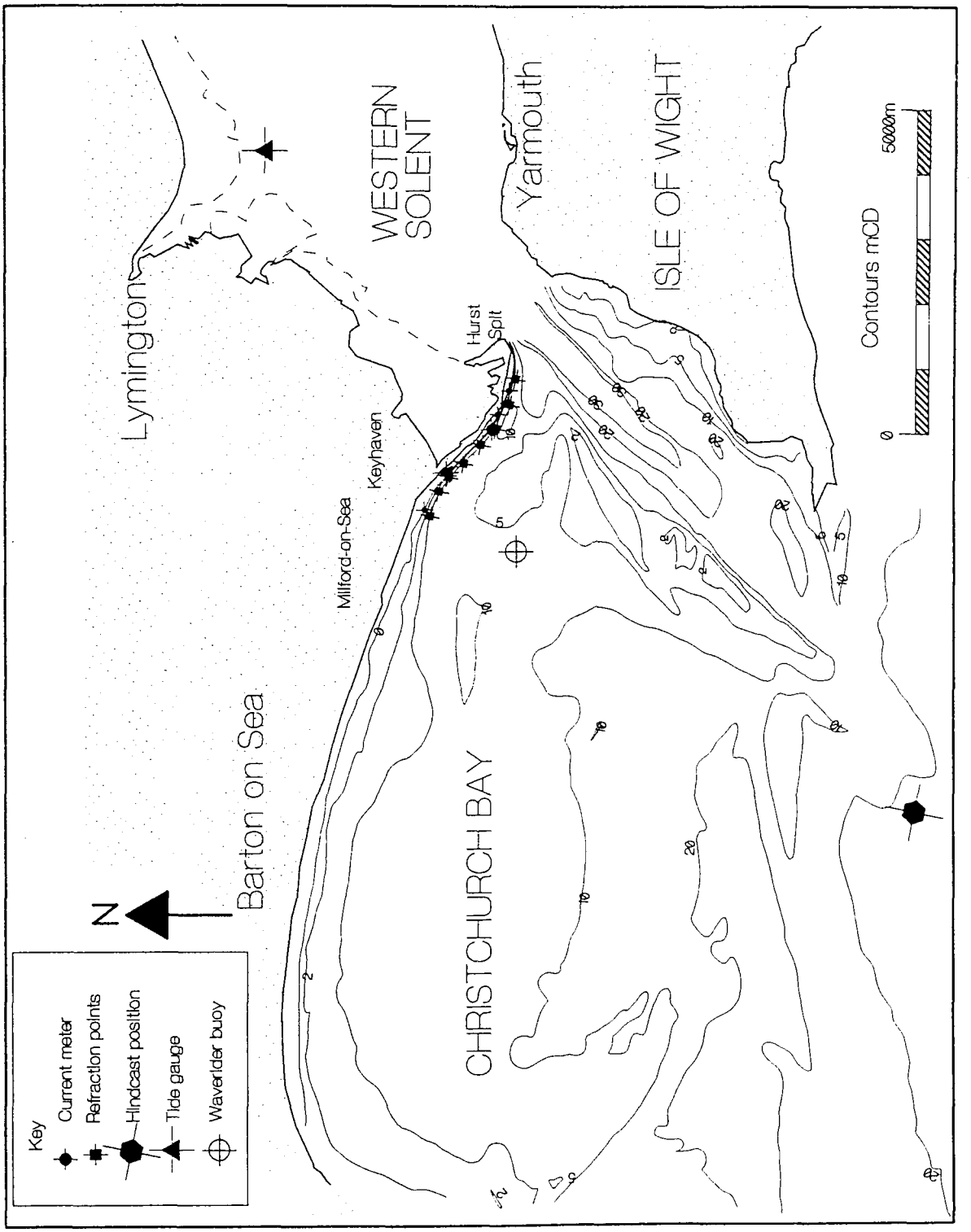

Figure 4.3 Location of hydrodynamic measurement positions and prediction points (bathymetry in m, relative to Chart Datum)

Attempts were made to install instrumentation to measure each of the variables; to compare results with numerical modelling methods; and to provide background data on each of long-term wave climate, extreme conditions and individual storm events. Although it was intended that all instrumentation should be installed and logged over the same period of time, the time spent in designing and preparing the various stages of the experimental and fieldwork programmes, and financial constraints resulted in a staged implementation of the hydrodynamic measurement programme.

Although the early stages of the programme lacked direct simultaneous measurements of some of the hydrodynamic variables, a comprehensive long-term field measurement programme was established before the end of the fieldwork. This permitted validation of the methodology used during the earlier phases of the research, providing full-scale testing of the hypotheses developed during the research programme.

(a) Current measurements

The cross-shore profile response of shingle barrier beaches changes primarily as the result of high cross-shore velocities generated by wave activity: this has been demonstrated locally at Hurst Spit during the course of field studies. The profile remains largely unaltered during periods of calm (Nicholls, 1985). Wave action was considered to be the main forcing mechanism for such changes. Nonetheless, the complex bathymetry of the approaches to Hurst Spit results in varied currents along its length; these may have a significant effect on longshore transport, particularly of the finer fraction of sediment which lies lower on the beach profile.

Investigations undertaken by Nicholls (1985) and Velegrakis (1994) have considered previously the effects of currents with respect to longshore transport at this site, although these have not recorded near-bed currents in the North Channel (adjacent to Hurst Spit). In order that currents and wave current interaction could be considered, it was necessary to carry out a series of field measurements.

Current measurements were recorded using a Valeport Braystoke direct reading current meter, deployed at 4 locations, over both spring and neap tidal cycles. The

instrument was deployed from a fishing vessel with a wooden hull, at a fixed level of 1m above the bed (i.e. the -3m ODN contour). Sites selected for current metering corresponded with the 4 segments for the physical model studies of Hurst Spit (Figure 4.9); these are shown in Figure 4.4. Measurements were recorded over a 13 hour (tidal) cycle during each deployment of the current meter. Additional velocity/depth profiles were obtained through the water column, at each of the sites. Data recorded during each deployment included the average current speed and direction observed over a time period of 100 s. Samples were recorded every ten minutes. The current measurement surveys took place during periods of calm weather.

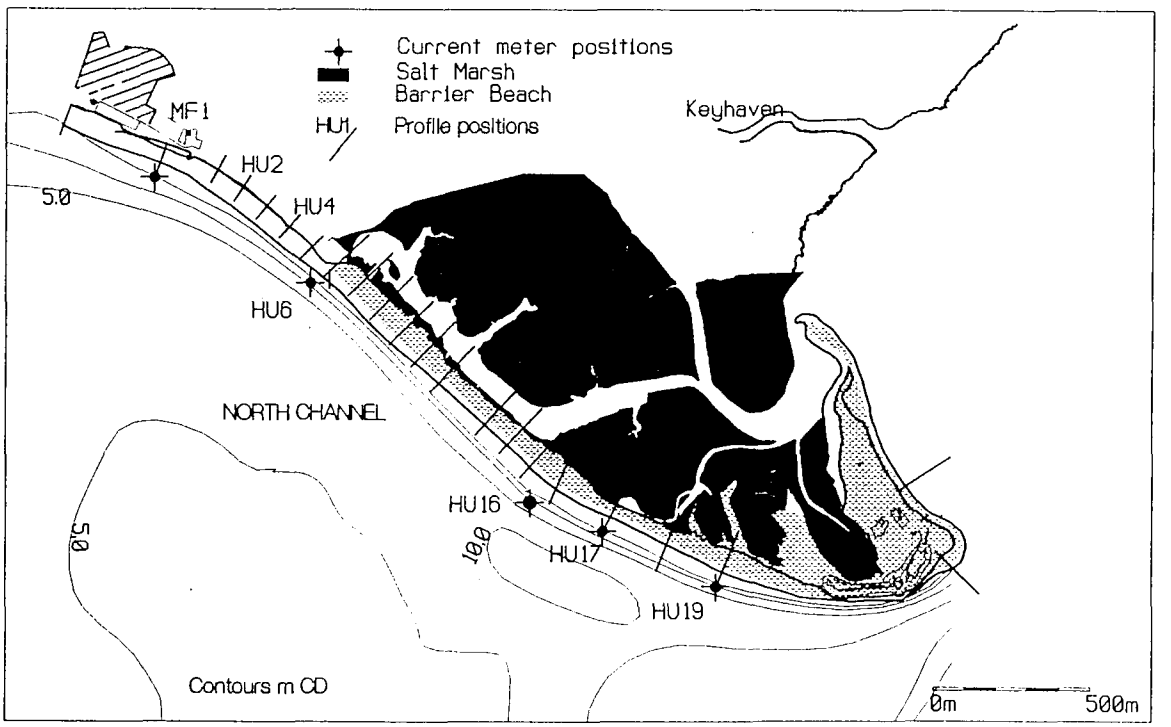

Figure 4.4 Location of current meter measurement sites adjacent to Hurst Spit (bathymetry in m, relative to CD)

(b) Wave measurements

A number of regional studies of Christchurch and Poole Bays have previously included measurements of wave conditions (Wright, 1982, Hydraulics Research, 1989a, b). However, these studies have not provided the appropriate combinations of duration or continuity of record, location of measurement points, or detail of individual storm events and extreme wave climate prediction. The large range of fetches and the complexity of the bathymetry in the study area (Figure 4.3) results in widely-varying wave conditions along the shoreline of Christchurch Bay; therefore, any such studies must be highly localised.

As the main objective of the study was to analyse the profile response of shingle beaches to storm waves, it was necessary to measure wave data close to the study site. Section 2.2.7 highlights the limitations of earlier studies which lack this data. Numerical models are of considerable use but have limitations, especially in areas of complex bathymetry. Consequently, previous attempts to model the study area have had only limited success due to the relatively coarse (grid) nature of models used; the limitations of the physics used to describe processes within the models; and the complex bathymetry. Used in combination with real wave data, numerical modelling can provide a valuable input to a regional wave climate study; thus, this approach was adopted here.

The crest of a barrier beach changes in response largely to various combinations of localised extreme wave conditions and water levels. Ideally the wave climate should be determined on the basis of a long time-series of wave measurements; these can then be extrapolated to predict extreme events. The short study duration precluded this, but a field measurement programme was designed to incorporate the long-term deployment of a waverider buoy. The buoy was deployed as a semi-permanent installation, to generate a long-term local wave climate. Ideally, measurements would include a number of extreme events, which could be analysed directly by comparison with measurements of beach response; however, these might not necessarily be expected to occur during the study period. The study carried out by Hydraulics Research (1989a) provided the most useful data to examine patterns, for direct comparison and validation with the results from deployments made during the present study.

Wave data were collected here using a Datawell Omni-directional waverider system (Figure 4.5). The 70cm diameter buoy was tethered to an elastic mooring and an accelerometer measured accelerations of the buoy, as it followed changes in the surface water level. The accelerations were integrated twice, with resultant measurements of the instantaneous water surface elevation used to modulate a radio transmitter. A shore-based radio receiver system was used to demodulate the radio wave, to record the vertical movements of the water surface on a PC based logging system (via an analogue to digital converter). Wave height, period and a full spectral analysis could be determined from the records.

The buoy transmitted continuously, whilst the receiver was programmed to record for a pre-selected time period at selected intervals. The sampling period was maintained at a constant length of 2048 data points, at a sampling frequency of 2Hz. Such a digitisation rate is suitable for measurement of the shape and magnitude of waves with periods ranging from 4 to 12 s: this provides a sample period of 17 min and 4 s. Prior to deployment, the buoy was calibrated by measuring the response of the accelerometers to periods of rotation of the buoy in a calibration rig, between 3 and 20 s on a fixed amplitude of 1.8m.

Receiving equipment was deployed at the New Forest District Council offices in Lymington - at distances of 6km and 7.25km from the data collection points in the North Channel and off Milford-on-Sea, respectively (see below). The onshore receiving equipment comprised an HF antenna, linked to a Datawell Warep receiver, and a PC logging system. Software used to carry out the data analysis was a bespoke software package, WAVELOG2; it consists of two elements; a logging segment and an analysis component. The analysis component provides for the calculation of significant wave height, mean wave period, maximum wave height and a full spectral analysis. A separate spectral analysis file was produced for each sample period. The analysis system also generated a file which contains a time-series of the summary data; significant wave height; mean wave period; and maximum wave height. This file was incremented automatically, after each sample period. Data was analysed and archived within a PC database.

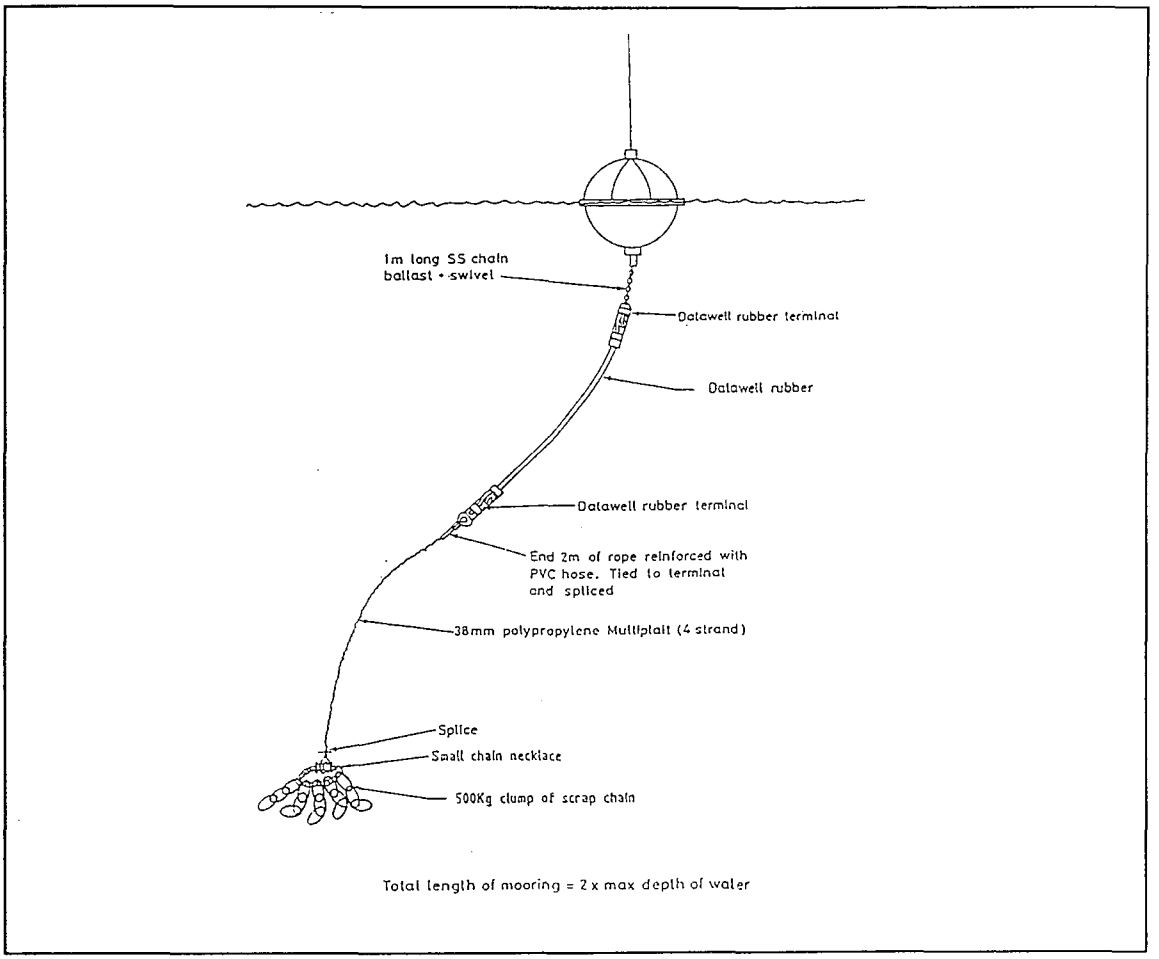

Figure 4.5 Waverider buoy configuration (from Hydraulics Research 1989b)

The buoy was deployed at two locations during the study period - both in much shallower water than is conventional for this type of instrumentation. The first site was in the North Channel in the lee of the Shingles Banks - a relatively sheltered site. The buoy was moored at 50^{o} 42.7' N, 1^{o} 36.8' W, in a mean water depth of 10 m between March 1994 and December 1995. The buoy was moved, in December 1995, to the location at which a waverider had previously been deployed between 1987 and 1989 (Hydraulics Research 1989a), i.e. 50^{o} 42' 30" N and 1^{o} 35' 36" W. It was hoped that this deployment would extend or prove the statistical validity of the earlier study, at this site. The buoy was, once again, moored in a mean water depth of approximately 10 m, approximately 1.5 km south of Milford-on-Sea and 5 km north of the Needles. The locations of waverider buoy deployments are shown in Figure 4.6.

The interval between sampling periods was varied throughout the data collection period. The commencement of each sampling period was maintained at an interval of 3 hr for the deployment in the North Channel, whilst hourly samples were collected at the Milford-on-Sea location.

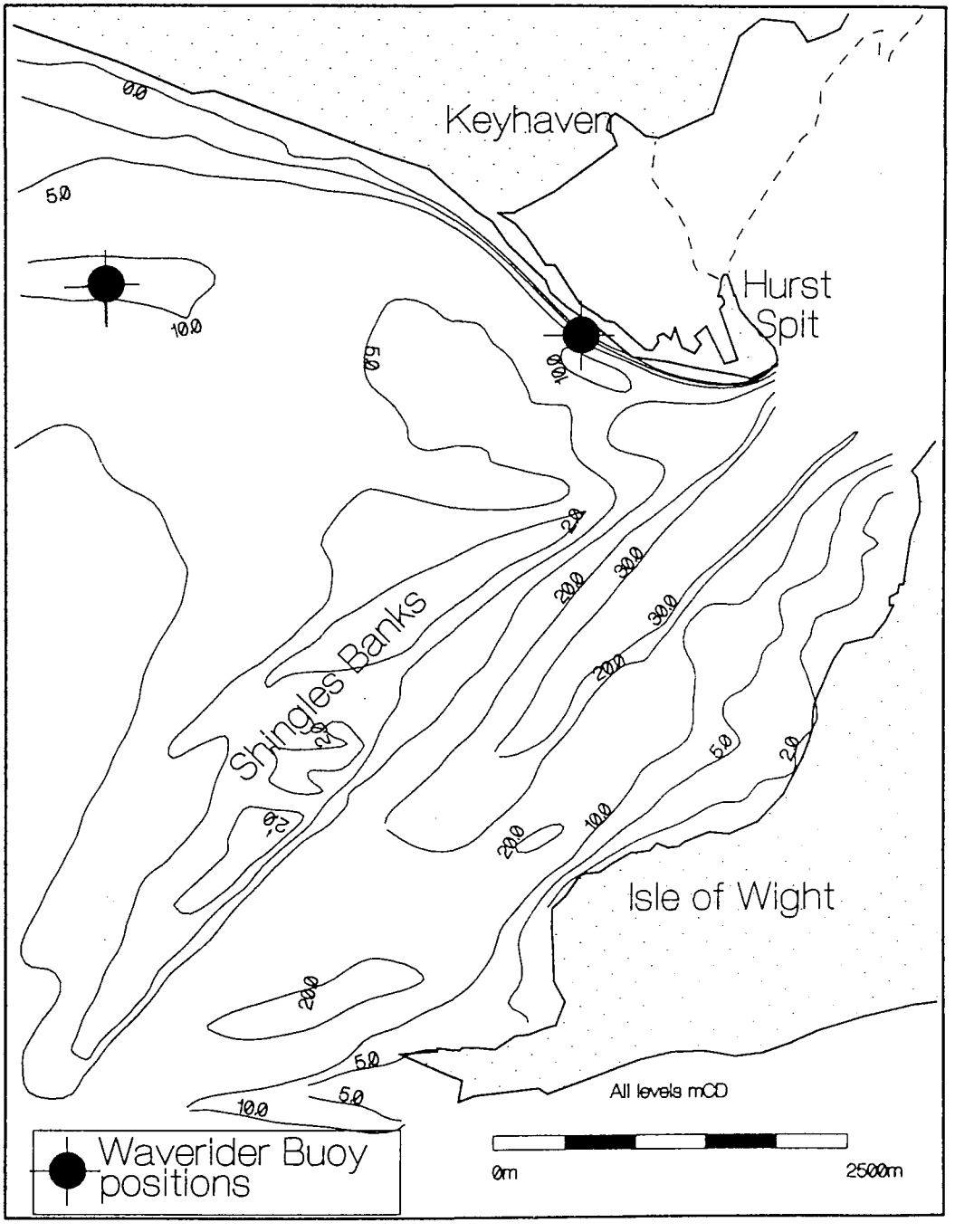

Figure 4.6 Locations of waverider buoy, during the study period (bathymetry in m, relative to CD).

(c) Tidal elevation measurements

Tidal water levels have a significant effect on the landward migration of shingle barrier beaches (Orford *et al*, 1993, 1995) Earlier studies in the area under investigation have identified tidal gradients (Blain, 1980) and provided predictions of extreme water levels (Nicholls, 1985). Likewise, a joint probability study of waves and water levels (Hague, 1992) has suggested alternative extreme water levels for the site. Only limited information is available on individual storm surge water levels and events at Hurst Spit; however, Nicholls (1985), has provided observations of extreme water levels at the site. On the basis of these data sets, a local tide gauge would provide the best method of determining extreme water levels.

The nearest and most appropriate location for such an installation was a yacht racing starters platform in the Western Solent (Figure 4.3). Consequently a tide gauge and anemometer were installed at this location. Limitations relate to the strong tidal gradient between the location of the gauge and the Christchurch Bay side of Hurst Spit (Nicholls, 1985; Blain, 1980); there is also a significant difference in tidal range between the two locations (see section 6.4.2).

A Vyner MF1001 radio tide gauge system was installed (see above). This system comprises a Druck pressure transducer linked to a calibration and transmission unit; it has a measurement accuracy of +/-10mm over the predicted tidal range (of approx. 4 m). The system was powered by 12 volt battery, which was replaced each month. A telemetry link enabled data to be transmitted to a remote logging station. A scaffold pipe housing, mounted on a timber pile, provided a stilling well for the pressure transducer; this was cabled to the power supply and telemetry unit in a secure location on the platform. A damping time constant of 60 s is applied to the data, which was sampled at 5Hz. Data were averaged over a period of 10 min and transmitted to the logging station at the Town Hall, Lymington (Figure 4.7). A barometer was linked also to the installation, to aid interpretation of the effects of atmospheric pressure on local storm surges.

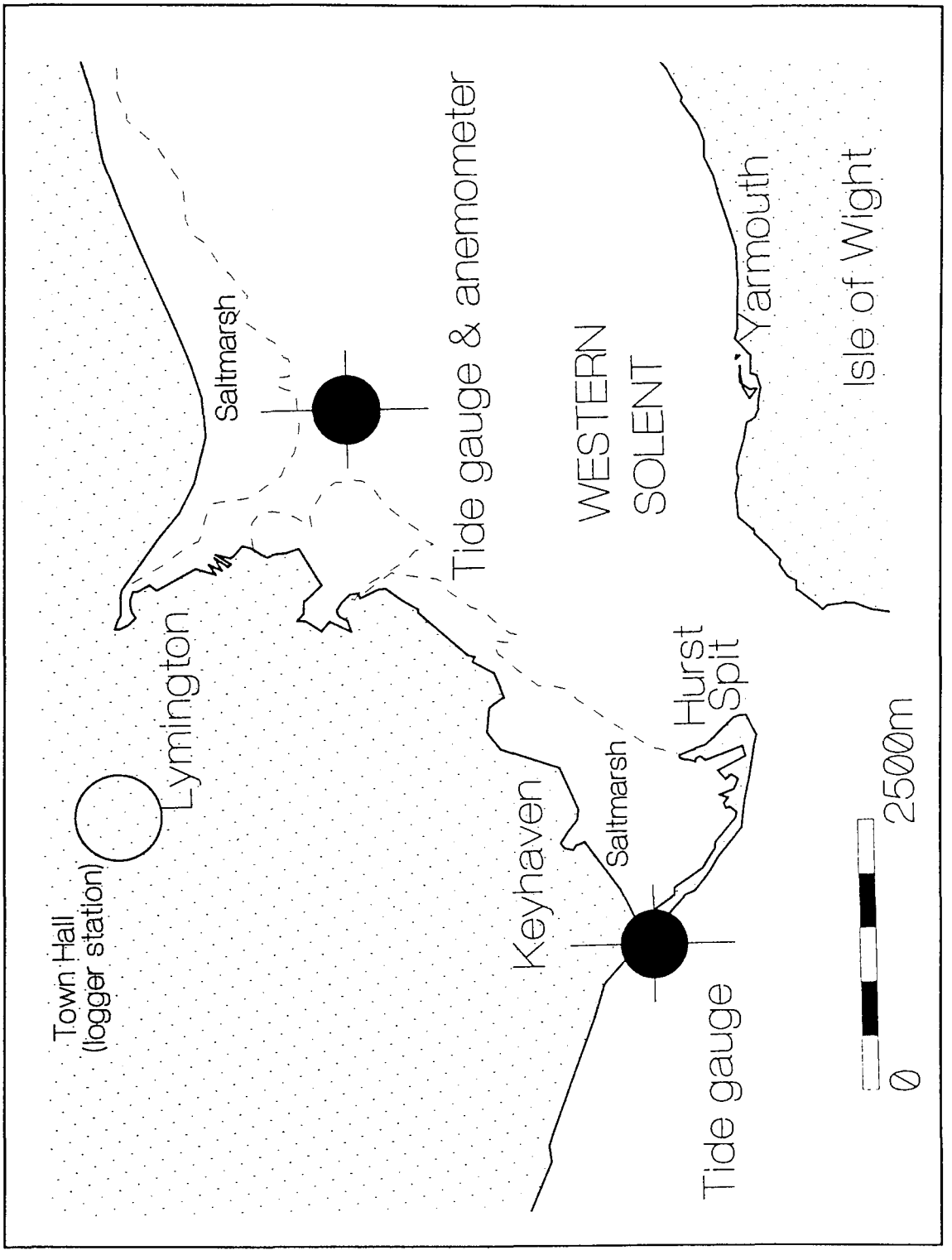

Figure 4.7 Location of the anemometer, tide gauges and logging station within the study area

Construction of a shore-detached breakwater adjacent to Hurst Spit, (during 1996) provided a more suitable site for a tide gauge, and a second gauge was deployed. Unfortunately, this latter installation was completed too late to provide a large quantity of data to this study. Although the data was limited, it should provide considerable benefits to future regional studies. This latter site is more exposed than the Lymington site, and dampening of waves is a more significant problem. The installation consisted of a 600mm diameter steel pipe, located within the rock armour; this formed an external core to the stilling well. A polyethylene pipe was located within this pipe, to provide additional damping; the pressure transducer was mounted inside this. A Hydrotide pressure transducer gauge was deployed at the site. A telemetry system was added to the installation, to provide real-time transmission of water levels to a logging station at the NFDC offices in Lymington (see above).

Both instruments were calibrated in a similar manner, by measuring the proportional change of the voltage output, compared to the depth of immersion of the transducer head. Compensation for atmospheric pressure was established through a vented tube, to the transducer. Similarly, the transducer head locations were levelled to Ordnance Datum; this provided a control relative to beach profile measurements. The gauges were levelled and co-ordinated using post-process static DGPS.

(d) Wind measurements

An alternative to the measurement of a regional wave climate, or individual storms, by direct measurement of wave conditions is to hindcast conditions synthetically, (using time-series of wind data). The tide gauge installation (Section 4.2.4) was made together with the deployment of an anemometer. Whilst the site was ideal in terms of its location, directly over an open expanse of water and with minimal local interference due to obstructions, wind conditions could reasonably be expected to be slightly less severe than in Christchurch Bay, where the conditions are more open.

The site was ideal location for the determination of wave conditions in the Western Solent; likewise, conditions impacting on the shoreline of the recurve spit at North Point could be hindcast with considerable confidence, using data from this installation. The JONSEY wave prediction model (Hydraulics Research, 1989c) was used, in

combination with wind data, to hindcast a series of storms during the study period, to determine the prevailing wave conditions. Data were collected with a view to calculating a wind wave correlation for local wave measurement sites. Earlier regional studies (Hydraulics Research, 1989b) examined the regional wave climate using wind data from Portland; wind-wave correlation studies were carried out using data from Portland and Milford-on-Sea (Hydraulics Research, 1989a); these were used for comparison with results of the present study (Section 6.4). Distributions of wind speed and direction were determined from hourly averages and wind roses derived for each month, each year and for the whole of the data collection period.

4.3 NUMERICAL MODELLING OF WAVE CLIMATE

Wave climate studies form an essential part of any regional study of beach response to storm conditions. Similarly, the development of physical and mathematical beach models require detailed analysis of the full range of nearshore wave conditions to describe specific storm events during the study period. Ideally wave climate data are provided by a long time-series of measured wave data. Since a minimum of 10 yr. of wave data are needed to develop a reliable local wave climate to derive extreme wave conditions for return period events of about 100 years (Hydraulics Research, 1989b), wave conditions were calculated using mathematical models of wave prediction, based upon historical wind data sets. The first step in the derivation of a wave climate using mathematical methods is the prediction of waves in deep water. Wave conditions are transformed inshore then, using refraction models; these simulate wave-seabed interaction.

4.3.1 Prediction of offshore wave climate- wave hindcasting

The HR HINDWAVE model, of wave-generation (Hydraulics Research, 1985; Hawkes, 1987), reproduces long-term wave conditions from wind data recorded at a local anemometer station (in this case, Portland). Extreme wave conditions and a wave climate were calculated using HINDWAVE for an offshore location in Christchurch Bay, during an earlier study for NFDC carried out by HR Wallingford (Hydraulics Research, 1989b). These data were used as the framework for the

derivation of offshore wave conditions for this study. The data set were extended using more recent data. The data were used to predict wave conditions for a location in approximately 20 m of water 10 km offshore of Milford-on-Sea (Figure 4.8).

The results produced by the model include a time-series of synthetic wave data, from which tables of distributions of wave height and direction and their probabilities of occurrence, and scatter diagrams of wave height and period can be produced. These data can be analysed typically in terms of seasonal, monthly or annual data-sets to determine temporal changes in the prevailing wave climate. Synthetic wave data can be analysed to predict extreme conditions within defined probabilities of occurrence (Hydraulics Research, 1989b). Further data can be extracted from the numerical model, to produce directional spectra for defined conditions; these can be used later as input to wave transformation models, for the determination of nearshore wave climate.

The HINDWAVE model has been prepared on the basis of the details of the geometry of the area relative to the wave prediction point; this is defined in terms of a series of (wave) rays, representing fetch lengths from the nearest land mass to the wave prediction point (typically at separations of 10^{o}). Wind data are used in combination with this geometric information, to derive wave conditions (using the JONSEY prediction program); this is based upon the JONSWAP method of wave generation, as modified by Seymour (1977). Initial calculations of wave conditions were carried out for a defined range of durations, from 1 to 24 hours. Calculations were repeated, for vectorially-averaged wind conditions, for each of the defined storm durations. A wave height, period and direction was calculated for every hour of the time-series; these data were stored, enabling the probabilities of occurrence to be derived. The model used for this study was set up, and calibrated, previously (Hydraulics Research, 1989b). The additional time-series data available to this study were used to supplement the earlier times series and extend the data set. The output was in a similar form to the earlier study, but additional extreme directional (wave) spectra were produced - as input to the nearshore wave transformation models.

4.3.2 Derivation of inshore wave climate wave refraction modelling

The bathymetry of Christchurch Bay is extremely complex (Section 3.1), particularly in its eastern part. This area includes a series of shallow offshore sand and shingle banks, where seabed friction and wave breaking reduce significantly the energy of waves. The most important of these features, as far as this study is concerned, is the Shingles Bank (Figure 4.6); this is situated close to Hurst Spit and has an extremely complex shallow bathymetry, which is modified constantly by the wave and tidal action.

Most waves are generated in deep open waters; in shallower waters, the effects of the seabed become increasingly important. For example, wave refraction and shoaling are both caused by spatial variations in water depth. Shoaling involves a change in wave height consequent upon the waves slowing down as they travel through water of decreasing depth. Refraction occurs when waves approach the coast at oblique angles of incidence; it involves a gradual change in the wave direction, as waves travel towards the coast. These processes are included in the standard refraction computer programs developed and used at Hydraulics Research (see below).

OUTRAY (Hydraulics Research, 1987) is a wave transformation model which reproduces linear processes (such as refraction and shoaling); it creates matrices which can be used to transform inshore, any offshore wave condition. Once transfer functions for the linear processes have been developed for the bathymetry and a selected water level, a large number of wave conditions can be transformed inshore rapidly, using the matrices. Directional wave spectra, derived from the offshore wave prediction model HINDWAVE (Hydraulics Research, 1985), are used as input to the model; these transfer functions can transform thousands of offshore wave conditions, into equivalent directional spectra at an inshore site.

Seabed friction and wave breaking are likely to have a significant effect on waves, as they travel over the offshore banks of the study area, e.g. the Shingles Banks. However, friction and breaking are non-linear processes, and cannot be reproduced within OUTRAY. Each combination of wave height, period and direction

has to be processed separately by another model to determine these shallow water effects.

An appropriate model for wave transformation in an area with a complicated seabed topography, such as in the eastern part of Christchurch Bay, is INRAY (Hydraulics Research, 1989e). The INRAY model can include the effects of seabed friction and wave breaking, as well as wave refraction and shoaling. However, only monochromatic waves can be used, to model these non-linear processes. Each wave condition is represented by a single wave height, period and direction. Therefore, the INRAY model was run for every single wave condition: this presents a significant disadvantage when compared with a spectral model such as OUTRAY.

(a) Use of the OUTRAY Model

The OUTRAY model was set up for use in Christchurch Bay. The Fair Sheets for the 1988 Admiralty survey were digitised and a model grid was developed, using a digital ground model. Bathymetric data were suitably dense to enable the complex bathymetry to be reproduced adequately, with a fine nearshore grid resolution of 100m. The model grids were expanded to allow for the influence of local wave generation from the west, as well as longer period waves from offshore. Transfer functions were produced for the Milford waverider site and 8 locations along Hurst Spit, along the -5m CD contour (Figure 4.8). The waverider site was used to check the results of the refraction models against recorded data, to help decide upon the friction factor to be used as input to the INRAY model. Results were required at 4 positions on the 5m depth contour, for the 4 beach sections in the physical model (Section 4.4.3). Initially, 8 points on this contour were examined (Figure 4.8) in order to determine the variation in wave conditions along Hurst Spit.

Transfer functions were created for a water level of MHWS, for all 9 points; they were created also for mean sea level and a 1m and 1.4m surge above MHWS, for the 8 points on the 5m contour. The wave periods chosen for creating the transfer functions were the same as those used in creating the offshore spectra i.e. 2 to 15s, in 1s increments.

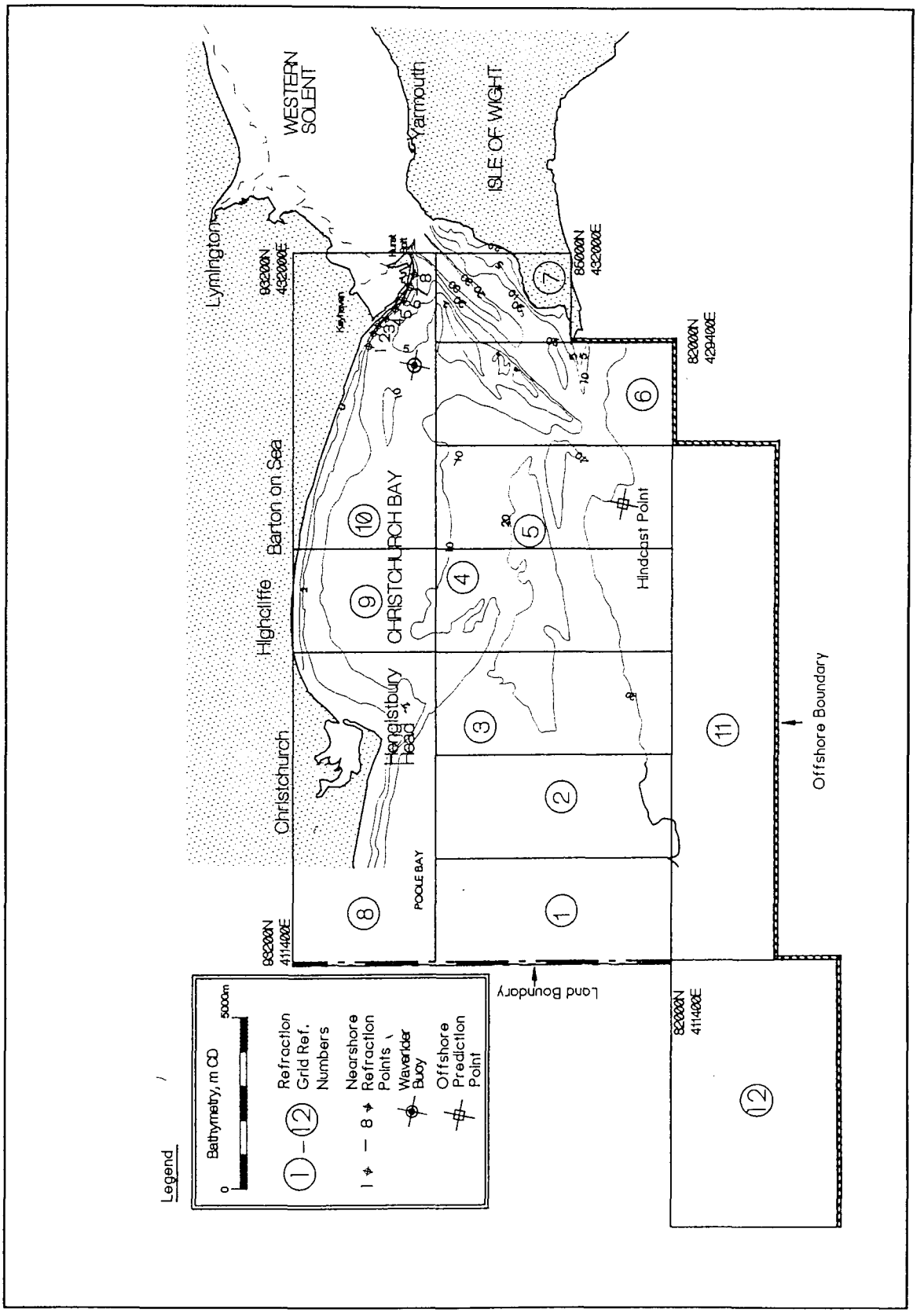

Figure 4.8 Refraction grids and wave prediction points, Christchurch Bay.

(b) Use of the INRAY Model

Wave rays are tracked across the gridded area using the same method as in OUTRAY, except that they are followed in their forward direction. Rays are sent out at equal intervals, from a line offshore; they are tracked inshore. Sufficient rays have to be tracked so that they adequately cover the inshore region of interest; this ray spacing depends on the complexity of the bathymetry. Grid elements are grouped into square - averaging regions. A ray-averaging method (Southgate, 1984) is used to determine the wave heights and directions at the centre of each region.

In the standard INRAY model the friction coefficient is assumed to be independent of wave height and water depth, likewise that it remains constant throughout the grid system. The water depth over the Shingles Bank is relatively shallow, hence the friction coefficient is likely to be higher here, than in other parts of the gridded area. The model was modified to allow a friction factor as input, from which a friction coefficient could be determined (depending upon wave height and water depth). In order to represent the propagation of a frequency spectrum fully with INRAY (see above), it is necessary to run the model for each of the 14 period components, then the wave heights are combined using linear superposition. Previous work (Smallman, 1987) has shown that a single run of the INRAY model, at the median wave period of the offshore frequency spectrum, will normally provide results that are close to those calculated from a combination of runs. Each offshore wave condition is represented in the model therefore, by the root-mean-square wave height, (H_{rms} = approx.H_s /1.414), the median period (the period which bisects the energy in the frequency spectrum) and the mean wave direction.

It was necessary to use a very small offshore ray separation in the analyses, of 5m for the 195-285°N direction sector and only 2.5m for the 120-195°N sector; this was in order for the wave rays to adequately cover the inshore region. The INRAY model was used only to determine the effects of friction and breaking, on the wave heights and directions. In order to achieve this, two runs of the model were required for each wave condition: one with friction and breaking, and one without. The ratio, of the inshore wave heights and the change in inshore direction between the two sets of results, was applied then to the inshore results from the OUTRAY model.

4.4 PHYSICAL MODEL STUDIES

4.4.1 Principles of physical modelling

(a) Background

Physical modelling techniques have been used to investigate the hydrodynamic performance of both natural processes and man-made structures in a range of environments since the mid 18th century (Hudson *et al* 1979). Model testing developed from early representations of steady state flow and rivers, to investigations of more complex processes associated with waves and tides (Yalin, 1971). Within the context of modelling laws, Reynolds (1887), Froude (1872) and Yalin (1963a) have made significant contributions to the scaling and validity of hydraulic modelling techniques (Sharp, 1981).

Much model research into beach dynamics has been carried out with the aid of regular wave testing; however, this can present significant limitations. Indeed, it has been suggested that parasitic secondary waves generated in shallow water, can affect formation of model beach profiles (Galvin, 1968). A comprehensive study of shingle beaches, under regular wave testing, is reported by Powell (1986), this draws attention to the limitations of this methodology, particularly with respect to the scaling of (beach) sediments.

Only since 1970 have random or irregular waves been used in physical modelling programmes (Dedow *et al*, 1976). Subsequently, modelling techniques have evolved to allow complex coastal processes to be reproduced, at small scales. The earliest reported studies of 3-dimensional mobile bed modelling of shingle beaches under random waves are those by Hydraulics Research (1985b, 1986); these are site specific in nature, based upon the theory developed of Yalin (1963a, b). The development of techniques, to provide reliable simulation of cross-shore and longshore shingle beach transport, are the result of relatively recent advances (Powell, 1990) (based upon the original work of Yalin (1963a, b)).

The limitations of mobile bed physical models include: the appropriate absorption of reflected waves from wave generators; and the boundary effects of the wave basin, or flume. The working water depth of the model test facility limits both water depth and wave conditions; similarly, the range of operational frequency of the wave generation equipment limits the wave conditions. Most wave models neglect the effects of tides, winds, and longshore currents (Powell, 1986). Although this can present difficulties when examining site specific problems, it is not a significant problem for the purposes of beach modelling of profile response under SWL conditions.

(b) Scales

If a model is to replicate the prototype processes accurately it must provide geometric, dynamic and kinematic similarity with the prototype system. Geometric similarity requires the ratios of all linear dimensions of the prototype and the model to be the same. Kinematic similarity requires similarity of motion, whilst dynamic similarity requires the same ratios for each of the forces (Powell, 1986).

$$\frac{(Fi)_p}{(Fi)_m} = \frac{(Fg)_p}{(Fg)_m} = \frac{(Fv)_p}{(Fv)_m} = \frac{(Fe)_p}{(Fe)_m} = \frac{(Ft)_p}{(Ft)_m} = \frac{(Fp)_p}{(Fp)_m} \qquad [4.1]$$

Dynamic similitude is related to Newtons 2nd Law of Motion and requires that the ratios of inertial forces of the model and prototype systems are equal to the vector sums of the active dynamic forces (of gravity, viscosity, elasticity, surface tension and pressure). However, it is considered impossible to satisfy equation 4.1 fully, except when the model scale is 1:1. Therefore, some compromise must be reached. Certain of the forces can be neglected safely, without adverse effect on performance, but the flow regime must be examined carefully. Models which examine the effects of wave action and sediment transport are not strongly dependant upon replication of the full-scale elastic and surface tension forces - within certain limits. The limiting factor is wave length; this must be greater than approximately 10cm, in order to overcome the effects of the surface tension. Inertial forces are always present in fluid flow; hence, dynamic similitude must be satisfied by equating the ratio of these to either gravity or viscous

forces. The Froude (model) Law equates the gravity forces whilst the Reynolds (model) Laws equates the ratio of viscous forces (Allen, 1947).

Froude (model) Law:

$$\frac{v_m}{(g_m l_m)^{1/2}} = \frac{v_p}{(g_p l_p)^{1/2}} \qquad [4.2]$$

Reynolds (model) Law:

$$\frac{\gamma_m v_m l_m}{\mu_m} = \frac{\gamma_p v_p l_p}{\mu_p} \qquad [4.3]$$

Within the surf zone on a beach profile and material, viscous forces are extremely small (relative to turbulence). Gravity effects acting parallel with the beach slope, together with turbulent flow close to the seabed are the primary inertia forces acting within the system. The Froude (model) Law is best suited to the examination of wave forces on a beach; in this, the ratios of inertia and gravity forces are the same, in both model and prototype. Wave models must be constructed, in general, without distorted horizontal to vertical scales, as wave steepness would not be reproduced correctly. As gravity is the same in both the prototype and model systems, then scale factors can be derived from (Equation 4.2):

$$\frac{v_m}{(l_m)^{1/2}} = \frac{v_p}{(l_p)^{1/2}} \qquad [4.3]$$

and

$$\frac{v_m}{v_p} = \left(\frac{l_m}{l_p}\right)^{1/2}$$

For the time scale,

$$\frac{t_m}{t_p} = \frac{l_m}{v_m}\frac{v_p}{l_p}$$

and

$$\frac{t_m}{t_p} = \left(\frac{l_m}{l_p}\right)^{1/2}$$

In general, scale effects may be defined as any hydraulic inaccuracy in performance, due to the scale of the model. Considerations given to the design of the model studies here have included examination of the effects of neglecting viscous, elastic and surface tension forces. Whilst the combined influence of these forces is small, the model may suffer from this scale effect, which is dependant upon the Reynolds number. Drag and lift forces on the bed load transport of the beach material vary with Reynolds number; these were considered when determining the model scale and in particular the scaling of the model sediment.

(c) Modelling sediment transport

Two alternative techniques are used commonly to examine the movement of sediments in physical models: (i) to represent the entire beach, as a mobile structure, using correctly-scaled sediments: and (ii) to represent only sediment transport pathways. In the latter case, no account needs to be taken of the characteristics of the beach itself (e.g. permeability, profile response). Scaling is somewhat simplified, as sediment tracers are injected into the system to identify flow paths. In the present investigation, however, it was necessary to model: the cross-sectional profile response of the beach; longshore transport; and their interaction with rock structures. Consequently, it was necessary to model the complete mobile section of the shingle.

Whilst the reproduction of waves and the geometry of the model can be described adequately using Froude's (model) Law, the scaling of mobile materials within mobile bed physical models is complicated further by: the nature of the beach materials; and the interaction of the beach with the waves. Further considerations must be given to the correct reproduction of the dynamic response of the beach.

The impacts of permeability on the slope angle of the beach have been discussed previously (Chapter 2). Simple geometric scaling of the model sediment would result in a model beach of incorrect permeability. Regular wave tests, using two grades of shingle in flume studies, and using simple geometric scaling have been conducted (Powell, 1986). Elsewhere, a single model scale for studies of shingle beaches has been used (Van der Meer, 1988). For beach response to replicate the full-scale, the model sediment should ideally satisfy three criteria:

(i) that the permeability of the shingle should be reproduced correctly;

(ii) the relative magnitudes of onshore and offshore motion should be correctly represented; and

(iii) the threshold of motion criteria should be scaled correctly.

(i) Permeability

Beach slope is governed by permeability, and indirectly by grain size. A method of scaling of shingle beaches, which allowed both the correct permeability and drag forces to be reproduced in the model, has been described (Yalin, 1963a).This approach suggests that the percolation slope must be identical, in both model and prototype, to ensure that the permeability is reproduced correctly, in an undistorted model:

$$J = \frac{k(Re_v)v^2}{gD_{10}} \qquad [4.4]$$

Where:

J	=	percolation slope
k	=	permeability, $k = f(Re_v)$
Re_v	=	voids Reynolds number, vD_{10}/υ
v	=	water velocity through the voids
D_{10}	=	10% undersize of the sediment
ν	=	kinematic viscosity
λ	=	Froude scale ratio

For identical percolation slopes, in the model and at full-scale, this gives:

$$\frac{\lambda_v^{\,2}\lambda_k}{\lambda_D} = 1$$

Where λ is the model scale (full-scale / model scale ratio). Assuming that the model is operated according to Froude's Law then $\lambda_v^{\,2} = \lambda$ (the geometric scale) so that:

$$\frac{\lambda\lambda_k}{\lambda_D} = 1 \qquad [4.5]$$

As permeability is a non-linear function of Re_v, Yalin (1963a) proposed a steady-state flow law and generated a recommended curve of k against Re_v. This curve can be approximated by the expression:

$$\log k = 3.17 - 1.134 \log Re_{v.} + 0.155 \log^2 Re_{v.} ,$$

for the range $1 < Re_{v.} < 200$

With such a non-linear expression, the scaling law will depend on the representative value of the full-scale (prototype) permeability. If this is designated k_p and the Reynolds number is Re_p then:

$$\lambda_k = \frac{k_p}{k_m} = \frac{\lambda_D}{\lambda}$$

$$\lambda_D = \frac{\lambda k_p}{k_m}$$

Now, $k_m = k\,(\mathrm{Re}_m)$. Where Re_m is the model Reynolds number, so

$$k_m = k\left(\frac{\mathrm{Re}_p}{\lambda_v \lambda_D}\right) = k\left(\frac{\mathrm{Re}_p}{\lambda^{1/2} \lambda_D}\right)$$

By substituting this expression, the implied equation for λ_D is obtained as

$$\lambda_D = \lambda k_p \,/\, k\left(\mathrm{Re}_p \big/ \lambda^{1/2} \lambda_D\right) \qquad [4.6]$$

Assuming that k_p, Re_p and the form of the function $k(\mathrm{Re}_v)$ are known, then this equation can be solved by successive approximation - to define the particle size for the model sediment, which will achieve the correct permeability within the model.

(ii) Onshore/offshore movement

It has been postulated that the relative tendency for sediments to move onshore or offshore depends upon the dimensionless parameter $H_b / W_T T_m$, (van der Meer, 1988). In this expression, H_b is the breaking wave height, T_m is the mean zero crossing period and W_T is the settling velocity of the sediment particles. If $H_b / W_T T_m < 1$, then

sediment moves onshore; if $H_b / W_T T_m > 1$, offshore movement occurs. In physical terms, the parameter represents the ratio between wave height and the distance which the sediment particle can settle during a single wave period. Therefore, for the correct reproduction of the relative magnitudes of onshore and offshore movement, the model scales must be such that:

$$\frac{\lambda_{Hb}}{\lambda_{WT}\lambda_{Tm}} = 1$$

Under Froudian model scaling $\lambda_T = \lambda^{1/2}$; assuming that the beach slope is modelled correctly then, $\lambda H_b = \lambda$, which gives $\lambda_{WT} = \lambda^{1/2}$

The general form of the settling velocity is given by:

$$W_T^2 = \frac{4gD(\rho_s - \rho_f)}{3C_D\rho_f}$$

where ρ_r and ρ_f are the specific gravities of the sediment and the fluid, respectively, and C_D is the drag coefficient for the settling particles.

For modelling purposes,

$$\lambda_{WT} = \frac{\lambda_D^{1/2}\lambda_\Delta^{1/2}}{\lambda_{CD}^{1/2}} = \lambda^{1/2}$$

$$\lambda_\Delta = \frac{\lambda\lambda_{CD}}{\lambda_D} \qquad [4.7]$$

where Δ is $(\rho_s - \rho_f) / \rho_f$

C_D is also a non-linear function; in this case, a function of the sediment particle Reynolds number ($Re_T = W_T D/\upsilon$). Thus, the actual scaling depends upon a typical value used for the prototype drag coefficient. Denoting this prototype value as C_{DP} and applying the appropriate Reynolds number Re_{TP},

$$\lambda_{CD} = \frac{C_{D_p}}{C_{D_m}} = \frac{C_{D_p}}{C_D(\mathrm{Re}_m)} = \frac{C_{D_p}}{C_D(\mathrm{Re}_p / \lambda_{WT}^{1/2}\lambda_D)} =$$

$$\lambda_{CD} = \frac{C_{D_p}}{C_D(\mathrm{Re}_p / \lambda^{1/2}\lambda_D)} \qquad [4.8]$$

If C_{D_p} and Re_p are known and λ_D has also been determined (for example from the permeability scaling) then equation [E4.8] can be solved for λC_D. The derived value can be inserted then into equation [E4.7] to derive ρ_s, the specific gravity of the model sediment. If both model and prototype sediments are coarse-grained (i.e. greater than 4mm) then $\lambda C_D \sim 1$ giving $\lambda_\Delta \sim \lambda / \lambda_D$

(iii) Reproduction of the threshold of motion

Komar and Miller (1973) have proposed that, for sediment sizes above 0.5mm and under oscillatory flow, the threshold of movement is defined by the expression

$$\frac{U_m^{\,2}}{\Delta g D} = 0.46\pi\left(\frac{d_o}{D}\right)^{1/4}$$

where U_m is the peak value of the near-bed wave orbital velocity at the threshold of motion, and d_o is the near-bed orbital diameter. Since the mean diameter in both the model and prototype materials lie above 0.5mm, this method would seem to be appropriate for application to shingle size sediment.

Since $U_m = \pi d_o / T_m$, this expression can be rewritten as

$$\frac{U_m^{7/4}}{(\Delta D^{3/4} T^{1/4})} = 0.46\pi^{3/4} g$$

The maximum near bed orbital velocity, to the first order, is given by

$$U_m = \frac{\pi H}{T_m Sinh(2\pi d / L)}$$

where L is the wavelength

Substituting this expression and rearranging gives the threshold, in terms of wave height and period, as:

$$\frac{H^{7/4} A^{7/4}}{(\Delta D^{3/4} T^2)} = \frac{0.46g}{\pi}$$

where A is the depth attenuation factor *(1/Sinh (2πd/l))*

For the appropriate modelling of the threshold of motion, therefore, the following expression is given

$$\frac{\lambda_H{}^{7/4} \lambda_A{}^{7/4}}{(\lambda_\Delta \lambda_D{}^{3/4} \lambda_T{}^2)} = 1$$

In a Froudian model $\lambda_H = \lambda_L = \lambda_d = \lambda$ and $\lambda_T = \lambda^{1/2}$; therefore, $\lambda_A = 1$, which gives:

$$\lambda_\Delta \lambda_D{}^{3/4} = \lambda^{3/4} \qquad [4.9]$$

4.4.2 Objectives of the physical model studies

Prior to designing the model studies, a series of objectives were set out to determine the most appropriate modelling techniques for investigation of the complex wave and shoreline interaction relevant to the study area. Consequently, the objectives of the calibration phase of the site specific model studies of Hurst Spit were as follows:

a) to identify the various combinations of wave and water level conditions that cause overwashing of Hurst Spit; and

b) to identify threshold crest levels, and widths, prior to overwashing of the shingle barrier beach.

If this calibration procedure was successful, then the model could be developed to study the performance of a wider range of conditions. Likewise, a corresponding range of beach geometries could also be tested, providing much wider applicability to the derived model.

4.4.3 Design considerations for the physical model of Hurst Spit

A number of physical model studies of coastal processes have been successful in reproducing sediment movements on shingle beaches, in particular beach profile response, with the aid of mobile bed materials and under random wave conditions (Hydraulics Research, 1985b, 1986; Powell, 1990; and van der Meer, 1988). It is believed that a shingle barrier beach has not previously been reproduced and tested in such circumstances. No reports of such studies have been identified in the literature, although investigations of flow through Chesil Beach, in random wave flume tests, have been reported (HR Wallingford, 1985b). Field data measured on Hurst Spit and in Christchurch Bay, reported in Chapter 6 of this study, provided full-scale data which

was used as the basis for the design of the model: this was also used as empirical calibration data to assess the validity of the test methodology. A physical model of Hurst Spit should ideally be constructed at a sufficiently large scale to allow hydrodynamic processes and beach responses to be reproduced within the context of the scaling framework (Section 4.4.1).

Mathematical models were used to derive wave processes, to provide input to the physical model of Hurst Spit (Chapter 5). The study area lies at the eastern end of Christchurch Bay (Figure 4.7) and is subject to a severe wave climate. The wave climate in the study area is complicated by a complex offshore bathymetry, consisting of numerous offshore banks and channels, and the prevailing current patterns.

Analysis of the beach profile data (see below, Chapter 6) has indicated that damage to Hurst Spit, by overwashing, occurs most frequently under storm surges. Hence, a range of water levels, including extreme storm surges, were considered at the design stage.

The accuracy and reliability of the physical model improves dramatically with increasing scale size. A model scale of 1:90 was considered to be the minimum requirement for the response of mobile sediment, to ensure that viscous effects would be minimised. For example, Yalin's (1963a, b) investigations into the reproduction of mobile bed physical models suggests an optimum scale of 1:27, to ensure that the permeability and threshold of motion criteria are met when using light-weight sediments. The response and effectiveness of relatively small features, such as rock groynes, could be reproduced considerably more reliably, at scales preferably larger than 1:40. These requirements posed a considerable problem for the present study, as even at a scale of 1:90, the model size would have been considerably larger than the largest model wave basin available. In order to reproduce wave transformations correctly along the full length of Hurst Spit, the bathymetry must be reproduced to seawards of the offshore banks, into deep water.

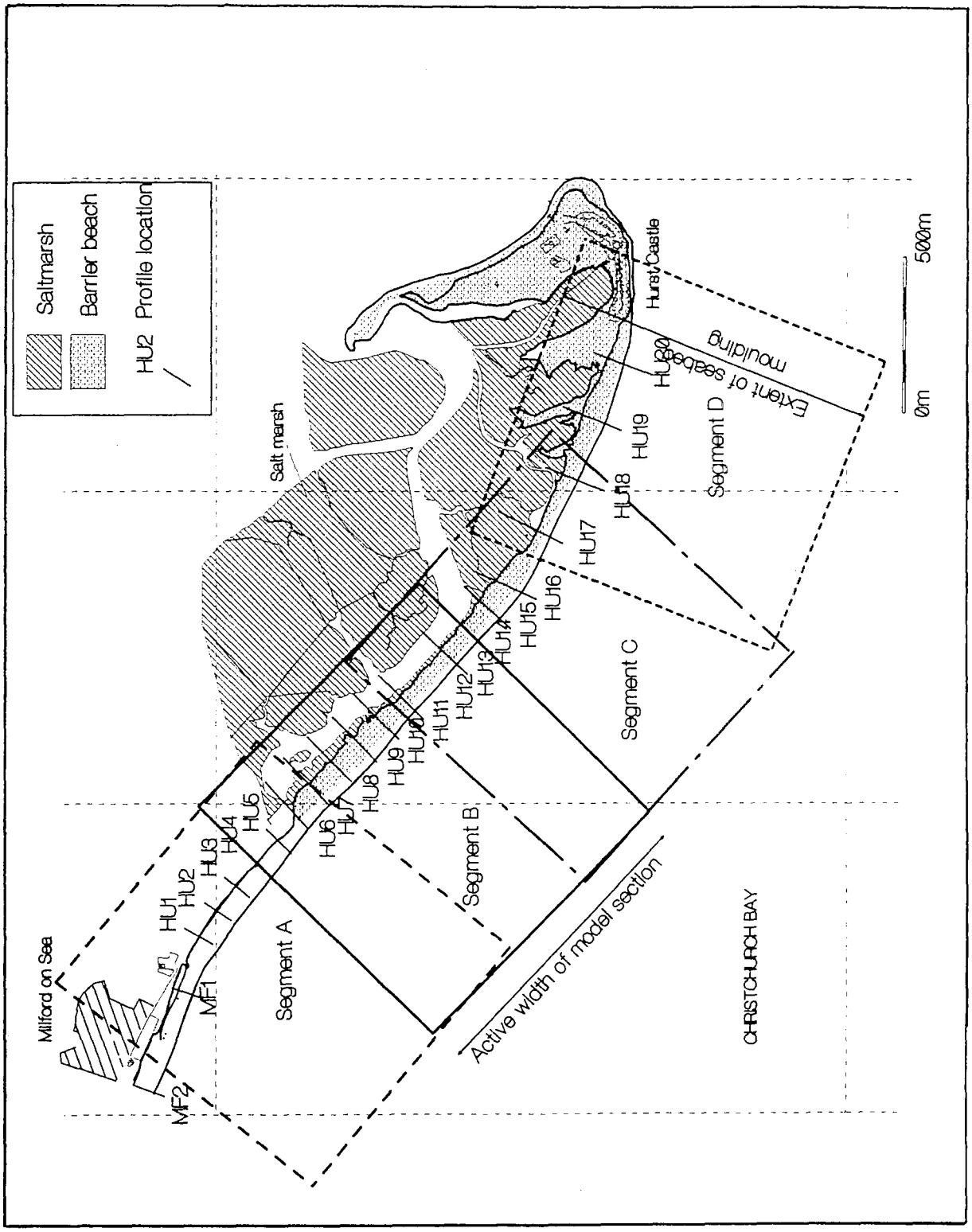

Figure 4.9 The overlapping segments of Hurst Spit reproduced in the physical model

The largest wave basin available for the physical model investigations had approximate dimensions of 35m by 25m, with a wave paddle of 25m in width (Figure 4.11). This arrangement limited the beach frontage in the model to 25m, under conditions of normally incident wave attack. Consequently, a model scale of 1:40 was selected; this allowed the spit to be modelled in 800m overlapping segments (Figure 4.9). In addition to allowing waves and currents to be reproduced accurately, at locations along the full length of the spit, the segmented approach to modelling had a number of other advantages. The relatively large model scale allowed: sediment response to waves to be reproduced with a high degree of confidence; and rock armour movement to be reproduced and monitored more accurately.

The model was designed subsequently, on the basis of the factors discussed above; and the test programme comprised the following elements:

a) mathematical modelling of the nearshore wave climate (Chapter 5);

b) physical modelling of four overlapping segments of Hurst Spit, at a scale of 1:40;

c) numerical modelling of sediment transport;

d) interactive modelling of the results from the physical and mathematical models; and

e) the physical modelling of a wide range of unrestrained shingle beach geometries and wave and water level conditions.

(a) Application of the Scaling Laws

In order that the selected mobile bed would simulate accurately the natural beach regime, it was necessary to ensure that sediment used in the model was representative of the natural deposits. Before model sediment could be scaled using the scaling laws discussed previously (Section 4.4.1), it was necessary to determine the sediment distribution. The sampling and analysis procedures adopted are discussed

further in Section 4.2.3. Samples obtained specifically for development of the physical model studies were collected at the low water mark, high water mark, and at the crest of the shingle beach. The sampling locations are shown in Figure 4.2.

Samples were sieved and divided at 2.0mm, into sand and shingle fractions. The shingle fractions were redistributed over all the samples and a typical shingle beach grading was derived, based upon an averaged combination of all the samples. The averaged distribution of the sediments is shown in Figure 4.10.

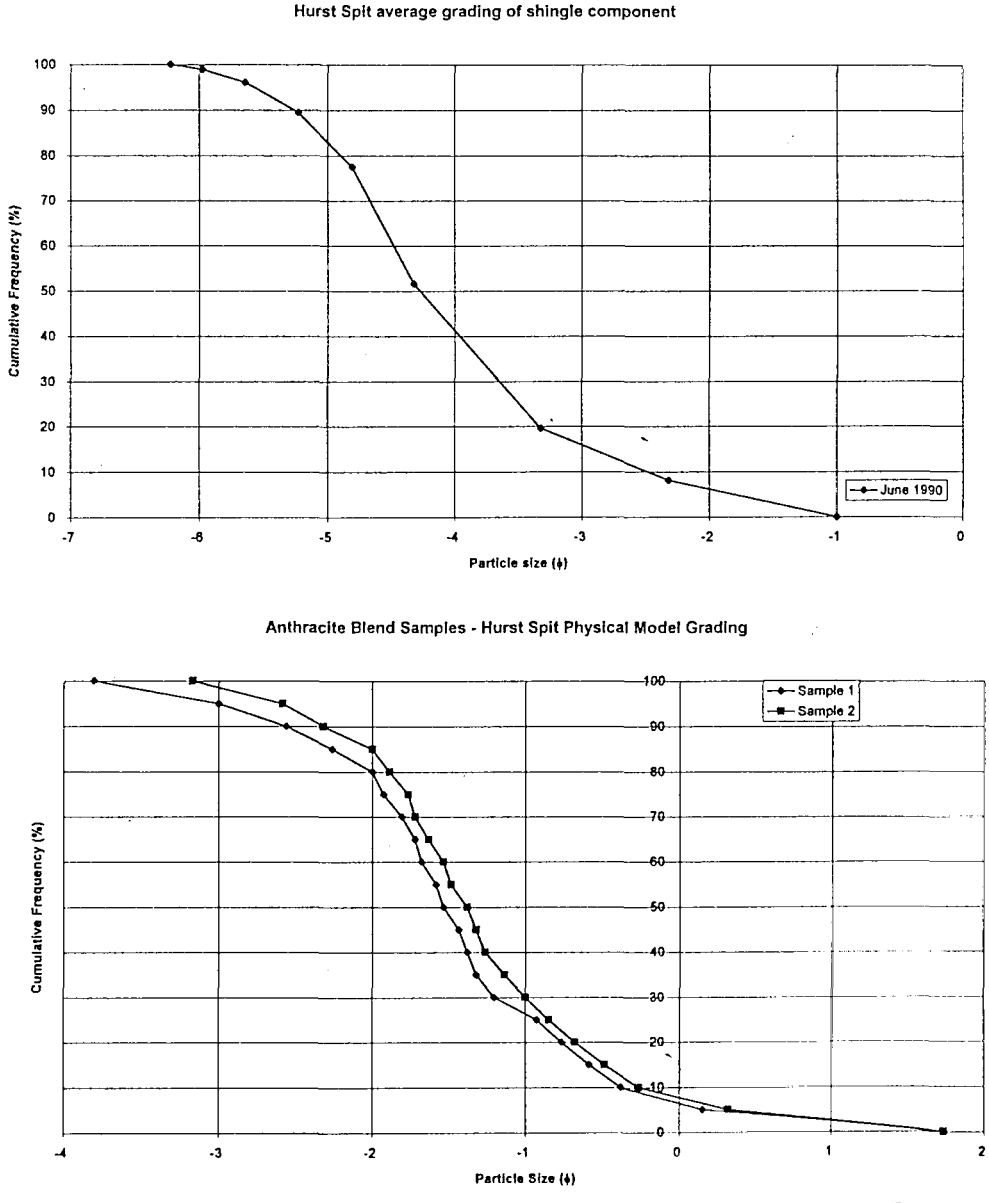

Figure 4.10 Averaged shingle gradings and model grading curves, for Hurst Spit sediments

On the basis of this distribution the shingle fraction of the beach is:

D_{50} = 20mm

D_{10} =6mm

ρ_s = 2.65 and

s = 4.25 (i.e. poorly sorted)

These values of D_{50}, D_{10}, ρ_s md, were used to calculate scaling factors for the mobile beach material, for a model constructed at a scale of 1:40.

Selection of model sediment

Beach material cannot be modelled with geometrically-scaled shingle, because it does not satisfy the requirements discussed in Section 4.4.1. If such shingle were used in the model, the profile response of the beach would be incorrect - as the beach permeability would not be represented correctly. Whilst there are three requirements to be satisfied (permeability; sediment mobility and the relative on-shore offshore movement), model sediment particles have only two main characteristics; size and specific gravity. As it is extremely unlikely that all three requirements can be achieved simultaneously, some compromise is necessary particularly as there are only a limited range of specific gravities amongst the readily-available materials.

To determine the permeability of the shingle beach, it is necessary to determine the rate of percolation through the voids; this changes constantly, under wave action, and full-scale measurements of permeability are not practical. An approximation must be made, based upon theoretical methods. In soil mechanics generally, the surface streamline is assumed usually to follow the shape of the bank (when there is rapid drawdown). At Hurst Spit, the shingle beaches typically have a slope of about 1:7 to 1:8 in the active zone. Using a percolation slope J of 1:7.5 and a D_{10} value of 6mm, gives:

$k_p(\mathrm{Re}_{vp})\, v_p^{\,2}$ = 7.38×10^{-3}

Re_{vp} = 85.7

v_p = 0.0143m/s

k_p = 36.1

Using equation 4.6 gives:

$$\lambda D = \frac{\lambda k_p}{k(\mathrm{Re} v_p / \lambda^{1/2} \lambda D)}$$

$$\lambda D = \frac{40x36.1}{k(60/40^{1/2} \lambda D)}$$

Using the function $k(\mathrm{Re}_v)$, given by Yalin (1963a), the solution of this equation by successive approximation gives:

Rev_m = 3.62

$k(\mathrm{Rev}_m)$ = 3.85

λ_D = 3.75

D_{50} = 5.33mm

Application of scaling for onshore offshore movement of shingle.

The settling velocity of 20mm shingle is 0.94m/s and with ρ_s=2.65 and ρ_f=1.03 this gives:

W_{TP} = 0.94 m/s

Re_{TP} = 19480

C_{Dp} = 0.44

If λ_D = 3.75 equation 4.8

$$\lambda_{C_D} = \frac{C_{D_p}}{C_D(Re_{Tp} / \lambda^{1/2} \lambda_D)}$$

$$\lambda_{C_D} = \frac{0.44}{C_D(19480 / \sqrt{40} x 3.75)}$$

Re_{Tm} = 821

C_{DM} = $10^{(1.6435-1.1242 \text{ Log Re} + 0.1558 (\text{LogRe})2)}$

= 0.49

λ_{CD} = 0.90

For the range $260 < Re_{Tp} < 1500$

Substitution into equation 4.7 gives

$$\lambda_\Delta = \frac{\lambda \lambda_{CD}}{\lambda_D} \qquad [4.7]$$

$$\lambda_\Delta = \frac{40x0.90}{3.75} = 9.59$$

The model sediment requires therefore a specific gravity of 1.16, to satisfy onshore/ offshore movement criteria.

Application of the threshold of motion

$$\lambda_{\Delta} = \frac{\lambda^{3/4}}{\lambda_D{}^{3/4}} = \frac{40^{3/4}}{3.75^{3/4}} = 5.90 \qquad [4.9]$$

The model sediment needs consequently, to have a specific gravity of 1.27 to meet the criteria for the correct reproduction of the threshold of motion.

Combination of the requirements

The scaling criteria (see above) suggest that the model sediments need the following characteristics, in order to reproduce correctly all aspects of the sediment motion at model scale:

D_{50} = 5.33mm, for correct permeability; [4.6]

Δ = 1.16, for correct onshore offshore movement; and [4.7]

Δ = 1.22, for the correct threshold of movement. [4.9]

Clearly, equations [4.7] and [4.9] derive conflicting requirements and further analysis is required. Similarly, no material was available which met the requirements. The choice of suitable materials is somewhat limited, for example perspex, (ρ_s = 1.2) and anthracite (ρ_s = 1.39). Unfortunately, the perspex material could not be produced economically, in the range of sizes required for the model. Thus, crushed anthracite provided the best initial approximation to the model requirements. This material has been used successfully to reproduce sediment in mobile bed models previously (Powell, 1990). The specific gravity of crushed anthracite is higher, however, than that required for either the threshold of motion or the onshore-offshore movement criteria. Since the

model tests were to be carried out under storm wave attack, the threshold of motion would be exceeded throughout the test programme. It was decided, therefore, to relax the threshold criterion. Since the specific gravity of the proposed material was greater than that required to meet the onshore-offshore movement criterion, it was necessary to compensate by varying the sediment size, (consequently, altering the effective permeability of the beach).

Whilst the profile response and onshore/offshore movement of the shingle is reproduced correctly, the rate of long-shore transport in the model will be much accelerated, because of the lower specific gravity of the model sediment. Calibration tests were required, to identify the distortion scale for the long-shore transport.

Specification of material for Hurst Spit

$$\rho_{s\,m} = 1.39$$

$$\lambda\rho_s = 4.03$$

For the correct threshold of movement,

$$\lambda_D = 6.23$$

$$D_{50} = 3.21\text{mm}$$

For the correct direction of movement,

$$\lambda_{CD} = 0.1008\ \lambda_D$$

and

$$0.1008\ \lambda_D = C_{DP} / C_D\ (\mathrm{Re}_{TP} / \lambda^{1/2}\lambda_D)$$

$$\lambda_D = 7.50$$

C_{dm} = 0.59

D_{50} = 2.68mm

The values for λ_D are therefore

Permeability λ_D = 3.75 D_{50} = 5.33mm

Direction of movement λ_D = 7.45 D_{50} = 2.68mm

Threshold of movement λ_D = 6.23 D_{50} = 3.21mm

The selected model scales were

$\lambda\Delta_m$ = 4.03

λ_D = 5.6 (an average of the permeability and direction of movement)

and D_{50} = 4.0 mm

(b) Limitations

The model design was appropriate only for the investigation of relatively severe wave conditions, which was appropriate to the requirements i.e. to examine the beach response to extreme events. Other processes which might affect the response, but which could not be reproduced included: the response of the salt marshes to wave attack, following breaching of the spit; erosion of the bed and the fine-grained sediments to seawards of Hurst Spit; the effects of sedimentation on flow in Mount Lake (Figure 4.13-4.14), in the lee of Hurst Spit; and the geotechnical response of the

salt marshes upon, which Hurst Spit is now founded (see below, Chapter 6). Finally, whilst tests could be carried out over a range of fixed water levels, the model did not have full tidal control.

The design of the model geometry and the hydrodynamic conditions used was based on Froudian similitude: hence, geometric scaling of the sea-bed and the cross section of the beach were proportional directly to the model scale of 1:40. The time and velocity scales are 1 in $\sqrt{40}$: consequently, wave events occurred approximately 6 times faster in the model, than in nature. Longshore sediment transport rates are subject to further distortion; these were higher in the model than in nature. Since the study area was to be modelled in segments, it was necessary to ensure that there was an appropriate overlap of each of the model segments. This allowed model end effects to be negated, providing a check on performance of overlapping segments of the model. The plan layout of the physical model segments is shown in Figure 4.9. The layout of each of the four model segments is shown in Figures 4.12-4.15.

4.4.4 Model construction - general layout

The models were constructed in a wave basin measuring 35m by 25m, in the laboratories at HR Wallingford. The layout of the model is shown in Figure 4.11. The model wave basin was prepared by installing large energy-dissipating beaches around its perimeter, to avoid artificial interference to the generated waves, by reflected waves. Wave generators in the test facility were capable of working over a range of water depths and the model bathymetry was designed to ensure an appropriate tidal range could be tested, (at the selected model scale of 1:40).

A sea-bed area was moulded in cement mortar for each of the model segments; each area covered a full-scale area of approximately 800m by 600m. The moulded area extended from the salt marsh area in the lee of Hurst Spit, to the -12mODN contour (Figures 4.12-4.15). Contours and levels were derived from hydrographic and topographic surveys of July 1990 (Section 4.2.2). The Mount Lake river channel was moulded in the lee of the spit, to enable the volume of sediment to be displaced correctly when the barrier beach 'rolled back' under storm action.

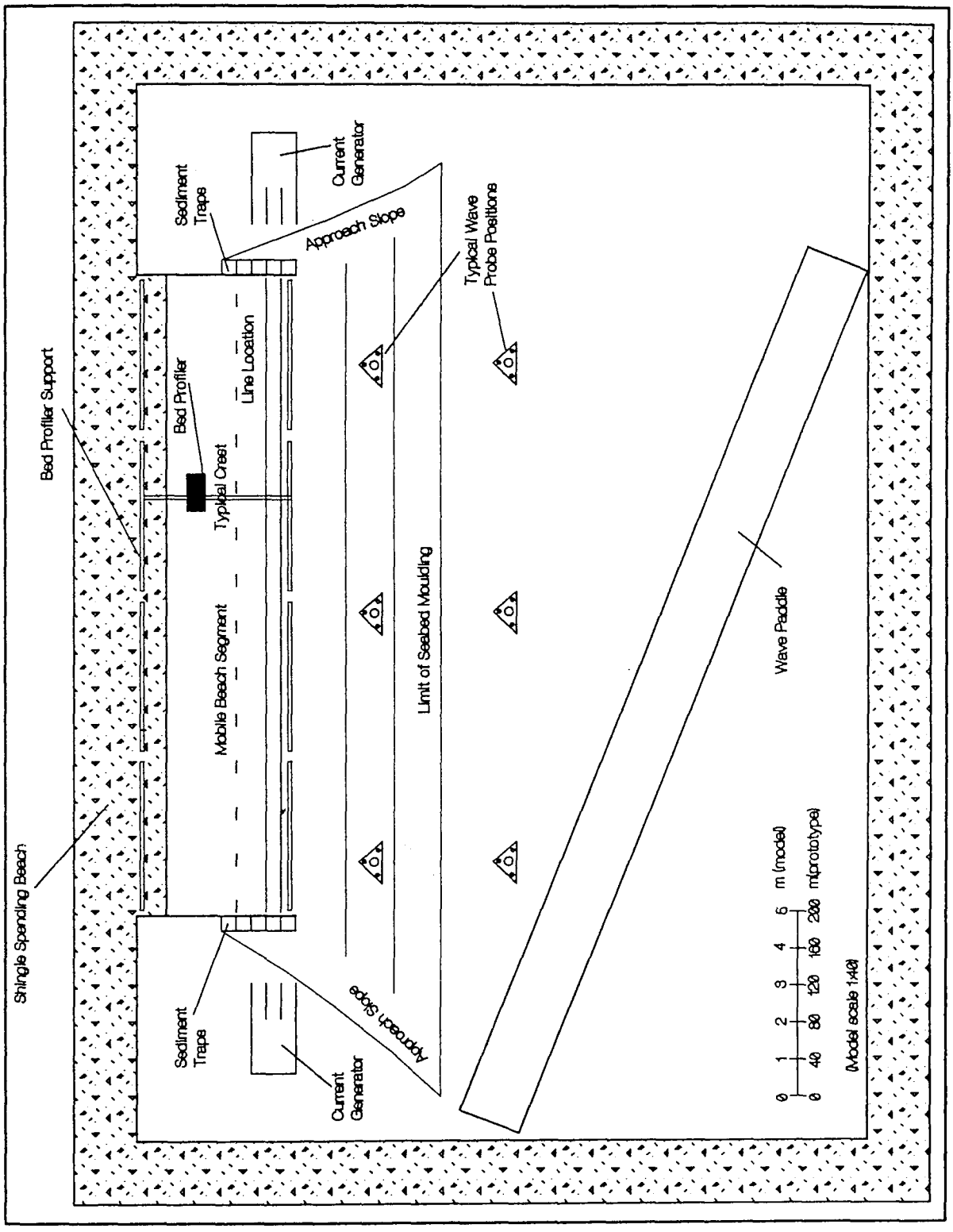

Figure 4.11 The layout of the wave basin and physical model used in the investigation

The assumed profile of the salt marsh surface beneath the shingle spit was moulded as an impermeable membrane: this was calculated on the basis of previous geotechnical results on differential compression (Nicholls, 1985) and from additional measurements made at the site.

Modifications to the idealised offshore bathymetry were made for each model segment, where appropriate. A 25 m long stretch of shingle beach was constructed for each model beach segment, representing 1 km in nature.

(a) Mobile beach and coastal structures

The mobile shingle beaches used in the model were based on the geometry of topographic and hydrographic surveys (see Chapter 6). Mobile beach material was moulded, initially, to cross sectional profiles surveyed prior to the severe storms of October and December, 1989. These surveys provided the basis for empirical calibration of the model; likewise, they allowed for the reproduction of these storms.

Since beach permeability is an important variable, it was necessary to ensure accurate reproduction of levels of the fixed bed beneath the beach. The shingle beach at Hurst Spit is founded on partially-compressed salt marsh. The weight of the shingle causes differential settlement, resulting in a prismoidal profile of the interface between the salt marsh and the permeable shingle. It was suspected that this change in cross sectional profile, with a maximum bed deviation from the normal surface of about 1m, would have a significant effect on the water flow path-ways through the shingle beach - (particularly when the beach had a small CSA). Therefore, an idealised permeable /impermeable interface was constructed, to the assumed profile of the salt marsh surface. The mobile beach zone was formed in mobile material. Following initial installation of the model beaches, they were subject to a period of wave activity; this ensured that the material was compacted properly. Beaches which were subject to testing were then constructed, by grading of the beach material to scaled templates of the actual beach profiles.

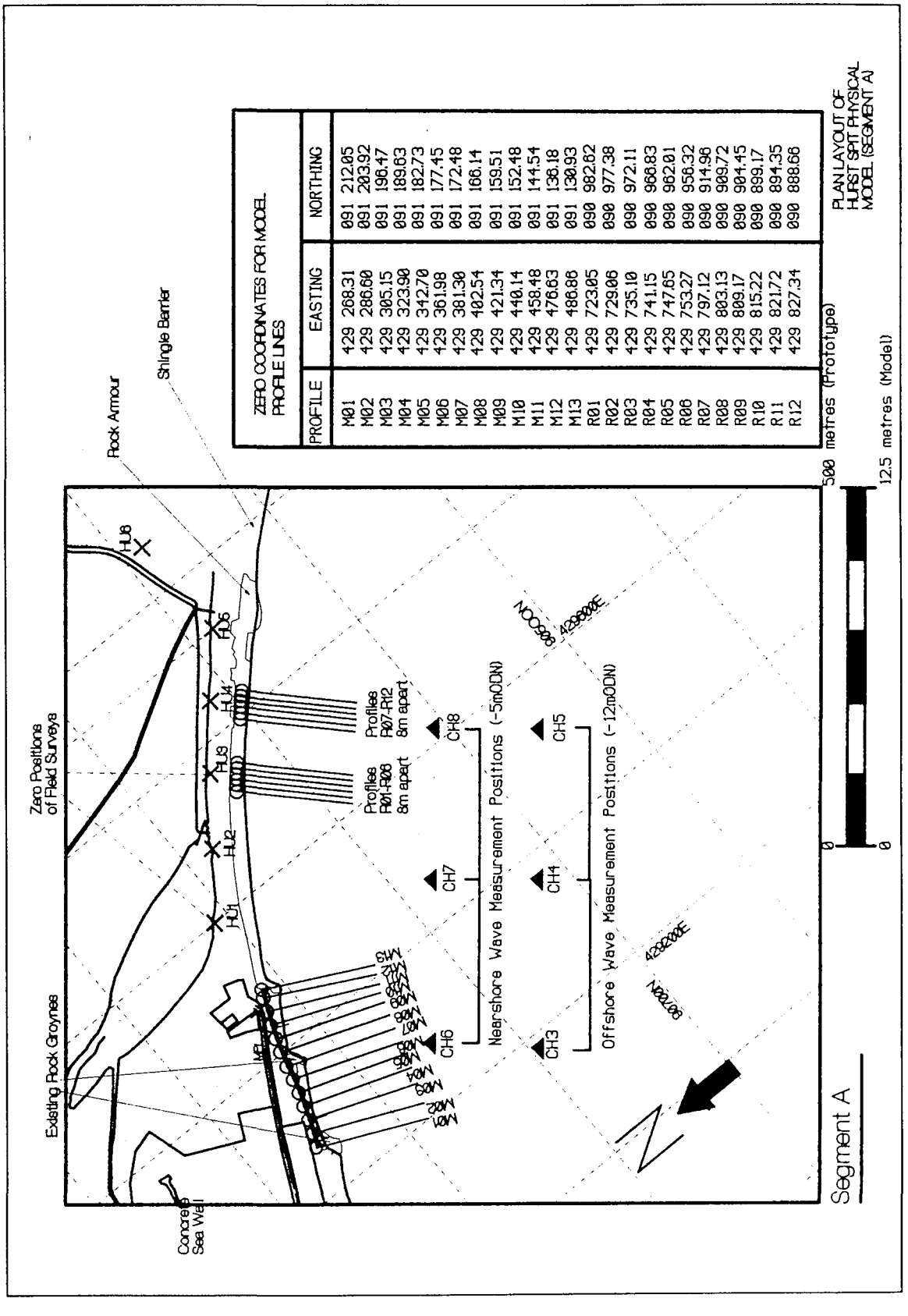

Figure 4.12 Model Test segment A

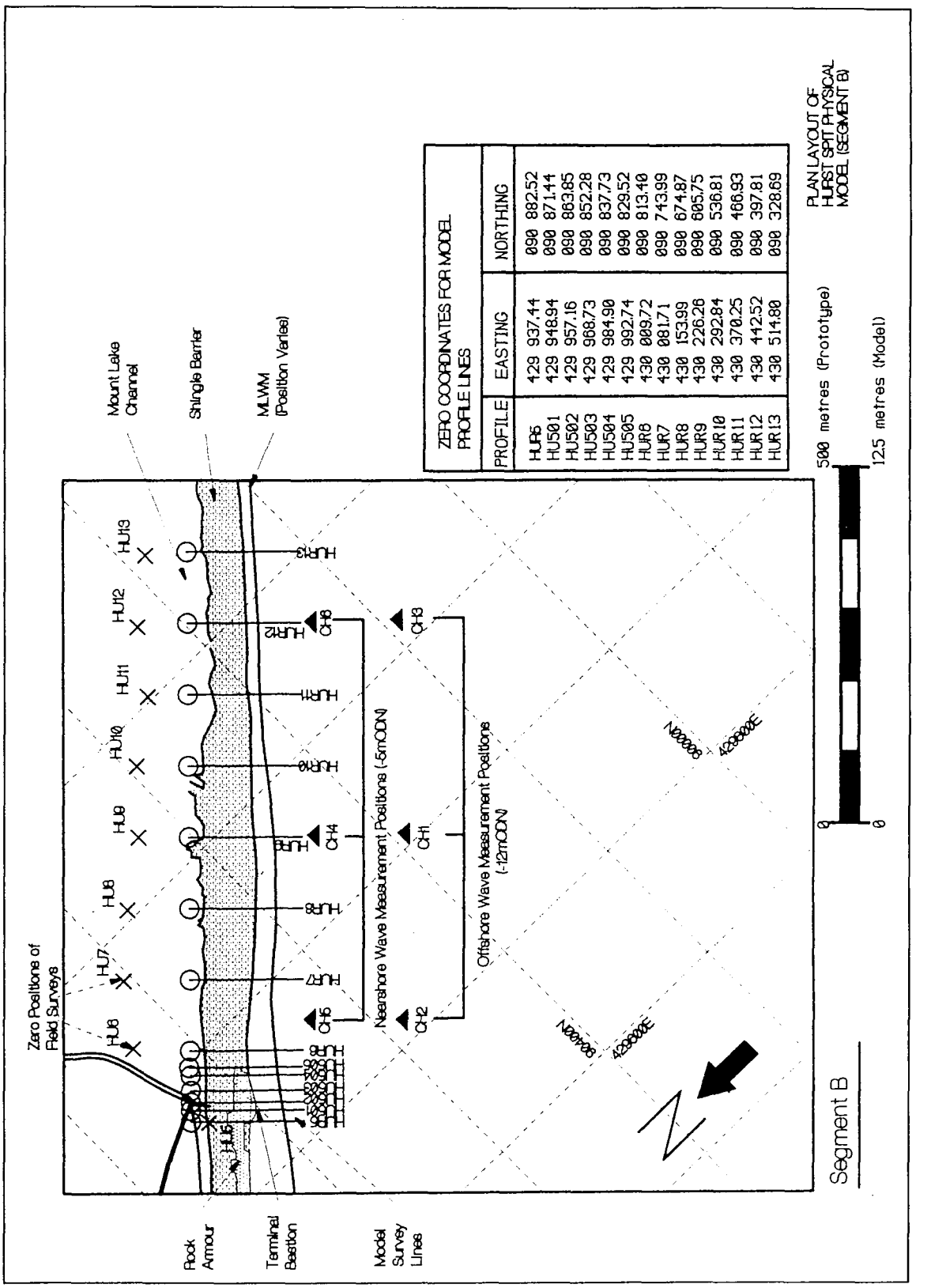

Figure 4.13 Model Test segment B

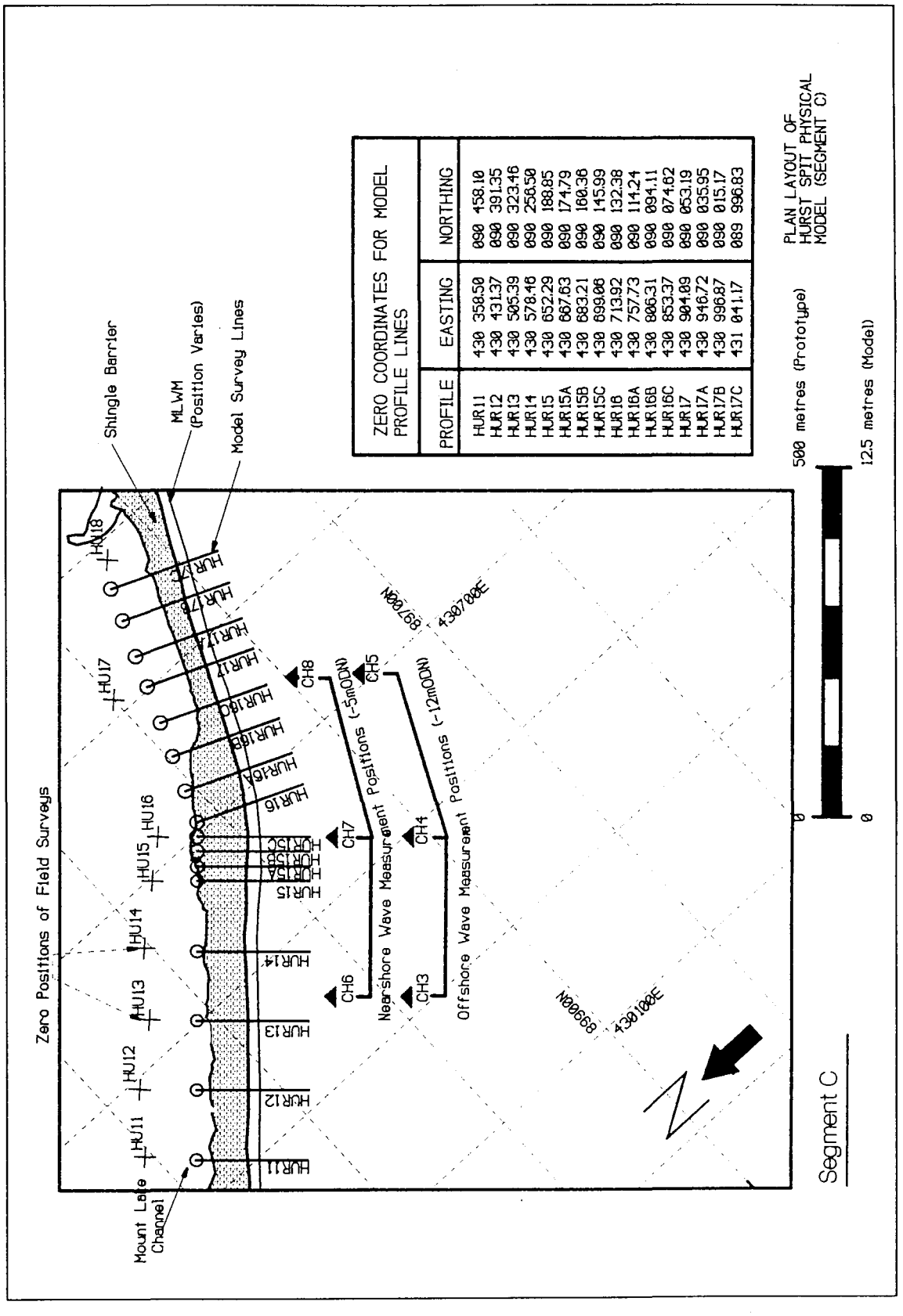

Figure 4.14 Model Test segment C

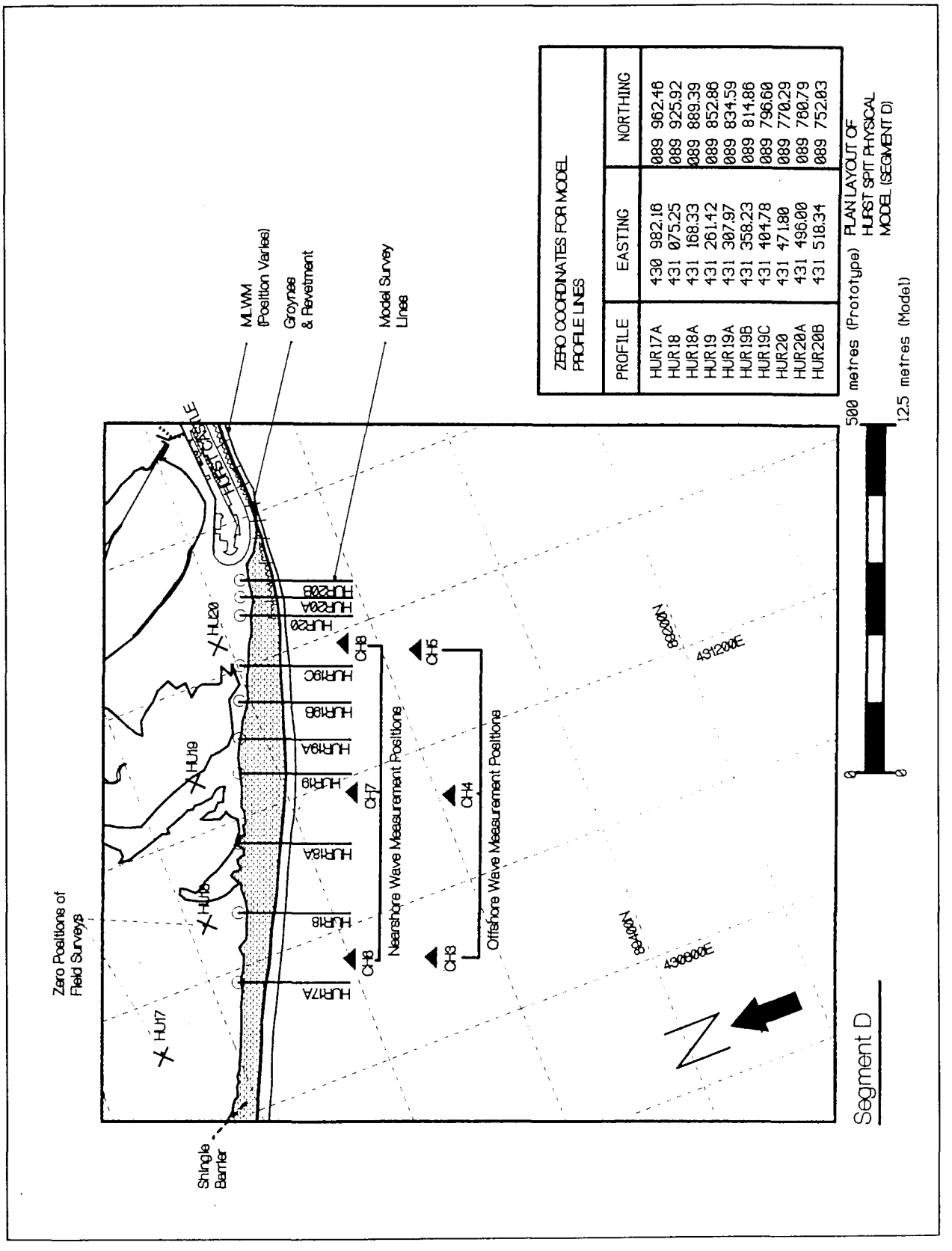

Figure 4.15 Model Test segment D

4.4.5 Model test variables

The model studies were designed using the results of the numerical modelling and field hydrodynamic studies (Chapters 5 and 6, see below). Key variables were selected to develop a framework for examination during the test programme. The most important forces acting on the beach at this site are storm waves, in combination with extreme water levels. Hence, a range of such conditions were defined that would allow the effects of various combinations of wave conditions and water levels to be examined.

(a) Wave Conditions

Wave variables tested in the model included significant wave height, period, direction and steepness. Site specific test conditions selected included (predicted) extreme storms, with probabilities of return period of 1 in 1, 5, 50 and 100 years. Additional wave conditions were tested in a systematic framework, to examine the influence of a range of wave variables. As wave conditions vary along the length of Hurst Spit (Section 5.4) it was necessary to reproduce different conditions, representative of the same events, for each of the four model segments. The severe storms of 1989 were reproduced to provide model validation against real events and identify the response of Hurst Spit to those events.

Whilst storm waves control the profile response of the spit, the longshore transport of shingle occurs throughout the year under significantly less severe conditions. Hence, longshore transport rates were compared for the various layouts. These tests were carried out using a morphological average wave condition, derived from the wave and sediment transport numerical models. A different incident wave condition was required for each model segment, to provide the morphological average.

Each wave condition for the model was defined using a standard spectral shape (JONSWAP), significant wave height and mean zero crossing period (Figure 4.16).

The wave approach angle varies at the beach, depending upon wind direction and wave refraction. As waves approach the spit, they become long-crested due to the influence of the bathymetry. Wave conditions at the shoreline may vary considerably along the

length of Hurst Spit (Section 5.4); consequently, different conditions might be expected at the shoreline for the same offshore condition in each of the model segments. A range of wave approach angles were tested, to accommodate this spatial variation. It was suspected that different incident wave angles would result in a different beach response, especially near to structures (such as groynes). Different angles of wave attack, representative of the likely range of incident conditions, were examined.

(b) Water Levels

Field observations of the response of Hurst Spit to storm action has indicated (see Chapter 6), that water level is a critical variable for describing the profile performance of a shingle barrier beach. Virtually all the storms which have caused overwashing of Hurst Spit occur at higher water levels than the normal tidal predictions. As the tidal range over the area is small (2.2m on springs), this surge component is extremely important; it can be greater than 50% of the maximum tidal range. Surge levels of 0.5m, 1m and 1.4m above MHWS were selected for testing, together with MHWS, on the basis of the results of earlier studies (Nicholls, 1985). These conditions provided a realistic range of extreme water levels which, in combination with various storm wave conditions, could be expected to result in significant changes to the beach profile. The same four water levels were used to provide a systematic analysis of the influence of water level, on all of the beach geometries tested. Freeboard conditions were varied further, by changing the crest elevation to investigate the influence of beach geometry on the profile development. The range of water levels tested also provided a method of analysing the influence of a depth-limited foreshore, for a range of wave and water level conditions.

4.4.6 Wave calibration

Waves were generated in the model using two mobile hydraulic wave paddles; these produced long crested waves, with a wave crest length of 25m (Plate 4.1). The paddles produced unidirectional waves, typical of the (long-crested) waves which form as waves refract towards the shoreline. The incident wave direction was varied by

moving the position of the wave paddles, relative to the shoreline. The paddles were driven by a double acting hydraulic ram, controlled by a servo system. The wave generation system allowed a random, but repeatable, sequence of waves of any defined spectral shape to be generated. Waves were generated from a time-varying voltage signal, driven by a computer program. On specification of a given spectral shape (e.g. JONSWAP), a time-series voltage signal was calculated which produced the specified spectral shape. On running the programme, the computer stepped through a binary shift register, to produce a time-varying voltage signal to the paddle actuator. Different transfer functions were calculated for each water level. Following calibration of the paddles, it was possible to drive the two paddles simultaneously to produce the same output signal.

The paddles could create any specified wave conditions, within their generating range of paddle stroke, frequency and working water depth; this permitted significant wave heights of up to 4.4m (i.e. 110mm in the model) to be generated. Storms which have occurred in the past, or which might statistically be expected to occur every 100 years, could be reproduced.

A series of wave calibration tests were run, prior to the model tests. Whilst the paddles could reliably reproduce waves of a given spectral shape, with a fixed peak period, the characteristic amplitude of the peak could be varied by a simple voltage gain control; this was used to calibrate the wave height.

Each wave condition was calibrated at each water level, to determine the appropriate gain setting. Waves were recorded in the model by twin wire resistance type wave probes, with an accuracy of +/- 0.25mm (or 0.01m, at prototype scale). The probes measured changes in instantaneous water levels, by detecting a change in the resistance across two wires as the water surface moves. A time-varying voltage analogue signal, proportional to the water level was sent, via an analogue to digital converter, to a PC computer; this recorded digital records of changes in water level, at the designated sampling frequency. The standard procedure adopted provided a digitisation rate of about 25 points per wave (approximately 25Hz), which was sufficient to describe the shape of the wave forms.

Waves were monitored at an array of wave probes set out in the wave basin. Six wave probes were used to calibrate and monitor the wave conditions; these were distributed in deep water, at the wave refraction prediction points and close to the toe of the beach (at locations in shallow water where wave breaking occurs) (Figures 4.12-4.15). Wave conditions, defined by refraction modelling provided the required conditions for the model testing: these were calibrated at the offshore wave probes. The inshore probes were used to monitor the attenuation of waves, as they move shorewards, thereby allowing the relationship between deep and shallow water (wave) conditions to be compared.

Two types of wave analysis were used, in both the model calibrations and the test programme. Spectral analysis, using a fast-fourier transform of the instantaneous surface elevations, was used to calibrate the wave conditions; this utilised analysis cycles of short sequences (typically, 300 waves). The analysis provided a measure of wave energy within 16 frequency bands, calculating the significant wave height using the method of moments ($H_S = 4Mo^{1/2}$) and the mean zero crossing period. Additionally, waves were monitored using a wave counting analysis program; this provided the opportunity to examine extremes and the probability distributions of very long sequences of waves, with the same spectral characteristics.

The calibration exercise was repeated for the wave conditions required, at each of the four water levels (see above). This process was repeated: (a) on each occasion that the paddle angle was altered; and (b) each time the sea bed bathymetry was remoulded. A summary of the calibrated wave conditions for the tests are shown in Table 4.1 and typical wave spectra are shown on Figure 4.16.

Test Segment (Fig. 4.9)	Hs (m)	Tm (s)	SWL (mODN)	Storm Return Period (Years)	Wave (^{O}N)	Surge height above MHWS(m)
B	2.7	8.4	0.87	1:1	225	0
B	3.0	8.4	1.37	1:1	225	0.5
B	3.1	8.3	1.87	1:1	225	1
B	3.4	8.3	2.27	1:1	225	1.4
B	3.0	9.0	0.87	1:5	225	0
B	3.1	9.0	1.37	1:5	225	0.5
B	3.3	8.8	1.87	1:5	225	1
B	3.7	8.8	2.27	1:5	225	1.4
B	3.4	9.6	0.87	1:100	225	0
B	3.4	9.6	1.37	1:100	225	0.5
B	3.6	9.4	1.87	1:100	225	1
B	3.6	9.4	2.27	1:100	225	1.4
C	2.6	9	0.87	1:1	225	0
C	2.6	9	1.37	1:1	225	0.5
C	2.7	9	1.87	1:1	225	1
C	2.8	9.1	2.27	1:1	225	1.4
C	2.9	9.5	0.87	1:5	225	0
C	2.9	9.5	1.37	1:5	225	0.5
C	3.1	9.5	1.87	1:5	225	1
C	3.1	9.7	2.27	1:5	225	1.4
C	3.5	10.4	0.87	1:100	225	0
C	3.3	10.4	1.37	1:100	225	0.5
C	3.3	10.4	1.87	1:100	225	1
C	3.5	10.4	2.27	1:100	225	1.4
D	2.1	9.6	0.87	1:1	220	0
D	2.4	9.1	1.37	1:1	220	0.5
D	2.4	9.1	1.87	1:1	220	1
D	2.7	9.1	2.27	1:1	220	1.4
D	2.4	10.2	0.87	1:5	220	0
D	2.6	9.7	1.37	1:5	220	0.5
D	2.6	9.7	1.87	1:5	220	1
D	2.7	9.6	2.27	1:5	220	1.4
D	3.0	10.9	0.87	1:100	220	0
D	3.0	10.6	1.37	1:100	220	0.5
D	3.0	10.6	1.87	1:100	220	1
A	2.9	8.4	0.87	1:1	220	0
A	3.1	8.4	1.37	1:1	220	0.5
A	3.3	8.4	1.87	1:1	220	1
A	3.6	8.4	2.27	1:1	220	1.4
A	3.0	9.7	0.87	1:5	220	0
A	3.7	9.6	1.37	1:5	220	0.5
A	3.7	9.6	1.87	1:5	220	1
A	3.8	9.6	2.27	1:5	220	1.4
A	4.1	8.4	0.87	1:100	220	0
A	4.4	8.4	1.87	1:100	220	1

Table 4.1 **Summary of wave calibrations used for storm response test programme.**

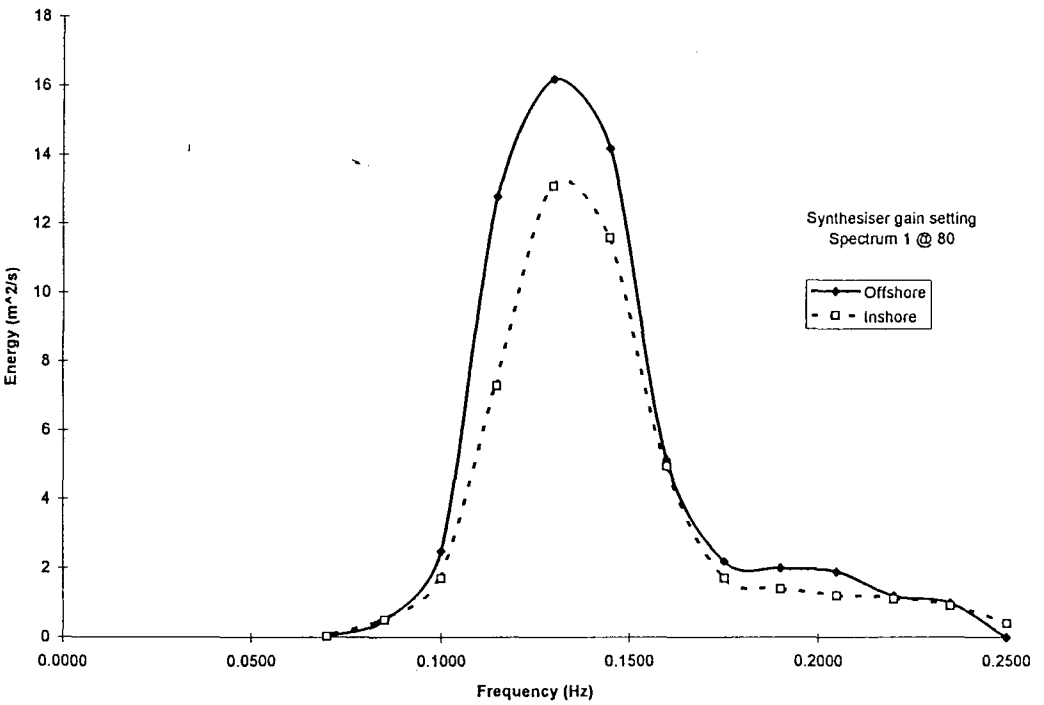

Figure 4.16 JONSWAP wave spectra measured during the model calibration

4.4.7 Test programme

Following completion of wave calibrations, further calibration studies were carried out to investigate the mobile bed model performance. Whilst mobile bed physical modelling using lightweight sediments is well established for assessing the profile performance of shingle beaches, it has not been used to evaluate the 'roll-back' of a shingle spit, subject to overwashing. Data derived from the field surveys of the response of Hurst Spit to the severe storms of October and December 1989 (Section 6.5), together with the corresponding records of wave and water level conditions, provided an ideal combination of conditions for validation of the model. Consequently, tests were designed to reproduce these events (see Chapter 7).

Following calibration, the first phase of the (model) tests was to identify the response of Hurst Spit (together with proposals for beach renourishment), to severe storm action. Test conditions were derived from the statistical analysis of the results of the numerical modelling of waves (Chapter 5).

The second phase of testing was designed to expand the validity of the model test results, to a much wider range of conditions. A wide range of combinations of structure geometry, wave and water level conditions and bathymetry were tested; this was subsequent to the site specific studies at Hurst Spit; providing the basis for an extensive empirical framework of results. The objectives of this phase of the studies drew upon the results of the site-specific studies at Hurst Spit, allowing variables to be extended (see below).

(i) Identify the influence of beach geometry variables on profile response of the shingle beach, including: crest width; crest elevation (freeboard); foreshore slope angle; initial beach slope angle; and beach cross sectional area.

(ii) Identify and quantify the influence of each of the following force variables, on the response of the shingle beach: wave height parameters; mean zero crossing wave period; spectral shape; wave steepness; water depth at the toe; and freeboard.

Details of the range of conditions tested are summarised below (Table 4.2) and presented in full in Appendix 3.

Variable	Range
Significant wave height	1.0 to 4.1m
Mean wave period	7.4 to 10.9s
Incident wave angle (relative to beach normal)	0 to15^{O}
Freeboard	-0.4 to 7.8m
Beach width at water level	0 to110m
CSA above still water level	0 to 400m^2
Water level	1.4m

Table 4.2 Summary of the ranges in variable used in the model tests.

4.4.8 Model test procedures and data collection

A common test procedure was adopted for the whole of the test programme; this enabled the direct comparison of results to be undertaken, for each different model configuration. Certain of the data collection techniques were common to all the tests; others were carried out for specific purposes. Each test was recorded by using an aerial view video camera and the collection of observations, to describe the beach and structure response. Waves were recorded in all of the tests, at each of the 6 wave probes (Figure 4.11). A wave-counting analysis programme WARP was used to analyse the wave data.

(a) Beach Profile Measurements

Each beach cross section was constructed by moulding the beach to templates, either to the design profile or to a surveyed profile. Following construction, each section was surveyed along a number of predefined profile lines (at a longshore interval not exceeding 100m), with a computer-controlled bed profiler (Plate 4.1). Closely-spaced lines were surveyed in some of the tests; this was in order to examine spatial variation of the beach response, or where the performance of specific structures were monitored. The plan layout and location of the survey lines are shown in Figures 4.12-4.15. Beach profiles were resurveyed following each of the tests, at a nominal horizontal increment of 1m. This approach provided sufficient information to describe the profile, which was typically 100-150 m in length, and which tends to change shape gradually. Although the high-resolution profiling system provided data at vertical and horizontal resolution of +/-1mm (model) or +/-40mm (prototype), the very steep upper beach profile is not described in detail; this is due to the horizontal digitisation rate. Ideally, digitisation of the beach profile should be at a closer spacing, to describe the changes over the steep upper part of the beach profile.

The bed profiler (Plate 4.2) was originally designed to provide continuous profiles over sand beaches (Hydraulics Research, 1988, HR, 1991); this was adapted for use on anthracite beaches, utilising an incremental control system.

(b) Beach profile response tests

Water levels were set to a pre-determined level for each of the tests; a sequence of waves, corresponding to the calibrated conditions were then run. The test duration was fixed at 3 hours (at full-scale) for the profile response tests (Appendix 3). This was sufficiently long to enable an equilibrium beach profile to form at the water level tested. For comparison, previous work (Powell, 1990) has shown that the beach profile form will stabilise after approximately 500 waves.

The standard procedure adopted for the site specific studies was to run the 1:1 year return period wave conditions, at each of the (four) water levels; this commenced at the lowest level, stepping upwards through the sequence. The water level was lowered then to the lowest level, with the process being repeated for the 1:5 year and 1:100 year storms: this approach was utilised for the site specific tests at Hurst Spit together with more generalised tests on beaches of other geometries. In many of the early tests, the full sequence of tests could not be run, as the test section failed due to breaching of the shingle beach. Additionally, the model test section was rebuilt after some of the site specific tests, in order to establish which (if any) single event would cause breaching of Hurst Spit.

Plate 4.1 ***The layout of the model wave basin, at HR Wallingford***

Plate 4.2 ***Details of the bed profiler used in the model tests, at HR Wallingford***

CHAPTER 5: RESULTS AND DISCUSSION - NUMERICAL MODELLING OF WAVE CLIMATE

5.1 OFFSHORE CONDITIONS

An offshore directional wave climate was derived for Christchurch Bay, during an earlier study, using wind data from Portland for the period 1974-1988 (Hydraulics Research, 1989b). The original time-series of wind records was extended to February 1990 for this investigation, using additional data from the meteorological office. A revised offshore wave climate was generated, using the same model and calibration as in the earlier (Hydraulics Research, *op cit*) study. The HINDWAVE model together with the method used to calculate wave climate from wind data, are described by Hawkes(1987).

The updated scatter diagram of wave height against wave direction, at the offshore point (Figure 4.8), are listed in Table 5.1. The table presents the probability of any combination of significant wave height and wave direction occurring, in parts per 100,000. The distribution of wave heights and periods is similar to that for the period 1974 to 1988 (Hydraulics Research, *op. cit*). The spatial distribution and percentage of occurrence of bands of significant wave heights, derived from the updated hindcasting study, are shown in Figure 5.1. The distribution of wave conditions demonstrates that prevailing wave conditions occur within the 225 - 255^{O} (relative to North) direction sector. Significant wave heights in excess of 6 m were not generated outside of this sector; this represents the combined effects of predominant wind direction and fetch lengths, which are here in excess of 500 km. The data set indicates also a secondary peak, within the direction sector 105-135^{O}. Probabilistic analysis of the revised data set indicates that the probability of occurrence of waves greater than 6 m is 0.0001: this compares with a probability of 0.00007 for the same conditions, for an earlier study (Hydraulics Research, 1989b). As the same model was used, approximately 88% of the data was used in both cases; it is suggested that conditions between 1988-1990 were slightly more stormy than during the previous 15 years. This interpretation is confirmed by comparison of the scatter diagrams; these indicate a

higher frequency of occurrence for the more severe storm events, during 1988-1990. The distribution of probabilities of exceedence, for the two data sets is shown for significant wave heights >3 m in Figure 5.2. The variation demonstrates the value of using long and recent data sets, for the determination of a regional wave climate. It demonstrates also the problems of introducing bias into the data sets, using short time-series; it indicates the level of sensitivity of the probability distribution, to relatively small changes in the frequency of more extreme events.

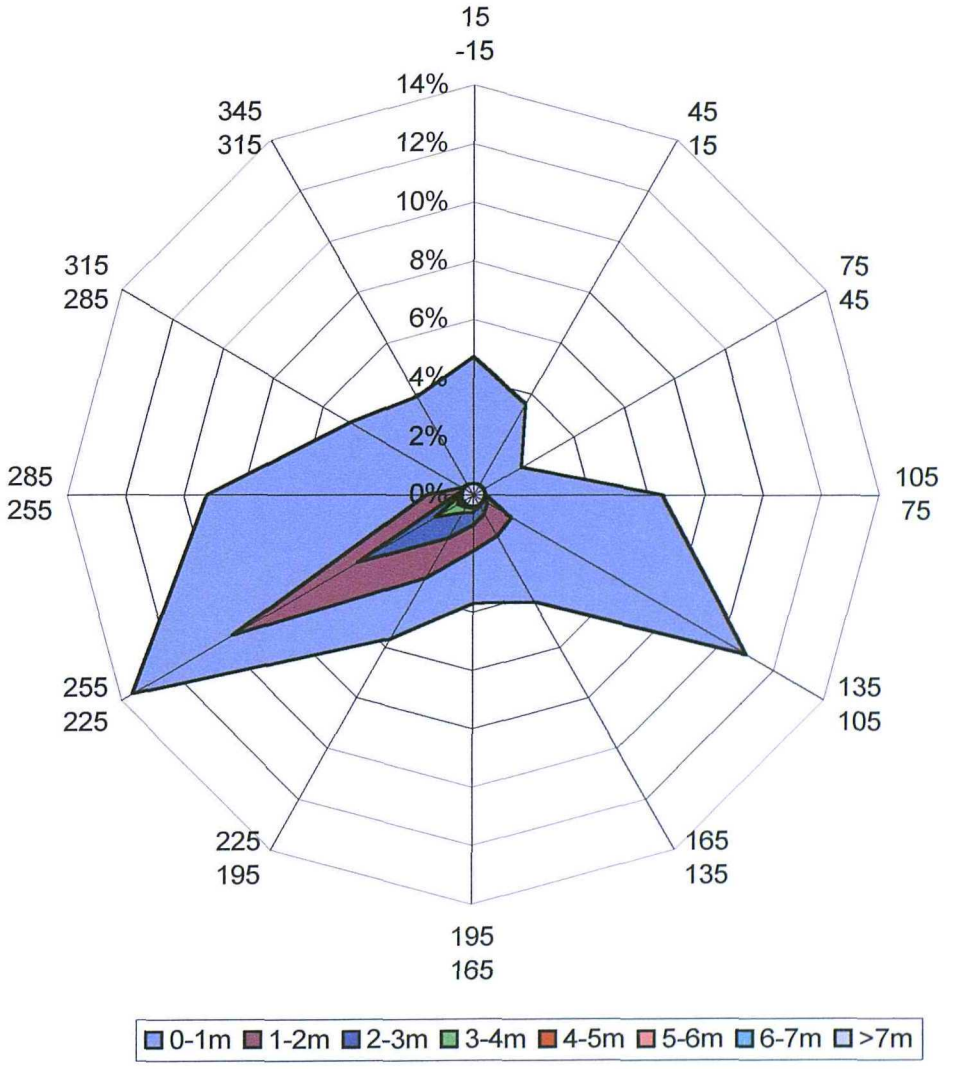

Figure 5.1 Wave direction and height scatter plot. Wave height distributions are shown in 1 m bands, in 30^{O} direction sectors and percentages of annual occurrence.

H1TO H2		P (H>H1)	Wave angle (° relative to North)											
			-15 15	15 45	45 75	75 105	105 135	135 165	165 195	195 225	225 255	255 285	285 315	315 345
0.0	0.2	0.9427	1130	615	366	1537	1560	288	235	241	438	1177	1429	1049
0.2	0.4	0.8421	1922	1765	646	2356	3464	1197	616	781	2246	2530	1351	1372
0.4	0.6	0.6396	898	646	387	1437	2857	944	1088	1667	2568	2112	668	478
0.6	0.8	0.4821	315	185	72	467	963	437	228	446	2381	1419	707	373
0.8	1.0	0.4022	36	8	17	265	1013	673	877	1741	3195	1015	224	158
1.0	1.2	0.3100	14	3	4	75	656	242	259	408	2324	525	160	54
1.2	1.4	0.2628	4	0	3	18	529	378	438	761	2485	493	51	11
1.4	1.6	0.2111	2	0	0	16	316	319	212	856	2505	285	11	4
1.6	1.8	0.1658	0	0	0	0	58	191	349	342	835	219	4	0
1.8	2.0	0.1459	0	0	0	0	138	219	243	433	2257	126	1	0
2.0	2.2	0.1117	0	0	0	0	83	131	285	511	1097	84	0	0
2.2	2.4	0.0898	0	0	0	0	67	90	105	227	976	78	0	0
2.4	2.6	0.0743	0	0	0	0	30	71	296	655	1512	43	0	0
2.6	2.8	0.0483	0	0	0	0	24	117	65	109	232	24	0	0
2.8	3.0	0.0426	0	0	0	0	9	31	52	191	1174	54	0	0
3.0	3.2	0.0275	0	0	0	0	20	49	112	102	331	2	0	0
3.2	3.4	0.0213	0	0	0	0	4	26	55	83	400	25	0	0
3.4	3.6	0.0154	0	0	0	0	0	16	54	63	235	1	0	0
3.6	3.8	0.0117	0	0	0	0	9	6	25	78	149	7	0	0
3.8	4.0	0.0089	0	0	0	0	0	8	7	42	184	16	0	0
4.0	4.2	0.0064	0	0	0	0	15	1	44	21	150	0	0	0
4.2	4.4	0.0041	0	0	0	0	0	2	17	20	24	4	0	0
4.4	4.6	0.0034	0	0	0	0	0	0	11	15	96	6	0	0
4.6	4.8	0.0021	0	0	0	0	0	1	6	16	80	0	0	0
4.8	5.0	0.0011	0	0	0	0	0	0	3	1	29	4	0	0
5.0	5.2	0.0007	0	0	0	0	0	1	3	7	3	0	0	0
5.2	5.4	0.0006	0	0	0	0	0	0	0	1	8	0	0	0
5.4	5.6	0.0005	0	0	0	0	0	0	3	1	14	2	0	0
5.6	5.8	0.0003	0	0	0	0	0	0	4	2	3	0	0	0
5.8	6.0	0.0002	0	0	0	0	0	0	0	0	8	0	0	0
6.0	6.2	0.0001	0	0	0	0	0	0	0	0	4	0	0	0
6.2	6.4	0.0001	0	0	0	0	0	0	0	0	0	0	0	0
6.4	6.6	0.0001	0	0	0	0	0	0	0	0	3	0	0	0
6.6	6.8	0.0001	0	0	0	0	0	0	0	0	6	0	0	0
6.8	7.0	0.0000	0	0	0	0	0	0	0	0	0	0	0	0
7.0	7.2	0.0000	0	0	0	0	0	0	0	0	0	0	0	0
7.2	7.4	0.0000	0	0	0	0	0	0	0	0	1	0	0	0
Parts per thousand for each direction			46	34	16	65	125	58	60	104	296	109	49	37

Table 5.1 Annual distribution of wave height and direction - Offshore

Notes: (i) Location - Offshore, Christchurch Bay 1/1/74 - 28/2/90, data in parts per hundred thousand, significant wave height in m

(ii) Significant wave height in m.

(iii) Data source HR Wallingford

5.2 EXTREME OFFSHORE WAVE CONDITIONS

The effects on the probability distribution of offshore significant wave heights, of the inclusion of data collected between 1988-1990, are demonstrated in Figure 5.2; this describes the probability distributions for significant wave heights >3 m, for both data sets. The extreme significant wave heights and their associated directional offshore wave energy spectra were recalculated, to include data derived between 1989 and 1990. Probabilities determined from the wave scatter plot (Table 5.1) have been extrapolated, utilising a three parameter Weibull distribution; this was fitted to the distributions of significant wave heights for each of the direction sectors, to determine the extreme conditions: the methodology is discussed in detail by Hydraulics Research (1985, 1989b). The extreme predicted offshore conditions were not significantly different from those derived in the study undertaken by Hydraulics Research (1989b). This conclusion is not surprising, despite the short-term variations in the distribution of wave heights; it indicates that the hindcast conditions for 1989-1990 were fairly typical of the longer data set, which was used in the earlier study.

The distribution and magnitude of wave heights and periods, for selected 30^{O} direction sectors, are listed in Table 5.2 . Conditions were calculated only for those directions centred between 120-255^{O}N. The fetches outside of this sector are all less than 25 km; these would not produce wave conditions which would impact on crest evolution of Hurst Spit. The largest predicted offshore significant wave heights arise from the direction sector 225-255^{O}N.

Full directional spectra were generated for each of the extreme predictions, using the JONSEY element of the HINDWAVE model. These data provided the input to the wave refraction models which were used, in turn, to provide extreme input conditions to the physical model studies. The mean wave periods associated with the wave conditions were also determined; these demonstrate high dimensionless wave steepnesses, ranging between 0.0518 - 0.0690, for the extreme conditions. Such wave steepnesses are characteristic of rapidly-developing storm conditions. The wave steepness tends to increase with the return period, although wave conditions generated from the 240^{O} sector have slightly lower steepnesses. Such conditions correspond with

a longer generation time and a more fully-developed sea state; this, in turn, reflects the longer fetches across this sector.

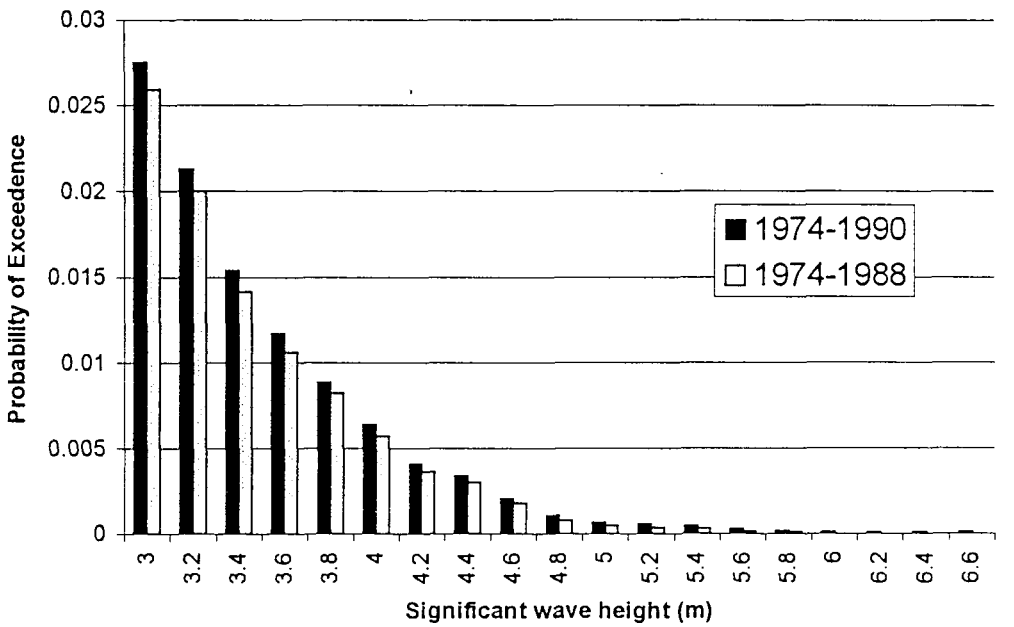

Figure 5.2 Comparison of probabilities of exceedence of significant wave heights derived by hindcasting, for data sets collected between 1974 - 1988 and 1974-1990

Wave Direction (°N)	Return period (years)	Significant Wave Height (H_s (m))	Significant Wave Period (T_m (s))
135	1	3.72	6.5
	5	4.65	7.1
	20	5.47	7.5
	50	6.02	7.8
	100	6.44	8.0
150	1	3.90	6.5
	5	4.53	6.9
	20	5.03	7.1
	50	5.34	7.3
	100	5.57	7.4
180	1	4.91	7.1
	5	5.71	7.5
	20	6.36	7.8
	50	6.77	8.0
	100	7.07	8.1
210	1	4.82	7.3
	5	5.52	7.7
	20	6.02	8.0
	50	6.42	8.2
	100	6.68	8.3
240	1	5.84	8.5
	5	6.60	8.9
	20	7.22	9.3
	50	7.61	9.5
	100	7.90	9.6
All Directions	1	5.91	8.6
	5	6.65	8.9
	20	7.26	9.3
	50	7.65	9.5
	100	7.94	9.6

Table 5.2: Predicted extreme offshore wave conditions

Note: the above figures are derived from 17 years of simulated wave data (1974-1990) at 50° 38.63'N 1° 38.17'W. The extreme conditions are averaged over a period of 1 hour. (Data source HR Wallingford)

5.3 *NEARSHORE WAVE CLIMATE*

Back-tracking ray modelling -(OUTRAY)

A series of transfer functions were generated using the OUTRAY model, for each of three water levels and directions of offshore wave attack, at each of a number of locations (Figure 5.4). These transfer functions convert directional wave climate matrices, derived from the HINDWAVE model, to provide nearshore wave conditions; these take into account the effects of refraction and shoaling, but not wave breaking. The data derived is in the form of directional spectra (Figure 5.3).

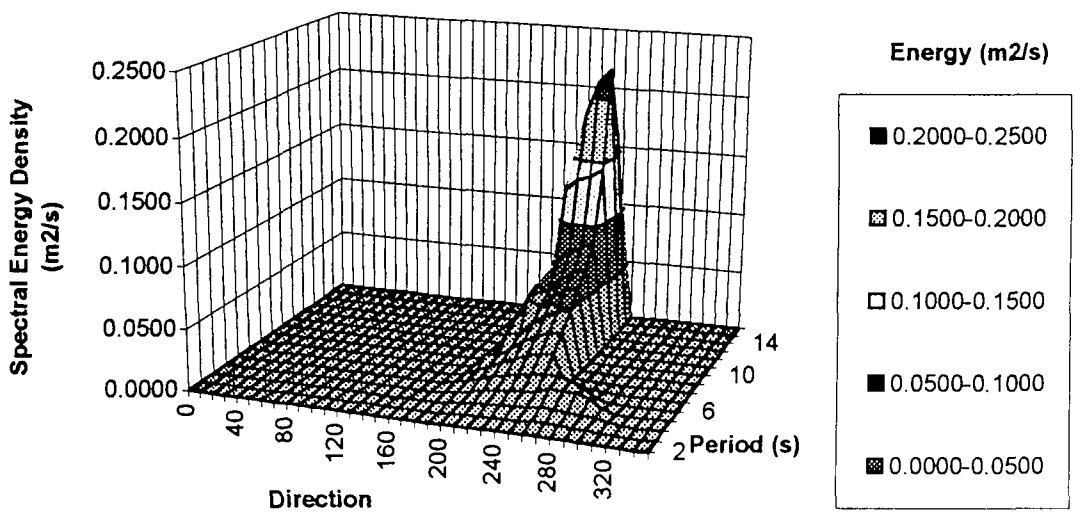

Figure 5.3 Example of hindcast offshore directional wave energy spectrum, derived using the JONSEY wave prediction program. (H_s =6.9m, T= 9.6s, Direction = 240^O Hindcast point = 50^O 38.61' N, 1^O 38.17'W Christchurch Bay, (see Figure 4.3) Conditions derived for wind speed = 31.4 m/s, wind direction = 258^O, generation period = 24 hours)

Forward-tracking ray modelling (INRAY)

Initial runs of the INRAY model showed wave rays (orthogonals) converging and crossing each other, as they travelled over the western half of Dolphin Sands (about 6 km to the south of Hengistbury Head), for an offshore direction of 240N^{O} and high wave periods (Hawkes *pers com*): this phenomenon is known as a caustic. Caustics have been reproduced using laboratory experiments and identified by studying aerial photographs of the ocean (Chao and Pierson, 1971). Studies undertaken in wave basins and theoretical analysis have demonstrated that, if a wave ray passes through a caustic region, it follows eventually the original ray path and wave conditions can be determined as if no caustic activity had occurred. The region of interest in the present study is well outside the caustic influence; it should therefore, have no effect on wave conditions incident on Hurst Spit. The minimum water depth over Dolphin Sand, at the lowest water level to be used in the model, is about 12.3m; hence, wave breaking is unlikely to occur in this area. However, the reduction in wave height, due to breaking, is dependent upon wave height; wave period and water depth. Since the wave height was increased unrealistically by the model, in the region of the caustic, an excessive amount of energy was dissipated by wave breaking over Dolphin Sand (Figure 3.1). Hence, the inshore wave height was much smaller than might reasonably be expected. To solve this particular problem, wave breaking was restricted in the model for waves around Dolphin Sand, if the significant wave height (H_s) was less than 0.66 times the total water depth (Hawkes, *pers com*).

Validation of numerical modelling

The deployment of a waverider buoy in Christchurch Bay, between 1987-1989 (Hydraulics Research, 1989a), presented an opportunity to assess the validity of the numerical modelling methods and to provide calibration to the synthetic wave data. Tests were carried out to determine the effect of wave breaking and the friction factor, within the wave refraction model, on the wave height at the waverider site. The wave condition for the 1 in 100 year storm from 240^{O}N (Hydraulics Research, *op. cit*) was used as input to the model, for these calibration tests. This wave condition also provided the highest offshore wave height to be used as input to the physical model, during this investigation.

The results from the tests indicated that, when friction effects are excluded from the model, the reduction in inshore wave height due to breaking is about 40%. Two

friction factors were used as input to the model: (i) a value which has been generally found to provide reasonable results at other sites where friction was important (0.016) (Hydraulics Research, 1989d); and (ii) a very much higher value (0.5). Wave breaking was included in these test runs. The reduction in inshore wave height due to friction and breaking was 46.1%, for results derived when using the average friction factor: the very high friction factor resulted in an 86% reduction (Hawkes, *pers com*).

The INRAY model was run also with a constant friction coefficient for the whole of the model grid, before it was eventually reconfigured to calculate a friction coefficient (from the friction factor), wave height and water depth at each grid node. Once again, a value was used which has been found to give good results at other sites, where friction has been important. The reduction in wave height, due to friction and breaking in this case, was 33%.

The wave height (H_S) obtained from OUTRAY at the 1987-1989 waverider site, for the 1 in 100 year storm from 240^{o} offshore, was 6.15m (without breaking or friction effects being taken into account). Using the average friction factor, the wave height including friction and breaking is:

$$6.15 \times (1 - 0.461) = 3.31\text{m}$$

When the high friction factor was used, the wave height predicted by INRAY at the waverider site (Figure 4.8) was 0.86m: the model suggested an H_S of 4.12m, using the configuration of INRAY with the constant average friction coefficient.

A comparison was made between the numerical modelling results, from the synthetic wave refraction data, with wave data recorded in the study area. An extremes analysis was performed on the data obtained for the period April 1987 to May 1989 (Hydraulics Research, 1989a): the significant wave height expected to be exceeded once in 100 years was predicted at 3.17m . The extremes calculated from the synthetic wave data were based upon hourly-averaged data, whilst those calculated from the measured data were based on 3-hourly records: a small difference is expected therefore. The one-hourly based wave height corresponding to 3.17m was re-calculated to be 3.32m: this indicates a remarkable level of agreement between the measured and synthetic wave data.

The extremes analysis for the waves offshore in Christchurch Bay are highest for the direction sector centred on 240°N. The extreme wave height derived from the predictions, transformed inshore using an average friction factor, compares well with the extreme from the measured data. The friction factor (of 0.5) is too high and the constant friction coefficient version of INRAY does not reduce the wave heights enough, unless a very high coefficient is used. It was decided, therefore, to use the friction factor of 0.016 in the INRAY model.

Comparisons between the measured and synthetic data demonstrate that the model predicts the wave heights well, as they travel towards the waverider site in a zone of relatively straightforward bathymetry. The assumptions made about seabed friction for wave conditions further inshore, in the shelter of the Shingles Banks and adjacent to Hurst Spit (Figure 3.1), could not be tested in a similar manner, however, since there was no validation data available. Hence, the numerical model transformations have to be used without any additional calibration. The complex bathymetry and the wide range of large-scale bed forms in this area (Velegrakis, 1994) present further complications; these may not be dealt with adequately by the numerical model. For example, the effects of friction and breaking are likely to be more significant. Features such as large sand waves and gravel mega-ripples are not taken into account by the model; this is likely to result in the over-prediction of wave heights. Nearshore wave periods may also be affected by the complex bathymetry: in some instances, waves may break and reform at shorter periods as they pass over the Shingles Banks.

Relatively short period waves (3-5 s) have been observed in the North Channel (Figure 3.2) on a number of occasions, when the wind conditions resulted in hindcast waves of 7 - 9 s. Observations made 2 km to the west, outside of the influence of the Shingles Banks, resulted in observed wave periods of 7-9 s, as predicted by the hindcasting methods. Such variation is worthy of further investigation, to determine the range of validity of the numerical models, for the transformation of wave conditions in areas of complex bathymetry and bedforms.

Having established the basic calibration of the numerical model, a series of calculations were carried out to determine wave transformations for a few of the offshore extreme conditions, at 8 locations along Hurst Spit, on the -5m CD contour: this provided a sensitivity analysis of the nearshore wave climate variability along a 3

km stretch of shoreline. The test refraction points were numbered 1 to 8, from west to east (Figure 5.4).

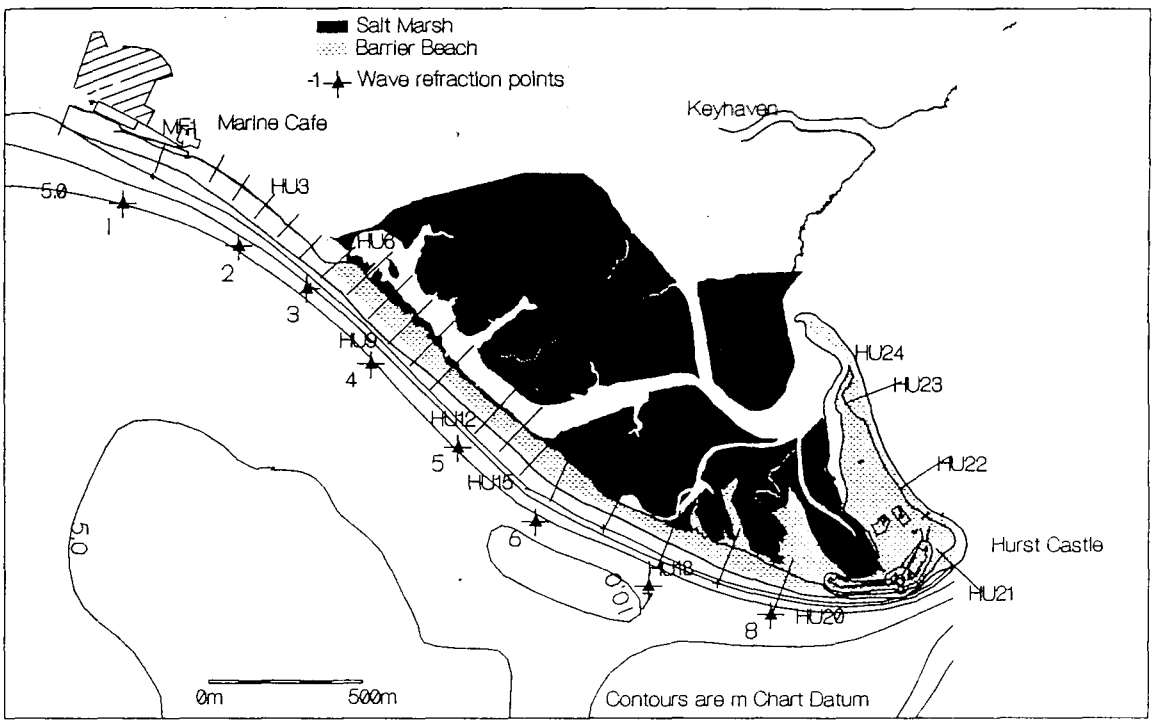

Figure 5.4 Location of Wave Refraction Points off Hurst Spit

Initial examination of the bathymetric charts of the study area have indicated that the complex bathymetry might result in varied conditions, along a relatively short stretch of coastline. Results were required as input to each of the four physical model segments (Figures 4.12-4.15); this required the production of four representative wave-climate data sets. The points representing the centres of the four model beach sections are 2, 4, 6 and 7 (Figure 5.4). The general trend is for the highest wave heights to peak close to the western end of Hurst Spit; they decrease eastwards, along the spit. This pattern is not surprising, as the energy dissipating effects of the Shingles Banks become more significant to the east. However, the trend is complicated by the initial offshore direction of the waves, and the local bathymetry.

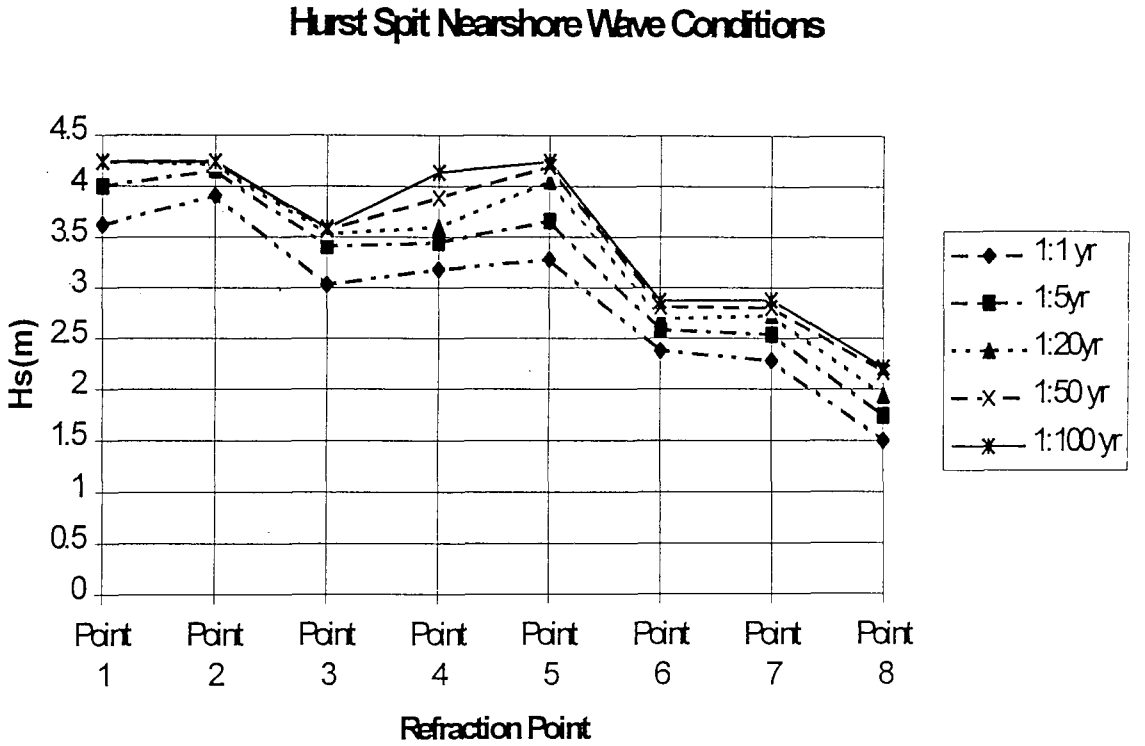

Figure 5.5 Distribution of nearshore wave heights along Hurst Spit, for waves originating from an offshore approach angle of 240^{O}, for different return periods.

Note: for location of refraction points see Figure 5.4.

Extreme waves travelling inshore, from 240^{O} (Figure 5.5), maintain a fairly constant longshore significant wave height on the 5mCD (-6.83m ODN) contour, between Points 1 and 5. This pattern represents the limited influence of the offshore Shingles Banks, towards the western end of the study area, in response to the wave approach angle. The slight reduction in significant wave height at Point 3 represents the localised effects of nearshore bathymetric changes, which cause more energy loss. This local effect has also been noted at the same position, for other offshore angles of wave attack.

There is a rapid reduction in longshore wave height, to the east of refraction Point 5 (Figure 5.5). Wave heights associated with the most extreme events fall by up to 35%,

within a distance of 340m, at Point 6. The significant wave height at Point 8, adjacent to the western flank of Hurst Castle, is reduced to 48% of the wave height at Point 5, within a distance of 1150m, for the most extreme conditions. The longshore reductions in wave height become proportionally smaller for less extreme events, but reductions in wave heights of 50% are still observed for the 1:1 year return period conditions, between Points 5 and 8.

The dramatic effects on the energy reduction at the shoreline can be illustrated in terms of the empirical stability formula used for rock armour (van der Meer, 1988): the term used to incorporate the effects of wave height in these formulae suggests that stability approximates to the cube of the wave height. The ray plots indicate considerable disturbance along the crestline of the Shingles Banks, when waves approach from an offshore angle of 240^{O}N. Some of the wave rays cross each other, resulting in energy loss across the spine of the banks and much reduced wave energy at the eastern end of Hurst Spit. The complex effects generated by the numerical models are realistic in this sense; such patterns can be viewed from the air, across the Shingles Banks.

Changes in wave heights follow a slightly different pattern for waves from 210^{O} offshore (Figure 5.6); these increase in height between refraction Points 1 and 4, where the energy peaks. Slight convergence of the wave rays occurs near to the edge of the offshore banks, in the area of the North Head, resulting in focusing at Point 4. A rapid reduction in wave conditions occurs to the east of Point 4. This change in the longshore significant wave height pattern represents the more marked effects of the Shingles Banks and the Needles Channel (Figure 3.2) at the eastern end of Hurst Spit. An examination of the ray plots produced from the INRAY model indicates considerable losses of energy across the Shingles Banks and North Head (see below).

The sensitivity tests indicate that there is no significant longshore change in the nearshore wave periods at the refraction points; these remain largely unaltered along the length of Hurst Spit. There is clear evidence, however, of a lengthening of the period between the offshore and nearshore sites, due to the effects of refraction. This effect is entirely consistent with the theoretical changes to wave period, which might be expected for the range of conditions examined. Wave periods increase typically by about 10-15% for offshore approach angles lying between 210-240^{O} offshore. This

effect is, not surprisingly, more pronounced for wave conditions which originate from offshore wave angles farthest from the shore-normal.

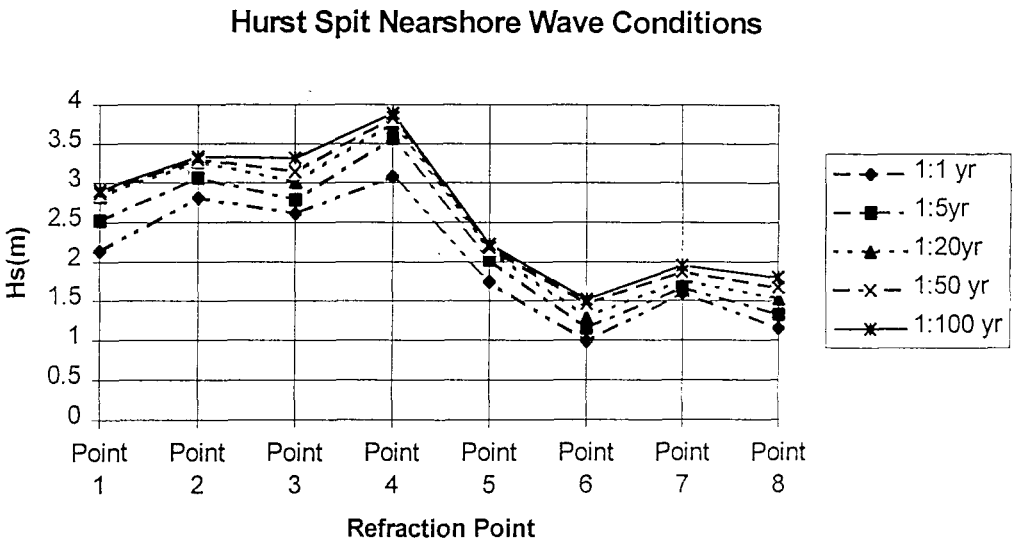

Figure 5.6 Distribution of nearshore wave heights along Hurst Spit for waves originating from an offshore approach angle of 210^{O}, for different return periods.

Note: for location of refraction points see Figure 5.4.

Incident wave directions derived by the model indicate that wave directions turn towards the beach normal as they travel inshore, as anticipated. The ray plots produced by the INRAY model indicate fairly minor direction changes in the angle of approach for waves originating from an offshore direction of 210^{O} N; this is primarily as the waves are already within 15^{O} of the shore-normal (225^{O}N, at the eastern end of Hurst Spit). The model suggests that the extreme wave conditions are likely to approach the shoreline at an angle which is within 5^{O} of the beach-normal in each case, for waves originating from an offshore angle of 210^{O}. Limited refraction occurs for waves originating from an offshore approach angle of 210^{O} (Figure 5.7). Field observations made during storms of the winter of 1996 (Section 6.5.1) support the results of the numerical models in this respect. The expected range of accuracy of the numerical models is +/- 5^{O} at best, even when the bathymetry is reasonably simple and when the grid is at a fine resolution.

The numerical models suggest that waves from 240°N tend to be deflected through the beach normal, so that their inshore direction is more southerly than waves originating from 210°N; this is due to the effects of the complex bathymetry of the offshore bank systems. Closer inspection of the ray paths (Figure 5.8) shows that, for an offshore wave direction of 240°N, the wave energy is split into two directions when it crosses the Dolphin Sands (Figure 3.1). The wave ray traces are plotted at a filtered spacing of 250 m for clarity: the ray spacing actually used, for the determination of nearshore conditions was 5 m. Some energy travels straight over the bank towards Hurst Spit, whilst the remainder is refracted over the Shingles and the deep channel behind it; this is then refracted and partially reflected, towards Hurst Spit. The inshore conditions for this direction are, therefore, a combination of two wave trains: one from around 240°N, with the other from the sector 160-220°N. Unfortunately, these wave trains could not be separated numerically in the models, to provide the relative magnitudes of the bi-directional wave climate; this is a significant limitation of the modelling. In particular, the conditions predicted at Point 7, which is most affected by this anomaly, may be less reliable than those at other prediction points.

A further limitation of the modelling arises as a result of the energy reflected from the deep water channel. The theory used by the model calculates that the whole of the incident energy is reflected, or refracted, by the deep water channel; no allowance is made within the model for energy dissipation by the reflection process. The conditions produced by the models simply combine all of the energy and produce an average wave height and incident direction. In reality, this is not the case: energy losses will occur and waves will arrive at the shoreline in two separate wave trains, each with separate height and period characteristics.

The trend of west to east reduction in energy is broken locally between Points 6 and 7, where a slight increase in energy occurs, but, energy continues to reduce farther to the east (Figure 5.4). The increase in energy towards Point 7 is explained by the recombination of energy from the two wave trains, as they focus close to the shoreline. This explanation is supported by observations at Hurst Spit.

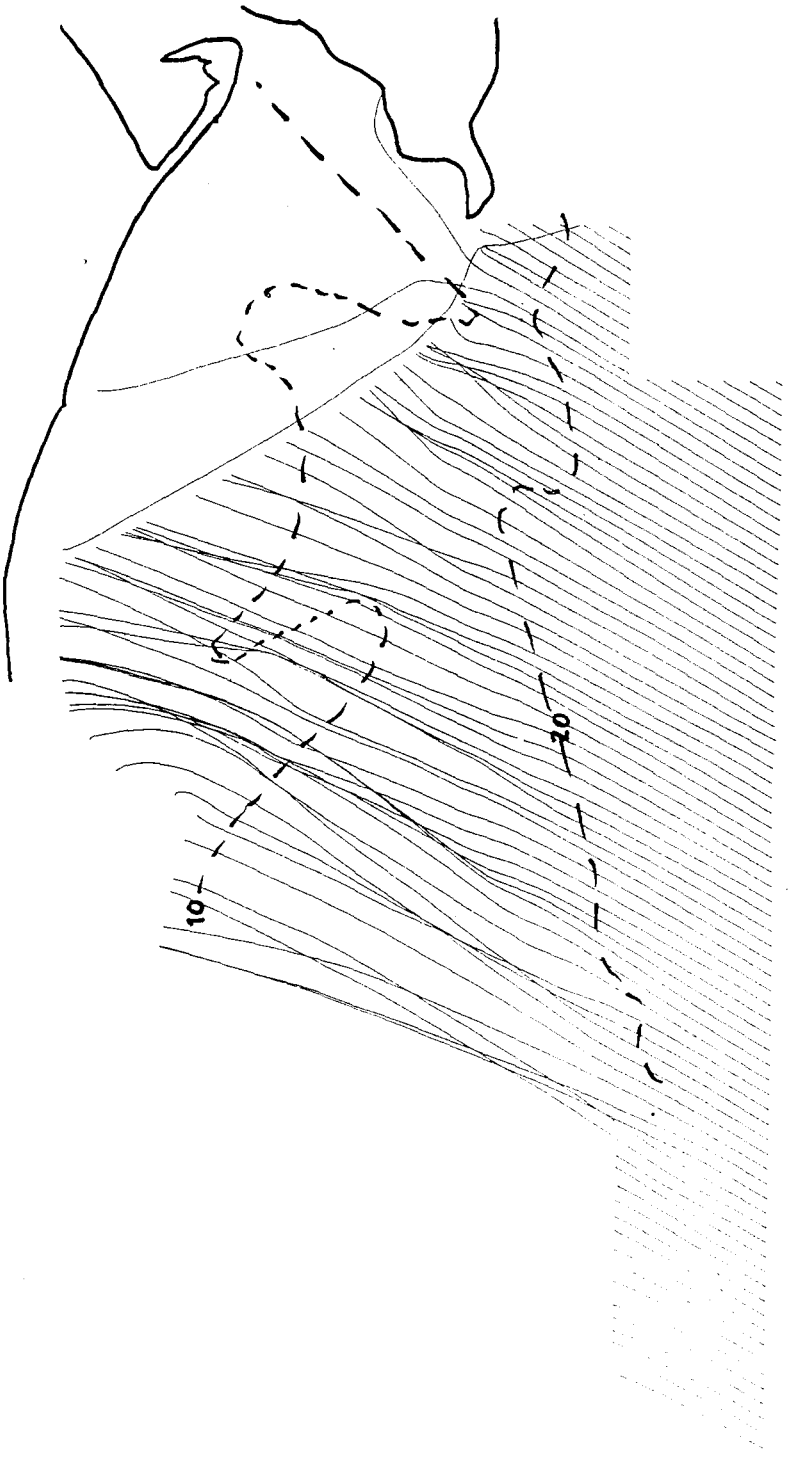

Figure 5.7 Typical output from INRAY showing wave rays for offshore waves from 210^{O}. Offshore storm conditions H_s = 6.7m, T_m = 8.3s (1:100 year return period), water level = 0.87mODN (equivalent to MHWS).

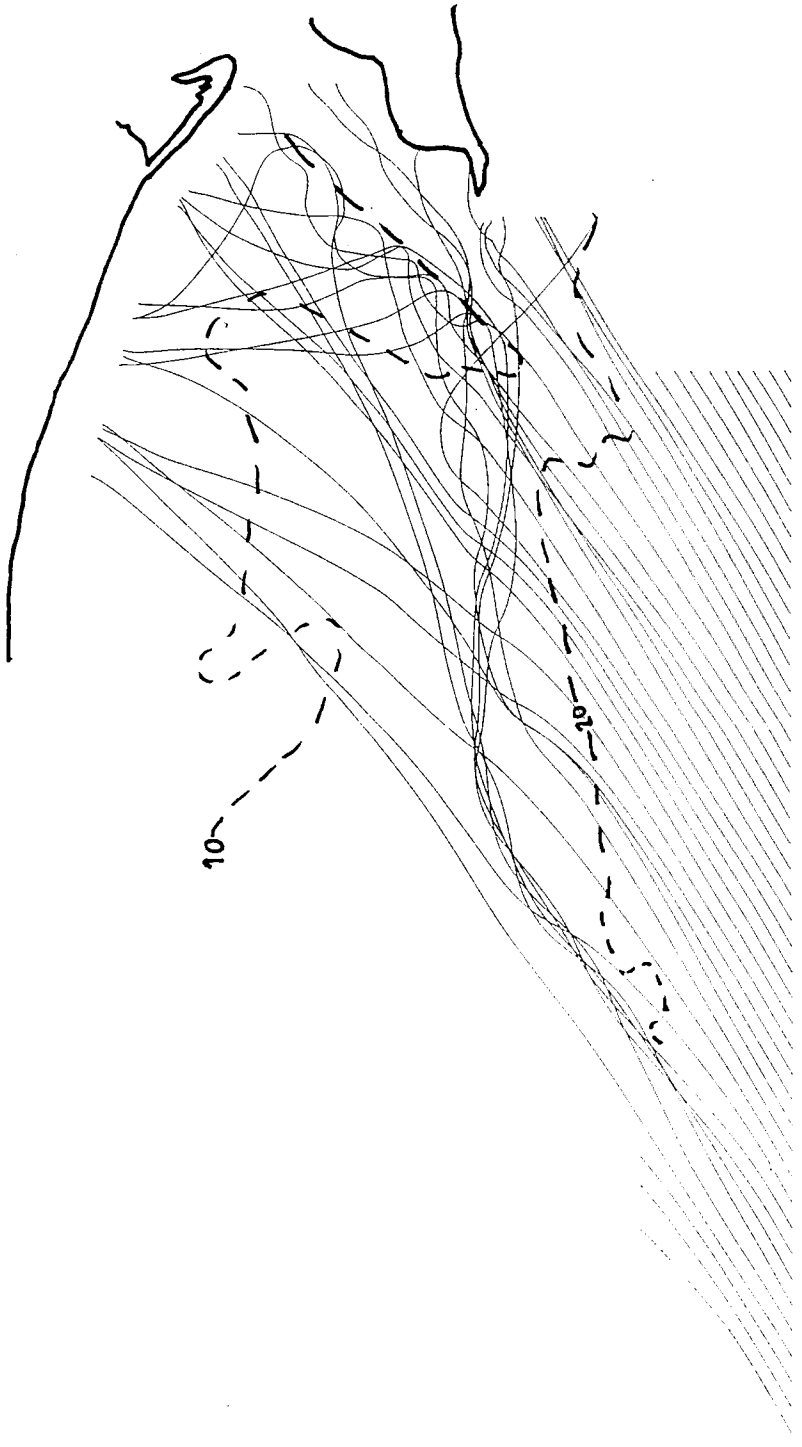

Figure 5.8 Typical output from INRAY showing wave rays crossing on Shingles Banks for offshore waves from 240^{O} Offshore storm conditions H_s = 5.6m, T_m = 11.0s, water level = 0.87mODN (equivalent to MHWS).

The effects of separation and recombination of wave trains creates a localised prediction problem, within the eastern-most kilometre, adjacent to Hurst Spit. The direction of wave attack, together with the relative magnitude of the two energy components at the shoreline, is somewhat confused within the model, due to the unknown proportional combination of the refracted and reflected wave conditions. Hence, the incident wave direction provided by the model appears to be unreliable; this is illustrated further as the output from the model is fed into sediment transport formulae. Directional spectra results indicate a net sediment transport direction towards the west, part way along the spit, suggesting a drift divide. In contrast field data demonstrate that this is clearly not the case.

Henderson (1979) carried out a study of wave climate in Poole and Christchurch Bays; this included a study of wave refraction. Several wave refraction methods were used including older versions of the subroutines used by INRAY (the method of Brampton). However, the grid for the study was much coarser than that used for this study, i.e. 1000m x 250m compared to 100m x 100m. The ray plots presented were for 'average' wave periods, compared with storm periods. Likewise, the charts used to digitise the depths for this study were more up to date. Against this background, the results are somewhat incompatible.

Diffraction is another process which is not included within the modelling process used here. This process may become important in the area around the Needles (Figure 3.1), particularly for waves originating from the south to south east sectors; it is a less significant process for waves from the south west, which provide the most extreme conditions.

The results of the sensitivity analysis, carried out for 10 combinations of wave conditions, at the 8 wave refraction points (Figure 5.4) have indicated that the 4 points selected for the physical model were suitably representative of conditions along the Spit, (although it is acknowledged that the offshore bathymetry actually results in a constantly-varying longshore wave climate). Conditions predicted at the eastern end of the spit are likely to be less reliable, in absolute terms, than those at the less complex western end. Since the data were to be used primarily as input of 'typical' extreme conditions to the physical model (Chapter 7), for comparative studies, the

results were accepted conditionally. The results relative to Points 2, 4, 6 and 7 were considered in detail for the remainder of this study.

Following the initial sensitivity tests to examine the longshore variability in wave climate, a series of more detailed model runs were carried out to provide local wave climates; these were derived for each of the inshore sites (Points 2,4,6 and 7), using a water level of 1.6m CD (MSL). The first phase of the HINDWAVE model produced a wave forecasting table (Table 5.1) for the offshore location (Figure 4.8); this provided the predicted wave height, period and wave direction for a wide range of wind speeds, directions and duration. Inshore wave climate conditions were converted in this way, using information from the OUTRAY and INRAY models. The inshore wave forecasting table was used then in the second phase of HINDWAVE, in the same way as the offshore table.

Examples of the wave height reduction factors, used to obtain the inshore wave forecasting table for each of the four inshore points, are listed in Table 5.3. The factors take into account the change in wave height due to shoaling, refraction, friction and breaking. If, for example, the offshore wave height is 4m and the wind direction is 240^{o}N, then the wave height at Point 2 is 2.27m (4.0 x 0.568). The factors reduce as the wave height increases; this is because the waves interact more with the seabed; hence, there is more friction, breaking, refraction and shoaling. In general, the factors are highest at the western point (Point 2) and reduce eastwards; here the banks have their greatest influence. The table gives examples of the wave height multiplication factors for obtaining inshore wave heights from the offshore wave height for a water level of -0.23mODN (MSL).

Summaries of the inshore wave climates are shown in Figures 5.9-5.12 and tabulated in Appendix 4, in the form of distributions of wave height and wave direction for each inshore point.

Location and Hs(m)	Offshore Wind direction (Degrees North)						
	120	150	180	210	240	270	300
Point 2							
2m	0.222	0.246	0.464	0.635	0.661	0.663	0.635
4m	0.157	0.259	0.378	0.517	0.568	0.583	NA
6m	NA	NA	0.326	0.461	0.521	0.517	NA
Point 4							
2m	0.193	0.247	0.511	0.563	0.621	0.616	0.619
4m	0.175	0.238	0.358	0.551	0.578	0.574	NA
6m	NA	NA	0.277	0.476	0.537	0.534	NA
Point 6							
2m	0.140	0.180	0.347	0.343	0.419	0.435	0.456
4m	0.126	0.155	0.223	0.266	0.331	0.360	NA
6m	NA	NA	0.197	0.215	0.311	0.347	NA
Point 7							
2m	0.181	0.271	0.352	0.315	0.379	0.389	0.440
4m	0.146	0.196	0.322	0.276	0.329	0.340	NA
6m	NA	NA	0.197	0.203	0.270	0.297	NA

Table 5.3. Wave height reduction factors for obtaining inshore wave heights, for a water level of -0.23m ODN (MSL).

Note: NA - Not applicable, because this particular wave height did not occur during the hindcast period. (Data source, HR Wallingford)

The highest waves at Point 2 occur with incident wave directions of 235°-245°N. However, there are no wave heights of between 0.4 and 2.2m from this direction; this may seem extraordinary but may be explained by the fact that waves with inshore heights <0.4m are generated mostly, locally, from within Poole and Christchurch Bay. The directional variation in longshore energy distribution is expressed in terms of percentage occurrence, in one metre significant wave height bands in Figures 5.9-5.12. Overall, these figures demonstrate that the wave heights at the 2 eastern points are significantly lower than at the 2 western points. The probability of occurrence of wave heights is listed, in 0.2m, bands for each of the four refraction points, in Table 5.4.

H1 (m)	P(H>H1)) Point 2	P(H>H1)) Point 4	P(H>H1)) Point 6	P(H>H1)) Point 8
0.0	0.8175	0.8175	0.8766	0.7596
0.2	0.4937	0.4944	0.4815	0.4508
0.4	0.3749	0.3757	0.2775	0.2824
0.6	0.2794	0.2722	0.1891	0.1713
0.8	0.2157	0.2084	0.1005	0.0837
1.0	0.1452	0.1373	0.0602	0.0397
1.2	0.1252	0.0922	0.0137	0.0135
1.4	0.0787	0.0729	0.0029	0.0021
1.6	0.0565	0.0411	0.0017	0.0002
1.8	0.0351	0.0221	0.0002	0.0001
2.0	0.0189	0.0140	0.0001	
2.2	0.0073	0.0069		
2.4	0.0029	0.0041		
2.6	0.0017	0.0017		
2.8	0.0005	0.0005		
3.0	0.0004	0.0004		
3.2	0.0001	0.0001		

Table 5.4 Longshore probability of occurrence of wave heights: Christchurch Bay, 1/1/74 - 28/2/90, (significant wave height in m)

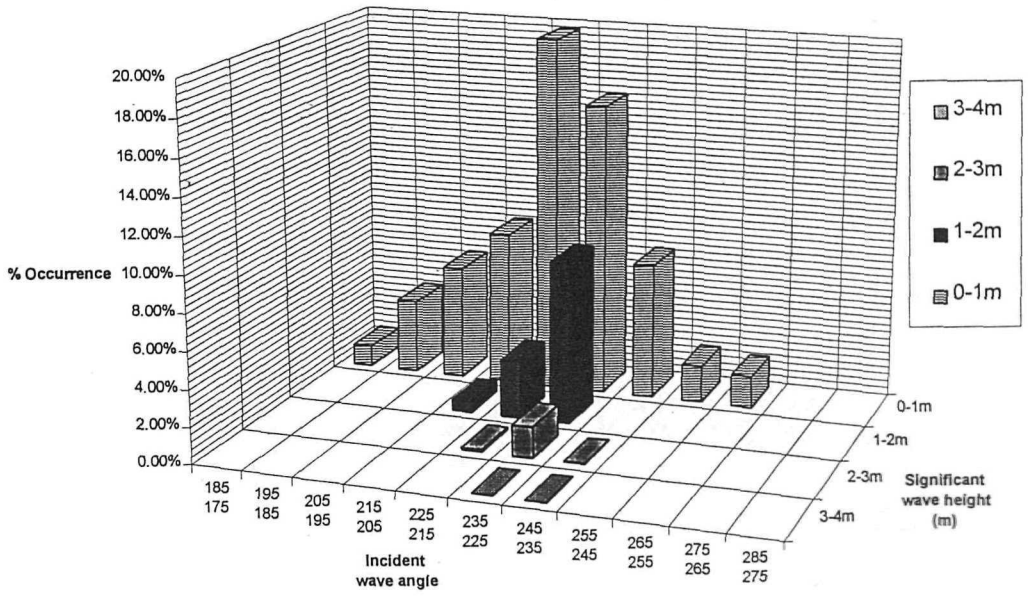

Figure 5.9 Annual distribution of significant wave heights: refraction Point 2, Christchurch Bay (1/1/74 - 28/2/90)

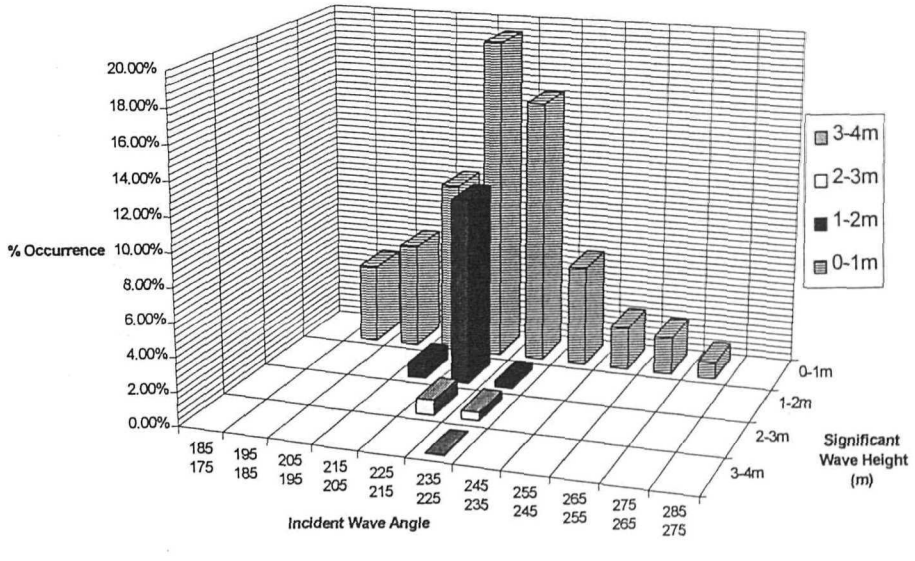

Figure 5.10 Annual distribution of significant wave heights: refraction Point 4, Christchurch Bay (1/1/74 - 28/2/90)

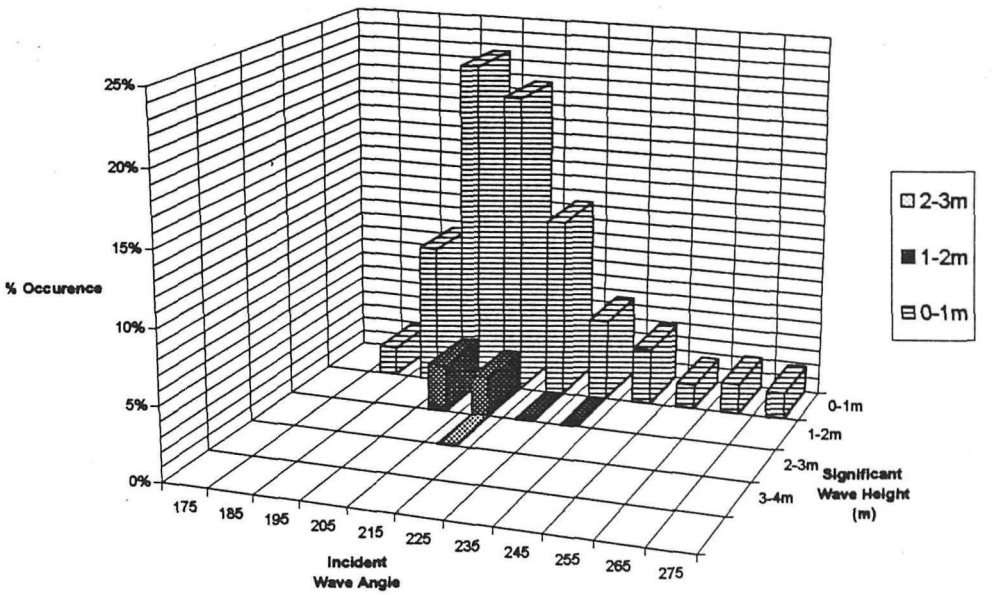

Figure 5.11 Annual distribution of wave height and direction: refraction Point 6, Christchurch Bay (1/1/74 - 28/2/90)

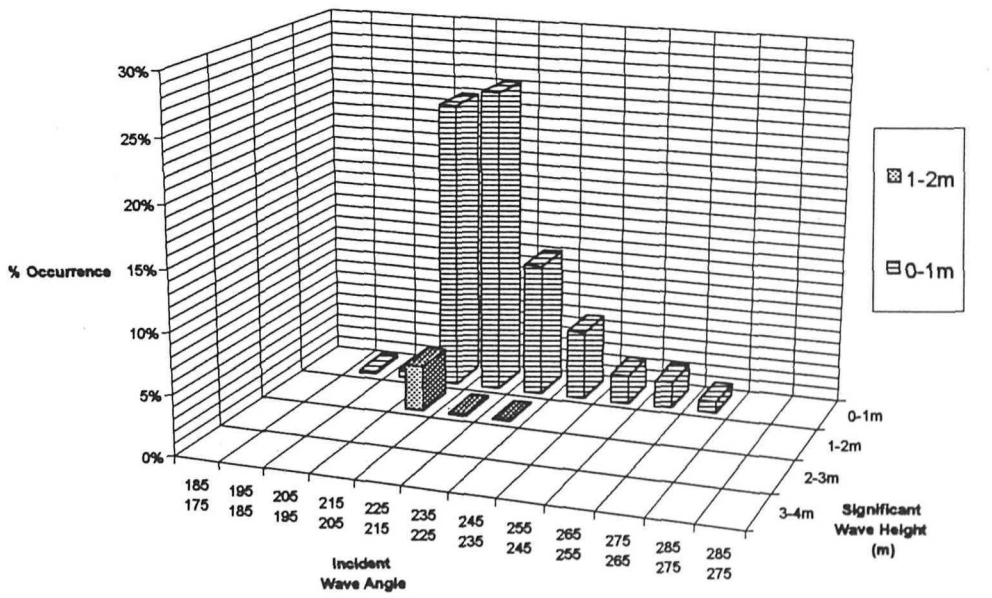

Figure 5.12 Annual distribution of wave height and direction. Location - refraction Point 7, Christchurch Bay (1/1/74 - 28/2/90)

5.4 EXTREME NEARSHORE WAVE CONDITIONS

The extreme offshore wave conditions derived from the HINDWAVE model, are summarised in Table 5.2. The full data sets comprise directional spectra for each condition (see for example Figure 5.3). The results were used to provide directional wave spectra for each of the storms, providing the input to the OUTRAY model. Each component was multiplied by the corresponding component in the transfer function matrices, to give the inshore wave conditions, without taking friction and breaking into account. The INRAY model results were then used to convert the wave conditions, to include the effects of wave breaking and friction.

The results for the predicted extreme conditions are given in Tables 5.5-5.7. The maximum breaking wave height (H_S), in a total water depth (d), is shown to be approximately 0.55 x d. However, INRAY does not account for this depth limiting effect and, in some cases, this was exceeded. On such occasions, the values calculated by INRAY have been replaced by the maximum wave height expected to occur in that water depth; these values have been calculated using the theoretical breaking wave heights (Goda, 1975) (see Tables 5.5-5.7).

The INRAY model was run for each of the extreme wave conditions for each of three water levels MHWS (Table 5.5), MHWS + 1m surge (Table 5.6) and MHWS + 1.4m surge (Table 5.7) - to provide information for the running of the physical model (Section 4.4).

Offshore Wave Direction (°N)	Return Period Years	Inshore Position: Point 2 Hs (m)	Point 2 Tm (s)	Point 2 θ (°N)	Point 4 Hs (m)	Point 4 Tm (s)	Point 4 θ (°N)	Point 6 Hs (m)	Point 6 Tm (s)	Point 6 θ (°N)	Point 7 Hs (m)	Point 7 Tm (s)	Point 7 θ (°N)
135	1	0.90	7.4	215	0.81	7.6	201	0.55	7.5	210	0.40	7.5	220
	5	0.95	7.9	217	0.86	8.4	204	0.61	8.0	210	0.53	8.2	217
	20	0.99	8.3	217	0.93	9.1	206	0.66	8.7	212	0.65	8.7	217
	50	1.05	8.6	217	0.96	9.4	206	0.69	9.2	210	0.73	9.1	216
	100	1.09	8.9	218	1.05	9.7	207	0.71	9.5	205	0.81	9.4	216
150	1	1.05	6.8	208	0.79	6.8	208	0.49	6.9	209	0.57	6.9	213
	5	1.21	7.2	209	1.12	7.3	208	0.59	7.3	208	0.60	7.3	213
	20	1.32	7.4	209	1.26	7.7	208	0.67	7.6	206	0.62	7.6	214
	50	1.35	7.6	210	1.34	8.0	208	0.77	7.8	206	0.74	7.8	214
	100	1.37	7.7	211	1.51	8.1	207	0.87	7.9	205	0.84	7.9	214
180	1	1.58	7.7	207	1.97	8.2	210	1.30	7.9	208	1.57	7.9	212
	5	1.73	8.1	206	2.17	8.7	208	1.46	8.3	208	1.72	8.4	211
	20	1.83	8.5	206	2.23	9.1	208	1.55	8.7	207	1.79	8.8	210
	50	1.89	8.8	206	2.41	9.3	208	1.63	8.9	207	1.87	9.1	210
	100	2.03	8.9	207	2.53	9.4	207	1.69	9.1	206	1.92	9.2	209
210	1	2.89	8.1	220	2.74	8.4	225	1.18	8.0	220	1.64	8.2	215
	5	2.99	8.6	221	3.00	9.0	225	1.39	8.5	220	1.68	8.8	215
	20	3.23	9.1	221	3.21	9.3	225	1.57	8.9	220	1.74	9.2	215
	50	3.40	9.3	221	3.30	9.5	226	1.67	9.1	220	1.79	9.4	215
	100	3.52	9.4	220	3.34	9.6	225	1.75	9.3	220	1.82	9.5	215
240	1	3.57	9.9	221	3.42	9.8	219	2.57	9.0	214	2.10	9.6	209
	5	3.82	10.4	222	3.79	10.3	219	2.86	9.5	214	2.34	10.2	210
	20	4.07	10.8	223	3.96	10.6	219	3.07	10.0	214	2.51	10.6	210
	50	4.13	11.1	224	4.05	10.8	219	3.17	10.2	214	2.76	10.8	210
	100	4.14	11.2	224	4.09	10.9	219	3.25	10.4	213	3.10	10.9	211

Key: θ=mean inshore wave direction; * Maximum breaking wave height; Hs=Significant wave height; Tm = mean wave period; (Data source, HR Wallingford)

Table 5.5 Extreme inshore wave conditions at MHWS (0.87mODN) for Hurst Spit (for location of points see Figure 5.4)

Offshore Wave Direction (°N)	Return Period (Years)	Inshore Position: Point 2 Hs (m)	Point 2 Tm (s)	Point 2 θ (°N)	Point 4 Hs (m)	Point 4 Tm (s)	Point 4 θ (°N)	Point 6 Hs (m)	Point 6 Tm (s)	Point 6 θ (°N)	Point 7 Hs (m)	Point 7 Tm (s)	Point 7 θ (°N)
135	1	1.01	7.1	207	0.89	7.5	205	0.58	7.4	209	0.88	8.5	220
	5	1.13	7.7	208	0.94	8.2	204	0.66	7.7	207	1.12	9.1	218
	20	1.20	8.1	208	0.96	8.8	205	0.74	8.2	207	1.21	9.6	219
	50	1.22	8.4	209	1.05	9.2	205	0.79	8.5	207	1.25	9.8	219
	100	1.26	8.6	209	1.09	9.4	204	0.82	8.8	205	1.27	10.0	220
150	1	1.00	6.6	205	1.12	6.8	209	0.96	6.8	210	0.89	7.3	213
	5	1.22	6.9	206	1.23	7.3	209	1.21	7.2	210	1.29	7.8	214
	20	1.39	7.2	207	1.34	7.6	210	1.41	7.4	209	1.58	8.2	214
	50	1.45	7.4	207	1.41	7.8	210	1.55	7.6	209	1.67	8.4	214
	100	1.49	7.5	207	1.45	8.0	210	1.66	7.7	209	1.71	8.5	214
180	1	2.17	7.7	206	2.10	8.2	210	1.68	7.9	207	1.67	8.0	213
	5	2.28	8.2	205	2.33	8.7	209	1.95	8.3	207	1.73	8.4	211
	20	2.45	8.5	204	2.51	9.1	208	2.08	8.7	206	1.95	8.8	210
	50	2.55	8.8	204	2.60	9.4	208	2.13	8.9	206	2.08	9.0	208
	100	2.62	8.9	204	2.67	9.6	206	2.16	9.0	206	2.17	9.2	207
210	1	3.29	8.2	218	3.19	8.3	218	1.87	8.0	217	1.85	8.1	219
	5	3.64	8.7	218	3.25	8.9	218	2.06	8.5	217	2.00	8.5	219
	20	3.92	9.1	218	3.59	9.4	217	2.18	8.9	216	2.10	8.9	219
	50	4.05	9.3	217	3.78	9.6	217	2.23	9.1	216	2.16	9.1	219
	100	4.20	9.5	216	3.92	9.8	217	2.28	9.3	216	2.21	9.2	219
240	1	3.97	9.9	216	3.27	9.8	209	2.71	9.0	210	2.41	9.1	206
	5	4.39	10.4	217	3.75	10.3	210	3.09	9.5	210	2.62	9.7	206
	20	4.59	10.7	217	4.13	10.7	211	3.30	9.9	209	2.77	10.2	206
	50	4.78	10.9	217	4.46	10.9	212	3.36	10.1	209	2.93	10.4	205
	100	4.79*	11.1	218	4.55	11.1	212	3.39	10.3	209	2.95	10.6	205

Key: θ=mean inshore wave direction; * Maximum breaking wave height; Hs=Significant wave height; Tm = mean wave period; (Data source, HR Wallingford)

Table 5.6. Inshore wave conditions for extremes at MHWS +1m surge (1.87mODN) for Hurst Spit (for location of points see Figure 5.4)

Offshore wave direction (°N)	Return Period (years)	Inshore Position: Point 2 Hs (m)	Point 2 Tm (s)	Point 2 θ (°N)	Point 4 Hs (m)	Point 4 Tm (s)	Point 4 θ (°N)	Point 6 Hs (m)	Point 6 Tm (s)	Point 6 θ (°N)	Point 7 Hs (m)	Point 7 Tm (s)	Point 7 θ (°N)
135	1	1.19	7.2	205	0.72	7.3	202	0.50	6.7	213	0.92	8.4	222
	5	1.42	7.7	207	0.93	8.3	201	0.55	6.9	213	1.29	9.1	221
	20	1.63	8.2	208	0.97	9.0	202	0.59	7.4	212	1.54	9.6	220
	50	1.69	8.5	209	1.01	9.4	202	0.64	7.8	211	1.62	9.9	220
	100	1.71	8.8	211	1.04	9.6	202	0.66	8.1	210	1.64	10.1	220
150	1	1.48	6.7	203	1.28	6.7	206	1.06	6.4	207	0.71	7.2	220
	5	1.59	7.1	204	1.34	7.2	207	1.11	6.8	206	1.27	7.7	219
	20	1.66	7.3	205	1.36	7.6	207	1.38	7.1	204	1.67	8.1	218
	50	1.68	7.5	205	1.44	7.8	208	1.49	7.3	204	1.79	8.2	217
	100	1.72	7.7	206	1.48	8.0	209	1.57	7.4	204	1.87	8.4	216
180	1	2.38	7.6	205	2.11	8.1	205	1.61	7.9	203	1.83	8.1	215
	5	2.41	8.1	205	2.40	8.6	207	1.82	8.4	204	1.92	8.5	215
	20	2.58	8.5	204	2.60	9.0	209	1.99	8.8	205	2.01	8.8	214
	50	2.66	8.8	204	2.69	9.3	209	2.07	9.0	206	2.05	9.0	214
	100	2.69	8.9	204	2.78	9.4	209	2.12	9.2	207	2.07	9.1	214
210	1	3.58	8.1	217	3.43	8.3	214	1.82	8.1	216	2.10	8.2	216
	5	3.81	8.7	218	3.70	8.8	214	2.36	8.7	216	2.23	8.7	216
	20	4.02	9.1	219	4.06	9.3	214	2.63	9.1	216	2.30	9.0	216
	50	4.34	9.3	218	4.25	9.5	214	2.85	9.3	216	2.36	9.2	217
	100	4.60	9.5	220	4.32	9.7	214	2.98	9.5	216	2.39	9.3	218
240	1	3.76	10.0	218	3.37	9.7	209	2.75	9.1	214	2.68	9.1	208
	5	4.50	10.5	217	4.15	10.3	209	3.13	9.7	215	2.70	9.6	207
	20	4.93	10.8	216	4.24	10.7	210	3.38	10.1	215	2.74	9.9	207
	50	5.01*	11.0	217	4.44	11.0	211	3.46	10.3	215	2.76	10.1	207
	100	5.01*	11.1	217	4.49	11.1	212	3.48	10.4	214	2.99	10.2	207

Key: θ=mean inshore wave direction; * Maximum breaking wave height; Hs=Significant wave height; Tm = mean wave period; (Data source, HR Wallingford)

Table 5.7 Inshore wave conditions for extremes at MHWS +1.4m surge (2.27mODN) for Hurst Spit (for location of points see Figure 5.4)

5.5 *THE STORMS OF 29 OCTOBER AND 17 DECEMBER, 1989*

Individual storm events were synthesised, by hindcasting and refraction modelling; these provided the wave conditions which were used later for calibration of the physical model (Section 4.4). The first storm (29 October) occurred when the peak water level was around MHWS (i.e. 0.87m ODN): the second (17 December), when there was an extreme high water level of 2.27m ODN.

Hourly-predicted offshore wave conditions were obtained, from HINDWAVE, for the period October 1989 to February 1990. The peak of the storms, on the two dates, were identified from the time-series generated from the wind records. Time-series wave data, derived from hindcasting are shown in Figure 5.13.

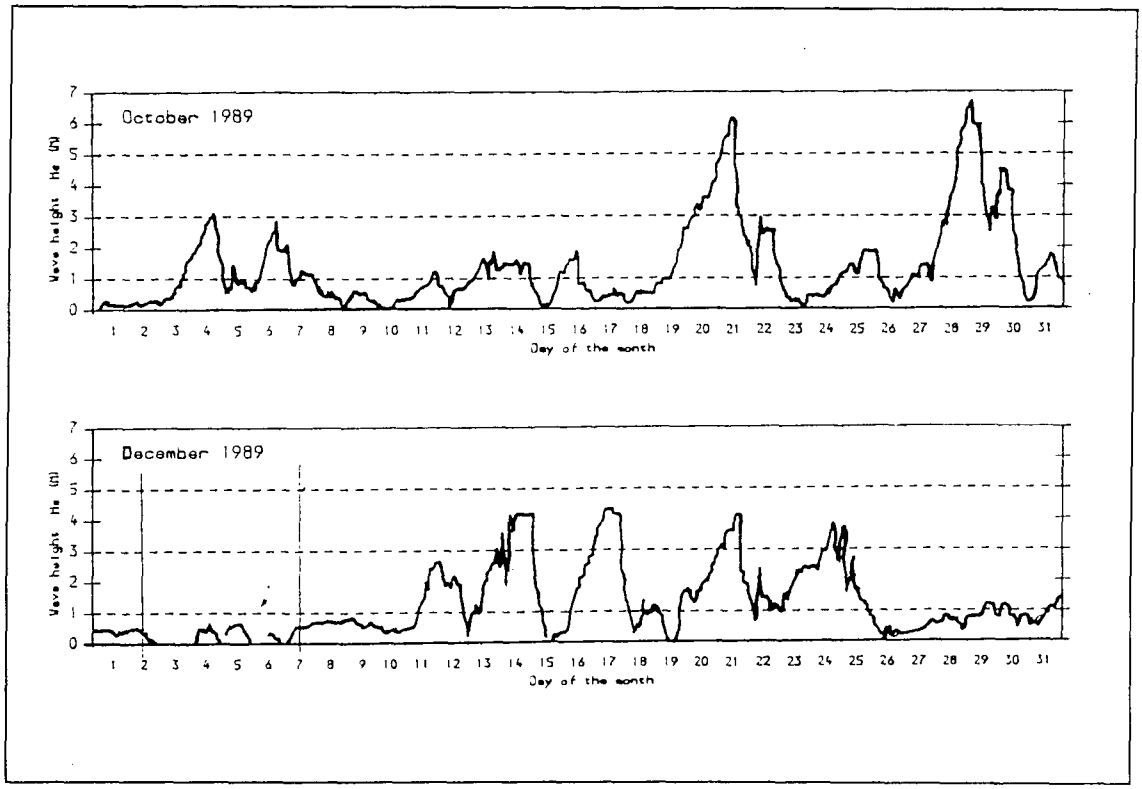

Figure 5.13 The time-series of wave data derived from the HINDWAVE model, for October and December 1989

Directional wave spectra for the storms were derived on the basis of the input of wind conditions into the JONSEY element of the HINDWAVE model (Hydraulics Research, 1989c). The storms of 29/10/89 and 17/12/89 had hindcast offshore significant wave heights of 6.7m and 4.2m, respectively. Further details are presented in Tables 5.8 and 5.9. Whilst the Portland Meteorological Office data used for the hindcasting has been assumed to be accurate, this has not been confirmed. Indeed, the data indicates a rather unusual 'flat top' cut-off to the wave height maxima, at the peak of the storms in December (Figure 5.13). Wave conditions were transformed inshore, using the OUTRAY and INRAY models (Section 5.3). Inshore wave conditions derived for the four refraction points, are displayed in Tables 5.8 and 5.9.

Location	**H_s (m)**	**T_m (s)**	**θ ^{o}N**	**Water level (m ODN)**
Offshore	6.72	8.8	240	0.87
Inshore				
Point 2	3.58	10.2	221	0.87
Point 4	3.78	10.1	220	0.87
Point 6	2.90	9.5	214	0.87
Point 7	2.59	10.0	210	0.87

Table 5.8 Predicted wave conditions for the 29/10/89 storm period

Admiralty Tidal Predictions (determined using TIDECALC software) indicate an anticipated tidal elevation peak at a level of 0.63m ODN, at Hurst Point on 29 October 1989. The storm peak occurred over the period 23:00 hr 28/10/89 to 02:00 hr 29/10/89, when a water level of 0.87mODN was reached; this relates to a surge component within the range 0.2-0.5m. The incident wave direction during the storm resulted in shore-normal wave approach along much of the beach. Energy dissipation (in response to shoaling, friction, refraction and wave breaking) follows a similar east - west trend, as predicted for many of the extreme conditions (Section 5.4). A probabilistic assessment of the storm characteristics, based on extrapolation of the 16 year time series of wind data (Table 5.1), suggests that the offshore wave conditions were representative of a storm with a return period occurrence of 1:5 years. The offshore sea steepness of this storm was 0.055: this is indicative of a sea condition

formed typically over a period of 1-3 hours. The offshore storm conditions exceeded a significant wave height of 6 m for a period of 6 hours, whilst the peak of the storm occurred over a period of 3 hours.

Location	H_s (m)	T_m (s)	θ ^{o}N	Water level (mODN)
Offshore	4.18	7.0	230	2.27 (MHWS +1.4m)
Inshore				
Point 2	2.94	7.7	219	2.27 (MHWS +1.4m)
Point 4	2.58	7.7	210	2.27 (MHWS +1.4m)
Point 6	2.51	7.4	208	2.27 (MHWS +1.4m)
Point 7	2.42	7.5	204	2.27 (MHWS +1.4m)

Table 5.9 Predicted wave conditions for the 17/12/89 storm period

The most significant storm event which occurred during the study period, with respect to barrier beach rollback processes, occurred on 17/12/89. The storm coincided with spring tides, during a period of extreme low pressure (975mb): it resulted in an extreme water level at the site, estimated at 2.27m ODN (determined on the basis of interpolation between measurements at Christchurch and Lymington). The wind records indicate that the storm was of extended duration (approx. 16 hr), with a peak of around 3 hr over a high water period. Wave refraction modelling has suggested that incident waves refracted past the shore-normal, resulting in wave attack towards the up-drift direction; these data may reflect limitations in the modelling process, but may be an accurate representation. Observations made from the Coastguard helicopter on the morning following the peak of the storm suggest that normally-incident waves approached the beach; this is demonstrated in Plate 6.7, which shows the eastern part of Hurst Beach under wave attack. However, the storm peak occurred at night, and conditions may have altered subsequently. The refraction modelling of this event should be more reliable than for the October 1989 storm, as the offshore waves occurred from an angle of 230^{o}; this is outside of the range of angles which result in reflections from the deep water channel.

The offshore wave conditions during the 17/12/89 event were not particularly severe: they have a probability of exceedence of 0.0041(all directions), whilst the probability of exceedence within the 225-255^{O} direction sector is 0.0028. Similar wave conditions could be expected to occur, statistically, for an average duration of 24 hr per year, within the 225-255^{O} direction sector. At the time of the storm, the influence of the offshore banks on wave breaking and friction was reduced, due to the extreme water level (at least 1.4 m above the predicted tidal elevation); this permitted much larger waves to reach the shoreline, than can occur during normal (astronomical) spring tides. The combination of the extreme water level, with moderate wave conditions, resulted in an extremely damaging event. This storm event provided another important, contrasting, extreme combination of waves and water levels; this could be used for validation of the physical model, in parallel with the field measurements of shoreline response.

5.6 CONCLUDING REMARKS

The range of differences between significant wave height conditions for extreme offshore events varies within the range 1.67- 2.72m, for the 1:1 and 1:100 year return period events, respectively for the directional sectors 135-240^{O}. The nearshore transformations of the same offshore conditions result in much closer groupings of wave heights, due to the energy loss processes. The corresponding band width of wave heights for extreme conditions, at mean high water spring tides, is between 0.18m and 1.0m for the same range of offshore sectors.

The relative significant wave height conditions on the 5m CD (-6.83m ODN) depth contour, at each of the centres of the physical model test segments, for wave directions resulting from offshore directions of 210^{O} and 240^{O}, are shown in Figure 5.14. An asymptotic trend is observed for waves originating from 240^{O}, as the significant wave heights approach the maximum breaking wave heights for each of the water depths. A similar trend does not occur for waves originating from 210^{O}, as the conditions are less severe and do not reach breaking wave limits. The trends shown for refraction Point 7 are slightly different for wave conditions originating

from 240^{O} offshore: this is probably the result of the complex separation and recombination of the bi-directional wave climate (see above).

The range of nearshore significant wave heights lies within a band 0.3 -1.25m wide, at all the wave refraction points: for the whole range of extreme storm events examined (from 1:1 year to 1:100 years); at any of the water levels tested; for both 210^{O} and 240^{O} directions. Although the range of significant wave heights at each of the water levels is fairly narrow, the combined set of results for the three water levels provided a range of significant wave heights between 1-5m. This range of conditions provided a sensible framework for the development of the physical model test programme.

A range of nearshore mean wave periods, between 7 - 11 s, were derived from the numerical modelling. In contrast to the wave heights, the mean wave periods associated with the extreme events are relatively unaffected by the wave transformation processes: longer periods are associated consistently with more extreme events. The period is increased generally by 10-15%, between the nearshore and offshore conditions, as a result of the wave transformation processes. However, the water depth has only minimal influence on the nearshore wave periods. The wave periods rarely differ by more than 0.1 s for any of the water levels, for the same input offshore conditions.

The dependence of nearshore significant wave heights on the water level, together with the effects of the offshore banks on energy dissipation, are illustrated well by comparison of nearshore wave conditions, with similar offshore conditions over a range of water levels (Figure 5.14). An increase in water depth results in significantly more severe wave conditions at the refraction points, for each of the offshore conditions. The effect on the shoreline is compounded, as a higher water level also allows wave attack to occur higher, and further to landwards, on the beach profile.

The incident wave angle can vary significantly as a result of changes in water level; it is also dependant upon the interaction between the waves and the bathymetry, the degree of refraction and the initial angle of approach. Variations in the incident wave

angle, resulting from water level variation, are rarely greater than 10^{O}; they are generally within the range 4-6^{O}, across the full range of water levels tested (1.4m). The largest variation occurs for the 135^{O} sector, which is the farthest sector from beach-normal. The limitations of the modelling process do not allow the incident wave angle to be determined more accurately than +/- 5^{O}. The results for each offshore direction and water level combination are generally scattered across bands of 4-5^{O}. This accuracy provided a range of input wave angles for each of the model segments, within these limits.

The four physical model segments were tested from as many as three incident wave angles, across a representative range of angles based upon the above results. The range of incident angles selected for physical model testing spanned 15^{O} either side of beach-normal, on the basis of the numerical model test results. Some doubts were cast upon the validity of the incident wave angles, on the basis of field observations of both waves and sediment transport during storms (Section 6.5); it is suggested that the incident wave angles for some of the extreme conditions were as much as 10^{O} in error, resulting in waves approaching the beach and transporting beach material in the opposite direction to that which actually occurs for the given offshore (wave) conditions. These conditions were examined during the calibration phase of the physical model studies (Section 7.1).

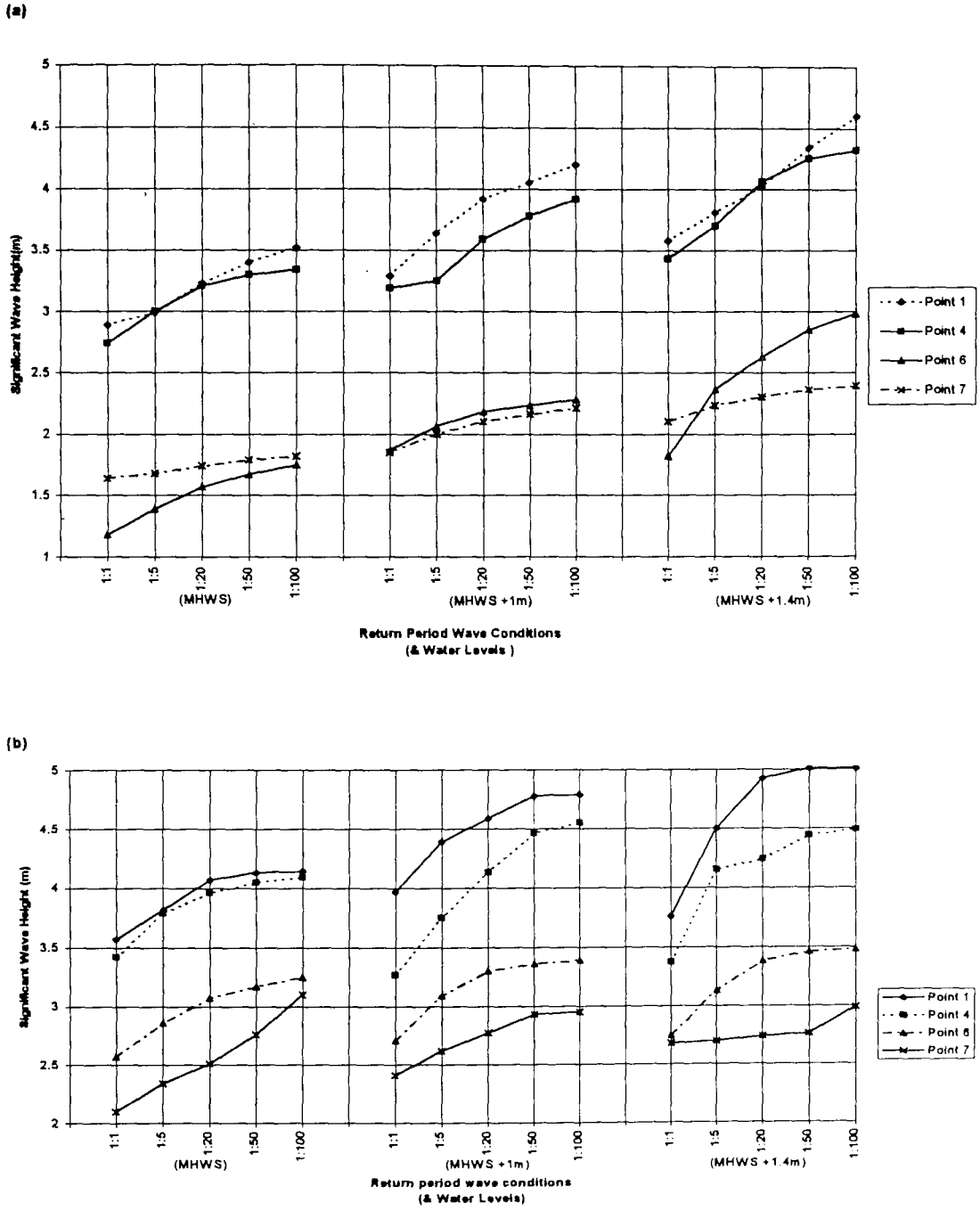

Figure 5.14 Effects of surge water level on extreme significant wave heights at refraction points on the 5m CD (-6.83m ODN) depth contour adjacent to Hurst Spit, for offshore wave conditions originating from 210^{0} (a) and 240^{0} (b). (for location of points see Figure 5.4)

CHAPTER 6: RESULTS AND DISCUSSION - FIELD STUDIES

6.1 ANALYSIS OF FIELD DATA

Data presented demonstrates beach evolution at two time scales: sub-decadal and individual storm events. The extensive sets of hydrodynamic, PSD and beach response time-series data, collected during the study programme, are stored in a SANDS (Halcrow, 1995) database; this is used as a management tool for beach maintenance along the New Forest District Council coastline (Appendix 2). In excess of 1200 profiles were surveyed between 1987-93, describing sub-decadal evolution of beaches within the study area. Typical beach profile data show the contrasting evolutionary profile response of Hurst Spit barrier beach with a simple open beach at Hordle Cliff (Figure 6.1). The beach at Hurst Spit has migrated, with frequent changes in barrier width, crest elevation and cross-section; at the same time, the beach at Hordle has remained almost static. The beach profile data were supplemented by a nearly continuous time-series data set of tides, wind speed, direction and barometric pressure (from 1991-1997), and wave data collected at two local nearshore sites (between 1994-95 and 1996-1997) (Figure 4.6).

The analyses presented here focuses upon examination of beach profile response to extreme events, by reference to hydrodynamic variables and to a parametric model of profile response (Powell, 1990). Storm events were analysed, both prior to and on completion of a major beach recharge scheme which took place on Hurst Spit in 1996 (Bradbury and Powell, 1992; Bradbury and Kidd, 1998). Extreme events analysed prior to the beach recharge scheme resulted in overwashing of the beach and crest modification. Similar hydrodynamic conditions following the completion of the beach recharge project resulted in a contrasting profile response with no overwashing. Data are presented for selected extreme events, together with explanations of the spatial variability in the performance of Hurst Spit. The limitations of field investigations as an approach to quantify the parameters resulting in overwashing are demonstrated and discussed. Comparisons are made also with earlier studies of the prevailing hydrodynamic conditions (Hydraulics Research, 1989a,b), with emphasis on the validity and prediction of extreme events.

(a)

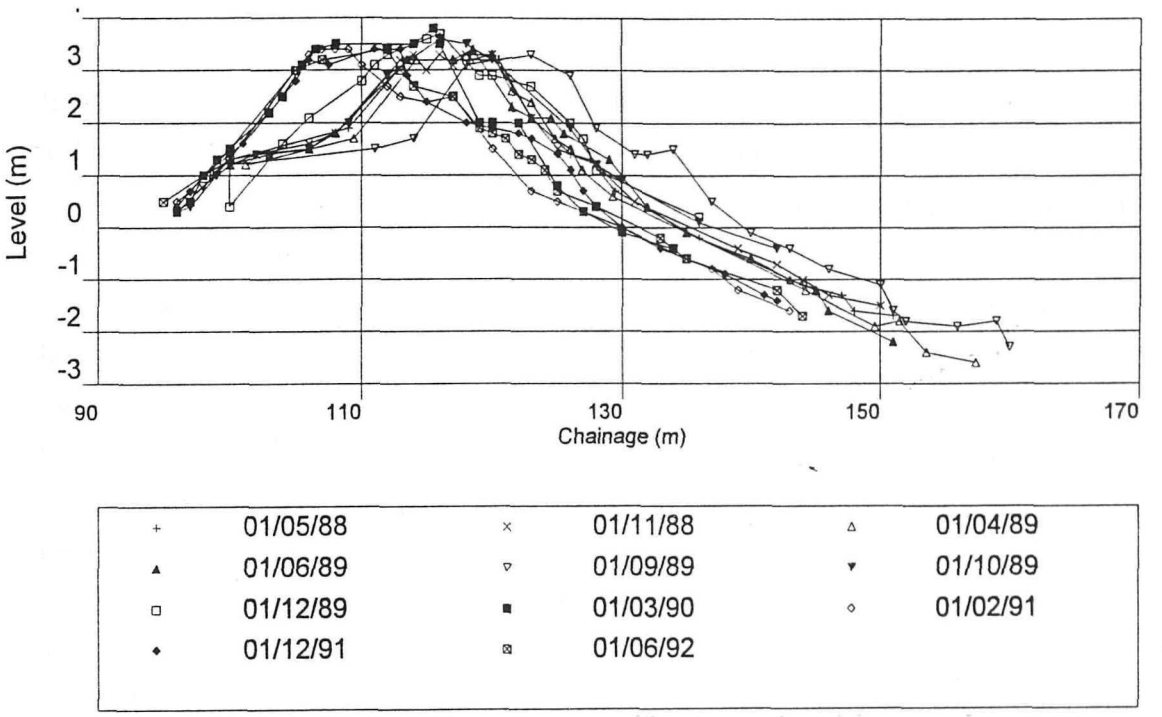

(b)

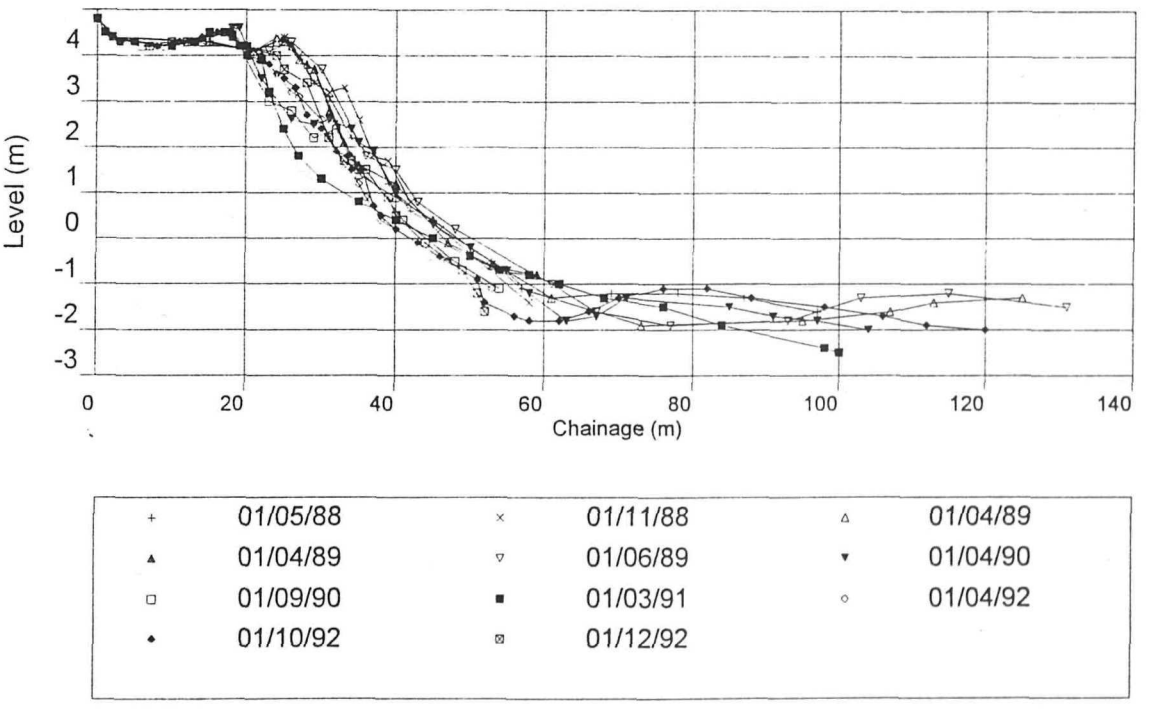

Figure 6.1 Evolution of typical beach cross sections between 1987 -1993 at HU17, Hurst Spit (a) and MF6, Hordle (b)(for location of profiles, see figure 4.1)

6.2 SUB-DECADAL BEACH PROFILE EVOLUTION

Initial examination of the time-series of profile data (prior to the 1996 beach recharge, at Hurst Spit) demonstrates a strong linear relationship between beach CSA and beach span at mean high water (Figure 6.2); similarly, the crest elevation and CSA shows a strong linear relationship. An exception to this trend is noted following the 17/12/89 storm, where the data is widely scattered; this suggests an exceptional barrier response to this event, probably due to the sluicing overwash conditions which resulted in barrier breakdown. Disorder identified as a result of this event is consistent with the hypothesis of catastrophic transition, from stable to unstable morphodynamic states, and rapid evolution during phases of instability (Carter *et al*, 1993a). Variability of the relationship between cross section and span reflects the various stages of barrier evolution, identifying phases of berm and crest build-up, crest reduction and maintenance; this is consistent with a conceptual barrier beach evolutionary model (Orford *et al* 1991a). In addition to these phases of barrier evolution, variations may also reflect such site specific factors as the back barrier and lagoon geometry, preferential loss from the root of the spit due to longshore transport, saltmarsh compression due to the weight of washover sediments, and the bi-directional wave climate which affects the easternmost segment of Hurst Spit.

Changes in beach span between barrier mean high water marks, from 1987-1993 (Figure 6.3), reflect the evolutionary variability of each of the profiles over the monitoring period; this provides further evidence in support of a conceptual model (Orford and Carter, 1991a). Spatial variability of the barrier geometry is demonstrated also by the data set. An artificial step in the data may be noted (Figure 6.3); this resulted from minor beach recharge and regrading work, following the storm of 17/12/89. The same pattern is shown in Figure 6.4, which identifies spatial and temporal change in barrier cross-section area above mean high water; this demonstrates the barrier instability in a similar manner. Beach CSAs and widths were measured previously at Hurst Spit (Nicholls, 1985), using data derived from historical studies of maps, supplemented by surveys (Table 6.1). These data showed similar local trends, suggesting that the evolution at both decadal and sub-decadal scales is similar, in terms of change in barrier width and area. The field data described here identifies a general reduction in beach CSA and crest elevation, from west to east; this may reflect variations in wave climate along the length of the spit (Chapter 5). The rate of

recession remains fairly constant along the length of the swash aligned structure; this may represent a relationship between beach CSA and the local wave climate, which reduces in severity from west to east. (Section 5.3). This is examined further in Chapter 8, by reference to the hydrodynamic variables.

Year	Average Width (m) at MHW	CSA (m^2) above MHW
1867*	48.6	88.2
1898*	44.6	80.9
1908*	46.6	84.5
1939*	62.6	113.6
1967*	45.4	82.4
1982*	43.9	79.6
1987	46.2	68.7
1988	45.1	74.7
1989	42.8	69.4

* from Nicholls (1985)

Table 6.1 Temporal changes in average beach width and area at Hurst Spit (1867-1989)

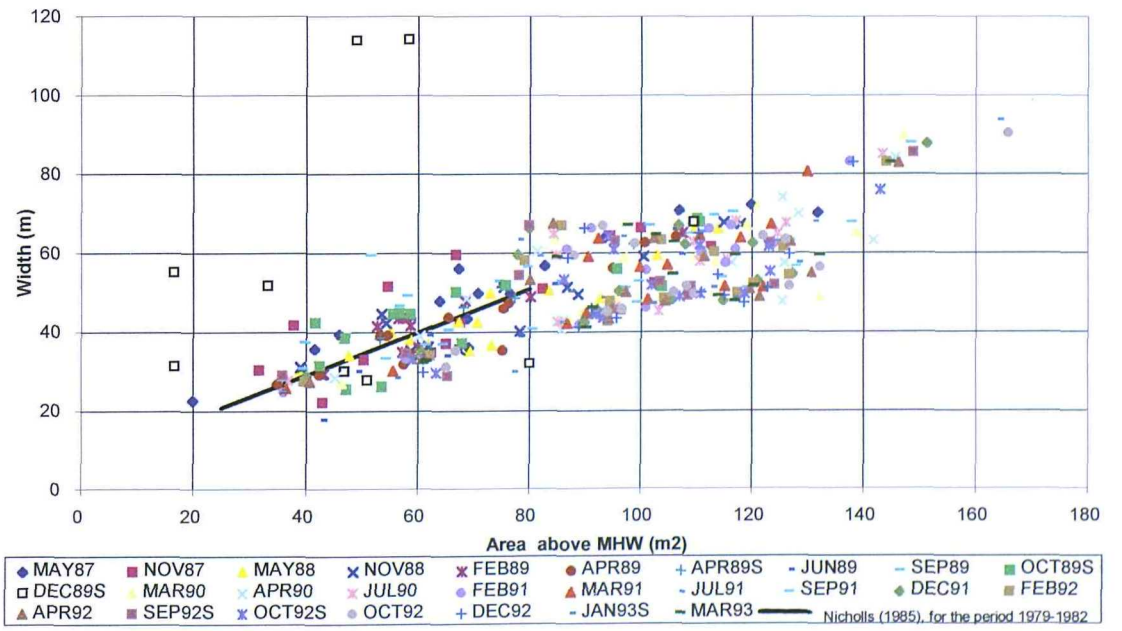

Figure 6.2 Relationship between beach CSA, above mean high water, and beach span at mean high water, between 1987-1993.

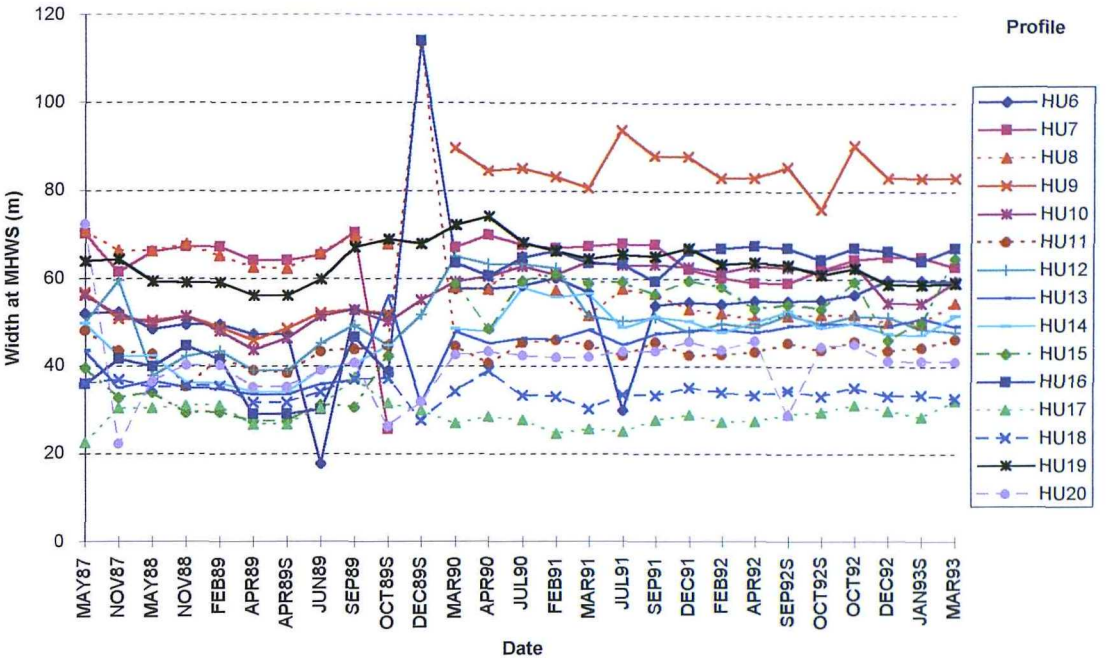

Figure 6.3 Changes in beach span at Hurst Spit between mean high water marks (1987-1993)(profile positions are located on Figure 6.13)

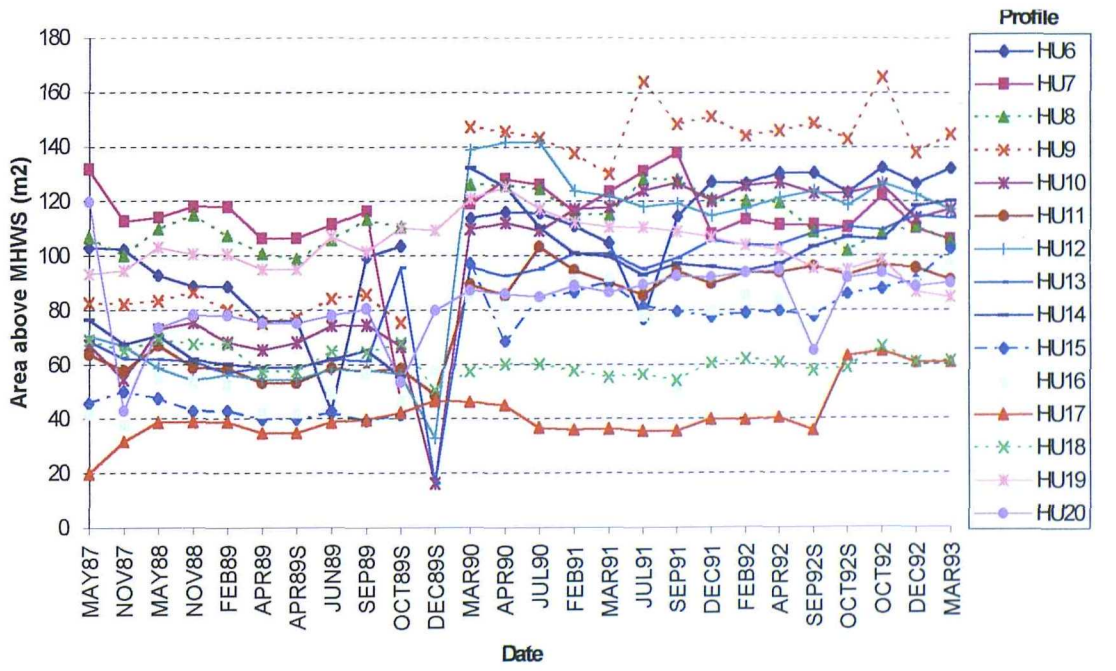

Figure 6.4 Changes in CSA, at Hurst Spit, between mean high water marks (1987-1993) (profile positions are located on Figure 6.13)

The maximum barrier crest elevation was considered to be a significant variable, (Nicholls, 1985; Orford and Carter, 1991); these earlier investigations suggest that the main variables governing sub-decadal evolution of the barrier are; beach geometry; sea level and mean sea state. Temporal and spatial changes in barrier crest elevation, between 1987-1989, are shown in Figure 6.5: the data set identifies considerable changes during the winter 1989. Elevations shown on profiles HU6-HU7 are largely artificial, due to earlier maintenance in this area. The trends represent both spatial variation in longshore wave climate, and also the intensity of storm conditions which have modified the beach crest. A similar data set obtained for 1990-1993 (not shown here), following a small (15,000m^3) beach recharge operation and reshaping of the barrier after the storm of 14/12/89, identified less frequent changes to the artificially-increased crest elevation.

Figure 6.5 Spatial and temporal changes in maximum crest elevation at Hurst Spit 1987-1989 (profile positions are located on Figure 6.13)

Evolution of the barrier crest of Hurst Spit was confined to extreme storm events, during the study period. Previous analysis of shingle barrier evolution, at a decadal level (Nicholls, 1985; Nicholls and Webber, 1987a,b) provides strong evidence for an acceleration of recession rates at Hurst Spit, from 1.5m/ year between 1867-1968, to 3.5m/year between 1968-1982 (Figure 6.6) (based upon the analysis of maps and aerial photographs). The recession rate can be attributed to a minimal supply of sediment from updrift beaches, and a net loss from the system, due to longshore transport. The beach volume declined by 14,600m^3 during a study period between 1980-1982 (Nicholls, *op.cit*); this is reflected in the rate of rollback. Alignment of the root of the spit was held artificially during this period. This trend continued at the eastern end of the site until 1989, at a similar rate; it was interrupted in 1996, due to beach recharge along the full length of the beach. The evolutionary rate was interrupted by the 17/12/89 storm, which caused partial barrier breakdown, due to sluicing overwashing. The beach response resulted in barrier migration as fast as 20 times the annual average rate, during a single storm.

Recession is affected also by a number of local variables; these include the composition of the lower foreshore, and the geometry leewards of the back barrier toe. The saltmarsh system in the lee of the barrier comprises channels and saltmarsh flats; these ranged in elevation between a maximum of 0.8m ODN on the surface of the saltmarsh, to a minimum of -2.2m ODN in the deepest parts of the shore-parallel channel, which lies to leewards of Hurst Spit over part of its length. (Figure 6.13). The varied back barrier geometry affects the evolutionary pattern: the natural rate of migration is controlled by relatively high zones of saltmarsh surface and relict recurves, which lie at a constant level, at the eastern end of Hurst Spit. In contrast, a channel ran parallel with the western 800m during the current investigation. Overwashing events resulted in migration and displacement of the barrier into the channel, reducing the effective CSA of the barrier, relative to storm water levels. This alteration allows greater volumes and frequency of overtopping discharge; consequently, higher rates of recession occur than farther to the east, where the CSA is maintained by overwashing.

The contrasting back barrier geometry is illustrated in Plates 6.1 and 6.2. The impacts of the geological structure underlying Hurst Spit also affect recession rates. Saltmarsh

deposits, which underlie the barrier, influence the effective beach volume, due to differential settlement resulting from loading by the washover deposits. Instantaneous loading by washover can result in rapid settlement of the marsh deposits, which is most rapid immediately after loading (Nicholls, 1985). When instantaneous loading is high, shearing and mass displacement of the marsh deposits may occur, due to their low shear strength: this was observed following artificial loading during beach recharge in 1996 (Bradbury and Kidd, 1998). Saltmarsh deposits directly beneath the shingle barrier, which generally lie below a level of 0.8m ODN, provide also an erodible zone which will not contribute to the local coarse sediment budget. The resultant effect is of erosion and steepening of the lower foreshore zone, which can increase the wave conditions at the beach toe; this results in a net loss of volume from the beach. Local longshore variations in wave climate have been identified in this study (Section 5.3); these will contribute also, to the spatial distribution of barrier recession. Plan shape changes to Hurst Spit, during the study period, reflect swash alignment: beach alignment changes occur in response to the bi-directional wave climate (Section 5.3).

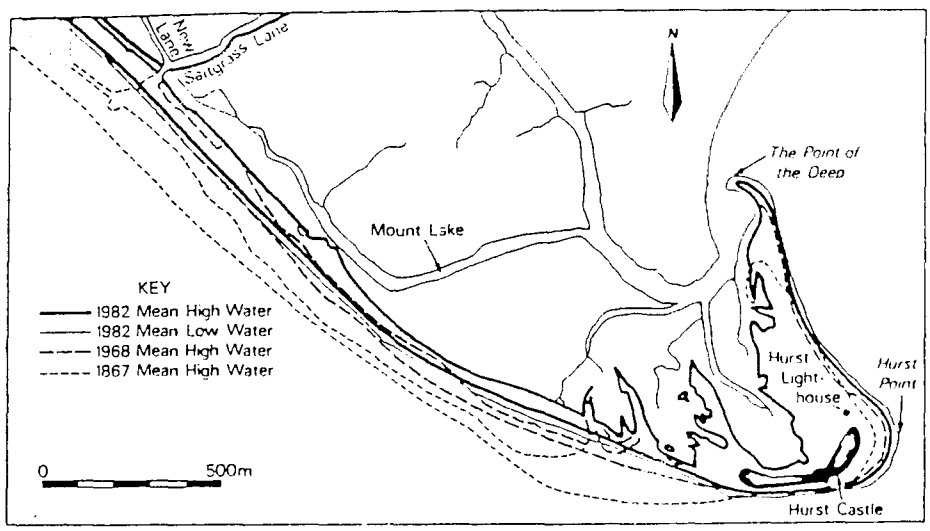

Figure 6.6 Barrier crest roll back between 1987-1993 from Nicholls and Webber (1987a)

Plate 6.1 Deposition of washover fan into the barrier lagoon near profile HU12, Hurst Spit, in December 1989 (location is shown on Figure 6.13)

Plate 6.2 Aerial view of washover deposits on saltmarsh between profiles HU13 and HU17, Hurst Spit, in 1984 (location is shown on Figure 6.13) (Photograph, courtesy New Forest District Council)

6.3 GRAIN SIZE ANALYSIS OF SEDIMENTS

The primary objectives of particle size distribution (PSD) analysis were to provide design data for the physical model and the beach recharge schemes; likewise to provide appropriate variables for use in assessment and development of empirical cross-shore prediction formulae. The significance of grain size distribution, on the hydrodynamic response of shingle and mixed beaches, has been recognised elsewhere (Mason, 1997). This investigator has suggested that considerable reduction in permeability and energy dissipation occurs, when the sand composition exceeds 10-20% of the beach volume. Grain size has been suggested as a significant variable (Powell, 1990; van der Meer, 1988). These authors utilise D_{50} within dimensionless parameter groupings, in their analysis of beach profile response. Powell (1993) examined subsequently the significance of a grading width variable (D_{85}/D_{15}) including this in further analysis.

Extensive studies of cross-shore grain size distribution on Hurst Spit (Nicholls, 1985) has provided suitable background data, for the assessment of : site-specific representativeness; and decadal temporal changes. Variations in particle roundness and maximum projection sphericity, of indigenous shingle at Hurst Spit, are also discussed by Nicholls (*op. cit*). Shingle in the study area has a composition which relates closely to the constituents of the Pleistocene Gravel; its composition is predominantly sub-angular to angular flint, with a small proportion of well rounded pebbles. Comparisons of the two data sets has confirmed that the samples collected for the current investigation were representative of the indigenous composition. Similarly, that the grading had not altered significantly between 1982 and 1990.

A series of PSD curves were produced, and the ratios of D_{85}/D_{15} were determined. The data for each of the sampling exercises (Section 4.2.3) was combined, to provide a 'typical' beach grading for the whole of the barrier. Data shown in Figure 6.7 were used: (a) as the basis for the design of the physical model of Hurst Spit; (b) for the subsequent design of the beach recharge material for Hurst Spit; and (c) as a variable in the dimensional analysis of barrier forcing (Section 7.5). Similar analyses of beach recharge sediments (Figure 6.8) were carried out during the 1996 beach recharge programme: this utilised sediment dredged from the Shingles Banks (Figure 3.1). The results correspond well with the data presented on the geological structure of the Shingles Banks (Velegrakis, 1994). However, the analyses indicates that the material

may be coarser than was suggested originally, in this earlier investigation; this may be a function of the vibracore sampling used in the earlier study (which limits the maximum particle size collected).

Although the PSD varies across the beach profile, with a tendency for natural sorting (resulting in preferential coarsening upwards of the sediments), analysis of the effects of cross-shore sorting were not included further within these investigations. Analysis of the influence of sediment size is confined to determination of a typical beach grain size, based upon the averaging of a series of cross-shore surface and depth samples. The significance of cross-shore grain size variability, sediment shape and sorting is recognised; these influence the evolution of beach profiles, under storm conditions. Future studies could usefully extend the validity of this research, by examination of the influence of sorting and size variables. The influence of cross-shore sediment sorting is perhaps less significant on overwashing barrier beaches, than on restrained beaches; this is due primarily to the large-scale re-mixing of sediments, carried across the beach crest in washover.

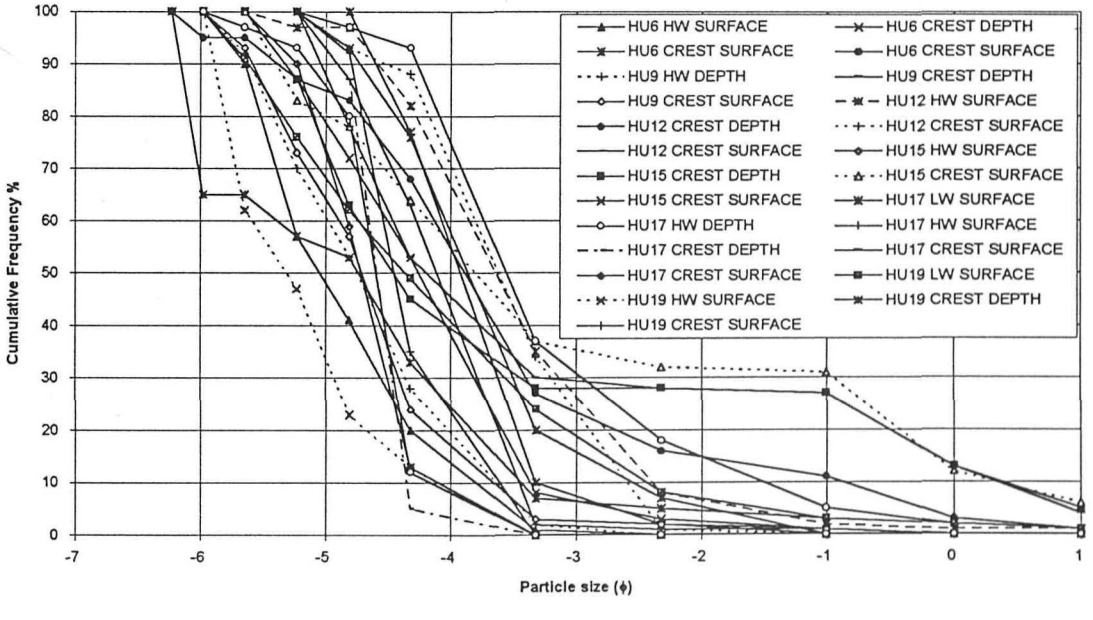

Figure 6.7 Particle size distribution curves for sediments from, Hurst Spit, (1990)

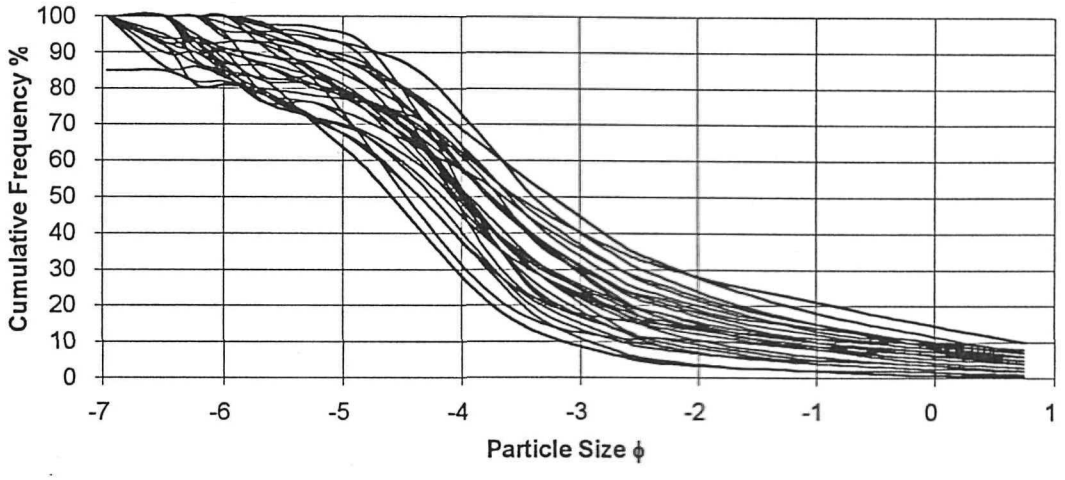

Figure 6.8 Particle size distribution curves for the beach recharge materials (from Shingles Banks) used at Hurst Spit, 1996.

6.4 HYDRODYNAMIC CONDITIONS

Hydrodynamic measurements have provided calibration data for the numerical modelling programme (Section 5.3), data for the design of the physical model (Section 4.4.3); they have provided also direct measurement conditions for the analysis of storm events, during the latter stages of the study programme (Section 6.5.4). Simultaneous time-series of each of the hydrodynamic variables were used to describe the intensity of the storms. Key variables were determined, for the analysis of each storm event: i.e. storm peak water level, significant wave height, wave period, wave direction and spectral shape were measured.

6.4.1 Wave measurements

Data collected during waverider buoy deployments were analysed using various approaches. The deployment at Milford-on-Sea provided a virtually continuous time-series between January 1996 and October 1997; data recovery rates were high, exceeding 92% for the period. Several periods of lost data occurred; the longest being

during September 1996, when the buoy was temporarily removed for repairs. The data set was of a similar duration to an earlier deployment at this location (Hydraulics Research, 1989a).

Analysis of hourly averaged summaries of significant wave height and wave period has provided data for the recalculation of the probability distribution of wave conditions, and to predict the extreme conditions. This analysis has been compared directly with the earlier investigation (Hydraulics Research, *op. cit*). Comparison of the two time-series suggests that the winter period 1996-97 was particularly severe. A typical 1:100 year storm (based on an extreme prediction using a 3-parameter Weibull extrapolation of the 1987-1989 dataset) was exceeded on four occasions during the winter of 1996-97. This period included: 14 storm events with H_s>2m; three storm events with H_s>3m; and 1 storm event with H_s=4.1m. The comparison demonstrates the potential problems of extrapolation of time-series, to predict extreme events, when relatively short time-series are used: it questions the statistical validity of the earlier extreme wave predictions (Hydraulics Research, *op.cit*). Figure 6.10 shows the distribution of wave conditions during part of the winter measurement period.

The omni-directional wave data were used, in parallel with wind speed and direction data and the wave refraction model, to determine nearshore directional data for the analysis of individual storm events. Although a full spectral analysis was determined for each hourly sampling period, only the summary spectral characteristics (H_s and T_m) were used in subsequent analysis of beach response to storm events. Spectral shape was not considered as a variable, within the analytical framework, although it may have a significant effect on barrier profile response. Previous studies of shingle beach profile response have not suggested any significance of spectral shape on profile response (Powell, 1990; van der Meer, 1988). The measured spectral shape of storm events was generally narrow-banded, characteristic of a JONSWAP spectral shape, resulting from rapidly-developing conditions. A significant long period component was observed in a number of storm events, resulting in a twin peaked bi-modal spectrum (Figure 6.9). However, the significance of this has not been identified, in terms of profile response. This sea state characteristic is masked, when describing the sea state in terms of significant wave height and peak or mean wave period alone. Inclusion of a significant swell component within the spectra was, not surprisingly, confined to those events which had developed over a number of days. Long period (>12s) waves, within the

wave train, may have a significant impact on wave run-up and overtopping and are worthy of further investigation. The significance of long period components may be greater on a barrier beach, than on a restrained beach: occasional high volume long period waves within a wave train can result in overtopping and perhaps overwashing of the beach crest. At the same time, the majority of waves, in frequency bands close to the spectral peak, may reach much lower run-up levels. The impacts of such a process can only be analysed effectively on a 'wave by wave' basis; they cannot be determined by inference of the spectral shape, or beach response characteristics.

A short deployment of the waverider buoy in the North Channel, during 1994, has provided the opportunity to measure waves close to the toe of the beach, in the lee of the Shingles Banks. Wave periods were consistently lower than those predicted by the numerical modelling methods; wave heights were also lower. Only a single severe storm event occurred during this deployment; this is analysed in Section 6.5.3.

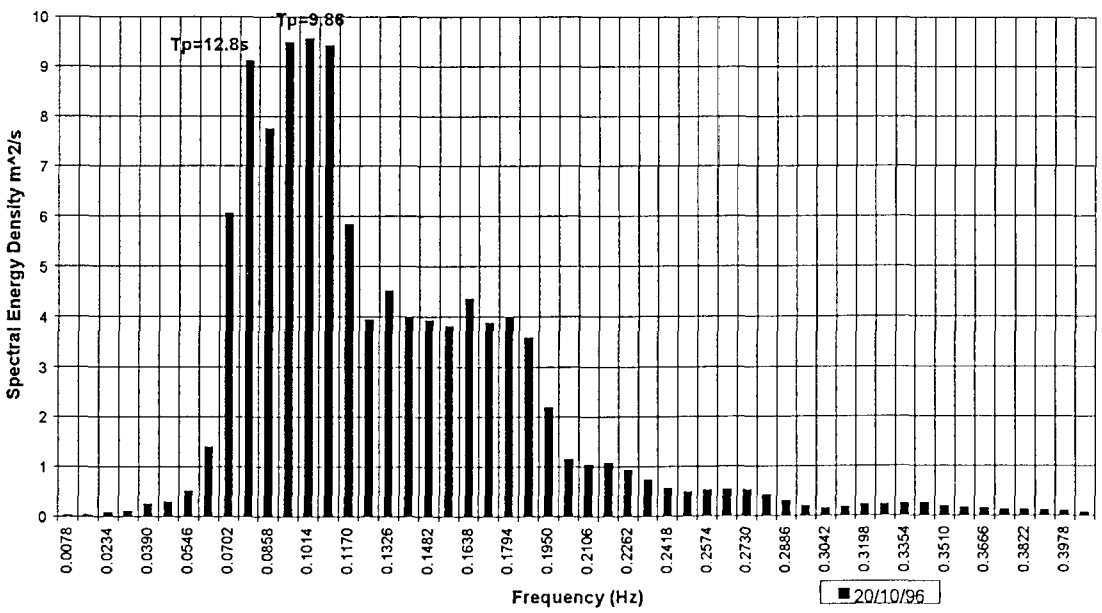

Figure 6.9 Spectral analysis of wave conditions on 28/10/96, for the Milford-on Sea Waverider, (for location see Figure 4.6) showing a dual peaked spectrum

(a)

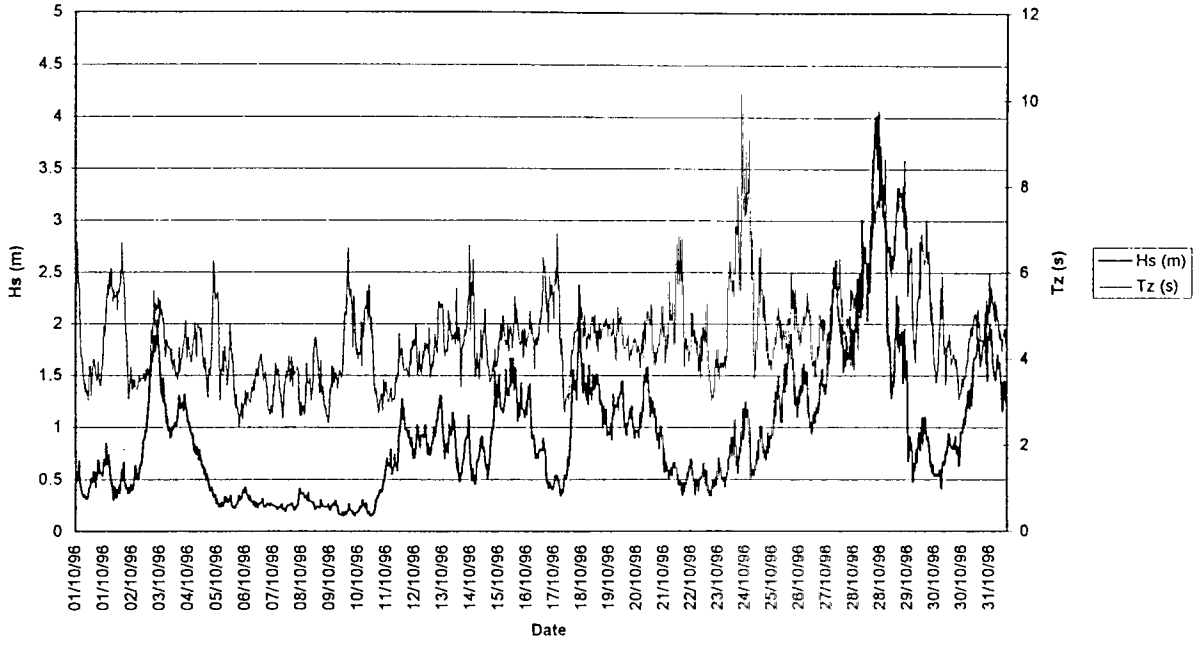

(b)

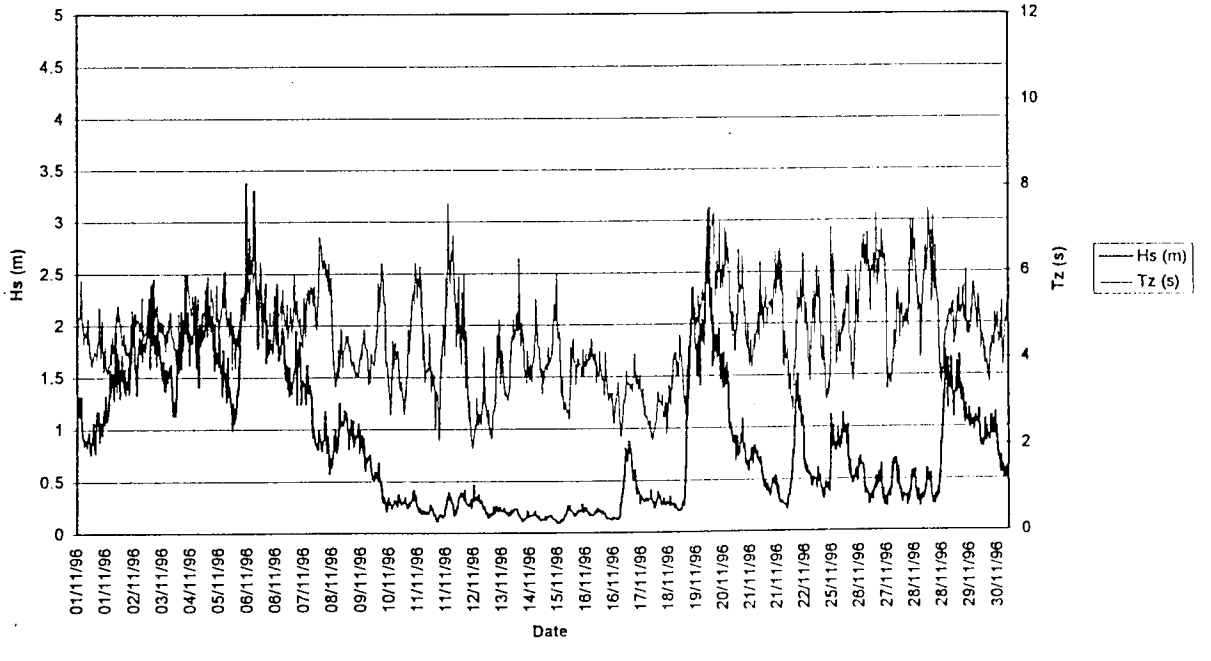

Figure 6.10 Time-series of wave data for the winter period 1996-97, from Milford-on-Sea waverider buoy: (a) October 1996; (b) November 1996.

6.4.2 Tides and surges

The tidal regime of the study area is complex as it lies within a region where the amplitude of the M_2 constituent is relatively weak, combined with a strong shallow water M_4 tidal component; this results in a double high water, with a long high water stand. The site is mesotidal, with a mean spring tidal range of 2.2m and neap tidal range of 1m. A typical spring tidal curve is shown, for the storm event of 28/10/96, in Figure 6.44, - the long high water stand results in water levels being maintained within a range of 0.2m, for a period of 4.5-5 hours.

As the lee and seaward sides of Hurst Spit, which is typically 30-80m wide at MHW, are separated by a water distance of up to 5km, due to the tidal propagation between Christchurch Bay and the Western Solent (Figure 4.7), differential levels are to be expected. Contrasting Spring and Neap tidal curves are shown, for the Lymington and Hurst Spit tide gauges, in Figure 6.11. Tidal elevations demonstrate a maximum differential level of 0.7m, between the gauges; the tidal curves are out of phase, despite the small distance between them. These observations are similar to those made in earlier investigations (Nicholls, 1985). Maximum differences of 0.75m were observed on a rising tide and 0.4m on a falling tide: these differential water levels may have a significant effect on the hydrodynamic stability of Hurst Spit.

Crestal changes to the shingle barrier occurred only over high water periods, in combination with storm surges, during this investigation. Surges greater than 0.8m had the most profound effect on the barrier crest response. The significance of the surge component is twofold. Firstly, the point of attack on the barrier is moved to landwards by the ratio of beach slope to surge height. A 1m surge on a beach with a mean slope of 1:7 will move the point of attack landwards by 7m; this is highly significant on a barrier which is only 30m wide at MHW. Secondly, the increased water depth at the beach toe allows higher and longer period waves to attack the beach, prior to breaking. A 1:100 year return period water level of 1.68m has been suggested (Nicholls, 1985): this seems unlikely, as this level was exceeded on 7 occasions during the study period. The current investigation has provided a relatively short term time-series of data, which is too short to be used to be used for accurate long-term forecasting of extreme water levels. Instrumentation and an analysis programme is in place, to permit long-term data collection and the potential for future

extreme water level analysis at the site. The effects of extreme water level events are examined on an event by event basis in Section 6.5.

Deployments of tide gauges in the Western Solent and adjacent to Hurst Spit provided, simple, elevation time-series data - required for analysis of storm events. Data was extracted from the time-series records to provide information across the storm peak; an example is shown in combination with wave data in Figure 6.44, for the storm event of 28/10/96.

6.4.3 Current measurements

Whilst it was considered unlikely that velocities generated by longshore tidal currents would have an impact on the cross-shore evolution of the shingle barrier during extreme storm events, a brief investigation of the nearshore currents was undertaken. Such a study was undertaken to aid the design of the physical model, allowing the modification of waves by tides to be incorporated into the modelling process.

Current measurements collected in the North Channel (Figure 4.4) are shown in Figure 6.12, for spring and neap tidal cycles. Velocities increase from west to east, and run generally shore-parallel, from west to east on a flood tide and from east to west on an ebb tide. The substitution of peak near-bed velocities into sediment transport formulae indicated that the threshold of motion for shingle was not exceeded at the high water level conditions, which result in barrier crest evolution.

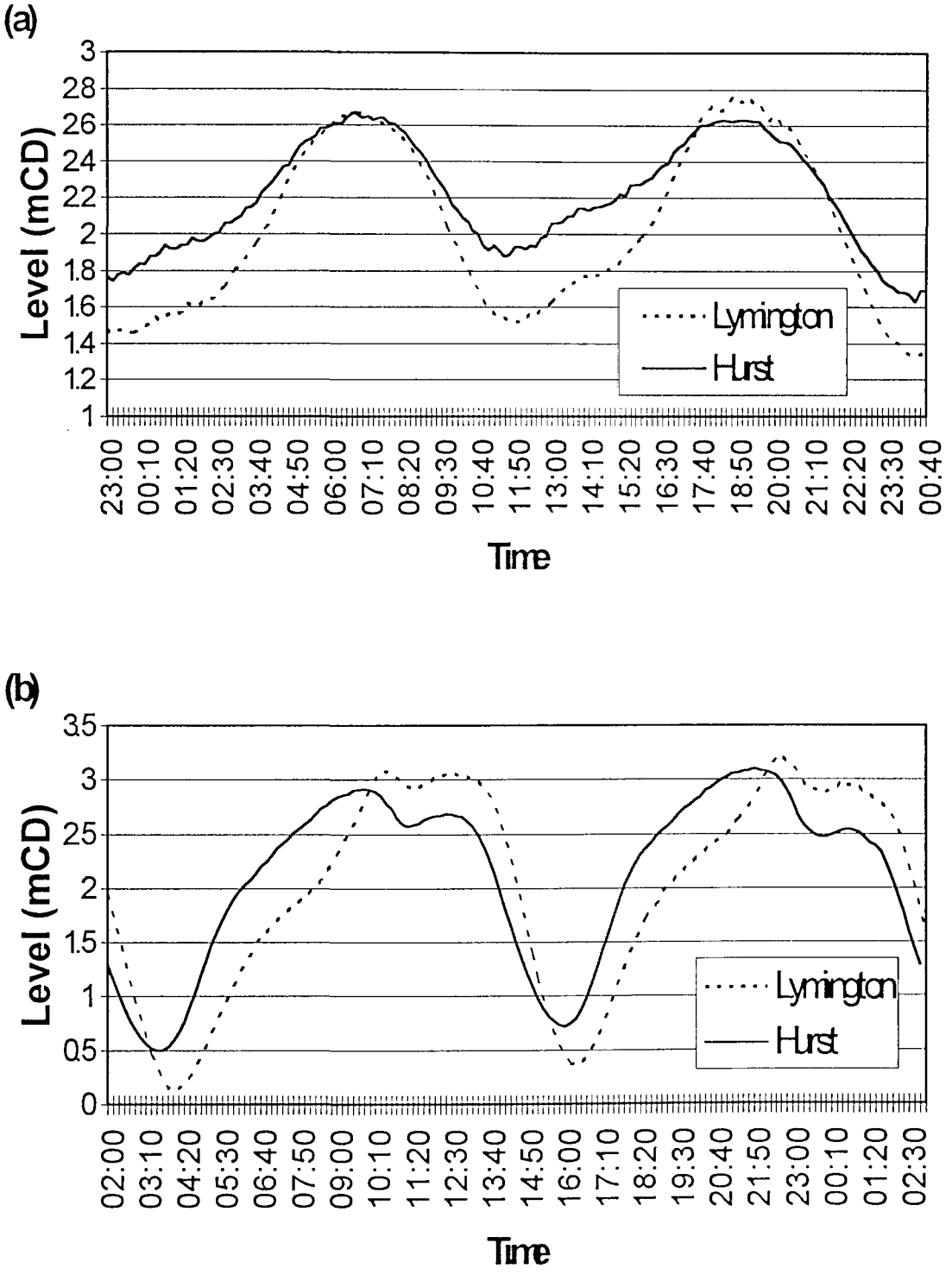

Figure 6.11 Comparison of neap (a) and spring (b) tidal cycles for locations at Hurst Spit and Lymington

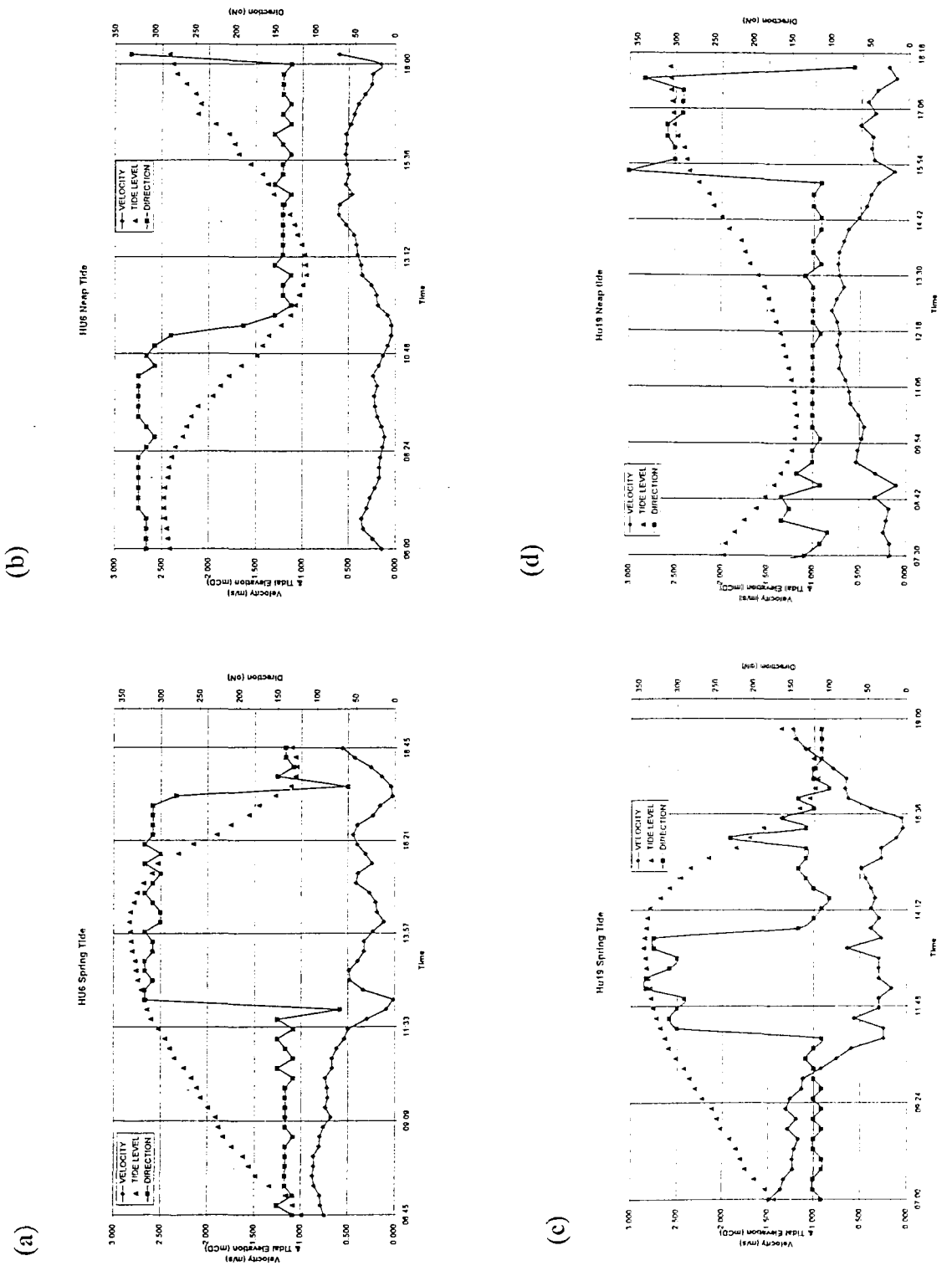

Figure 6.12 Tidal currents, for spring and neap tides at North Channel sites: (a) HU6 Spring tide; (b) HU6 Neap tide; (c) HU19 Spring tide; (d) HU19 Neap tide (for locations, see Figure 4.4)

6.5 STORM EVENTS

Whilst average rates of migration provide an indication of barrier response, trends identified at a decadal or sub-decadal scale, related to changes in mean sea level, may be masked by the incidence of extreme events, (which can bias strongly average rates). This pattern is demonstrated by the storm event of 17/12/89, which resulted in the equivalent of between 5-20 average years of change overnight. Hence, average migration rates discussed at a decadal scale (Orford *et al* ,1991a, 1993, 1995) must be considered with some caution. The frequency of overwashing events increased, during the period of monitoring prior to the commencement of the study; this was due to the decline in supply of sediment from the west and a consequent reduction in the beach cross section. Data collected prior to commencement of the study (by NFDC) provided evidence of crest rollback during the period 1987-1988. Regrettably, the data gathered during this period were collected without simultaneous records of wave conditions and water level data.

Analysis of field data consisted of examination of the profile response of Hurst Spit to those storm events which caused significant modifications to the upper beach profile, which were surveyed both pre- and post-storm: time-series of wind-, wave-, and water-level-data, providing hydrodynamic input and; post-storm morphological observations to support analysis of the events. Data sets demonstrate considerable spatial variation and the development of a range of combinations of beach response, within individual storm events: this is consistent with similar observations made in earlier investigations (Orford and Carter, 1982). The extreme events analysed include similar storm events on both the natural shingle barrier and the recharged barrier; this provided a contrast between overtopping and non-overtopping conditions. Two overwashing events occurred prior to the physical modelling phase of the test programme: thus, these have provided the design and calibration data for the physical model (Section 7.1).

Storms are discussed on an 'event by event' basis, to investigate the effects on profile response, of: beach geometry; and spatial variation of environmental parameters. The combined effects of hydrodynamic variables and profile response characteristics are examined qualitatively at the end of this Chapter. The data are subsequently included in the parametric analysis, together with the model data in Chapter 8.

Data collection conditions varied between the various events. Nevertheless, several important restrictions have limited the range of applicability of the field data sets; these have demonstrated the need for alternative methods of study. The implications of these restrictions are outlined below.

Pre-storm profiles provided reasonable survey coverage of the beach toe, mostly reaching an elevation of -2m ODN; this is below the level at which the theoretical break point (p_t, h_t) is likely to occur under high water storm wave conditions. However, the level is some way above the expected closure depth of the dynamic equilibrium profile expected for storm events, according an earlier parametric model (Powell, 1990).

Post-storm profiles did not extend as low onto the foreshore, rarely extending below a level of 0m ODN: this is the result of the decay of wave conditions following storms, which limited the safe and practical extent of the topographic surveys. Conditions were unsuitable for hydrographic surveying. Consequently, no profile information was available for the sub-tidal segment of the beach profile. The beach was not profiled immediately after storms, because of the continued heavy seas, which followed the storm peak. Further modification of the storm profile, after the storm peak, usually resulted in development of a modified ephemeral run-up berm, to seawards of the barrier crest. Thus, measured post-storm profiles are a combination of the response to the storm peak, which modifies the beach crest, and further development of a modified seaward profile. This combination of conditions presents some analytical difficulties, with reference to the parametric profile prediction model (Powell, *op.cit*); this is designed to examine the response of a known profile to a single set of hydrodynamic conditions.

Profile response is affected by a number of man made factors adjacent to the root of Hurst Spit. The present root position of the barrier beach is some 600m west of its natural position; this is controlled by a rock armoured revetment, constructed originally in 1963 and later extended to its present position (Nicholls, 1985). The junction of the barrier beach with a rock revetment provides a change in the hydrodynamic regime, between the statically-stable structure and the dynamic barrier. A transition zone of 300 m was considered appropriate, to differentiate between the open barrier and the rock revetment. Data were compared, to investigate the relative

performance of the open barrier and a zone affected by local coastal protection structures. Observations made during storm events have demonstrated that the rate of sediment transport is lower along the toe of the rock revetment, than along the barrier; consequently there is no mass balance and sediment starvation occurs at the junction.

The duration of the study and the limitation of overwashing events to extreme storms restricted the occurrence of suitable storm events to analysis. However, a combination of storms has provided a wide framework of conditions. Further analysis of each of the events is presented later, in a synthesis of field data, in combination with the physical model data in Chapter 8.

6.5.1 October 29 1989

Profiles collected on 28/09/89 provided a pre-storm data-set. A relatively calm period between the survey and storm will certainly have modified the lower beach profile, although the crest profile geometry could not have been altered by wave activity. Pre-storm profiles are characterised here by wide run-up berms to seawards of the crest ridge. Such data indicate a period of beach accumulation at the toe of the barrier crest; this is consistent with previously proposed conceptual evolution hypotheses (Carter and Orford ,1993, 1993a). The run-up berm ridge, (p_c, h_c) is a characteristic clearly defined point on the beach profile; it provides an indication of the wave climate during recent high water conditions (Powell, 1990). This berm elevation fell from west to east, representing the longshore spatial reduction in wave intensity, (Section 5.3). Spatial variation of the pre-storm crest ridge position and elevation varied, from 1.8m ODN at HU6 to 1.3m ODN at profile HU19 (Figure 6.13). This pattern is shown clearly by the pre-storm profiles (Figures 6.14-6.19).

A berm elevation of between 1.7-1.8m ODN occurred over a distance of 800m, between profiles HU6-HU14; this suggests that spatial variation of wave climate is small, over this distance, under relatively calm conditions. This beach zone corresponds with physical model Segment B, (Figure 4.13). Back calculation of the conditions leading to the development of such a profile using the parametric profile prediction model (Powell, 1990), suggests wave conditions with H_s=1.25m and T_m =4.25s, at a water level of 0.6m ODN. Berm elevation fell by 0.4m, to an elevation of

1.3m ODN, over a distance of 800m, between profiles HU14-HU20. This observation confirms the dissipative influence of the offshore bank system, even under relatively calm conditions; it demonstrates also the significant longshore variation in wave climate (this is illustrated numerically in Figures 5.9-5.12).

Spatial variations in the initial geometry and effective barrier crest level has resulted in spatially variable reductions, in both crest level and beach CSA, above the storm peak water level, (0.87m ODN). Variability in key geometric characteristics of the pre- and post-storm profiles are shown in Figures 6.14-6.19. Key variables are presented in Table 6.2.

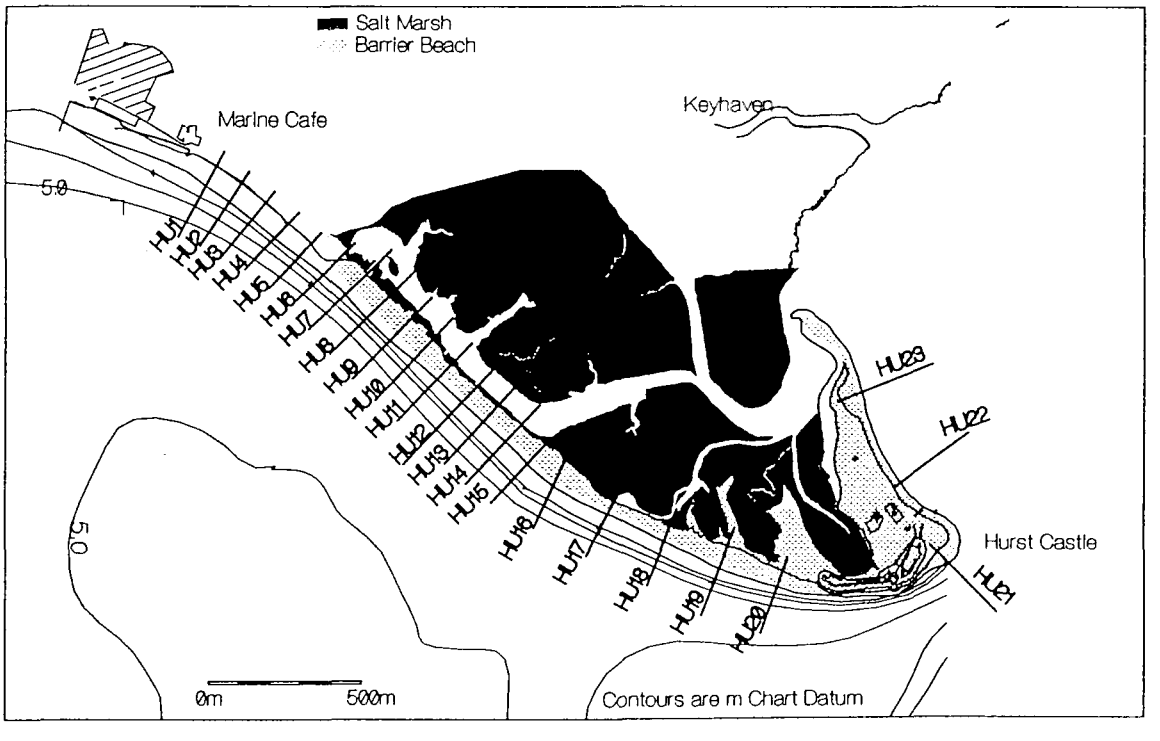

Figure 6.13 Location of the beach profile survey lines at Hurst Spit

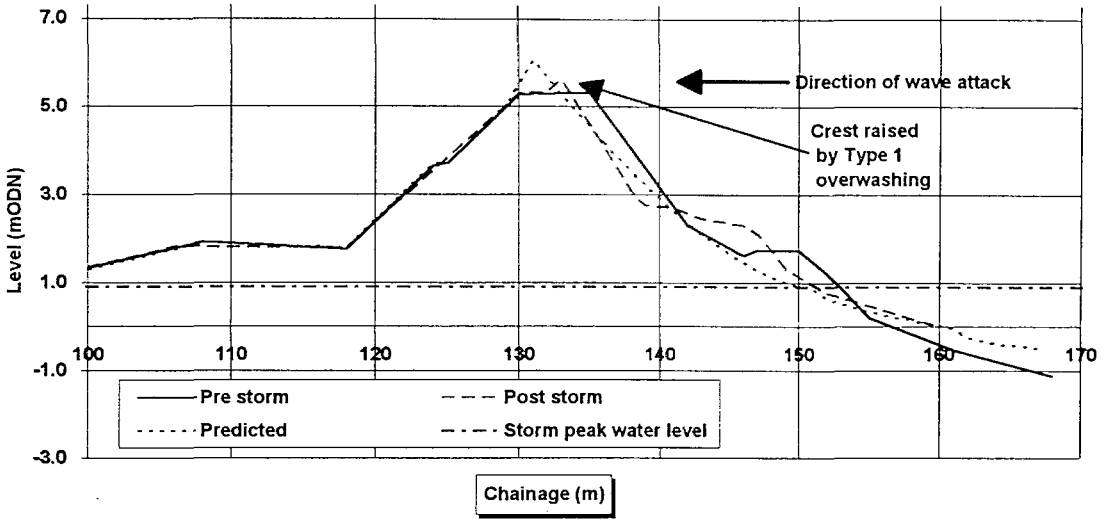

Figure 6.14 Measured pre- and post-storm profiles and predicted profile response for the storm of 29/10/89, at HU6 (see Figure 6.13) for storm conditions: Hs =3.8m; Tm=10.1s; SWL=0.87 m ODN

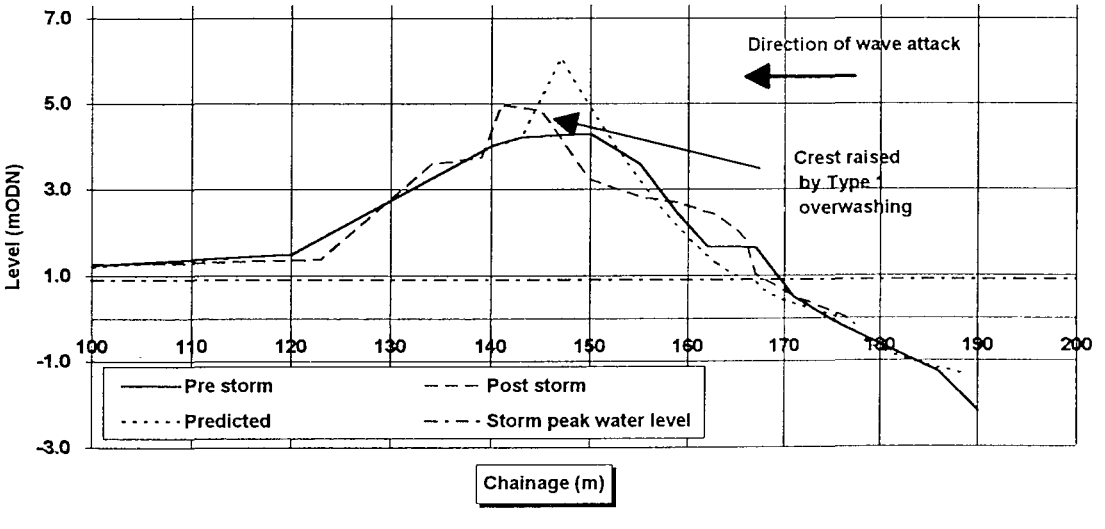

Figure 6.15 Measured pre- and post-storm profiles and predicted profile response for the storm of 29/10/89, at HU8 (see Figure 6.13) for storm conditions: Hs =3.8m; Tm=10.1s; SWL=0.87 m ODN

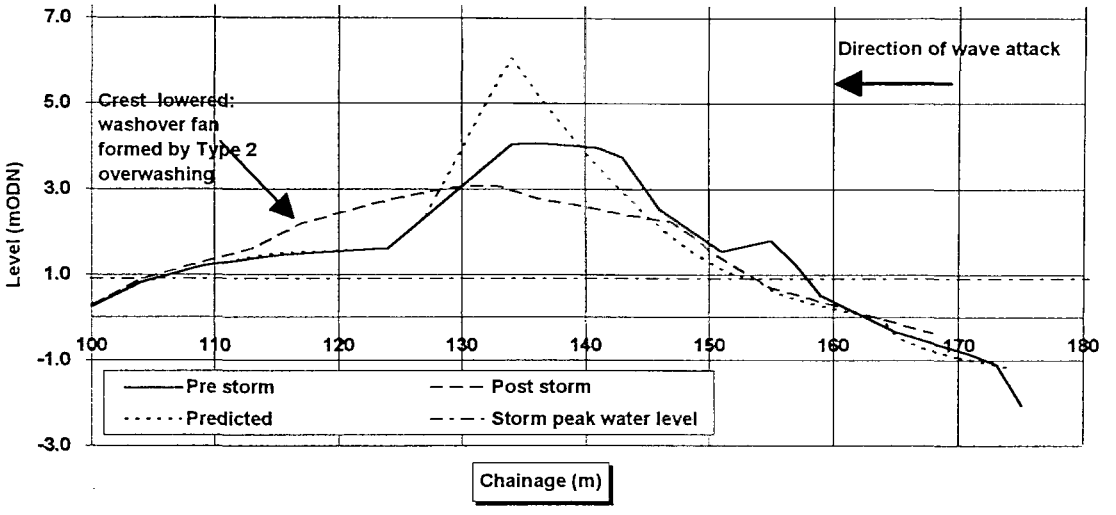

Figure 6.16 Measured pre- and post-storm profiles and predicted profile response for the storm of 29/10/89, at HU10 (see Figure 6.13) for storm conditions:Hs =3.8m; Tm=10.1s; SWL=0.87 m ODN

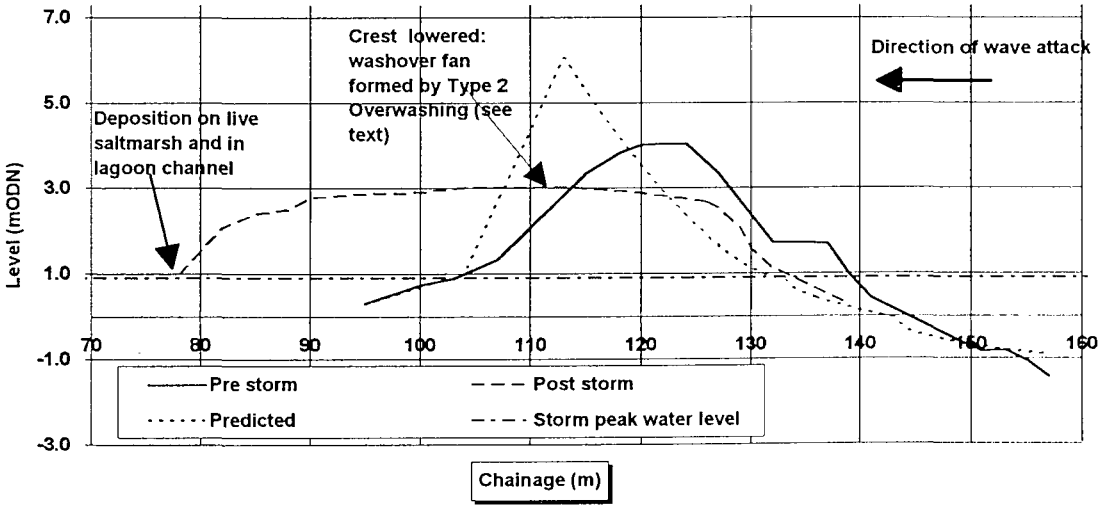

Figure 6.17 Measured pre- and post-storm profiles and predicted profile response for the storm of 29/10/89, at HU13 (see Figure 6.13) for storm conditions: Hs =3.8m; Tm=10.1s; SWL=0.87 m ODN

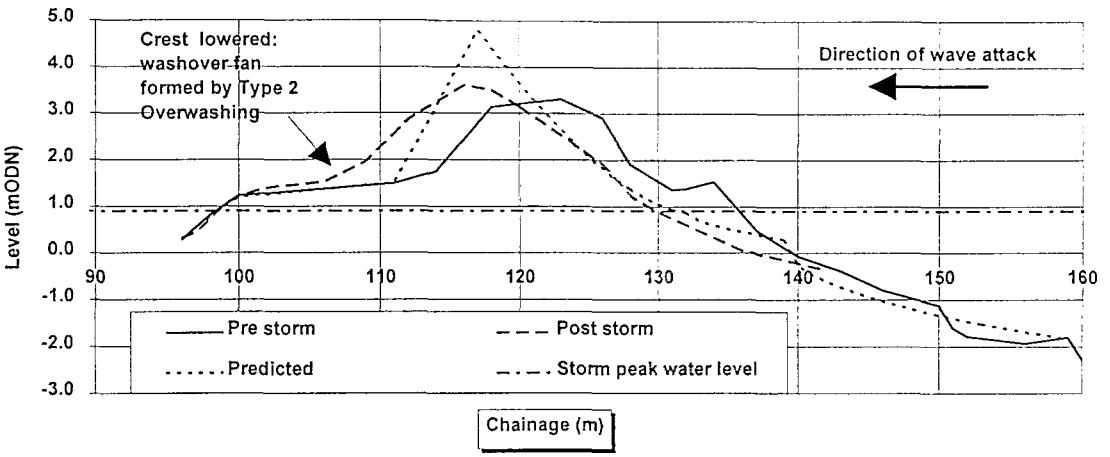

Figure 6.18 Measured pre- and post-storm profiles and predicted profile response for the storm of 29/10/89, at HU17 (see Figure 6.13) for storm conditions: Hs =2.9 m; Tm=9.5s; SWL=0.87 m ODN

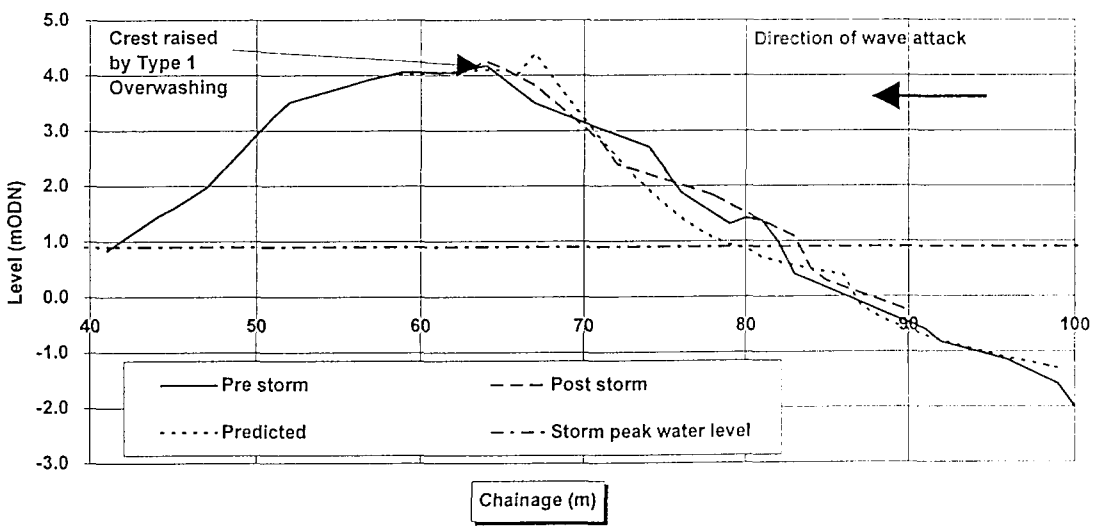

Figure 6.19 Measured pre- and post-storm profiles and predicted profile response for the storm of 29/10/89, at HU20 (see Figure 6.13) for storm conditions:Hs =2.9m; Tm=9.5s; SWL=0.87 m ODN

(a) Hydrodynamic conditions

Numerical modelling has indicated (Section 5.5) that the intensity of wave conditions reduced from west to east, during the storm. H_s fell from 3.9m at the prediction point offshore of profile HU8, to 2.9m offshore of profile HU14, and to 2.6m at profile HU19 (Figure 6.13). Predicted wave periods varied between 9.5-10.2 s. A storm peak water level of 0.87m occurred. It has been suggested (Section 5.5) that lengthening of wave period, due to shallow water processes, is exaggerated by wave refraction modelling; this is largely as a result of the complex bathymetry in the study area: actual nearshore wave periods may have been shorter than those predicted. Offshore wave conditions suggest a deep water period of 8.8s. Limitations of the wave modelling are further supported by field observations, subsequent monitoring of wave conditions (Section 6.4.1), and comparison of hindcast wave data with measured wave data, during extreme events with similar storm profiles.

(b) Profile analysis

Pre-and post-storm profiles were plotted to identify changes, resulting from storm conditions. Numerical comparisons of the barrier profile response were made by integrating the area under each of the beach profiles, in 0.1m thick horizontal slices; this provided both the beach span, at a defined level, and also the CSA above that level. Comparisons of the pre- and post-storm span and area data, based upon the difference of the integrated values, demonstrates the levels and quantities of the area and span changes during the storm; they describe also the geometric changes of barrier crest elevation.

Contrasting evolutionary steps are represented in Figures 6.20-6.22, which demonstrate, respectively; (a) crest lowering, roll back and an increase in span at low levels; (b) crest roll back, with an increase in crest elevation and steepening of the profile; and (c) minor crest changes with beach steepening. Each phase of barrier evolution is characterised by span- and area-curves of differing shapes and trends. A cross-shore mass balance was not achieved on any of the profiles, demonstrating a movement of material to lower levels than those profiled. This pattern is consistent with the expected beach profile response.

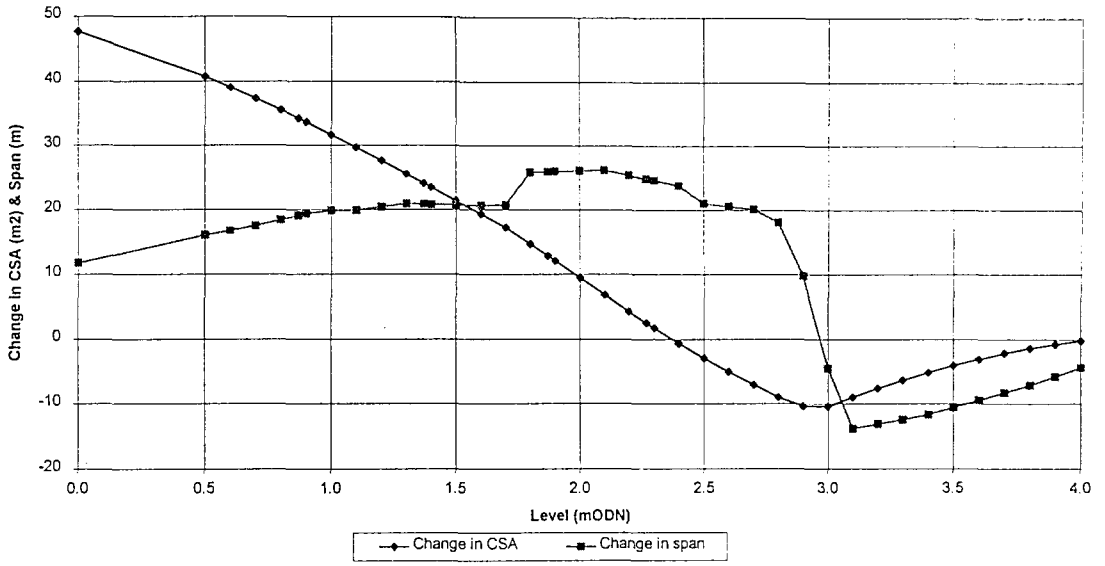

Figure 6.20 Changes in the barrier profile - span and CSA, shown in 0.1m vertical increments, due to the storm of 29/10/89 at Profile HU13

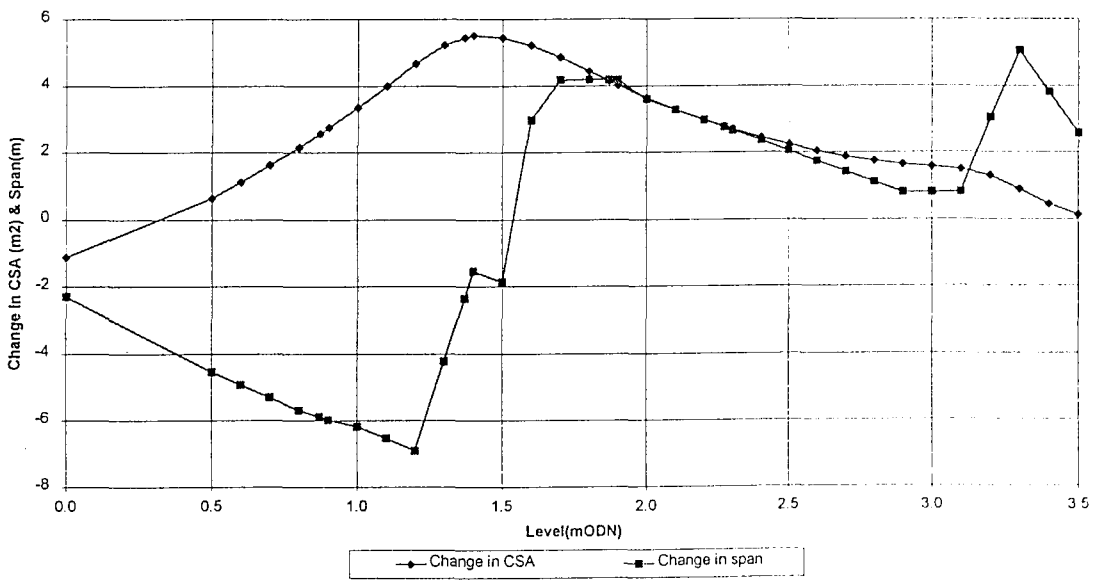

Figure 6.21 Changes in the barrier profile - span and CSA, shown in 0.1m vertical increments, due to the storm of 29/10/89 at Profile HU17

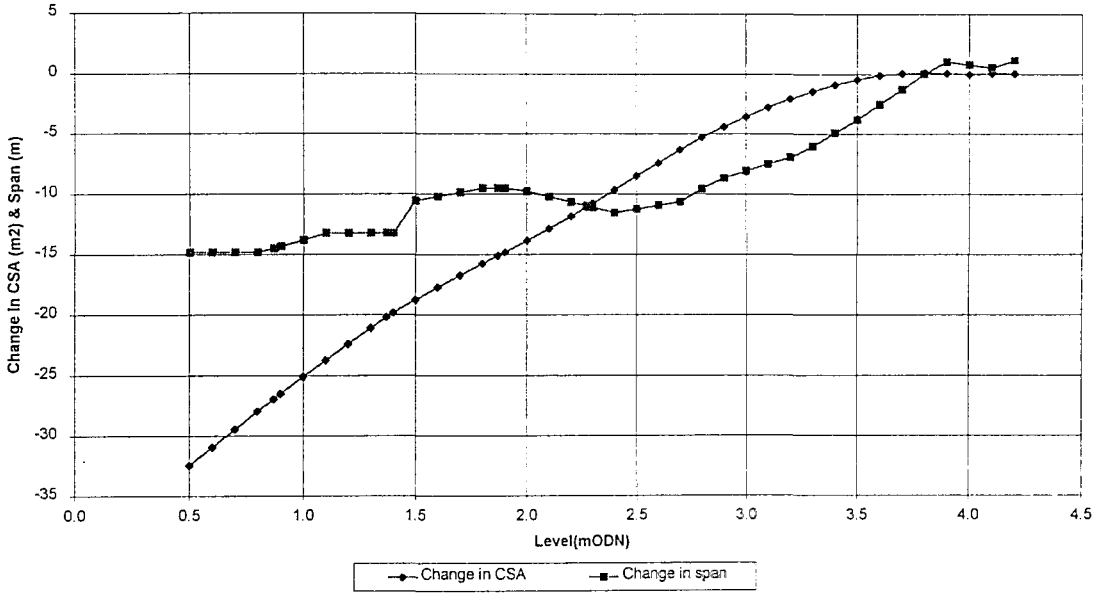

Figure 6.22 Changes in the barrier profile - span and CSA, shown in 0.1m vertical increments, due to the storm of 29/10/89 at Profile HU20

Further analysis of profile response was carried out by reference to parametric profile prediction equations (Powell, 1990), using measured profile and water level conditions. Synthetic wave data generated for analysis of this event is discussed further elsewhere (Section 5.5). Wave climate analysis suggests a return period of 1:5 years for this event, with a nearshore significant wave height (H_s) of 3.87m and period (T_m) of 10s, at the most exposed western end of the site. The profile response and hydrodynamic relationship is complicated further by longshore variability in the wave climate. Substitution of hydrodynamic conditions and measured profiles into the empirical framework presents a problem, as they lie beyond the outer limits of the validity of the profile prediction equations (Powell, 1990). Subsequent analysis and comparison of measured wave data, with synthetic wave conditions during 1996-1997, suggests that the wave refraction model over-predicts the nearshore wave period, by approximately 10-15%. This overestimation may represent the complexity of the nearshore bathymetry at this site: previous calibration of the same model, against real wave data, has not indicated similar variations (Hydraulics Research, 1989d). Reduction of the wave period, from 10s to 9s brings the hydrodynamic data within the range of validity of the model; in this case they appear to compare favourably with the limitations of the numerical modelling (discussed above). The

data was tested within the valid limits of the empirical framework, with a reduction in wave period from 10s to 9s.

The profile prediction model functions effectively only when a mass cross-shore pre- and post-storm profile balance can be achieved, within the volume of the pre-storm beach: this occurs during this particular storm event and the profile response should, theoretically, be predicted correctly by the model (Powell, 1990). However, the model is limited to prediction of profile development within a confined beach; it does not simulate the rollback process observed on shingle barrier beaches. It is not reasonable to expect direct comparison of the predicted and measured profile response, under such conditions (see Figures 6.14-6.19).

This (29/10/89) storm event has provided contrasting profile response along the length of Hurst Spit, demonstrating several phases of a conceptual barrier evolution model within a single storm event (Orford and Carter, 1982) (Figures 6.14- 6.19). Profiles HU6-HU9, spread over a longshore distance of 300 m (Figure 6.14-6.15), have demonstrated cut-back of the barrier crest. However, the whole of the storm profile developed within the existing beach without overwashing. Pre-storm barrier crest levels, widths and CSAs were larger than farther to the east, where overwashing and crest modification occurred. Profile response is similar throughout the western section of the beach, where the wave climate is consistent (according to numerical modelling) (Section 5.3).

Profile HU6 (Figure 6.14) was associated with a run-up crest at a level of 5.5m ODN, some 0.6m below the predicted run-up crest for the storm; this suggests, perhaps, that the wave period predicted by the numerical modelling may have been even lower than the reduced value used in the profile prediction formulae. Overtopping resulted in a small quantity of deposition at the barrier crest.

Profile HU7 shows an interesting response to the prevailing wave conditions: cut-back of the beach occurred at the leeward limit of the pre-storm beach crest ridge, leaving a 'knife-edge' crest at the pre-storm level. The crest width was reduced from 6m to 1m: and it should be noted that this profile is close to the limit of formation of a break-through breach. Whilst this type of profile response is not discussed elsewhere in the literature, it is an important form of barrier evolution: previous studies suggest that

barrier crest evolution results only from overtopping, as opposed to widening of the active beach profile. The profiles obtained suggest that overwashing did not take place, although the pre-storm profile occurred at the calculated maximum run-up level for the storm event (6.07m ODN). The profile was probably formed primarily by undermining and collapse of the barrier crest, developing as the active beach zone widened: this process is consistent with observations made during storms of 1997-1998, at the same location, when the crest was also above the run-up limit. Widening of the active beach zone is consistent with an increase in significant wave height, according to profile prediction (Powell, 1990).

Beach crest overtopping and overwashing occurred across all profiles to the east of Profile HU7, over a distance of 1600m (e.g. Figures 6.15-6.19). Beach response was variable, characterised by both 'Type 1 and Type 2 Overwashing', as defined by Nicholls (1985). Profile HU8 demonstrates 'Type 1 Overwashing', resulting in crest level accumulation and 'Type 2 Overwashing', resulting in the formation of a small washover fan on the lee face of the barrier. A crest level of 5m ODN was achieved, raising the original level by 0.7m and displacing the crest landwards by approximately 5m. Predicted crest elevation (h_c) is 1m higher than the measured post-storm crest, at a level of 6.07m ODN; it is also located farther to seawards, than the measured profile.

Extensive roll back and crest lowering of the beach crest resulted from overwashing, between profiles HU10-HU16 (Figures 6.16-17), over a distance of 700m. Profile response of the barrier is significantly different to that predicted by the parametric equations, throughout this section of the beach. The prediction model suggests: (a) a crest elevation (h_c), at an increased level of 6.07m ODN, and (b), a crest position (p_c) at a chainage of -20m to landwards of the SWL and beach-intersection: the predicted values of h_c and p_c reduce to 4.81m ODN and -15m, respectively, between profiles HU15-HU17.

In reality, the crest level was lowered on profiles HU10-HU16. Reductions in crest elevation, and consequent formation of washover fans and flats, resulted in the formation of a beach crest (at a level of between 2.9 and 3m ODN), between profiles HU10-HU14. Rollback of the barrier crest position accompanied crest level reduction; this ranged between 8-11m. Location of the lee-side toe of the beach also altered,

migrating on some of the overtopped profiles. Recession of the leeward beach toe varied spatially, in the range 0-25m, over the same distance: most of the profiles migrated by 10-15m. The landward edge of the barrier did not always migrate, despite crest rollback: this indicates a narrowing of the barrier (Figure 2.5), conforming with an earlier conceptual hypothesis (Orford *et al*, 1991a).

Profile response across the upper part of the beach profile is much more varied than when the profile is formed within a restrained profile; in the case of the latter, the beach run-up crest ridge forms at a constant level. Differences between the predicted and measured crest elevations exceeded 3m for this event (this error is well outside of the confidence limits for the prediction of h_c, which has an expected variance of $0.017H_s$=0.06m (Powell, 1990)). Application of the model is clearly not valid for this particular combination of hydrodynamic and geometric variables, even when there is sufficient volume of beach material available for the development of the theoretical profile.

Type 1 Overwashing and an increase in, or maintenance of, crest elevation occurred between profiles HU18 - HU20 (e.g. Figure 6.19), over a distance of 400m. The profile response of the beach compares more favourably with the empirical prediction equations, although these still over-predict elevation, for the conditions used within the equation framework. The predicted crest level varied, from the measured level, by 0.1-0.4m.

Other geometric variables were examined, to attempt to identify alternative response relationships between barrier geometry and hydrodynamic conditions. Results for this event are particularly useful, as they demonstrate several phases of barrier crest evolution (see above). Spatial variations of the barrier crest elevation, beach CSA and span, at the level of the storm peak (0.87m ODN), are examined in Figures 6.23 and 6.24: an oversimplification of beach response is presented, as no account is taken for the relative influence of longshore variation of nearshore wave conditions. The data suggest that crest evolution is related to a combination of barrier CSA, effective barrier crest elevation and prevailing hydrodynamic conditions, at a constant water level. This response supports the conceptual barrier inertia model framework suggested by Orford *et al* (1991a), providing quantitative hydrodynamic data focused on wave and freeboard conditions - in support of such a model.

The results suggest that critical threshold conditions, leading to crest lowering, were exceeded consistently between profiles HU10-HU16. Earlier research has suggested short, episodic, rapid reorganisation of barriers (Carter *et al,* 1993a), during which hydraulic jumps occur from one evolutionary mode to another; these are followed by long periods of slow evolution (Carter and Orford, 1993). Such a threshold was exceeded between profiles HU9-HU10 and HU16-HU17. Conditions determined by the numerical modelling have suggested that the significant wave height reduces from west to east; similarly that the mean wave period also varies. Hydrodynamic and grain size conditions varied little within the 200m between profiles HU8-HU10: it is suggested that the differing response over this distance is a representation of the initial beach geometry, which provides the only other combination of variables.

The barrier crest elevation varies between 4.2-4m ODN over this distance. Whilst this difference may be significant, the change is small when considered in terms of other linear elevation variables. The dimensionless barrier crest freeboard (R_c / H_s) varies within the range 0.86-0.80, between profiles HU8-HU10: the change in crest elevation is 6% of the freeboard, above the storm peak water level. The most significant difference is the pre-storm barrier CSA, above the storm peak water level; this fell from 113m^2, at profile HU8, to 75m^2 at HU10. The barrier crest elevation was lowered by overwashing when, both: (a) the beach cross-section was less than 76m^2; and (b) the barrier crest elevation was lower than 4.2m ODN (R_c = 3.33). These conditions were evident at all the locations, except at profiles HU17-HU18, where wave conditions were significantly less severe. This relationship is examined in more detail, in consideration with model results and in numerical terms, in Chapter 8.

The profiles between HU17 and HU20 all showed an increase in barrier crest level, due to crest accretion, resulting from overtopping: crest elevation was raised by as much as 0.3m within this beach zone. Changes in barrier CSA above the storm peak water level were relatively small (2 - 9m^2), whilst all of these profiles show net accumulation above this level. In contrast, beach span showed both increases and reductions in width, over the same zone. Pre-storm effective beach CSA ranged between 40-101m^2. The calculated significant wave height was 2.58m, for this particular zone.

Profile	*Pre-storm CSA above SWL (m^2)*	*Pre-storm crest level (m ODN)*	*Pre-storm span at SWL (m)*	*Post-storm CSA above SWL (m^2)*	*Post-storm crest level (m ODN)*	*Post-storm span at SWL (m)*	*Crest level change (m)*	*Extent of Crest Rollback (m)*
HU6	99.7	5.3	53	103.7	5.6	51.6	0.3	0
HU7	116.5	6.0	70.6	107.2	5.7	69.2	-0.3	0
HU8	113.3	4.3	69.8	110.7	4.9	68.0	0.6	5
HU9	85.9	4.2	53.1	75.7	4.2	52.1	0.0	0
HU10	74.7	4.1	53.1	66.8	3.0	50.3	-1.1	8
HU11	57.6	3.9	44	58.7	3.3	44.7	-0.6	10
HU12	58.1	3.9	49.4	56.6	2.9	44.9	-1.0	10
HU13	61.5	4.0	36.9	95.8	3.0	56.0	-1.0	11
HU14	65.4	3.9	40.7	55.6	2.8	44.7	-1.1	9
HU15	39.5	3.2	30.8	41.6	2.2	42.5	-1.0	11
HU16	56.7	3.2	46.8	47.0	3.0	38.6	-0.2	8
HU17	39.9	3.3	37.5	42.5	3.6	31.7	0.3	8
HU18	64.6	4.2	37.1	67.9	4.4	37.2	0.2	1
HU19	101.6	4.0	67.1	110.3	4.0	68.9	0.0	0
HU20	80.5	4.1	40.9	53.6	4.2	26.4	0.1	0

Table 6.2 The main geometric and hydrodynamic variables describing the beach profile response of the storm event of October 29, 1989.

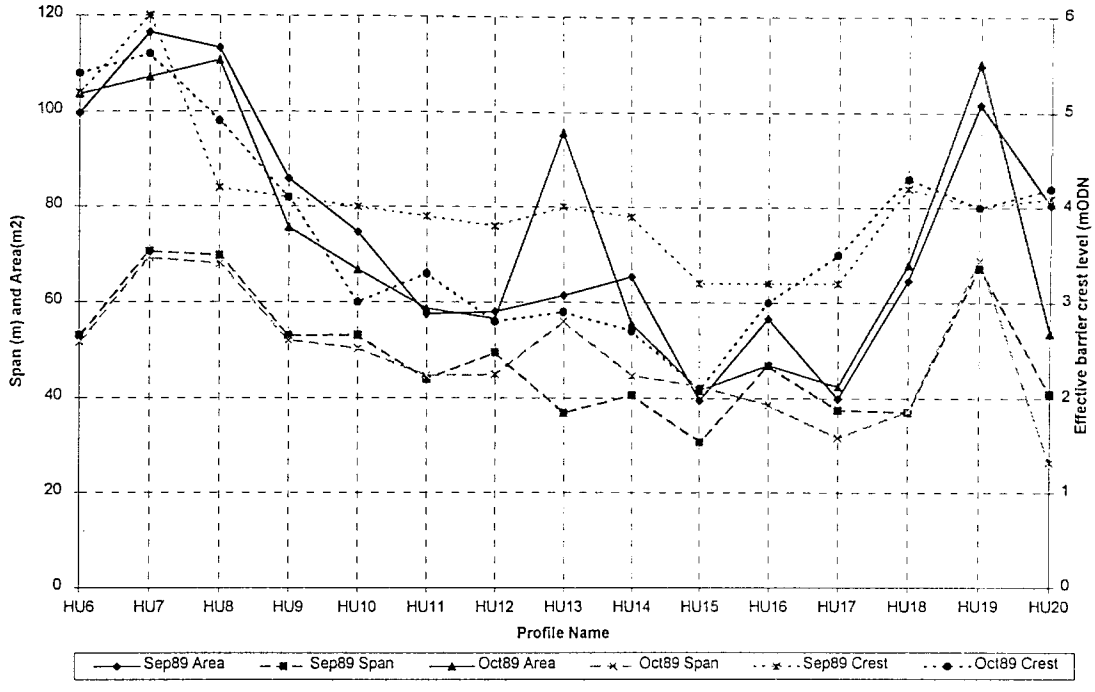

Figure 6.23 Spatial variation of barrier crest elevation, beach CSA, and span, at the level of the storm peak (0.87m ODN), for the storm of 29/10/89 at Hurst Spit (for the location of the profiles see Figure 6.13)

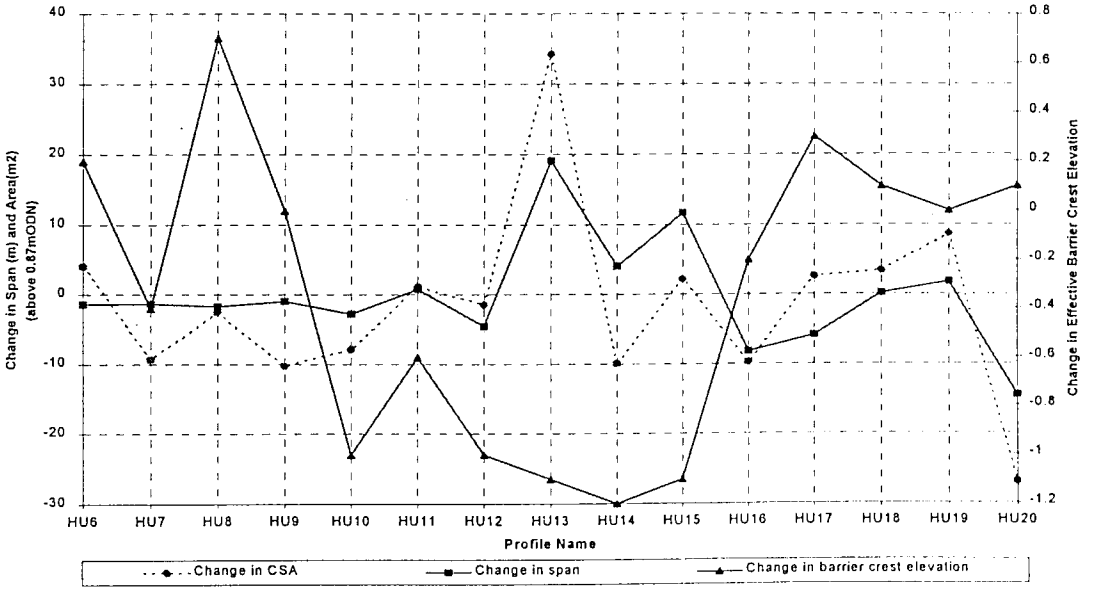

Figure 6.24 Differences in CSA and span (above the storm peak water level) and barrier crest elevation beach response, for the storm of 29/10/89 at Hurst Spit (for the location of the profiles, see Figure 6.13)

6.5.2 December 17 1989

The pre-storm profiles used in the analysis of the 17/12/89 storm event were the post-storm profiles measured following the 29/10/89 storm event: these were modified, by several relatively low intensity storms, between these events. Offshore conditions are shown in a hindcast time-series, in Figure 5.13. Whilst conditions between the two storms would have caused some modification of the profiles, no overtopping occurred.

Post-storm profiles were measured on 18/12/89, when water level conditions and waves prevented access to the beach below approximately 1m ODN. Profiling was restricted to the zone between profiles HU8 - HU20: it was not possible to measure full profiles to the west of profile HU8, due to the movement of heavy plant which was being used to reform the crest of the spit. Attempts were made to profile across the whole of the saltmarsh, exposed on the seaward side of the spit; however, its softened surface made this too dangerous to complete. Spatial variation of the initial geometry is discussed in Section 6.5.1, by relation to the 29/10/89 storm. The pre-storm barrier crest elevation was significantly lower than prior to the 29/10/89 storm: the freeboard was reduced further by the extreme water level.

(a) Hydrodynamics

The most significant hydrodynamic variable was the storm peak water level, which reached 2.27m ODN; this consisted of a combined surge and set-up component, 1.4 m above the predicted high water level. The water level recorded at Lymington was 2.1m ODN, including a surge component of 1.1m. An offshore water level of 1.32m ODN, in Christchurch Bay, has been suggested; including a surge component of 0.83m (Hague, 1992) at the storm peak. A larger surge component (1.18m) was identified later in the tidal cycle. Whilst the suggested surge component appears to be consistent with local measurements, the peak water level is significantly lower than that measured locally. Variability in the absolute levels is explained, perhaps, by the method of analysis used; this was based upon data interpolated between Portsmouth and Christchurch Harbour (Hague, *op. cit*).

Wave conditions, in contrast, were not particularly severe; they had a 225^{o}-255^{o} sector probability of occurrence of 0.0028 - an event that could be expected to occur, on average, for a duration of 24 hours each year. Offshore wave conditions of H_s=4.18m and T_m=7.0s were calculated (Section 5.5). Wave transformations to the nearshore refraction points suggest a significant wave height of 2.58m at profile HU6, falling to 2.42m at profile HU20. The longshore variability in wave conditions is far less marked than for the 29/10/89 event: this reflects the significantly higher storm peak water level and, consequently, less modification of the wave conditions. Wave periods varied between 7.4-7.7s, at the various wave refraction points.

An extended time-series of water level data was used elsewhere, in combination with extreme wave predictions, to determine a joint probability analysis of waves and tides, for the events of the winter of 1989-1990 (Hague, 1992): this investigator suggested that the joint probability occurrence of the 17/12/89 storm was 1:55 years. Whilst the return period might be correct, the water level data cannot be fully representative of conditions at Hurst Spit. Localised effects of nearshore wave setup are not considered in the analysis of deep water conditions; these may account for a local increase in water levels within the area under investigation. Subsequent discussions with Hague (*pers com*) confirm the uncertainty of the absolute values.

(b) Profile response

The 17/12/89 storm produced some dramatic changes to the barrier profile. The root of the barrier beach was cut back and a break-through breach formed. This area, at the junction of a rigid rock armoured structure with a dynamic shingle barrier beach, has historically been a weak point in the coastal defences (Nicholls, 1985); it is not representative of the barrier as a whole. The beach contained a high proportion of fines between profiles HU6- HU7; it consisted of a mixture of sand, clay and gravel, placed in an earlier beach recharge operation (Dobbies, 1984). The effects of the resistance of this semi-cohesive material are shown in Plate 6.3: areas of crescent shaped barrier, comprising this material, are shown above the main beach crest level. The barrier crest level was reduced along the whole of the length of Hurst Spit between profiles HU8-HU16: a flat and wide barrier formed, with its crest located below the storm peak water level. This change in beach geometry suggests that

sluicing overwash occurred within this zone. Overtopping and 'Type 2 Overwashing' also occurred between profiles HU16-HU20, although modifications to the barrier crest were significantly smaller.

(c) Influence of the saltmarsh on profile response

An extensive area of saltmarsh, normally only visible in the benign area to the lee of Hurst Spit, became exposed during this event: similar observations were made following less severe storm events, which occurred during 1979 (Nicholls, 1985). Plate 6.4 shows a survey control marker, to seawards of the barrier; this identified the leeward extent of the barrier profile, prior to the storm.

The profile data present some interesting changes to the levels of the marsh surface. The saltmarsh surface generally lies at a level of between 0.5-0.8m ODN, across an area of several square kilometres (Nicholls, 1985): this has been confirmed, by levelled observations of tidal coverage (water level) over the saltmarsh surface. Levels recorded on the saltmarsh, which was exposed on the foreshore following this storm, were often higher than the natural surface: *Spartina* surface levels of 1.3m ODN and 1.0m ODN were recorded on profiles HU10, and HU13 respectively (Plate 6.4).

Increased levels on the profiled marsh surface represent displacement of the sediments, by shearing and upward rotational slippage of the cohesive sediments. Instantaneous loading of the uncompressed sediments with shingle, during overwashing, resulted in vertical and lateral squeezing of the marsh, from beneath the shingle. Similar observations were made during post-storm engineering reinstatement of the beach: material which was bulldozed to reform the beach crest disappeared into the exposed marsh surface and resulted in upward displacement of the marsh sediments to seawards. These responses result from exceedence of the shear strength of the saltmarsh: consequent shearing of the thin, relatively strong and vegetated, crust of the marsh surface permitted large displacements of the relatively soft material beneath. These processes were analysed in an earlier investigation (Nicholls, 1985), but displacements were not quantified.

Rollback of the whole of the mobile shingle barrier occurred, across the saltmarsh surface, leaving active saltmarsh exposed over an area exceeding 600m^2. The geotechnical implications of saltmarsh displacements are significant in this instance: beach profile response cannot be described by parametric profile equations (Powell, 1990).

(d) Overwashing

Sluicing overwash and partial barrier break down is demonstrated in photographs taken on 18/12/89 (Plates 6.5-6.7); these identify clearly saltmarsh surface above the SWL, indicating a tidal elevation of approximately 0.6-0.8m ODN. Sluicing overwash is seen to continue along much of the length of the spit, despite the fact that the water level had fallen from the surge level reached at the storm peak.

General observations suggest that the changes resulted from a complex combination of hydrodynamic and geotechnical processes; these developed in several stages. Whilst recognising that the parametric equations (Powell, 1990) were not designed to deal with such a complex response, the profile data were compared with predicted response; this is shown, together with pre- and post-storm profiles, in Figures 6.25 - 6.32. The results demonstrate contrasts between the profile response of barrier- and restrained- beaches; limitations of the applicability of the parametric framework, to barrier beaches, are clearly demonstrated.

Beach profile development resulted in modification of the barrier crest, over a narrow range of levels, in those areas of the beach where sluicing overwash occurred. The barrier crest level formed at approximately 2m ODN, between profiles HU10-HU13; this was where the most extensive roll back occurred and was between 0.2-0.3m below the level of the storm peak. The shape of the beach profile formed under this extreme event did not reproduce either the classical S-shape profile, associated normally with a shingle beach, or the parametric descriptors (Powell, 1990). A convex upwards crest profile formed instead; the run-up berm, which is typically punctuated by a sharp run-up crest ridge, was completely absent from the profile. The complexity of the profile development is compounded by the duration of the storm, which continued for several days (Figure 5.13); however, the intensity of conditions reduced

dramatically following the storm peak. The overwashed lee slope of the barrier adopted a flat slope of approximately 1:40-1:90; at the same time, a much steeper intercept with the Mount Lake channel, which lies to landwards of the barrier.

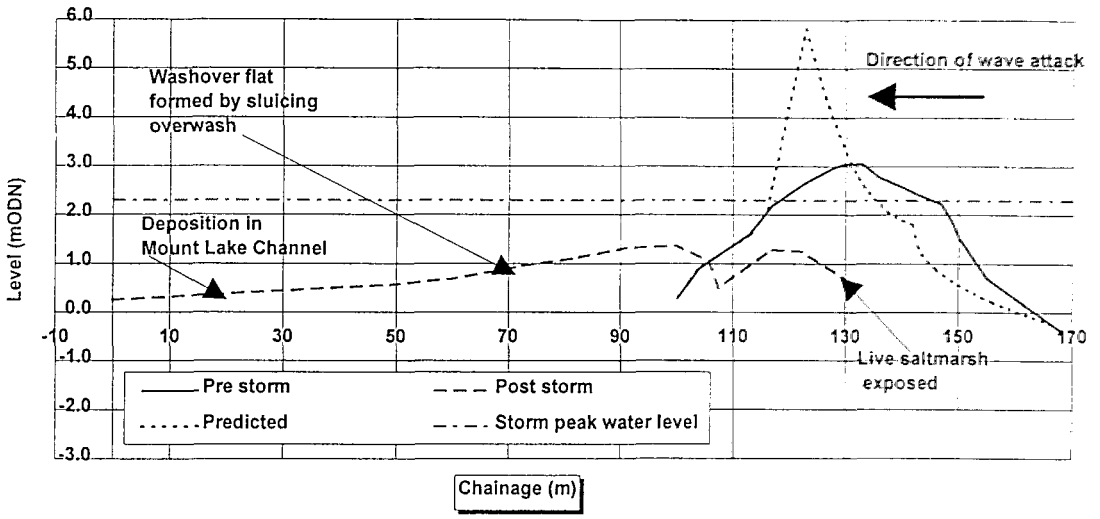

Figure 6.25 Measured pre- and post-storm profiles and predicted response for the storm of 17/12/89, at HU10 (see Figure 6.13), for storm conditions: Hs =2.6m; Tm=7.7s; SWL=2.27 m ODN

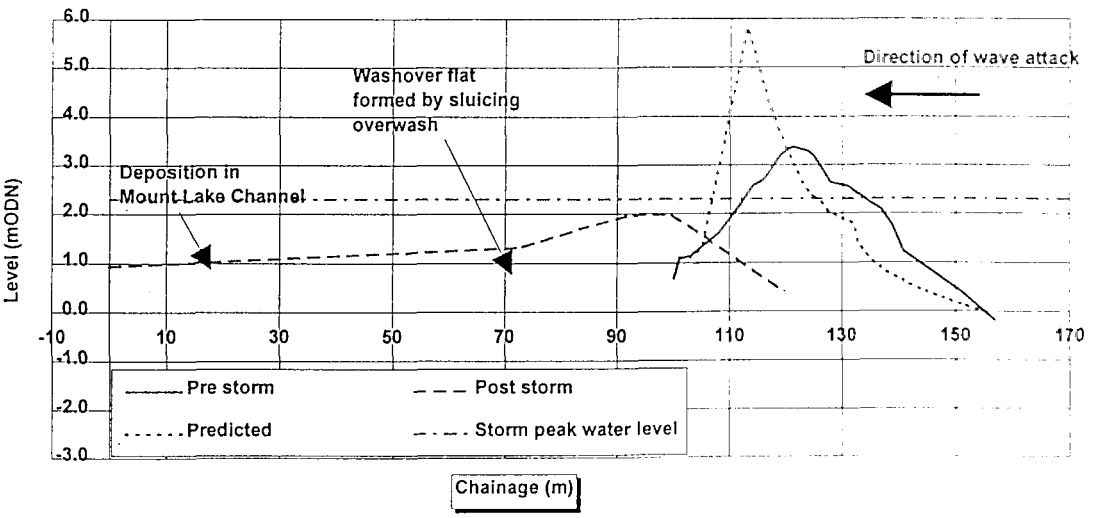

Figure 6.26 Measured pre- and post-storm profiles and predicted response for the storm of 17/12/89, at HU11 (see Figure 6.13), for storm conditions: Hs =2.58m; Tm=7.7s; SWL=2.27 m ODN

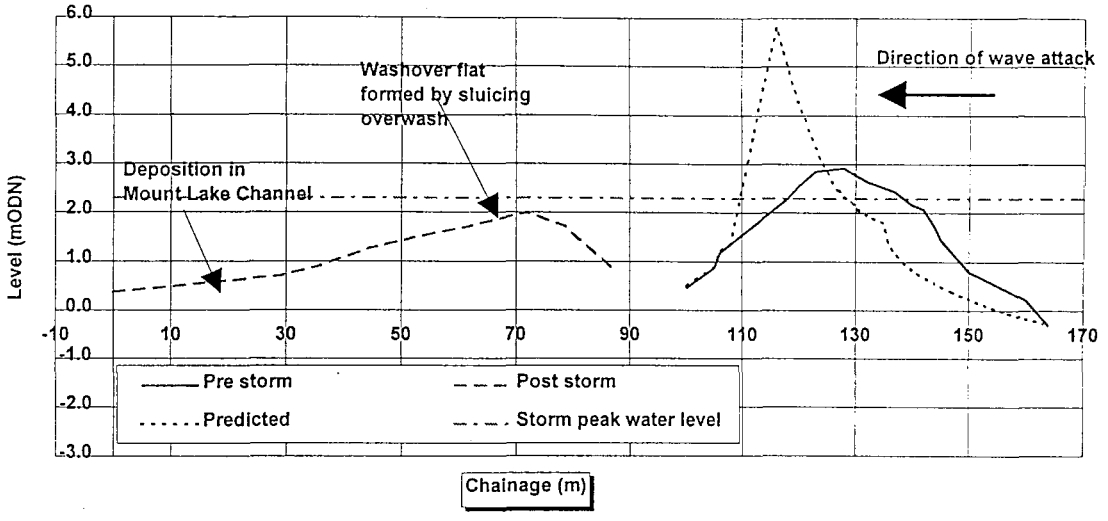

Figure 6.27 Measured pre- and post-storm profiles and predicted response for the storm of 17/12/89, at HU12 (see Figure 6.13), for storm conditions: Hs =2.58m; Tm=7.7s; SWL=2.27 m ODN

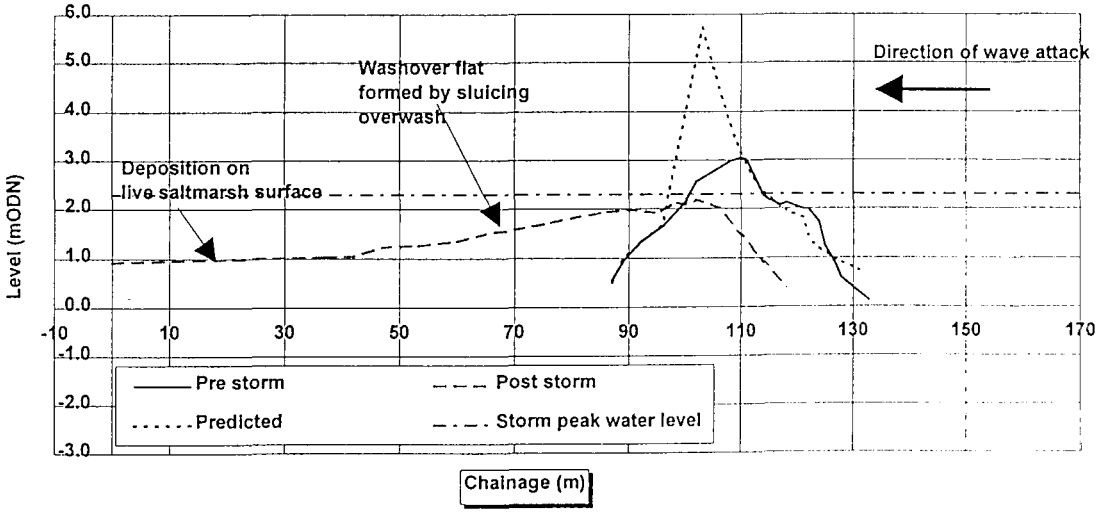

Figure 6.28 Measured pre- and post-storm profiles and predicted response for the storm of 17/12/89, at HU16 (see Figure 6.13), for storm conditions: Hs =2.5m; Tm=7.4s; SWL=2.27 m ODN

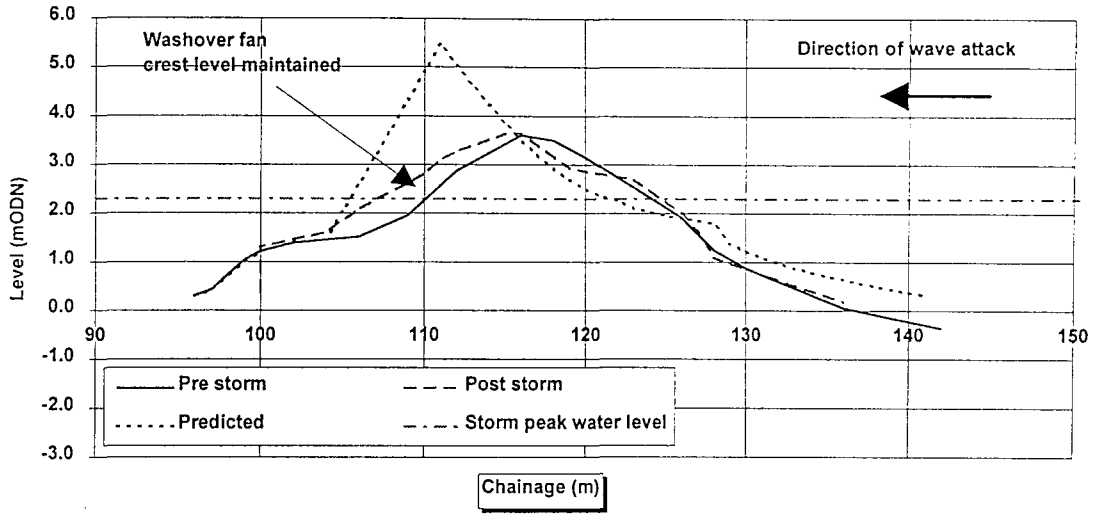

Figure 6.29 Measured pre- and post-storm profiles and predicted response for the storm of 17/12/89, at HU17 (see Figure 6.13), for storm conditions: Hs =2.5m; Tm=7.4s; SWL=2.27 m ODN

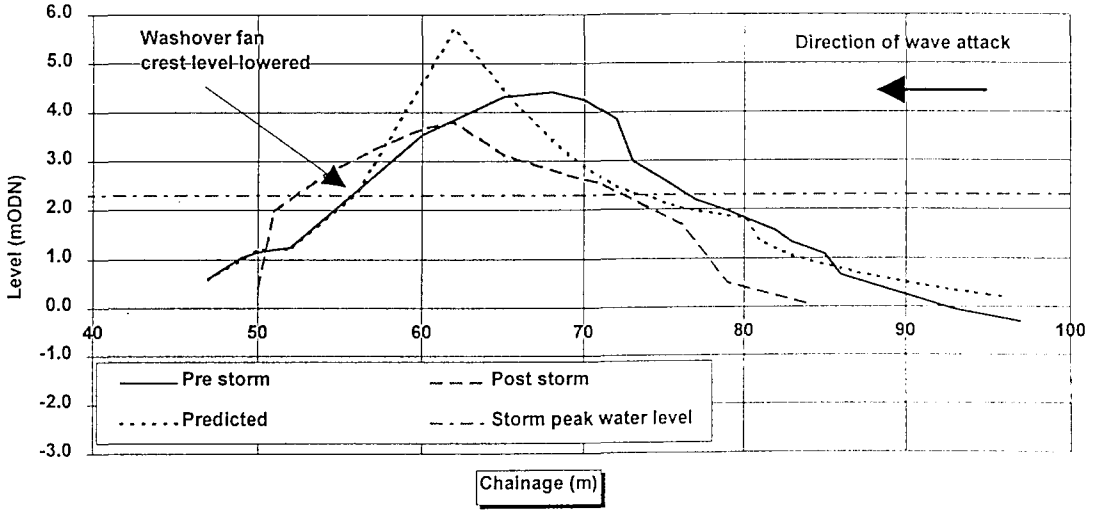

Figure 6.30 Measured pre- and post-storm profiles and predicted response for the storm of 17/12/89, at HU18 (see Figure 6.13), for storm conditions: Hs =2.5m; Tm=7.4s; SWL=2.27 m ODN

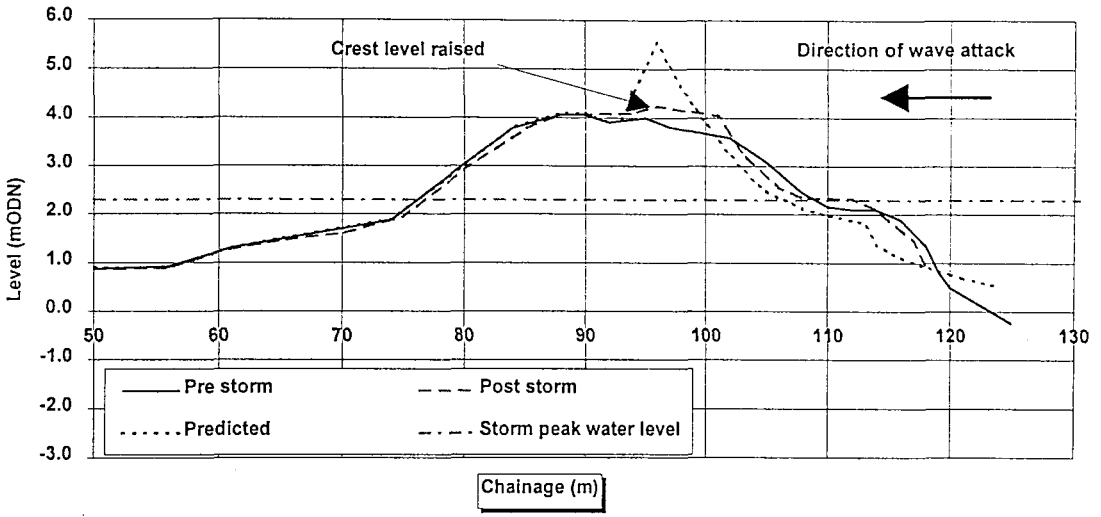

Figure 6.31 Measured pre- and post-storm profiles and predicted response for the storm of 17/12/89, at HU19 (see Figure 6.13), for storm conditions: Hs =2.42m; Tm=7.5s; SWL=2.27 m ODN

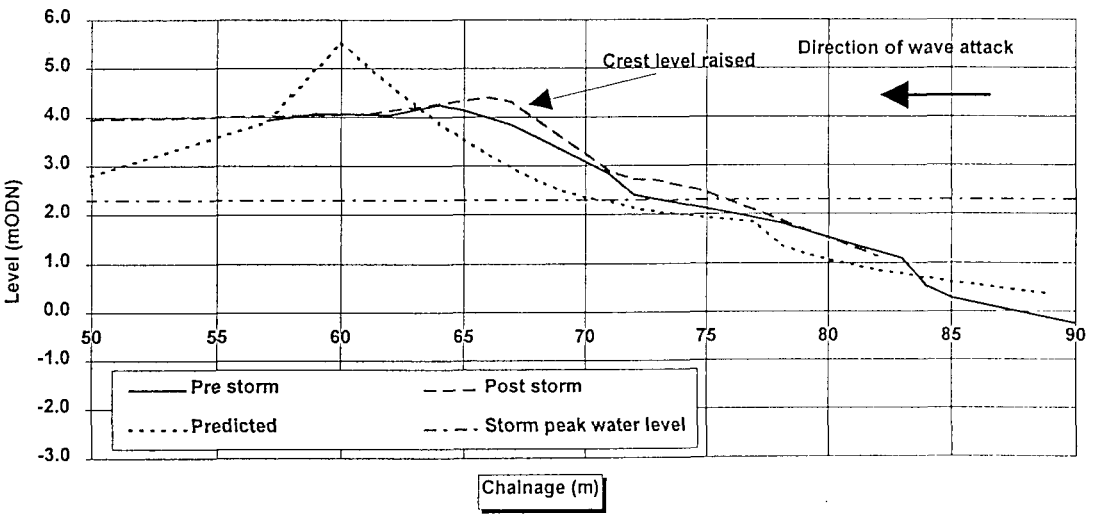

Figure 6.32 Measured pre- and post-storm profiles and predicted response for the storm of 17/12/89, at HU20 (see Figure 6.13), for storm conditions: Hs =2.42m; Tm=7.5s; SWL=2.27 m ODN

Plate 6.3 Exposure of semi-cohesive deposits, following partial barrier breakdown, adjacent to profile HU7

Plate 6.4 Exposure of saltmarsh on the southwestern side of Hurst Spit, following the storm of 17/12/89, near profile HU13

Plate 6.5 Sluicing overwash on Hurst Spit, viewed eastwards from HU6

Plate 6.6 Throat confined and sluicing overwashing on Hurst Spit, - aerial view from the Coastguard helicopter taken on 18/12/89 - following the storm peak.

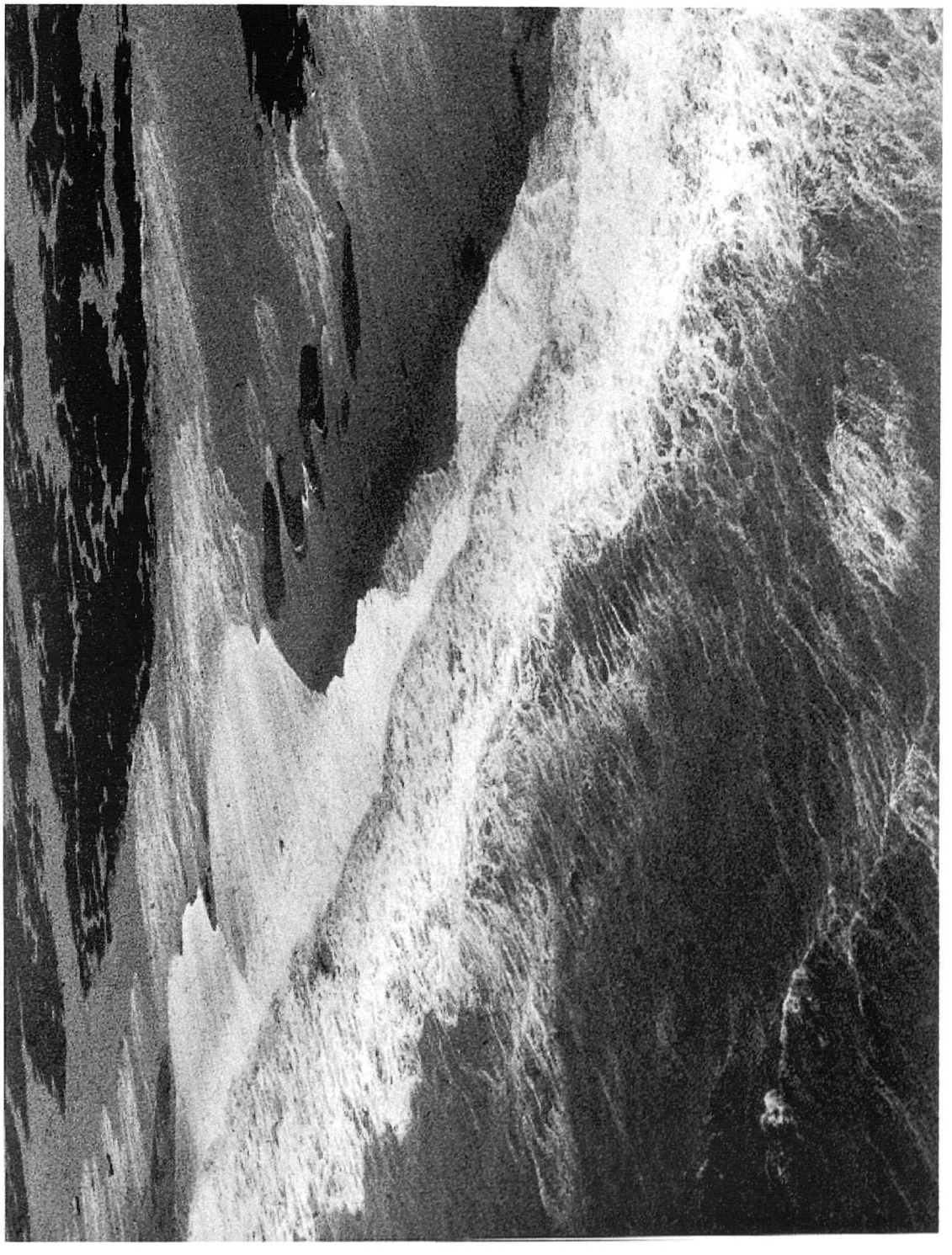

Plate 6.7 Sluicing overwash on Hurst Spit - aerial view from the Coastguard helicopter taken on 18/12/89 - following the storm peak

Figures 6.33-6.34 show the effects of sluicing overwash, on normalised profile response of the integrated CSA and beach span changes. Crest lowering results in redistribution of the barrier, by increasing its width at lower elevations on profile HU10 (Figure 6.33): displacement of the barrier into the Mount Lake channel resulted in reductions in both the span and the area, at all levels on profile HU13 (Figure 6.33). The examples presented represent the most extreme cases, identifying cross-shore redistribution of sediments. Comparison of pre- and post-storm span- and area-data indicates the extreme nature of changes in span and elevation of the barrier, during the storm. The lack of cross-shore mass balance represents movement of material to levels which are lower than those profiled; in this respect, this is a limitation to the measurements. Changes in effective beach volume are significant during this event, due to the displacement of large volumes of sediment into the channel on the leeside of Hurst Spit (Plate 6.1); these resulted in large losses of volume of material above mean high water level.

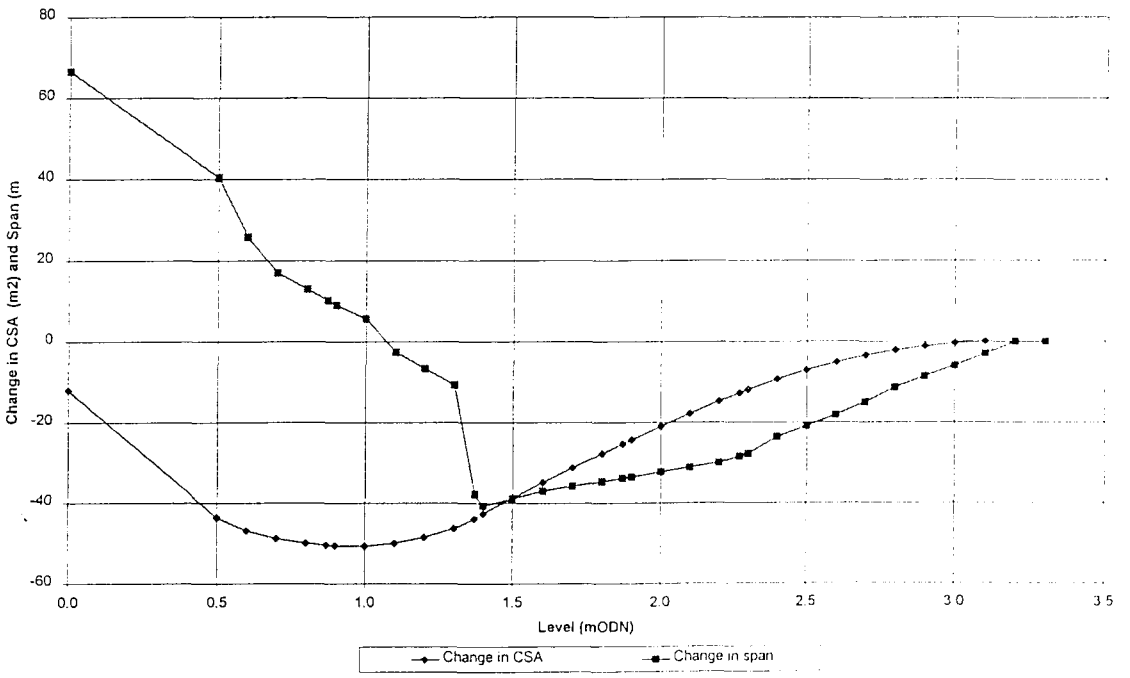

Figure 6.33 Changes in the barrier profile - span and CSA, shown in 0.1m vertical increments, due to the storm of 17/12/89 , on Profile HU10 (see Figure 6.13).

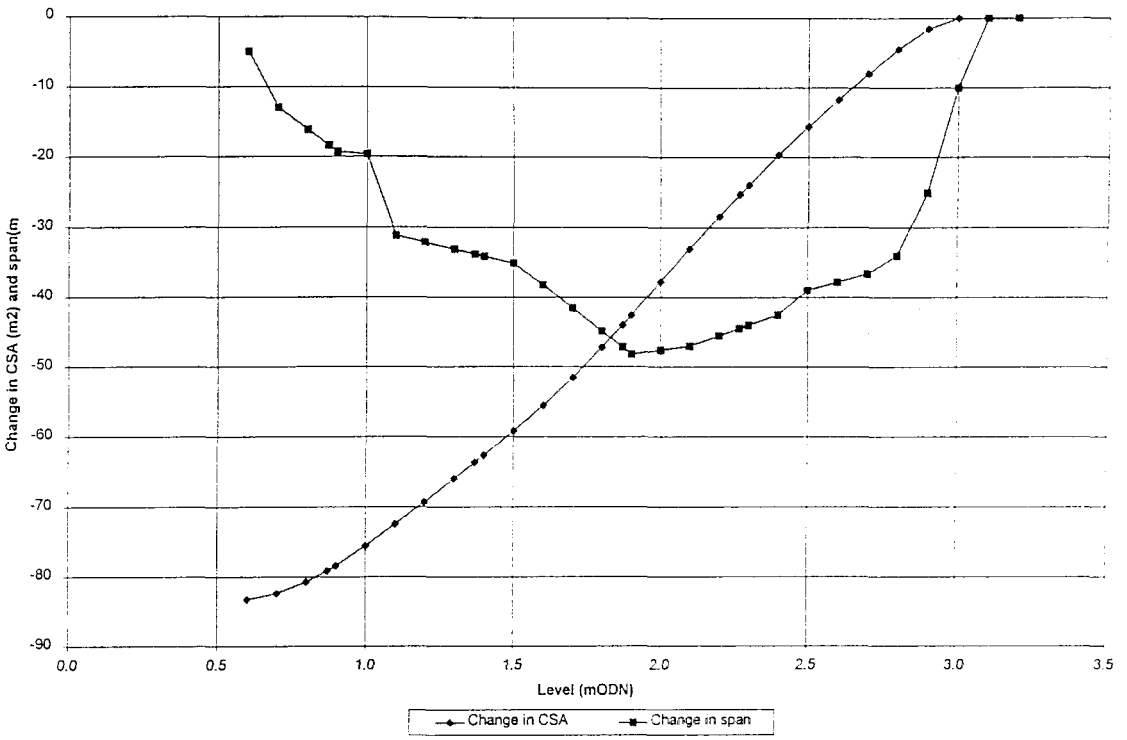

Figure 6.34 Changes in the barrier profile - span and CSA, shown in 0.1m vertical increments, due to the storm of 17/12/89 , on Profile HU13 (see Figure 6.13).

The total volume of material displaced by the storm is difficult to quantify, as the available profile data were limited. The fact that sluicing overwash was a predominant sediment transport process makes comparison of the volumes of material remaining above the storm peak water level somewhat meaningless, as the whole of the pre-storm volume was displaced below that level. The limited data sets provide insufficient information to calculate changes, at either mean low water or mean water level

CSAs and spans of pre- and post-storm profiles are shown, in relation to the storm peak water level, in Figure 6.35; both were reduced to zero, on a number of the profiles. This pattern reflects the severity of the overwash process, which lowered the crest below the storm peak SWL; it demonstrates a marked contrast with the response of the beach to the 29/10/89 storm (see above), when 'Type 2 Overwashing' occurred. However, on this occasion, the crest elevation was not reduced below the storm peak

water level. Sluicing overwash dominated during the 17/12/89 event; it is demonstrated where the CSA above the storm peak water level was reduced to zero, between profiles HU8-HU16, over a distance of 800m: a small surface emergent section remained east of profile HU7 (Plate 6.3). Pre-storm profiles show considerable variation in CSA, above the storm peak water level; this ranged from $42m^2$ at profile HU8 to $1m^2$ at profile HU16. Pre-storm crest elevation ranged between 4.9m ODN at profile HU8, to 2.3m at profile HU15 - virtually at the level of the storm peak water level. Crest lowering occurred as far east as profile HU16 (Figure 6.13).

The response was more variable between profiles HU17 -HU20, where both crest lowering and increases in crest elevation occurred (Figure 6.36); this reflects both 'Type 1' and 'Type 2 Overwashing' within this zone. Such variability may represent the increase in CSA of the beach and reflect, perhaps, the slight reduction in significant wave height at the eastern end of the beach. The plan-shape alignment of the beach also alters from profile HU16 to the east, representing the complex bi-directional wave climate (Section 5.3). The angle of incidence of waves on the beach, within this zone, may also influence profile response. In general, it seems reasonable to expect a different profile response within this area than farther to the west, due both to the variability of the longshore wave climate (Section 5.4) and the barrier geometry (Figures 6.25-6.32).

The profile response of the beach suggests that there are two significant threshold conditions separating different categories of profile change at the barrier crest, in response to crest lowering. Exceedence of the first of these thresholds results in the onset of ' Type 2 Overwashing' and crest lowering: a second threshold occurs at the point where sluicing overwash causes a reduction in the elevation of the barrier crest to a level below the storm peak water level. This latter mechanism corresponds with Orford and Carter's (1982) final stage of barrier breakdown, in their conceptual model.

Comparisons of the data associated with this particular storm with parametric equations (Powell, 1990)(Figures 6.25-6.32) indicates some considerable variation, except over the eastern end of the study area. The extent of the field data availability limits comparison of the profile response, to the upper part of the beach; none could be made to examine the response of either the breaking point, or the beach toe.

Longshore variability of wave conditions presented a further limitation; however, to some extent, sensitivity analysis of the possible narrow range of conditions has overcome this particular problem.

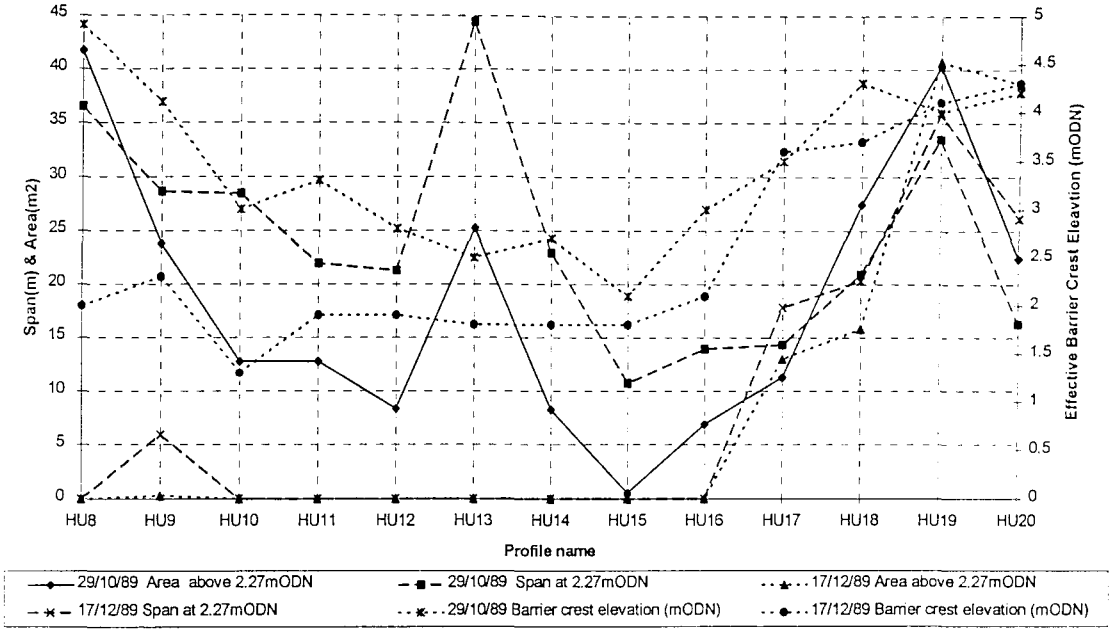

Figure 6.35 Spatial variation in the barrier crest elevation, beach CSA and span, at the level of the 17/12/89 storm peak (2.27m ODN) at Hurst Spit

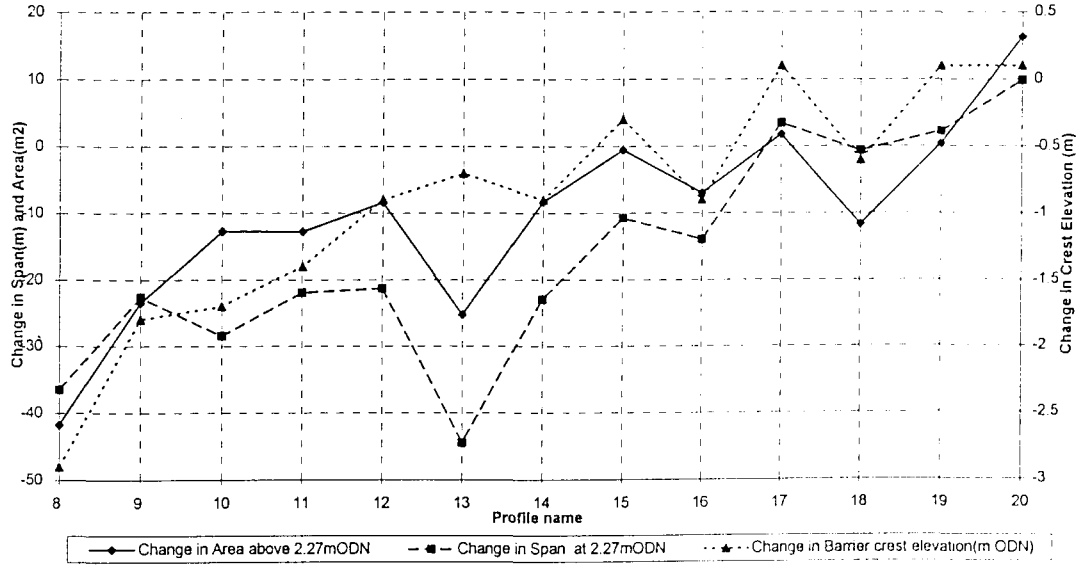

Figure 6.36 Differences of pre- and post-storm CSA and beach span above storm peak water level (2.27m ODN) and the barrier crest elevation, to the storm of 17/12/89, at Hurst Spit

(e) Roll-back

The horizontal extent of the beach roll-back varied considerably over the length of the beach; this was, perhaps, the most significant factor controlling beach evolution, during the storm. Measured crest roll-back ranged between 0 and 56m. Similarly, the landward extent of the washover deposits varied; the maximum measured movement of the lee toe of the barrier was 70m. Relocation of mean high water could not be determined, as the profiles did not extend far enough down the profile. However, it could be observed that the 1m ODN contour moved landwards, by between 26 and 64m, between profiles HU8-HU15. The landwards movement reduced to the east of HU16; this may reflect (partially) a smaller reduction in CSA, due to washover deposition on the surface of saltmarsh, at a level of approximately 0.8m ODN, (as opposed to within the Mount Lake river channel, where the deposits could be relocated at depths as low as -2.2m ODN).

Local topographic variations in the lee of the barrier, such as channels, can affect long-term barrier evolution by changing the effective barrier CSA, above a defined level. Examination of a series of aerial photographs has demonstrated that in-filling of channels, by washover deposition, has impacted upon the rate of recession of Hurst Spit. The reduction in significant wave height, from west to east, may also have contributed to the reduction in crest rollback. Although rollback also occurred at the eastern end of the spit, between profiles HU16-HU20, the extent was much lower and does not represent sluicing overwash conditions; it was characteristic of the 'Type 2 overwashing' that occurred on 29/10/89. These observations are consistent with the effects of the reduction in the severity of wave climate, from west to east.

(f) Crest elevation change

Significant changes occurred in the crest elevation, between profiles HU8-HU16, ranging from between -2.9m to +0.1m. Crest elevation was reduced below the storm peak water level in places, indicating partial barrier breakdown and sluicing overwash: post-storm crest levels were confined to a narrow band at 0.2 to 0.3m below storm peak water level. This pattern suggests that sluicing overwash can result in the formation of a constant crest elevation, irrespective of the crest elevation of the

initial beach geometry. Development of the beach profile, between profiles HU6 and HU8, may have been due partially to this process; it may also represent landward erosion of the steep beach face, resulting in the eventual collapse of the beach by undermining.

Crest elevation build-up (0.1m) was observed on profiles HU18-HU20, but an increase in the CSA of the beach above the storm peak water level occurred only on profile HU20. The combined geometric and hydrodynamic conditions were below the threshold for 'Type 2 Overwashing', but exceeded the threshold for 'Type 1 Overwashing' (see above). Both types of overwashing occurred within a distance of 400m, between profiles HU17-HU20; here, conditions were similar, in terms of angle of incidence, wave height and period. This similarity enabled examination of the response mechanism, purely in terms of geometric variables, against constant hydrodynamic conditions. This analysis provides still a complex picture, with significant spatial variations in: beach span at storm water level; CSA above storm peak water level; and barrier crest elevation. The influence of these variables could not be separated and a clear trend could not be identified on the basis of this data set alone. Data are considered further within the context of the physical model data, in Chapter 8.

The extreme nature of this storm event, together with the corresponding large-scale changes to beach geometry, are illustrated through comparison of the beach span and cross-sectional area relationship at a pre-defined water level. The long-term data set, consisting of profiles measured between 1987-1993, reveals the relationship between beach span and CSA above a given level (Figure 6.2); this shows a strong linear trend for all of the data sets except for the 17/12/89 profiles, which are scattered widely by comparison. This analysis demonstrates a differing response of the beach, to an extreme event, in which sluicing overwash was the predominant process.

6.5.3 April 1 1994

The analysis of this event has focused on a smaller area of the beach, but has provided more detail on spatial variation of the post-storm crest geometry; and the development, shape and extent of throat-confined washover fans. Pre-storm profiles

were measured on 23/3/94 and post-storm on 1/4/94. Profile measurements were grouped into two zones: one directly in line with the waverider buoy; the other some 500-600m to the west. No overwashing was evident at the first site, although the beach width and crest ridge was reduced.

Wave data were measured at a waverider buoy in the North Channel (Figure 4.6); conditions were less severe than those discussed in Sections 6.5.1-6.5.2, but extended the empirical framework to provide data on conditions close to the crest lowering threshold. A peak significant wave height of 2.12m (H_{max}=3.88m) and T_m of 4.81s were measured at 01:00 hr on 1/4/94. A storm peak water level of 1.73 m ODN occurred: predicted high water was 0.94m ODN. The dissipative effects of the Shingles Banks are demonstrated by cyclic changes in wave conditions in the North Channel, over the course of several tides (Figure 6.37).

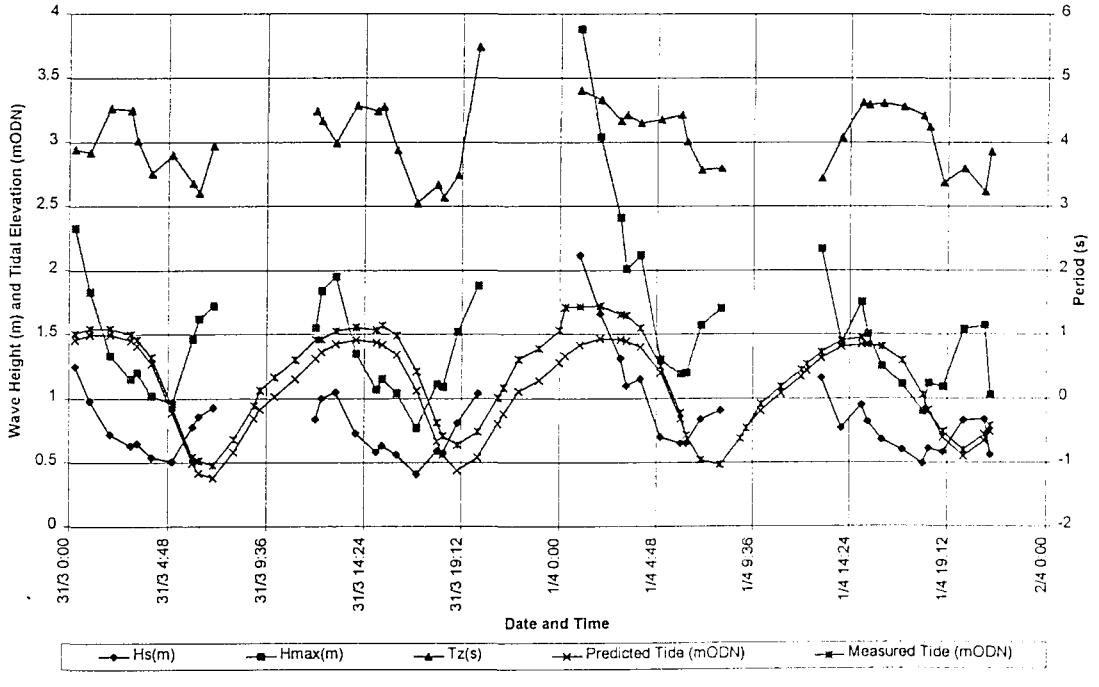

Figure 6.37 North Channel wave conditions (see Figure 4.6) and tidal elevations (see Figure 4.7), during the storm event of 1/4/94.

A series of five new washover fans formed within a 130m long zone, 700-800m to the west of the waverider, where conditions were significantly more severe (due to increased exposure). Crest elevation was reduced, in places, by as much as 2m.

Throats were of similar dimensions, each approximately 0.5m deep at their centre and 8-12m in width (Figure 6.38). The elevation of the base of the throats varied by 1.2m and they extended between 18-26m to landwards of the crest; some showed evidence of discrete layers of deposition, by superposition of washovers on a larger base fan. Comparisons between pre-storm crest elevation, interpolated between survey lines, and the post-storm crest ridge (Figure 6.39), suggest that crest lowering occurred throughout this zone. Although the crest was lowered along the whole length of the monitored zone, some of the reduction represents cut-back and undermining of the crest, as a result of widening of the active beach zone. The lee slope of the washover fans formed at varying slope angles, between 1: 4 and 1:7 (Figure 6.40). A narrow crest ridge (<1m wide) was formed in each case.

The combination of the hydrodynamic and geometric conditions was close to the overwashing threshold, as overwash was evident only at discrete locations. The limits of applicability of the predictive equations (Powell, 1990) were examined. Predicted profile response is plotted, against measured profiles, in Figure 6.40; this demonstrates a poor fit of the predictions, to the measured data. The profile response model suggests widening of the beach profile, but containment within the beach cross-section. Measured profiles obtained through the centre of the fans, plotted relative to a common lee toe position, showed considerable variability in shape. Although the seaward slopes of the profiles are parallel, run-up berms occurred at varied levels; this suggests that a short-term dynamic equilibrium profile was not achieved.

No overtopping or overwashing was evident on the beach, directly to landwards of the waverider buoy. Predicted profile response was reproduced reasonably well on the upper curve of the profile, but the lower profile was reproduced poorly (Figure 6.41). This limitation may be due to modification of the lower profile, during storm decay. Parametric predictors all lie outside of the confidence bands suggested (Powell, 1990).

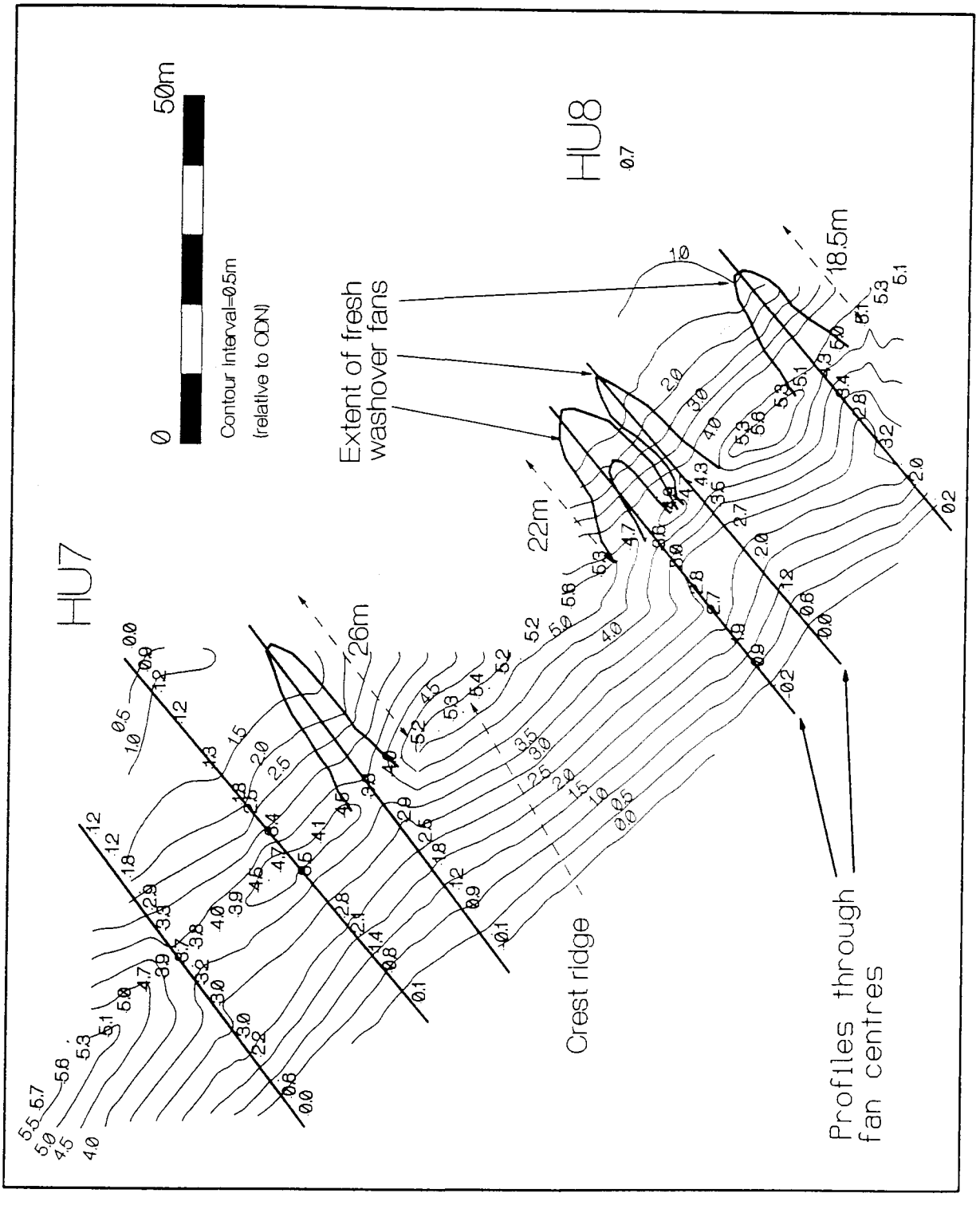

Figure 6.38 Plan shape development of the washover fans, during the storm of 1/4/94, at Hurst Spit.

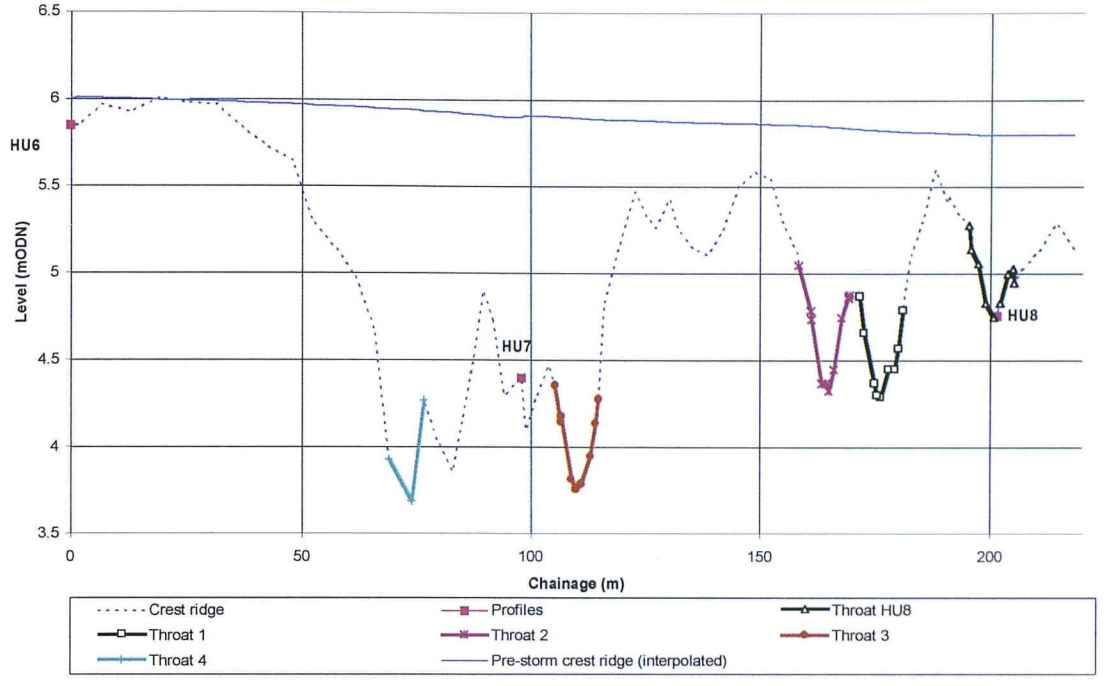

Figure 6.39 Spatial variation of throat-confined washover throats and the crest ridge, formed during the storm event of 1/4/1994, at Hurst Spit (shown relative to the elevation of the pre-storm crest ridge)

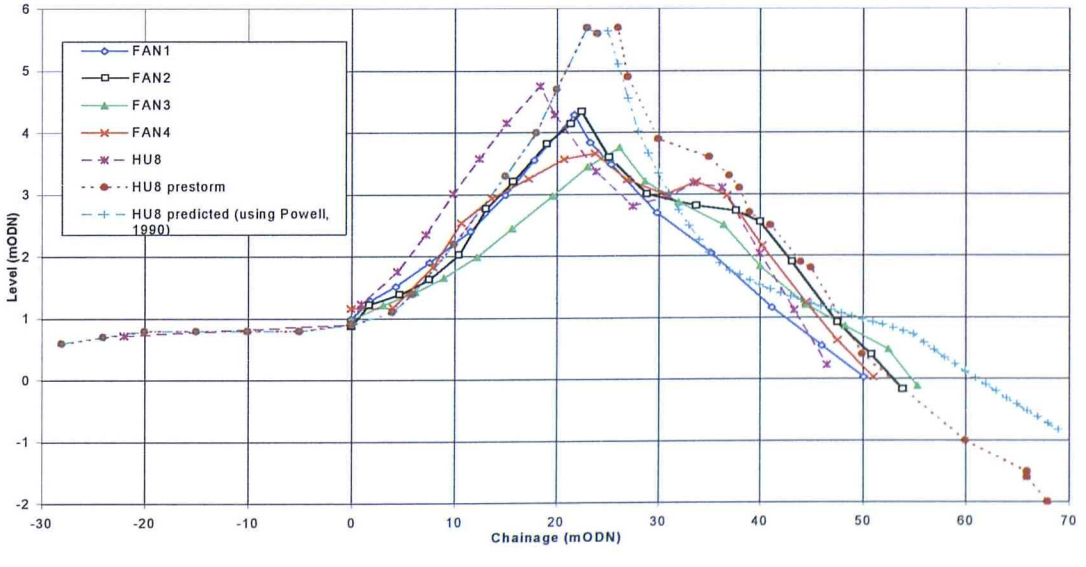

Figure 6.40 Measured profiles through the washover fans on Hurst Spit, for the storm of 1/4/94 (see Figure 6.38)

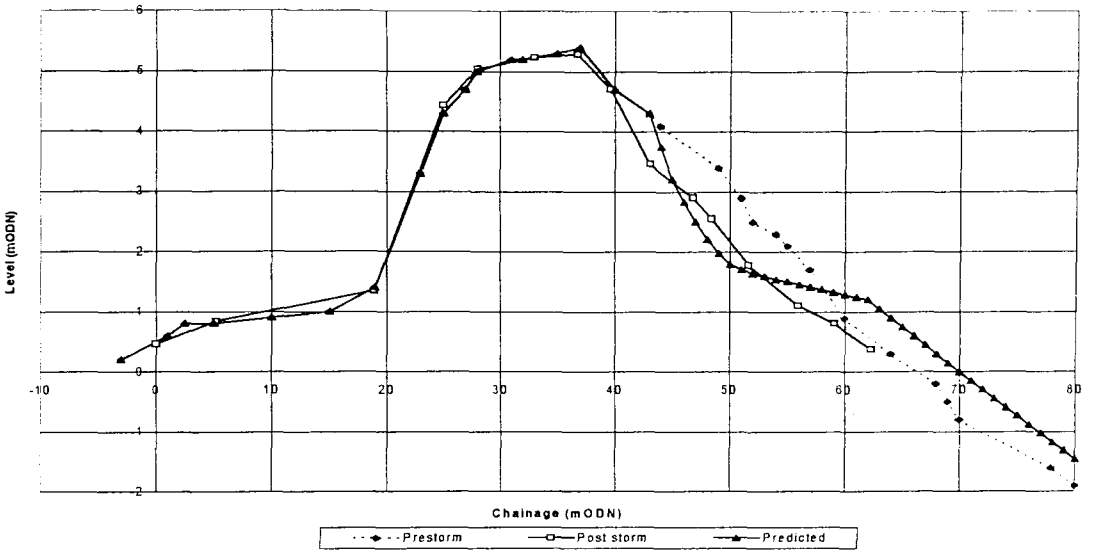

Figure 6.41 Measured and predicted profile response of Hurst Spit, to the storm of 1/4/94, at Profile HU14 (see Figure 6.13) for storm conditions: Hs =2.1m; Tm=4.8s; SWL=1.7 m ODN

6.5.4 Post beach recharge (1996) storm response.

The analysis has been confined to storms of similar hydrodynamic intensity, to those resulting in overwashing prior to the recharge. The profile response of each event was analysed by reference to parametric equations (Powell, 1990), using measured wave and tidal data. Events are discussed with reference to: hydrodynamic data gathered at a waverider buoy off Milford-on-Sea; wind speed, wind direction, tidal elevation and barometric pressure data gathered at the Lymington weather station; and tidal data from the Hurst Spit tide gauge (all shown on Figure 4.3). Data from two example storms are presented, although the results from several other events are included in the synthesis of the results (Section 6.6 and Chapter 8).

Beach profile data were restricted to the upper beach profile, due to the pre- and post-storm conditions which limited access to the lower foreshore. Surveys were carried out on the day prior to the storm and on the following day. Beach crest levels and cross-sections were increased substantially during the beach recharge operation. Although substantial modification of the profile occurred in these events, the artificially reformed barrier was not overtopped or overwashed.

Although substantial modification of the profile occurred in these events, the artificially reformed barrier was not overtopped or overwashed.

(a) October 28, 1996

The storm of 28/10/96 occurred during the construction phase of the beach recharge scheme. Much of the beach had been artificially-profiled and mixed, by the combination of the discharge pipe line and mechanical plant used to form the design profile of the beach recharge. The grading of the recharge material is shown in Figure 6.8. Wave height conditions corresponded with the predicted 1:100 year wave conditions, (Section 5.4). The relationship between significant wave height and wind speed is demonstrated in Figure 6.42: a phase lag response of 3 hr indicates that the storm was a locally-generated event. Typical pre- and post-storm profiles are shown in Figure 6.43, together with the predicted profile response.

The storm event is examined through the application of formulae, on an incremental basis. The time-series of wave and water level conditions (Figure 6.44) were applied to the pre-storm profile and, subsequently, to predicted profiles, through the storm peak and on an hourly basis. Extensive cut back of the barrier crest and draw-down of the toe is predicted when the significant wave height reached a maximum (4.1m), at approx mid-tide. The maximum run-up level occurred when the wave period lengthened (8.2s), but when water level was still below high water. A decay in wave conditions occurred as high water was approached, limiting run-up below the peak level (Figure 6.44). Subsequent profile changes resulted in the rebuilding of the eroded foreshore, as water levels fell and wave conditions decayed.

Profile predictors fit the measured data extremely well, within the confidence limits suggested (Powell, 1990), when this incremental approach is adopted: in contrast, a single application of storm peak conditions, to the pre-storm profile, does not provide a good fit of data. Examination of the upper profile, above the run-up limit, indicates a steeper measured profile than predicted. This difference represents artificial mixing and reduced permeability of the recharged beach; this provides greater resistance to erosion, and resulting in an effect known as 'cliffing' (McFarland *et al* 1996). Application of the procedure discussed above, to profiles along the length of the recharge scheme, have provided comparable results. Although 'cliffing' is generally

considered to be adverse in beach management terms, the over-steep profile resulting from storm action on the recharge actually slows the rate of crest erosion. The results from this storm demonstrate also large-scale volumetric displacements, which reflect adjustments to the artificial pre-storm profile.

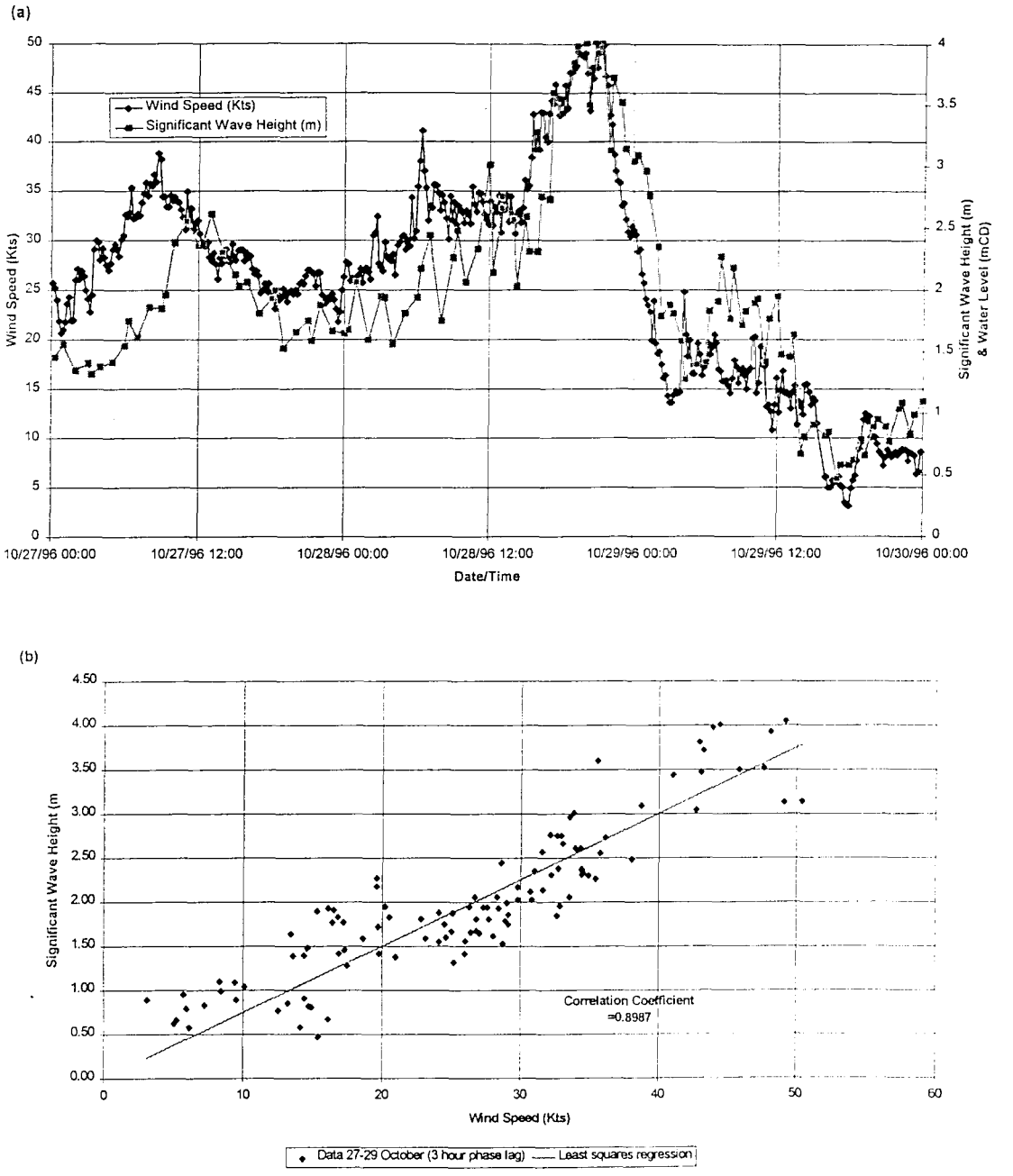

Figure 6.42 Wind and wave data for the period 27-29/10/96, for the Milford-on-Sea waverider buoy and Lymington weather station (see Figure 4.3), showing: (a) wind speed and wave heights; and (b) wind/ wave correlation

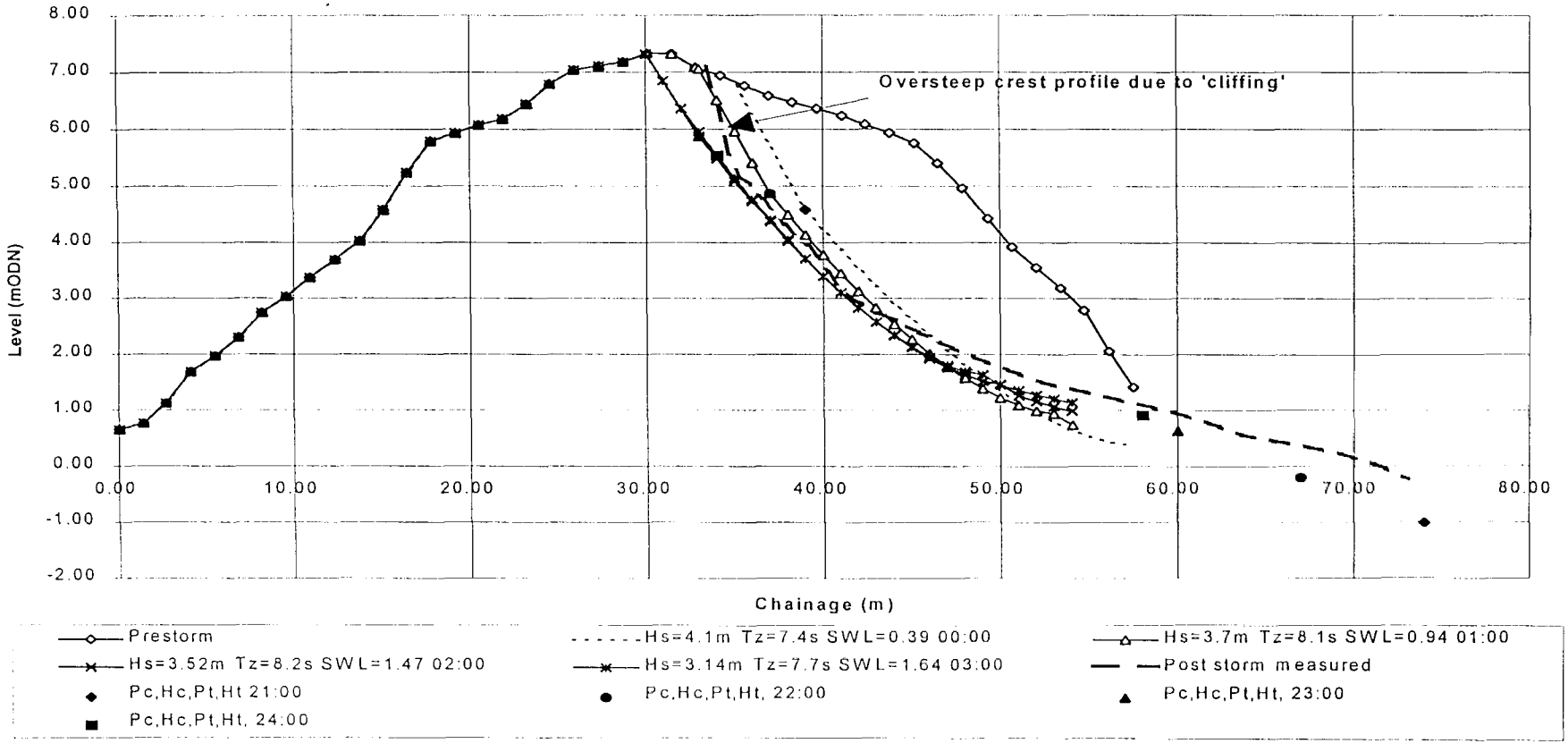

Figure 6.43 Profile response of HU15 (see Figure 6.13) to the storm event of 28/10/96, showing the predicted parametric profile descriptors (Powell, 1990) at intervals through the storm.

Key: p_c = crest position; h_c= crest elevation; p_t = step position; h_t=step elevation (all relative to static water level)

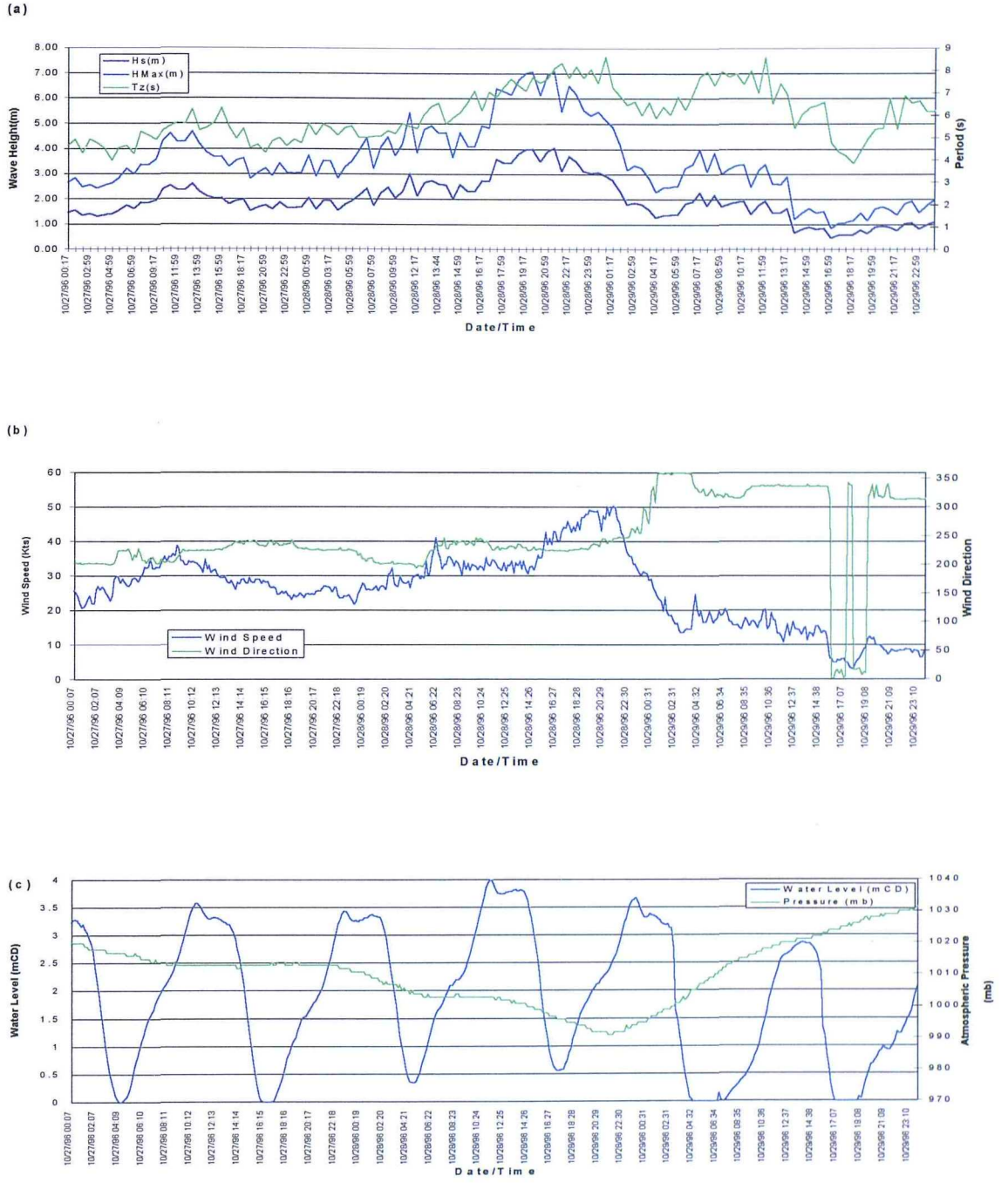

Figure 6.44 Hydrodynamic time-series for the period 27-29/10/96, showing: (a) wave heights and periods; (b) wind speed and direction; and (c) tidal elevation and barometric pressure (for measurement locations, see Figure 4.3).

(b) 4 January 1998

Severe wave attack, combined with a storm surge, resulted in large-scale displacement from the supratidal section of the barrier. Storm peak wave conditions coincided with both surge and tidal peaks (H_s=3.6m, T_m=6.9s and SWL=1.77m ODN) (Figure 6.46). The tidal surge component was 0.82m.

The whole of this event was observed from the beach crest by the writer. Considerable change occurred to the supratidal profile some 2-4 hr after low water, as the storm intensity increased. Changes to the supratidal zone slowed during the 2 hr prior to high water. The foreshore was drawn down, whilst undermining and cut-back of the barrier crest resulted in a widening of the active beach zone, as the dynamic equilibrium profile developed (Plate 6.8). A sustained period of south-westerly conditions, which had persisted generally at force 7-8 over a period of 3 days prior to the storm peak, had lowered previously the foreshore zone; this had rebuilt partially, prior to the post-storm survey. Waves approached at an angle of 5-10^{O} from the beach normal, throughout the event; this resulted in preferential erosion of the beach zone immediately down-drift of the terminal breakwater (Plate 6.9). Although run-up did not reach the beach crest, wind blown spray attacked the supratidal barrier, cutting deep (1-3m) runnels into the seaward crest. No overtopping occurred, except for the spray. The peak run-up reached a level of approximately 6m ODN.

Incremental prediction of the profile response over the storm indicates good correlation with measured data (Figure 6.45). The western end of the beach shows more cut back than is predicted, but this may represent the net loss of material from the zone down-drift of the breakwater, resulting from longshore transport. Despite the failure to produce a cross-shore mass balance, the shape of the predicted curves are maintained; they are simply offset from the predicted positions. The eastern part of the beach shows net accumulation, resulting from the feeding of material from the west.

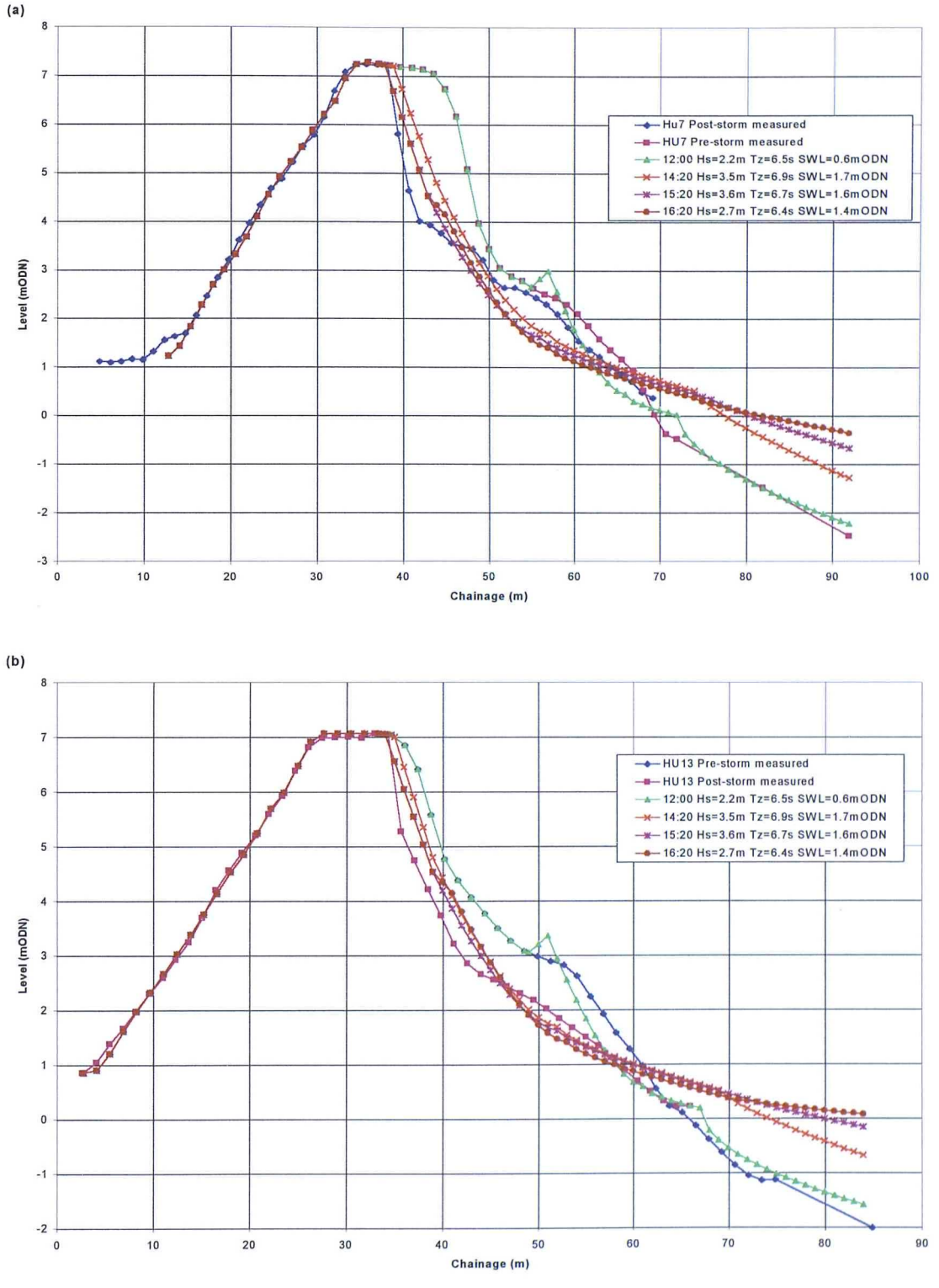

Figure 6.45 Measured and predicted profile response of Hurst Spit, to the storm event of 4/1/98 at: (a) HU7 and (b) HU13 (see Figure 6.13). The predicted profiles are shown at intervals through the storm.

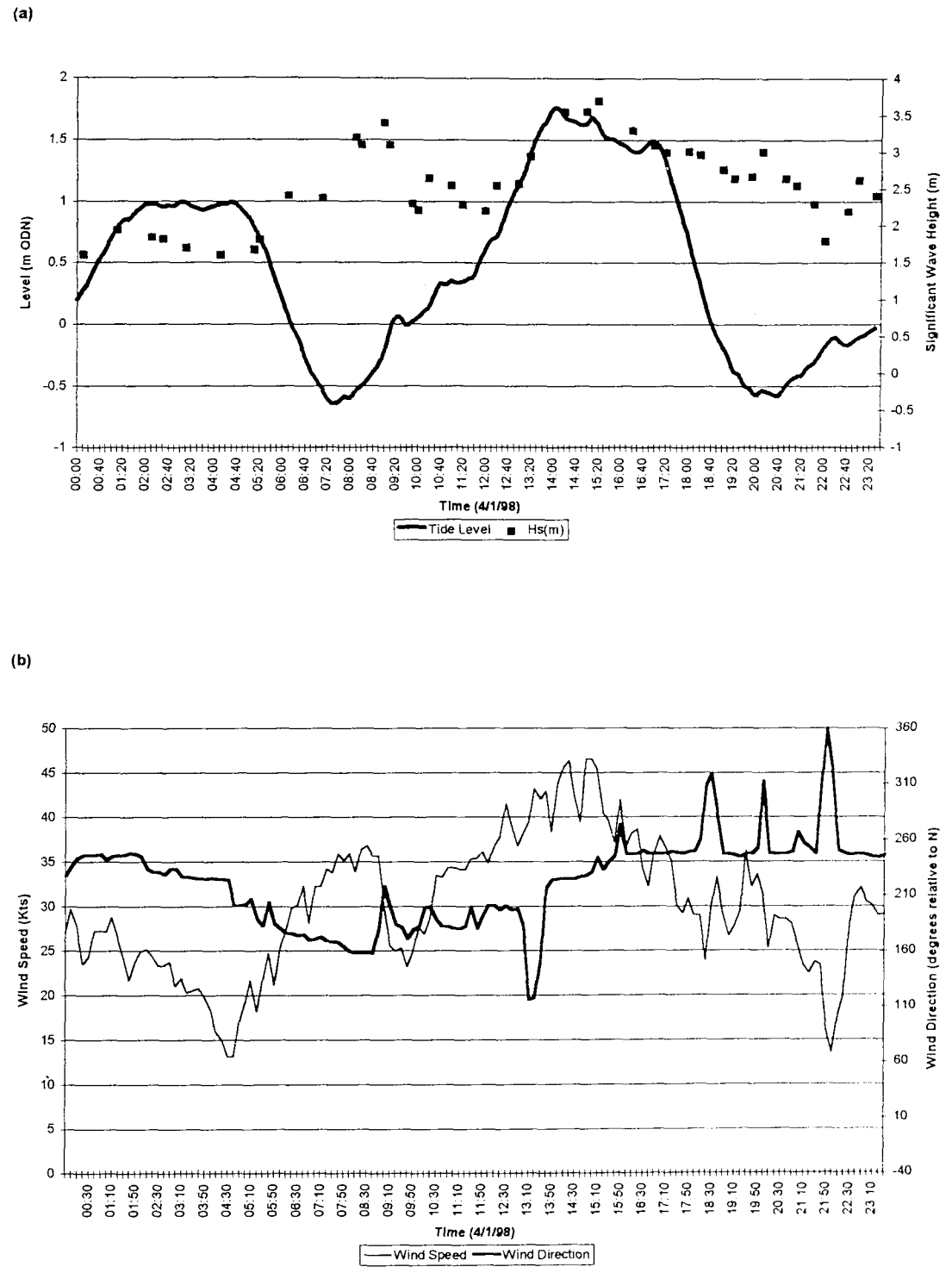

Figure 6.46 Hydrodynamic conditions for the storm event of 4/1/98 showing: (a) significant wave height and tidal elevation; and (b) wind speed and direction (for location of measurements see Figure 4.3).

Plate 6.8 Storm conditions, at high water on 4/1/98, adjacent to profile HU7 Hurst Spit

Plate 6.9 Cut-back of the barrier downdrift of the breakwater, adjacent to profile HU7, Hurst Spit

6.6 FIELD DATA PROFILE RESPONSE - SYNTHESIS

6.6.1 Profile response and parametric profile descriptors

The direct comparisons made between measured field data and the predicted profile response (Powell, 1990) have produced mixed results. The data are presented for the crest elevation parameter (h_c) in Figure 6.47, for both overtopping and non-overtopping events. Measured- and predicted responses do not agree, for overtopping and overwashing events: profiles measured on the recharged barrier provided a much better fit, when no overtopping occurred. Conditions approaching the margins of the overwashing threshold (Section 6.5.3) were not well reproduced by the predictive equations.

Profile prediction equations assume no net loss of volume across the profile; they locate the predicted profile in accordance with a mass balance calculation, related to the volume of beach material required to form the new profile. Although there was sufficient volume within the beach to achieve the predicted profile for each data-set, this was unable to be formed when overwashing occurred: measured values of h_c and p_c were consistently lower, and usually farther to landwards, than the predictions suggest. The results lay considerably outside of the suggested confidence limits (Powell, *op cit*). It is suggested that the pre-storm beach geometry affects the length of time (but not the final shape) taken for the dynamic equilibrium profile to form (Powell, *op cit):* this is clearly not the case for a barrier beach.

Measured and predicted profile responses compared more closely, when overtopping did not occur. Variance of the data was often outside of the predicted confidence limits, but this may represent the limited control of the geometric and hydrodynamic measurements: field data sets are relatively poorly controlled in comparison with those from the laboratory studies used to derive the formulae. A strong correlation was observed consistently only when predicted run-up was at least approx. 1m below the barrier crest. At such times, the barrier width was able to contain the dynamic profile: this suggests that relatively coarse hydrodynamic variables, such as significant wave height or mean wave period, may be insufficiently well refined to identify crest responses close to the overwashing threshold conditions. Analysis may be required on

a 'wave by wave' basis, to assess the effects of individual long period or high waves, when conditions approach the overwashing threshold.

Application of the predictive model on an incremental (hourly) basis, for the storm duration, provided convincing results when overtopping did not occur: such application of the model can resolve the post-storm changes, although the foreshore profile (formed at the storm peak) cannot be measured to confirm the predictions. The fact that incremental application of the formulae works well provides confidence in the equations, within a valid application range: any errors are likely to be exaggerated. It is suggested that the most appropriate method for testing the profile is by application of the model in 1-2 hr steps, throughout a tidal cycle, (depending up on changes in wave and water level combinations). Coates and Bona (1997) suggest that crest elevation and position formulae are valid, within the confidence limits provided, (Powell, 1990) at a number of south coast sites; however this analysis was based only on conditions at the storm peak.

Direct comparison (Table 6.3) was limited to measurement of the crest (h_c, p_c); other parametric descriptors could not be compared, due to the limited seaward extent of the surveys. Extrapolation of the measured data, towards the breaking point (h_t, p_t), infers that this segment of the curve is also predicted well, by the parametric model. No data were available to test the lower section of the profile curve. Differences between the measured data and predictions may be explained partially, as a result of the time interval between the storm and beach profile surveys; these limit direct comparison of the profiles to the supratidal zone. Variances may reflect the accuracy of the synthetic wave data, as opposed to the parametric prediction model. Unfortunately, there is no way of determining which of the variables is in error.

The analysis (Figure 6.47) demonstrates clearly, that the parametric framework (Powell, *op. cit*) is not valid for the determination of the crest response of a barrier beach: the response of shingle barrier beaches elsewhere (Orford *et al*, 1991a) confirms this limitation of the equations. Although earlier research (Powell, *op cit*) suggests that a dynamic equilibrium profile will form within the beach, provided that a cross-shore balance of the pre- and post-storm profiles can be made within the profiles, the parametric equations will not necessarily predict the profile response correctly. It appears that the profile prediction equations may be valid within certain

geometrically-controlled limits, but that combined geometric and hydrodynamic threshold conditions limit the range of validity. Threshold conditions cannot be identified from the field data; this is too limited to quantify the wide range of hydrodynamic and geometric variable limits. The predictive formulae worked reasonably well on the recharged barrier at Hurst Spit, but there is some considerable uncertainty when freeboard conditions are within approx 1 m of the barrier crest.

Date	Hs (m)	Tm (s)	SWL (m ODN)	Measured		Predicted	
				h_c	p_c	h_c	p_c
28/10/96	3.5	8.2	1.5	4.2	-13.5	4.1	-13
06/11/96	3.2	6.0	1.0	2.3	-10.3	2.3	-10
20/11/96	3.1	7.0	1.1	3.3	-13.2	3.2	-13
13/2/97	2.9	6.0	1.0	2.2	-11.3	2.3	-10
24/02/97	3.6	6.5	1.6	3.0	-12.4	3.1	-12
26/03/97	1.6	5.2	0.7	2.4	-8.5	2.3	-10
28/04/97	1.6	5.4	0.6	2.0	-6.0	1.9	-7
8/10/97	3.5	6.9	1.8	3.1	-14.1	3.1	-13
4/01/98	3.6	6.7	1.7	3.1	-14.2	3.1	-13

Table 6.3 Comparison of measured and predicted beach response to post-beach recharge storm events :

h_c= crest elevation relative to static water level; p_c = crest position relative to static water level

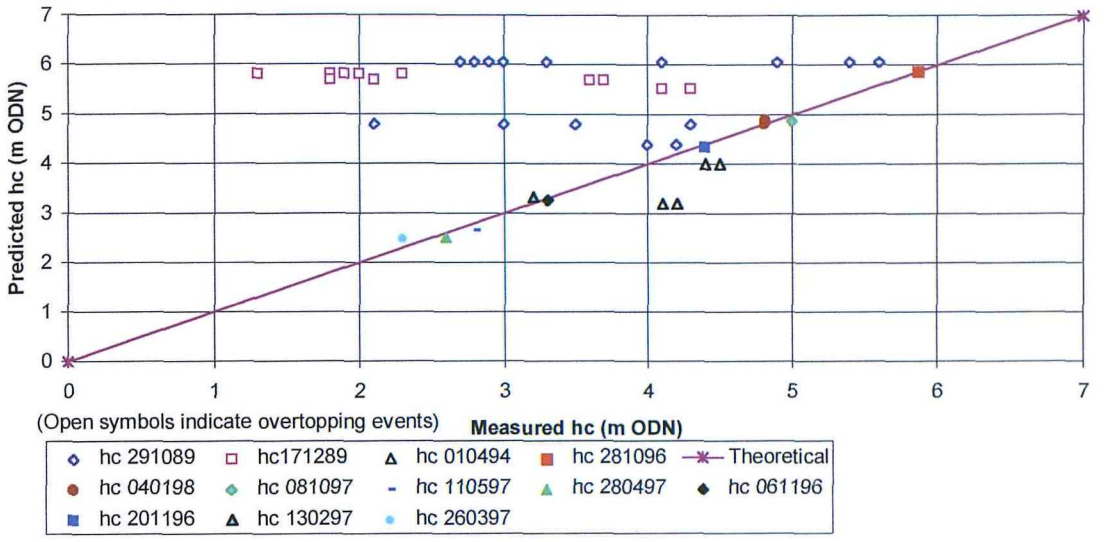

Figure 6.47 Comparison of predicted and measured parametric profile descriptors

6.6.2 Overwashing events

A wide range of profile responses occurred, covering the full range of conditions suggested in an earlier conceptual model of barrier evolution (Orford and Carter, 1982). Three storm-event data-sets provided a broad framework of overtopping and overwashing conditions; these ranged from throat-confined fan formation, to sluicing overwash and partial barrier breakdown.

Attempts to quantify the response of the beach, by relation to hydrodynamic variables, were partially successful; however, the spatial variability and limited control of the measurement of hydrodynamic and geometric variables presented a complicated and incomplete data set. Although the results demonstrated each of the conceptual phases of barrier evolution, analysis of just three overwashing events did not provide sufficient adequately-controlled data, to develop a statistically-valid predictive model which would be capable of quantifying threshold conditions. The events analysed provided a useful contrast, demonstrating the relative effects of extreme wave and water level conditions, by reference to the geometry of Hurst Spit. The extreme conditions monitored during the study could not have been expected, realistically, to be wider ranging.

The spatial variability in the local wave conditions complicates and limits the validity of the analysis. It is not reasonable to quantify the critical threshold for barrier crest elevation lowering, by overwashing, based purely upon the results of the field data sets described: there are too many interacting hydrodynamic and geometric variables to allow a simple relationship to be determined. A more systematic analysis of the data is needed, within the context of a wider range of better controlled conditions, before a numerical relationship can be established with any statistical validity. The following inter-relationships are examined later (Chapter 8): beach geometry; wave and water level conditions; and the thresholds of overtopping and overwashing of a barrier beach. In the analyses, the limited field data results are combined with the comprehensive and well-controlled laboratory study data sets.

Examination of the field data suggests a relationship might be established between geometric variables, hydrodynamic conditions and the barrier crest response. Analysis methods used to estimate overtopping discharges across coastal structures (Owen, 1980, and Bradbury *et al*, 1988) were applied, by plotting changes in crest elevation against the dimensionless freeboard (R_c/H_s). The results presented in Figure 6.48 suggest that the Type 2 overwashing threshold may be reached when $R_c/H_s = 0.88$-1.15: the threshold can be defined no more precisely, as is no data are available within this range. This hypothesis is opposed by the presence of a single point within the field data set. Further examination of the raw profile data indicates that the reduction in crest elevation of this point is not due to overtopping, but is a function of cut-back and undermining of the barrier. The statistical validity of this analysis is questionable; it is based upon a small population, subject to many poorly-defined variables; including the method of determination of the local wave climate and the timing of the surveys. The data have provided a framework for: the design and calibration of the physical model studies; delimiting a range of possible threshold conditions; and further development of an improved approach to measurement. The field data have been included within analysis of the laboratory studies, to provide confirmation of relationships identified by the model testing programme; this is discussed further in Chapters 7 and 8.

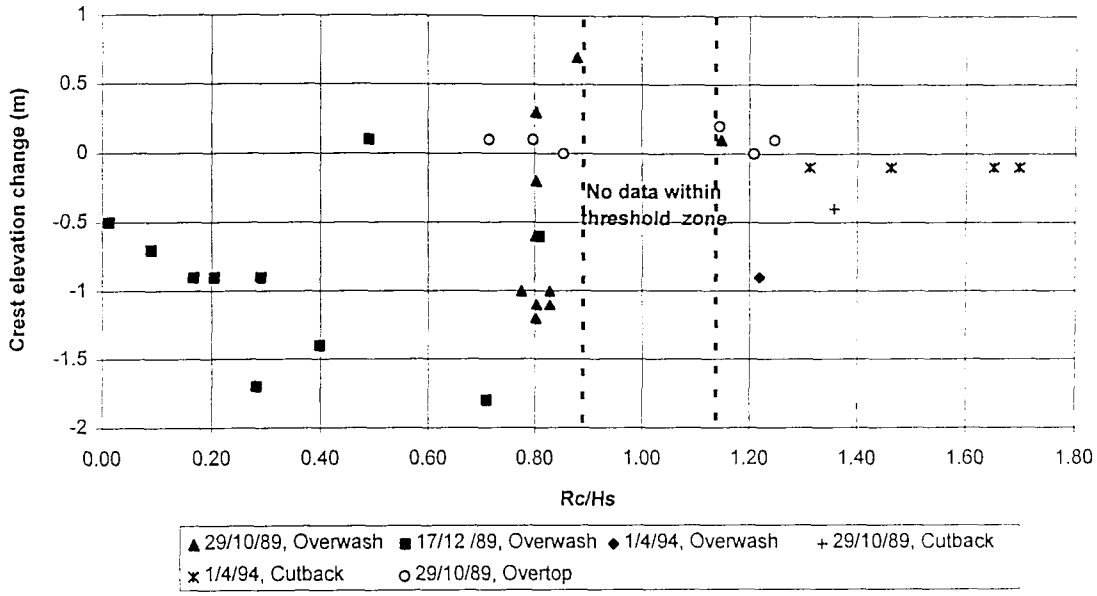

Figure 6.48 Barrier crest elevation change, compared against the dimensionless freeboard parameter.

(a) Change of effective barrier cross section

A reduction in crest elevation, resulting from overwashing, effects a change in the beach cross-section over a range of levels. It may effect no change above the storm peak water level but, where both crest elevation and CSA are reduced, the vulnerability of the beach to overwashing is increased during events of similar intensity. This effect is particularly significant when there is a reduction in volume, due to displacement into the adjacent channel or lagoon (Figure 6.26). Large-scale sluicing overwash at Hurst Spit resulted in deposition of considerable volumes of beach material into the Mount Lake Channel (Figure 3.2) and, consequently, a reduction in the volume of beach material above mean high water, on several occasions; this process reduced the resistance of the barrier to overwashing.

The geometry of the back-shore topography can affect the distribution of sedimentation following overwashing; this may affect the effective cross sectional area of the barrier, above a defined elevation. Three possible patterns of washover deposition can occur in various combinations on Hurst Spit: (i) deposition onto

existing washover deposits above the level of mean high water, with no change in effective CSA; (ii) deposition onto a flat surface, such as the *spartina* saltmarsh, which may lead to loss of volume by subsidence; and (iii) deposition into the Mount Lake Channel which lies below the barrier toe level.

6.7 CONCLUDING REMARKS

(a) Pre- and post-storm beach profiles did not extend sufficiently far seawards, to allow the profile response to be analysed to the depth of dynamic profile closure (Powell, 1990).

(b) Time-delays between storm events and the profile surveys resulted in measurement of profile response to a complex sequence of wave and water level conditions. Such conditions represented both modification of the upper profile to the storm peak, and subsequent modification of the lower profile following the storm peak.

(c) Longshore spatial variability in the wave conditions, local bathymetric variations and the complexity of the local bi-directional wave climate have limited the confidence in accuracy of the wave conditions used for the analysis of storm events.

(d) The parametric model (Powell, 1990) is shown to be appropriate for the prediction of profile response, under a limited range of conditions; it is unsuitable for the prediction of the profile response of the barrier beach crest, subject to overwashing conditions.

(e) The profile response of Hurst Spit is dependant upon the pre-storm beach geometry as well as wave and water level conditions.

(f) The geotechnical properties of the barrier basement geology may have a significant effect on the profile response, when overwashing and barrier roll back occurs across the saltmarsh surface.

(g) The topography of the back barrier area can affect the long-term development of the barrier.

(h) The profile response of Hurst Spit, to a series of extreme storm events, has provided suitable calibration data for the development of a physical model.

(i) The beach profiling and hydrodynamic measurement programme has provided evidence of the profile response of the Hurst Spit barrier beach to overtopping and overwashing events. The programme has demonstrated each of the phases of profile development, suggested by an earlier conceptual model of barrier response (Carter and Orford, 1982); it has provided quantification of hydrodynamic and geometric conditions required to achieve each of the evolutionary steps. Scattered data have suggested a complex beach profile response at the beach crest and a series of threshold conditions, delimiting the phases of crest evolution suggested by the conceptual model.

(j) The relatively short data collection programme has necessarily limited the number of extreme events which could be evaluated. Field data have included the analysis of extreme events, with the predicted return periods ranging from 1:1 yr. to 1:100 yrs.

CHAPTER 7: RESULTS AND DISCUSSION - LABORATORY STUDIES

7.1 VALIDATION OF TEST METHODOLOGY

Although mobile bed physical models have been used previously, to examine the response of restrained shingle beaches to storm waves, the published literature does not cite any investigations in which the crest development of shingle barrier beaches has been examined. Earlier studies (Powell, 1990) have demonstrated that profile response of the shingle beach crest could be reproduced realistically on a restrained beach.

A series of beach response calibration tests were undertaken, based upon actual storm events and the pre-storm geometry of Hurst Spit. Overtopping events were selected for investigation, which caused large scale morphological beach changes to Hurst Spit (Section 6.5). This approach provided a quantitative means of comparison of the model and full-scale beach response, to similar prevailing hydrodynamic conditions. Measurements were made of the following profile variables, pre- and post-storm:

(i) crest level;
(ii) crest position;
(iii) lee slope angle;
(iv) incidence and extent of roll-back; and
(v) model construction accuracy (comparison of nominal to measured profiles)

Some variations were to be expected, between the model and field measurements; this was due to the limitations of the field measurements (Section 6.5). Storms reproduced in the model were simulated for the full-scale equivalent of 3 hr duration, representing the peak of the storm. This approach ensured that the model represented profile development over the most intense period of storm activity, at water levels which permitted overwashing. Development of the profile was not reproduced following the storm peak, as it decayed and water levels fell. This decision impacts upon the

development of the lower part of the beach profile, but should have only a limited effect on the crest evolution. Synthetic wave data, derived by mathematical modelling, may cause further variations; these are discussed, in detail and in context within each of the tests. These limitations resulted inevitably in a less than perfectly controlled reproduction of the storm events; however, it has provided a comprehensive framework of results.

Although directly comparable quantitative measurements of profile response were made in both the laboratory tests and fieldwork, an element of qualitative analysis was required in the interpretation of the results. Direct comparison of model and field data had to be considered carefully in this context: likewise it was clear, that it would not be possible to reach a statistically-valid conclusion on the calibration tests, due to limitations in the field data. Video recordings and observations of beach development in the model provided further qualitative details of the processes.

7.1.1 Reproduction of the storm event of 17/12/89

The first series of physical model tests were designed to reproduce the peak of the storm surge and wave conditions experienced on 17/12/89 (Tests B01-B02). These tests were carried out under identical hydrodynamic conditions, in order to examine the repeatability of the test methodology. The model response appeared to provide a realistic reproduction of the beach development. The extreme storm peak water level (estimated at 2.27m ODN), together with the relatively low barrier crest, provided a low barrier freeboard; this was unable to contain waves with a significant wave height of 2.5m. A breach of the narrow surface emergent beach crest formed very rapidly, resulting in the formation of extensive washover fans and rapid 'roll-back' of the beach crest.

The beach crest was overtopped initially by waves with an estimated height of approximately 2m; this resulted in crest lowering and roll-back: following the overtopping, most of the waves in the test sequence passed over the beach crest. Sluicing overwash developed between profiles HU9-HU13, soon after the commencement of the test. Throat-confined washover fans formed, initially at topographic lows in the beach crest adjacent to profile HU9 (Figure 7.1(a)); these

occurred within a period of 20 T_m, waves from the start of the test. A large washover fan formed between profiles HU10-HU11. Runnels developed through the centre of the fans, lowering the throats within the time scale of several waves after their initial formation. The runnels acted as sediment transport pathways; they provided the means for the fans to extend rapidly to landwards of the original crest. Further crest lowering resulted in a reduction in the cross-sectional area of the beach above OD, due to displacement of shingle into the Mount Lake channel (Figure 4.13). The negative freeboard, resulting from the overwashing, caused sluicing overwash and enabled the waves to propagate across the beach and Mount Lake, towards the model boundary. Model and field observations of wave propagation are in agreement; this suggests that regular and direct wave attack will occur on the salt marshes, in the event of a breach of Hurst Spit, resulting from the sluicing overwash.

Most of the beach, between profiles HU7-HU14, was breached severely by the completion of the test; in this way, a series of large washover fans formed. Small areas of the beach crest remained 'surface emergent' at the end of the test: the whole of the beach was reduced, below the storm SWL between profiles HU12-HU14: the crest level was not reduced below 1.9m ODN (0.3 m below the SWL) at any location. Two 'surface emergent', crescent plan-shape areas (30 and 50 m in width) formed between profiles HU9 and HU11. Similar features were observed and photographed during the fieldwork programme (Plate 6.3). The horizontal 'roll-back' in the model extended to maxima of 80 m and 60 m, on the landward and seaward side of the barrier, respectively. The crest level was reduced below the level of the storm peak water level, to approx. 2m ODN, in many places.

Only limited offshore movement of shingle was observed during this particular part of the study. Most of the shingle movement took place to landwards: this contrasts with the response of a restrained shingle beach to storm wave attack, when the storm profile migrates seawards (Powell, 1990). Steep seaward faces formed where the overwashing did not occur (HU6-HU7); these resulted from a combination of waves failing to reach the beach crest and saturation of the beach by wave action, reducing the effective beach permeability. Some offshore movement of shingle occurred in this area, as the beach profile was drawn down and widened to absorb the wave energy. Wave crests approached the beach at an angle of approximately 10^{O} to the shoreline, over this section of beach: this is not an accurate representation of real storm

conditions along this section of the study area (Section 6.5). As the model wave paddles produced straight long-crested waves, a single orientation of waves was generated along the whole of the model offshore limit: subsequent wave transformations have relied upon the moulded bathymetry and shallow water conditions, between the paddles and the shoreline. Conditions were determined by numerical modelling of waves, at a point which was theoretically representative of the whole of the 800 m long model segment (Section 5.4). In reality, the wave height, period and orientation varies along this length. Whilst the incident wave angle was not reproduced correctly over the western most 200m, it was appropriate over the remainder of the model frontage.

Measurements of the model response were compared directly with the field measurements representative of the same event (Figures 7.1 and 7.2). Initial examination of the model profiles showed remarkable agreement with the full-scale measurements, for most of the beach profiles; however, there was some variation at the western end of the model (profiles HU6-HU7) and at profiles HU10-HU11. These variations can be attributed to a number of differences, between the model and the full-scale prototype. The incident wave direction predicted for the storm event suggests that waves approached from an angle of 210^{O}. Refracted waves were approximately 5^{O} from the shore normal at the shoreline along much of the model segment; westerly longshore transport also occurred. For comparison, the field evidence suggests that waves approached virtually normally incident to the beach, during this event: likewise, no build up of beach material occurred adjacent to the terminal groyne, at profile HU6 (Figure 4.13). The composition of the beach was assumed to be constant, although this is not accurate in reality, as several segments of the beach consisted of heavily compacted clay materials; these respond in a different manner to the unconsolidated beach. This particular zone is concentrated between profiles HU6-HU7.

There was insufficient field data available to describe the lower part of the beach profile, following the storm peak; this is due to the moderate wave conditions, which continued for several days after the storm peak. This limitation restricted the model validation to the upper part of the beach profile (above a level of 0.5m ODN).

(a)

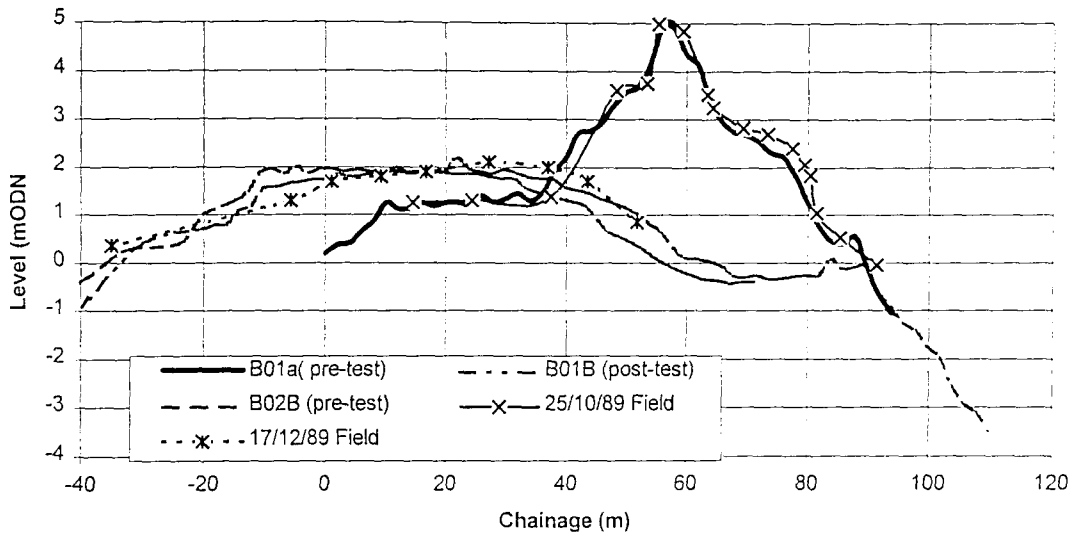

(b)

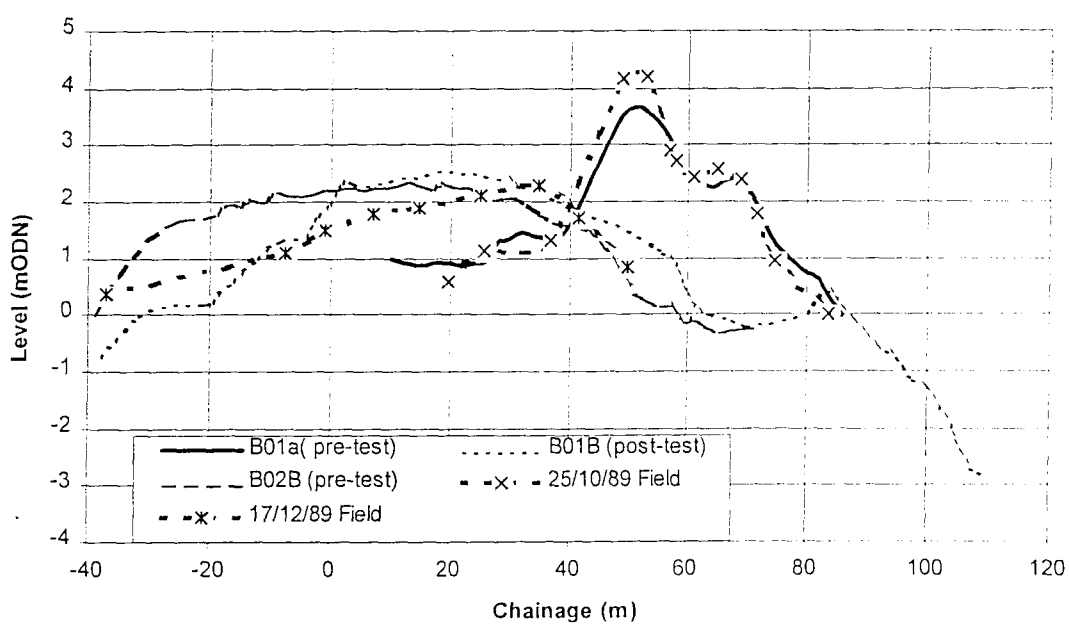

Figure 7.1 Comparative profile response of the model and field data, to the storm of December 17 1989, for profiles HU8 (a) and HU9 (b). Test conditions: SWL=2.27m ODN, H_s=2.5m, T_m=7.4s at an angle of 210^O

(a)

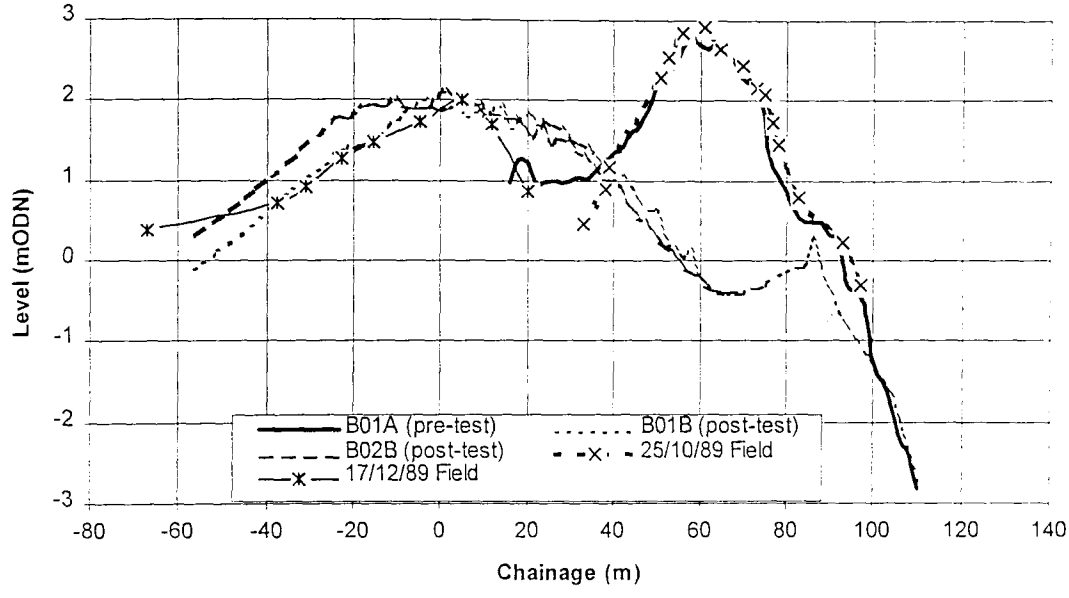

(b)

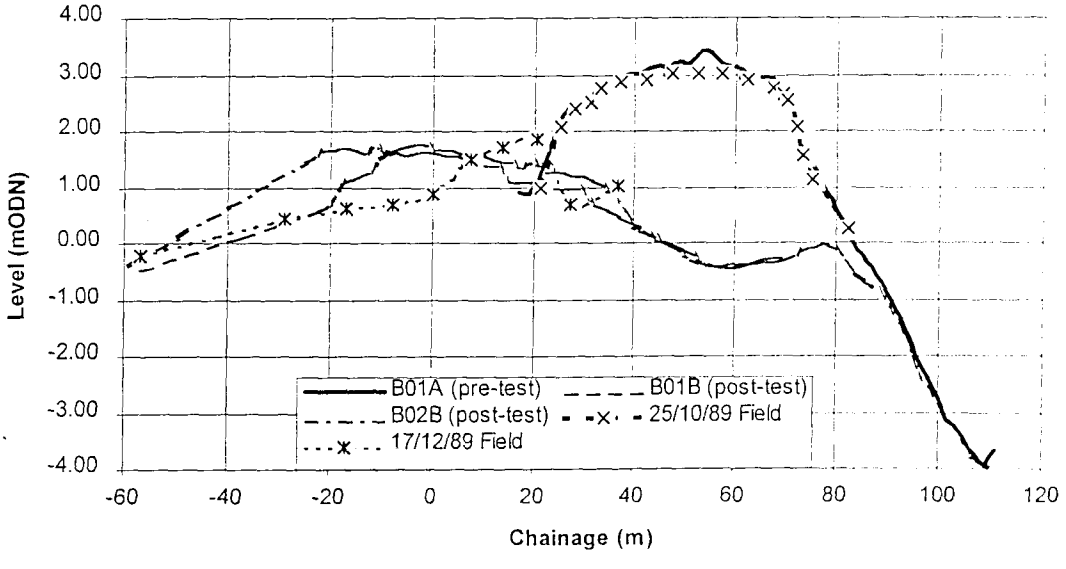

Figure 7.2 Comparative profile response of the model and field data, to the storm of December 17 1989, for profiles HU12 (a) and HU13 (b). Test conditions: SWL=2.27m ODN, Hs=2.5m, Tm=7.4s at an angle of 210^{o}

Validation of the methodology for the lower part of the beach was considered to be less important, as the procedure for modelling restrained shingle beaches has been well established over many years (Section 4.4.3). The lower part of the profile is affected, at full-scale, by the surface level of the underlying saltmarsh deposits; these form a boundary to the beach response, during overwashing events. Saltmarsh response processes (Section 6.5.2(c)) are not reproduced by the model.

(a) Crest lowering

Crest level was reproduced in the model with reasonable consistency, for profiles HU8-HU9 and HU12-HU13. The crest levels were within 0.2m of those recorded in the field, but were consistently higher in the model. Profiles HU10 and HU11 provided less compelling evidence of comparability. The crest profile was 1.7m higher in the model at HU10 and 1.3m higher at HU11. Examination of the field data has provided a possible explanation for this difference. The model data suggests that the barrier crest will form approximately 0.1-0.3 m below the storm peak water level, when sluicing overwash occurs. Field data show that the crest formed at a lower level than this, in some areas. This pattern suggests, perhaps, that sluicing overwash continued to occur for some period after the peak water level: this interpretation was confirmed by the examination of aerial photographs, taken from the Coastguard helicopter, which indicate more severe overtopping in this zone (Plate 6.7). Isolation of the sluicing overwash, to a narrow zone, may reflect longshore variations of the pre-storm beach cross-section: this was smaller between HU10-HU11 than between HU8-HU9, and the initial crest level was also lower. The process appears to be less significant farther to the east; this is perhaps indicative of the reduction in wave energy, from west to east. Such a difference becomes more significant as the tidal elevation falls, due to the effects of the offshore Shingles Banks (Figure 3.1).

The crest positions were more variable (in relation to the crest elevations): both the model and field data demonstrated crest roll-back at profiles HU8-HU13. The extent of roll-back in the model and the field was variable, although the same general trends were observed (Figure 7.3); this may represent modelling of the storm at a single water level. Some scatter in the data was expected, as overwashing waves can move the beach crest several metres within a single wave event. Lee slope angles were

reasonably consistent, although the model slope tended to be steeper than at full-scale (Figure 7.3); once again, this may represent modelling of the storm event at a single water level (see above). Although there were some measurable differences between the profile response of the model and the field measurements, the results were sufficiently similar to demonstrate that the model methodology could reproduce the behaviour of the barrier crest, as well as that of the lower beach profile. Comparisons with field conditions of the crest slopes, overtopped lee slopes, extent of overtopping, and the crest levels have all provided evidence that the model methodology was appropriate for this investigation. Further the results of tests B01-B02 have provided confirmation that the modelling procedure was repeatable.

The model geometry was not identical to that of the prototype profiles, in some instances, despite the use of templates to form the beach; this resulted in marginally lower profiles being formed within the model in Test B01, but was rectified in test B02. The probable cause of this inaccuracy was the method of screeding the model beach to the profile templates; this resulted in the top surface of the grains lying at the template surface (as opposed to the mean surface of the grains). The accuracy of model construction is demonstrated now, by comparison of model and field pre-storm profiles (Figures 7.1 and 7.2). Field and model data sets were combined and translated to common zero co-ordinates by "eye fit" of the data, for comparative purposes.

The same storm event was reproduced, later in the test programme, to provide calibration of the adjoining easterly model segment C (Figure 4.14). This approach provided the opportunity to examine the relative effects of the spatial variation in the beach geometry, together with the longshore reduction in the intensity of wave conditions (from west to east). Test C03 was carried out with waves generated at an angle of 210^{O}: concurrently, the beach response to a significant wave height of 2.5 m and period of 7.4 s was investigated.

Large and wide washover fans were formed rapidly and sluicing overwash was the dominant process throughout the test run. Most of the test section was overtopped, by virtually all the waves within the test. Three crescent-shaped 'surface emergent' areas formed, between profiles HU12-HU13. This test provided some unexpected results, when compared with the field measurements of the same storm. The model did not reproduce the expected direction of sediment transport (from west to east), although

the profile response of the barrier beach was comparable with that identified within the field data. Beach crest roll-back was greater in the model, than at full-scale, between profiles HU16 - HU18: this probably reflected reversal in the sediment transport direction within the model. The beach crest alignment formed almost parallel with the crest of the incident waves; this represents a significant realignment of the beach, during the storm. Such alignment indicates, also, a limitation to the uni-directional wave climate produced in the model. The results suggest that the waves refract to shorewards, impacting with an incident wave angle of 5^{O} (from the beach normal). Further examination of the wave climate data, together with the field observations, has resulted in a revised prediction of incident wave angle - for this storm, of 225^{O}. Limitations of wave climate modelling at the eastern end of the site are discussed further in Chapter 5.

Test C20 was run with the same wave conditions as Test C03, but with waves generated at an angle of 225^{O}. Observations made during the later test provided a more satisfactory comparison with the longshore response observed in the field data. Sluicing overwash occurred between profiles HU12 - HU16, resulting in crest lowering. The most severely damaged area lay between profiles HU12-HU15. A build-up of beach material occurred between profiles HU17 and HU18. The beach crest was realigned virtually parallel with the wave crests, as far east as profile HU17.

Although data generated by reproduction of the 17/12/89 storm provided some confidence in the modelling methodology, the event was exceptionally rare; it was not typical of most of the storm events resulting in overwashing and crest development. However, the storm probably provided an upper boundary condition, for examination of the effects of extreme water levels in combination with wave activity, for the Hurst Spit experimental site.

7.1.2 Reproduction of the storm event of 25/10/89

Field data were collected before and after the storm of 25/10/89. Wave climate studies suggest that this storm was characteristic of an event with a return period of once in five years (Section 5.4). The storm peak water level was determined at 0.87m ODN. Although overtopping and overwashing occurred, the prevailing conditions were far

less severe than those experienced during the 17/12/89 event: field data suggest that the beach response, measured following 25/10/89, is more typical of events resulting in crest modification. Hence, in this particular respect, the storm provides ideal conditions for calibration of the model methodology.

Tests C01, C02 and C19 examined beach response to the 25/10/89 storm. Similar problems were experienced during tests C01 and C02, to those discussed for test C03 (for 17/12/89): these were carried out with an incident wave angle of 210^{O} (see above). Little overtopping occurred between profiles HU10-HU11 and a steep, reflective, seaward face formed to seawards of the crest: a slight accumulation of material occurred in this area, representing east to west longshore transport. Overwashing resulted in the formation of throat-confined washover fans at a number of locations; these were linked by a narrow crest ridge, between profiles HU11-HU15. More severe overwashing occurred between profiles HU15-HU16, whilst a series of small washover fans developed between profiles HU16-HU18: overwashing was more limited in this area, during the full-scale storm event. Whilst the profiling (in the model) identified features which formed on pre-defined lines, detailed profile response information data were not gathered for all of the fans which formed. The profile response was similar to that observed during test C02.

The test was repeated using the same initial beach geometry and wave and water level conditions, but at a wave angle of approach of 225^{O}, to examine the sensitivity of the model to the incident wave angle. Similar trends were observed to those identified, for an approach angle of 210^{O} (see above). Roll-back levels measured were generally smaller in the model than in the field.

The comparative results between the model and field data are generally more scattered, for this event. However, such events, which are close to the overwashing threshold, are likely to produce more scattered results. Such scatter may represent differences between the synthetic and real wave conditions, as the crest elevation modifications are sensitive to small changes in beach geometry or hydrodynamic conditions.

7.1.3 Calibration tests - discussion

The combined data sets for the calibration tests are presented in Figure 7.3. Changes in crest elevation are reproduced reasonably well in the model, although the model tends to underpredict crest lowering. It may be suggested that this variance represents the fall in the tidal elevation, following the storm peak: sluicing overwash is likely to have continued for some period, resulting in further crest lowering. Most of the model crest data lie within +/-0.5m of the field data levels. Further, overwashing and crest lowering occurred in the model, at all of the locations profiled in the field (Section 6.5).

The extent of the crest roll-back (migration) follows similar trends, for both the model and the field data, although the data were scattered; this is not surprising, as individual waves can cause the crest to roll-back several metres. A maximum difference of 38m was measured, but most of the data varied by less than 15m (Figure 7.3(b)). Scatter tends to increase over the extreme range of movements, during the 17/12/89 event. The scatter during the 25/10/89 event may represent the close proximity to the overwashing threshold, together with the 'questionable' prediction of nearshore wave conditions (Section 5.5).

Field data controls are poor, relative to those within the physical model; consequently, the model and field data sets may be expected to differ. Most notably, wave conditions, used within the physical model for these particular tests, (determined by numerical modelling) may have differed from those which actually occurred (Section 6.5). Any differences between model and actual field wave conditions will affect directly the comparability of the beach profile response.

The field data have provided 2-dimensional profiles: however, no information was available between the profiles, to describe spatial variations in beach geometry. The response of the saltmarsh beneath Hurst Spit was not reproduced within the model: however, shearing, sliding and rotational movement of the saltmarsh surface impacted upon the profile response, at a number of locations during the 17/12/89 event (Section 6.5.2). This difference helps to explain variability between the field and model profile response at HU13 (Figure 7.2 (b)). The timing of the post-storm surveys, following the storm peak, affects the measured response of the seaward face of the barrier.

Local, small-scale spatial variations in the model and the full-scale topography may have affected the results, particularly where topographic lows occurred close to the measured profiles.

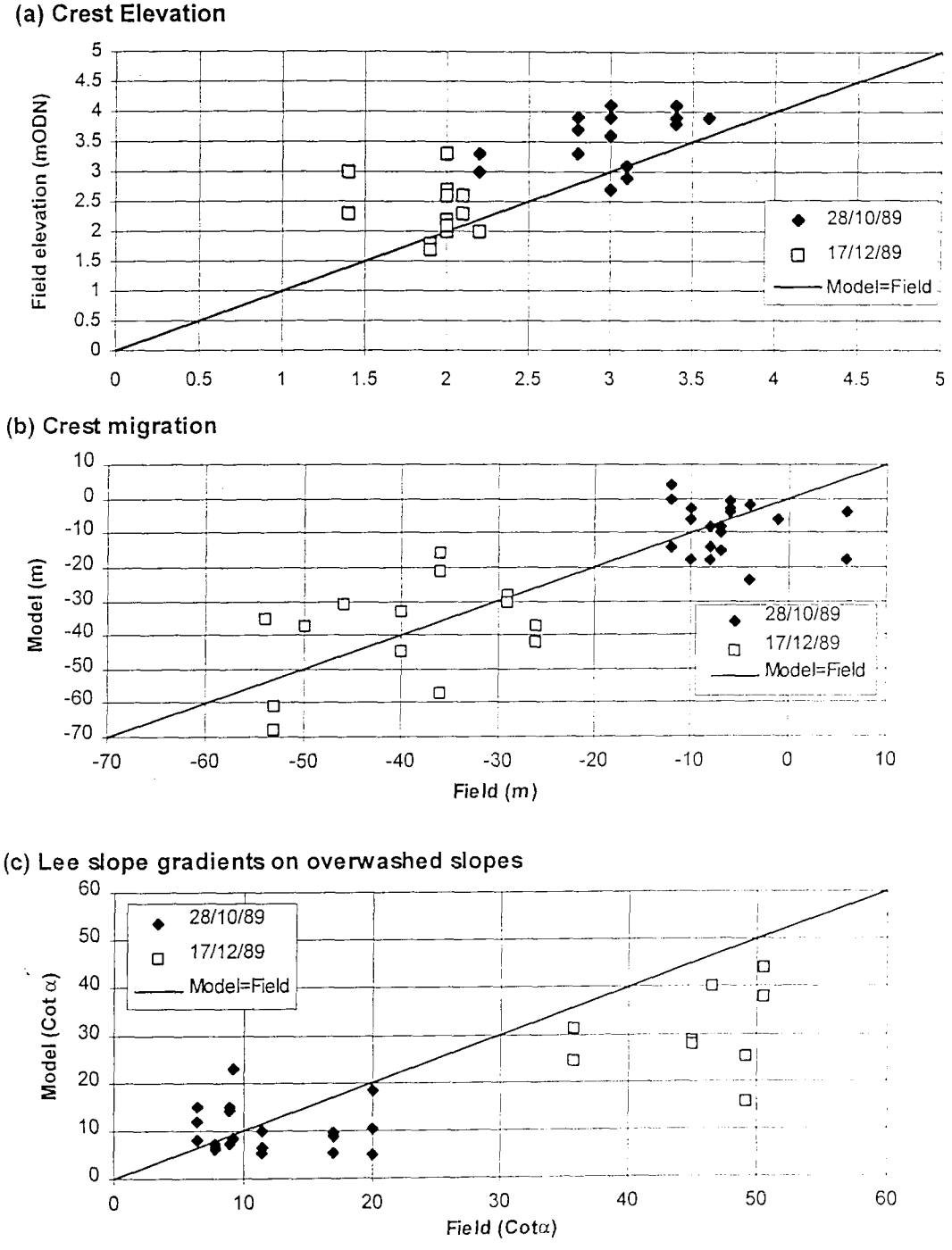

Figure 7.3 Comparison of field and model geometric response variables, during the calibration tests

Although it could be argued that the calibration phase of physical modelling of storm events lacked statistical rigor, in proving the methodology, the results obtained have provided compelling evidence that the beach response follows the same general pattern of change - in both model and at full-scale in the prototype. This conclusion is supported by: (a) observations made at full-scale during storms; (b) visual interpretation of profile data sets; and (c) the processes observed during the model tests. All of these considerations suggest that the overwashing processes are reproduced adequately. The scale of the washover features formed in the model were of similar dimensions and plan shape, to those observed at full-scale. The fact that the test methodology has been applied successfully to restrained shingle beaches previously (Hydraulics Research, 1985b; 1986) provides further support for the methodology. Studies undertaken on restrained beaches have produced run-up crests with similar characteristics to the crest of shingle barriers (Powell, 1990). Although the calibration tests do not prove conclusively that overtopping and overwashing processes were replicated accurately by the model, the evidence obtained was such that further testing of more varied test geometry could proceed. Such tests were undertaken, to determine model threshold conditions for overtopping and overwashing. This decision was made on the basis that further calibration data could be collected to confirm, or later refute, the methodology in future research programmes.

7.1.4 Recommendations for further empirical validation.

Calibration of the modelling methodology could be improved, with more detailed field data: however, this would be extremely difficult to achieve. Nonetheless, better controlled wave data might improve the analysis of the field data. Further support could be given to the model methodology, by undertaking more detailed field studies, but this would require an intensive programme. The studies should provide simultaneous full-scale measurements of the directional wave conditions, at a number of locations along Hurst Spit, together with the installation of a tide gauge at the field site. The response of the saltmarsh surface should be determined, under both pre- and post-storm conditions. A detailed grid of 3-dimensional levels are required across the whole of the 'surface emergent' section of the barrier, ideally at a grid spacing of approximately 2 m, extending to seawards to a water depth of approx. 8 m. This

information is required: over the low water period immediately prior to the storm; and immediately following the storm peak. This requirement presents a particular problem, as there is virtually always a period during which the storm decays and conditions are unsuitable for beach profiling: however, there is inevitably a period of beach recovery during this phase. The only way to overcome this restriction might be to utilise some form of remote sensing technique, which permits the high resolution measurement of the beach surface and nearshore bathymetry. Laser scanning technology presently under development, such as LIDAR, may permit such measurements in the future. Regrettably techniques are not yet sufficiently well developed to obtain results in the submerged zone. The timing of measurements presents a major problem which must be overcome, if model calibration is to be improved.

Alternative barrier sites, such as Chesil Beach (Dorset), may be more suitable for further calibration of the methodology: this latter site has the advantages of a larger tidal range (4.1 m on springs), simpler basement geology and less spatial variability of wave climate (Hydraulics Research, 1984).

7.2 CATEGORISATION OF BARRIER CREST EVOLUTION

Observations made during the model testing have identified a series of alternative beach crest responses, to hydrodynamic conditions; these are used in subsequent analysis, and are outlined below.

(a) No change occurs to the crest elevation and the profile is contained to seawards of the barrier crest. The beach responds in a similar manner to that described by the functional relationships observed in earlier studies (Powell, 1990).

(b) The crest elevation is raised in response to overtopping and limited overtopping of the barrier occurs. The waves modify the crest, by depositing thin layers of shingle and building a run-up berm in a similar manner to (a), above. Finally, the supratidal beach becomes higher and, usually, narrower.

(c) Roll-back occurs and crest elevation is reduced by overwashing. The waves exceed the crest-line, resulting in destructive modification of the profile. The crest is lowered and migrates landwards whilst deposition occurs on the back barrier and further to landwards.

(d) Roll-back occurs and the crest is raised by overwashing. The waves exceed the crest level, resulting in destructive modification of the crest profile. The crest is lowered initially, then migrates landwards; it subsequently rebuilds in a new position, at a higher elevation than the pre-storm level.

(e) The crest elevation is reduced, due to beach widening and cut-back of the barrier crest, with no overtopping. Waves do not exceed the barrier crest, but the active profile widens (between the run-up crest and the breaking point). Undermining of the beach crest occurs and the beach crest level reduces; this dynamic profile response is similar to that observed in earlier investigations (Powell, 1990).

The evolutionary modes discussed above can be described in numerical terms using profile descriptors. The criteria used to define the thresholds, for each evolutionary stages as outlined below.

(a) Crest elevation raised (build-up) by overtopping	$h_{bc(pre)} < h_{bc(post)}$, $p_{lc(pre)} <= p_{lc(post)}$, $h_{lc(pre)} <= h_{lc(post)}$
(b) Crest elevation reduced, by foreshore widening (cut back)	$p_{bc(pre)} > p_{bc(post)}$, $h_{bc(pre)} > h_{bc\ (post)}$, $p_{lc(pre)} = p_{lc(post)}$, $h_{lc(pre)} = h_{lc(post)}$
(c) Crest elevation raised and roll-back, by overwashing	$p_{bc(pre)} > p_{bc(post)}$, $h_{bc(pre)} < h_{bc\ (post)}$ $p_{lc(pre)} > p_{lc(post)}$
(d) Crest elevation lowered and roll-back, by overwashing	$p_{bc(pre)} > p_{bc(post)}$, $h_{bc(pre)} > h_{bc\ (post)}$
(e) No crest change	$p_{bc(pre)} = p_{bc(post)}$, $h_{bc(pre)} = h_{bc\ (post)}$ $p_{lc(pre)} = p_{lc(post)}$, $h_{lc(pre)} = h_{lc(post)}$

These evolutionary categories are illustrated, with reference to test conditions, in Figure 7.4.

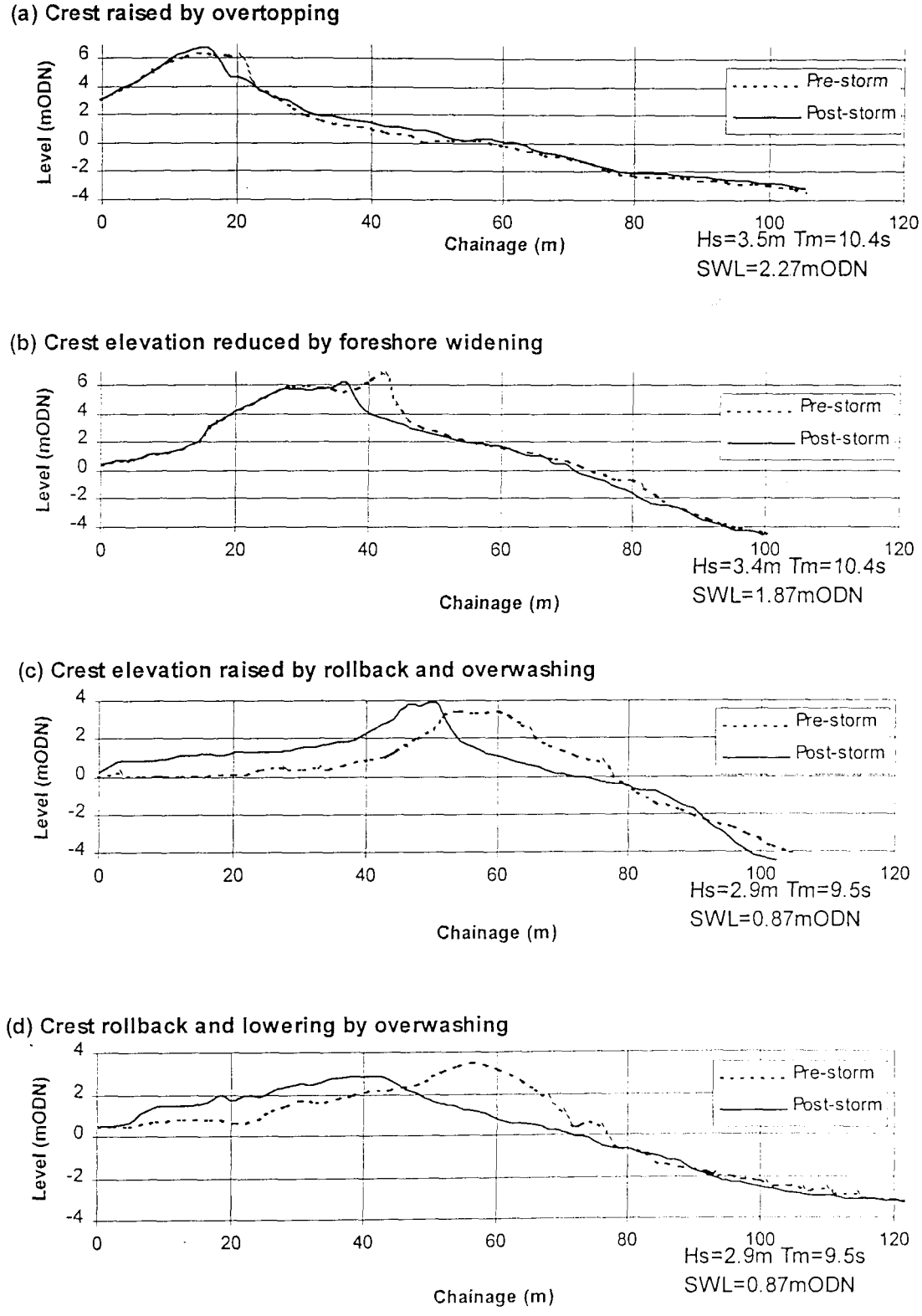

Figure 7.4 Categorisation of barrier crest evolution, based upon the model results (see text)

Category (b) conforms with the 'Type 1 Overwashing' mode (Nicholls, 1985), and the 'overtopping' category (Orford and Carter, 1982). Categories (c) and (d) provide subdivisions for 'Type 2 Overwashing' (Nicholls, *op. cit*) or 'overwashing' (Orford and Carter, 1982 *op. cit*). Category (e) provides a new crest evolution category, for shingle barriers, nonetheless, the dynamic profile response conforms with an earlier model of dynamic equilibrium profile development (Powell, 1990).

7.3 PROFILE RESPONSE OF HURST SPIT, TO EXTREME STORM EVENTS - QUALITATIVE ANALYSIS

A series of 41 tests were carried out to examine overwashing and overtopping thresholds of Hurst Spit, under a range of storm conditions. The test section was based upon the surveys undertaken during October 1990 (Segment B)(Figure 4.13) and February 1991 (Segment C) (Figure 4.14); these consisted of profiles with a range of spatially-variable, barrier geometry configurations. Tests were carried out with angles of nearshore wave approach of 210^{O} and 225^{O} (i.e. normally incident). An empirical framework of profile response and hydrodynamic conditions has identified a range of conditions, resulting in overwashing and overtopping. The test conditions are listed in Appendix 3.

Crest evolution thresholds were identified, by reference to variable wave, water level and freeboard conditions; this was achieved using crest evolution criteria (Section 7.2) and by qualitative comparison with return periods of wave conditions defined for Hurst Spit (Section 5.4). The results have demonstrated a relationship between freeboard, wave conditions, and crest elevation response: all five categories of crest evolution (Section 7.2) were observed. Figure 7.5 shows the influence of crest elevation and freeboard on crest evolution; the effects of wave period and barrier cross section are ignored. The range of wave steepnesses considered is narrow (0.015-0.033, at the offshore boundary); this may have some impact on the barrier response. The relationship between barrier cross-section, freeboard and barrier span is linear, over the range of conditions examined; therefore, these effects can be described by a single variable (R_c), for this barrier configuration. An overwashing threshold approximation was identified; this was based upon a linear relationship between H_s and R_c, for a single geometric configuration. Although the relationship appears to describe

threshold conditions reasonably well, its use is only of limited site specific value, as this relationship does not consider wave period or barrier geometry.

Numerical analysis of the beach performance, based upon the measurements of profiles, waves and water levels, is considered further in Section 7.7; this is carried out in parallel with a wider range of barrier geometry and hydrodynamic conditions. The results of the tests undertaken on Hurst Spit have provided a framework of results, used to identify conditions resulting in wave overtopping of a specific shingle barrier, of defined geometry. This framework was extended to examine a much wider range of geometric conditions, which might apply to barriers elsewhere, if analysed in a dimensionless form. Such data were used also to determine the design geometry of a beach renourishment project for Hurst Spit (Bradbury and Kidd, 1998).

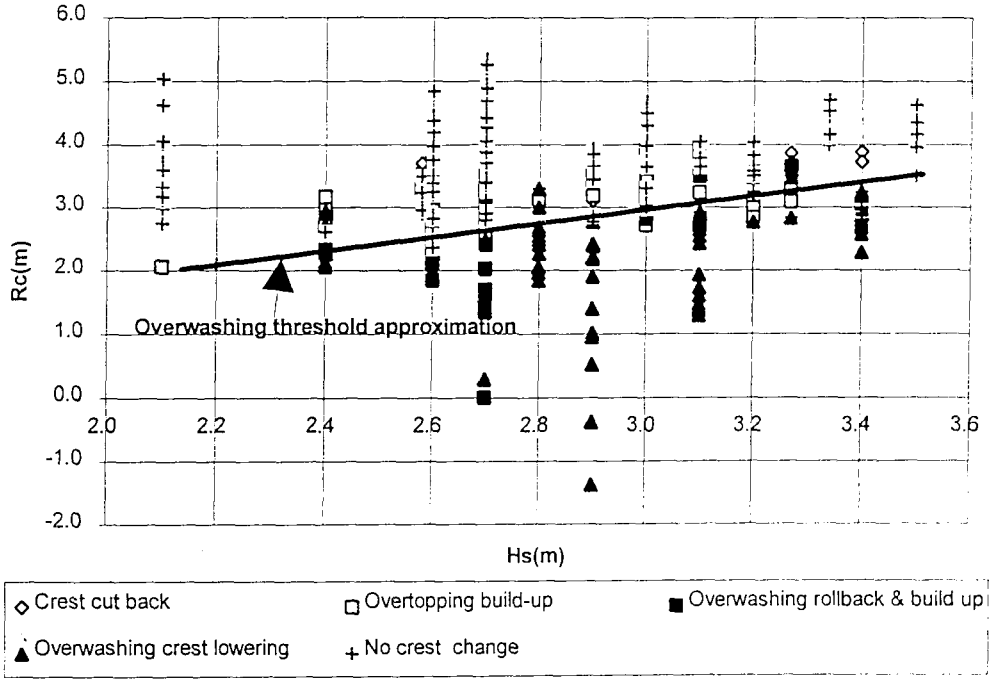

Figure 7.5 Effects of H_s and R_c on barrier crest evolution thresholds for Hurst Spit (1990 profiles)

The threshold conditions for the geometry of Hurst Spit, as surveyed in October 1990, varied along the length of the barrier: reproduction of the severe storms of December 1989 did not result in overtopping between profiles HU6 and HU11 (Test

B13). The barrier to the west of HU11 was more vulnerable to overtopping; it was subject to overwashing, with extensive overwash flats forming during the event.

A storm sequence consisting of the 17/12/89 storm, followed by a typical 1:1 year return period storm (Section 5.4), resulted in severe overwashing along the whole length of Hurst Spit.

Conditions generated during Test B12 (H_s=3.5m, T_m=10.4s, SWL=2.27m ODN) were very close to the overwashing threshold conditions, for the barrier geometry tested. Overwash fans formed between profiles HU10-13, whilst overtopping and crest build up occurred at HU8. The variability in the response represented the spatial variability of the test section freeboard.

Observations recorded during testing provided an improved understanding of rarely observed physical processes. As storms develop, the supratidal barrier width may reduce, due to widening of the active profile, as the beach approaches a new dynamic equilibrium profile. This modification is significant if the cross-shore volumetric balance is not maintained by longshore transport: undermining and thinning of the crest may result, ultimately forming a breach through the barrier. It is not necessary for waves to reach the elevation of the pre-storm barrier crest, for migration to occur under these circumstances; this demonstrates the importance of the CSA, as well as the crest level of the barrier. This process does not seem to be recognised in the established literature, within the context of barrier evolution. Where waves were unable to reach the crest, a steep supratidal face was carved into the barrier: this was often nearly vertical, with a maximum height of approximately 2-2.5 m, and characteristic of ramp deposits (Orford and Carter, 1985). Offshore movement of shingle is associated with such a condition, since a considerable proportion of the incident wave energy is reflected from the steep beach. This pattern was more obvious at lower water levels, than during high surge conditions, where higher wave run-up and associated backwash brought material down on to the foreshore from the crest. Feeding of the foreshore resulted generally from undermining of the toe of the supratidal beach, with severe wave activity at lower water levels. A reduction in the crest elevation may result from foreshore widening, without the waves reaching the crest.

A threshold condition was observed, when the combination of waves, water level and beach geometry resulted in waves reaching the crest; these had sufficient energy to spill onto the crest, but insufficient energy to wash completely over the crest. Less than 5% of the waves reached the crest, depositing a thin veneer of deposits at the crest, when this occurred. Accumulations of (up to) 0.7m thickness were measured at the crest in response to this process; this process was limited to a narrow range of conditions. The transition between overwashing and overtopping was restricted, and sensitive to small hydrodynamics changes.

When crest accumulation threshold conditions were exceeded, overwashing occurred and crest-lowering resulted. Small washover fans normally formed initially, followed by more extensive breaches through the barrier; these resulted in large-scale crest lowering. The size and method of washover fan formation depended upon the crest width, level and wave / water level conditions. If the crest was very narrow, a wide breach formed rapidly: waves were able to overtop the barrier and rapidly lower the crest. If the crest was wider, the rate and size of washover fan formation was significantly slower and smaller. As the crest level was reduced, the probability of waves reaching the crest increased. Consequently, the beach profile at the crest was modified by the formation of washover deposits. The seaward face of the beach was affected also, since a greater proportion of energy was dissipated in run-up and overtopping - than due to wave reflection from the front face. Once the crest level had been lowered, the rate of crest lowering increased rapidly, as the frequency of waves reaching the crest increased. The width of the initial washover fan ranged in size, from approximately 4m-25m, depending on the barrier geometry immediately prior to overtopping. Similarly, the length of the initial fan extended to landwards, by between approx. 1and 5 m. The rate of progression of the washover fan was also influenced, significantly, by back barrier geometry. Displacement of washover deposits into Mount Lake (Figure 3.2), following the initial fan formation, reduced the active barrier cross section. The rate of development of a fan or breach formation was influenced, clearly, by the cross section geometry of the beach.

Beach plan shape evolved rapidly, normally, following initial washover fan formation. The fans widened by outflanking, of upstanding throats on either side of the fan, under the action of overtopping waves. The fan itself provided a preferential flow path for the overtopping waves; throats tended to form through their centre. As the

waves flowed across the barrier, the fan became liquefied and flowed with the waves towards the lee side of the barrier. Fan progradation often extended as rapidly as 2-5m per individual wave. When the fan reached the base of the barrier, its shape altered; this depended upon the back barrier geometry. If the fan entered the lagoon, the rate of growth slowed; at the same time, the head spread and a steep slope formed at the entry point to the water. Spreading of the head was less evident when the fan extended over a solid surface. Wave grouping was important, following the initial fan formation: if the waves were small, then a ridge or berm formed often, to seawards of the crest ridge; this migrated occasionally, upwards towards the crest, blocking the throat and preventing further overtopping. In some instances, the wave grouping enabled a fan to form, but the initial breach closed; this demonstrates the need to study these processes under the influence of random (as opposed to regular) waves. Analysis on a wave-by-wave basis could provide a better explanation of crest evolution. The effects of wave grouping may explain the wide scatter of results, close to the overwashing and overtopping threshold.

In addition to overtopping, percolation of water occurred through the permeable shingle barrier; this resulted in the formation of streams and washout cans on the lee side of the barrier, close to the interface with the saltmarsh. This phenomenon, as well as being been noted on Hurst Spit, also relates to similar shingle barriers elsewhere (Section 2.2); it occurs when the surface emergent barrier cross-section is reduced by wave action, but where the waves are too small to reach the crest of the beach. This process was observed in the model, providing further evidence that the permeability characteristics of the beach were reproduced correctly.

The effects of various combinations of wave and water level conditions were examined, to establish combinations of storms which led to failure of the barrier. Sequences of closely-spaced storms have a significant impact on overwashing; they occur relatively regularly in nature: the winter storms of 1989 provide evidence of combinations of storms which resulted in overwashing. When such storms are widely-spaced in temporal terms, the barrier tends to build: the sediments become better sorted, whilst the profile becomes more dissipative and the active profile shortens (Carter and Orford, 1993).

7.4 VARIABLES CONTROLLING BARRIER PROFILE RESPONSE

Qualitative assessment of the profile response, measured within the model tests based upon the analysis of previous work has provided a list of controlling geometric and environmental variables, which may affect the evolution of barrier beach profiles.

7.4.1 Geometric variables

The beach profile, to seawards of the barrier crest, can be defined in terms of its principle geometric components (Powell, 1990), using numerical descriptors for key points on the profile, linked by defined curves (Section 2.3). A datum position is defined at the intersection of the seaward beach slope with SWL; this varies, with time, as the profile develops or the water level changes. The remaining features are described by co-ordinates relative to this datum (Figure 2.8). Crest position (p_c) and crest height (h_c), formed by run-up, are usually clearly-defined descriptors. The transition step position lies directly beneath the breaking wave location; it is a clearly developed feature, although it is less well-defined than the beach crest. This particular location is the most mobile and variable point on the profile.

Analysis of the barrier profiles obtained as part of the present investigation has identified additional features, which are common to all the profiles; these can be defined in relation to the same zero, as discussed above. A schematic barrier profile is presented in Figure 7.6. The maximum crest level of the barrier is a key feature of the profile: likewise, a series of ephemeral crest ridges co-exist commonly, on shingle barrier beach profiles. The highest and most landward crest is that resulting from the most severe combination of wave and water level conditions. The lowest crest is that which has occurred as the result of the most recent wave activity.

The maximum barrier level lies often above the clearly-defined maximum wave run-up crest; this may be due to any combination of a range of circumstances as outlined below

(a) Undermining of the beach crest may result from short period but high amplitude waves.

(b) The crest ridge may be degraded by aeolian processes such as wind and rain.

(c) Human activity may result in the degradation of the beach crest.

(d) Beach recharge may raise the barrier crest, artificially, above that normally formed by hydrodynamic processes: the beach profile may not show a clearly-defined wave run-up crest, until the beach has become well sorted and a new dynamic equilibrium profile has formed under storm action.

(e) Erosion of the beach crest may result in: the formation of washover deposits on the crest; deposits leeward of the crest; and erosion of the crest due to hydrodynamic processes, such as overtopping and overwashing.

(f) A relict degraded beach crest may result during periods of falling relative sea level.

The barrier- crest, freeboard and its position can be defined by simple profile descriptors, co-ordinated relative to the still water zero datum (p_{bc}, h_{bc}). Although the highest point on the beach crest can be defined simply, it is not always representative of the crest geometry. The lee crest (p_{lc}, h_{lc}) can be defined as the point of maximum wave run-up, to landwards of the barrier crest; it is often marked by a 'strand line' on the beach, which is ephemeral and often difficult to identify, and is used within the definitions of barrier crest elevation (Section 7.2).

Observations undertaken during the model tests suggest that crest width may be a useful variable to consider in analyses, although it is not easily defined. Qualitative analysis of the profiles has indicated that the profile is associated generally with a single turning point over a parabolic crest section. The single turning point at the crest has no width (nor area); the only exception to this is likely to be the presence of a flat crest berm, formed artificially by beach recharge. This situation is not appropriate for the general definition of the barrier crest, but may be relevant when assessing the design of beach recharge.

The landward limit of the back-barrier (p_{bb},h_{bb}) is used often to identify the rate of barrier progradation (Orford *et al*, 1991a) : it is not an appropriate variable for use in

the analysis of crest evolution. Evolution and location of the back-barrier toe is influenced by the basement topography, as well as the hydrodynamic variables.

Qualitative analysis of the model tests of barrier beaches has indicated that the beach span at SWL, and the surface emergent CSA are geometric variables which can control overtopping or overwashing. The SWL span (SWL_s) is defined as the barrier width at the zero datum level; similarly the CSA of the surface emergent profile can be calculated by integrating the area above this limit (Figure 7.6).

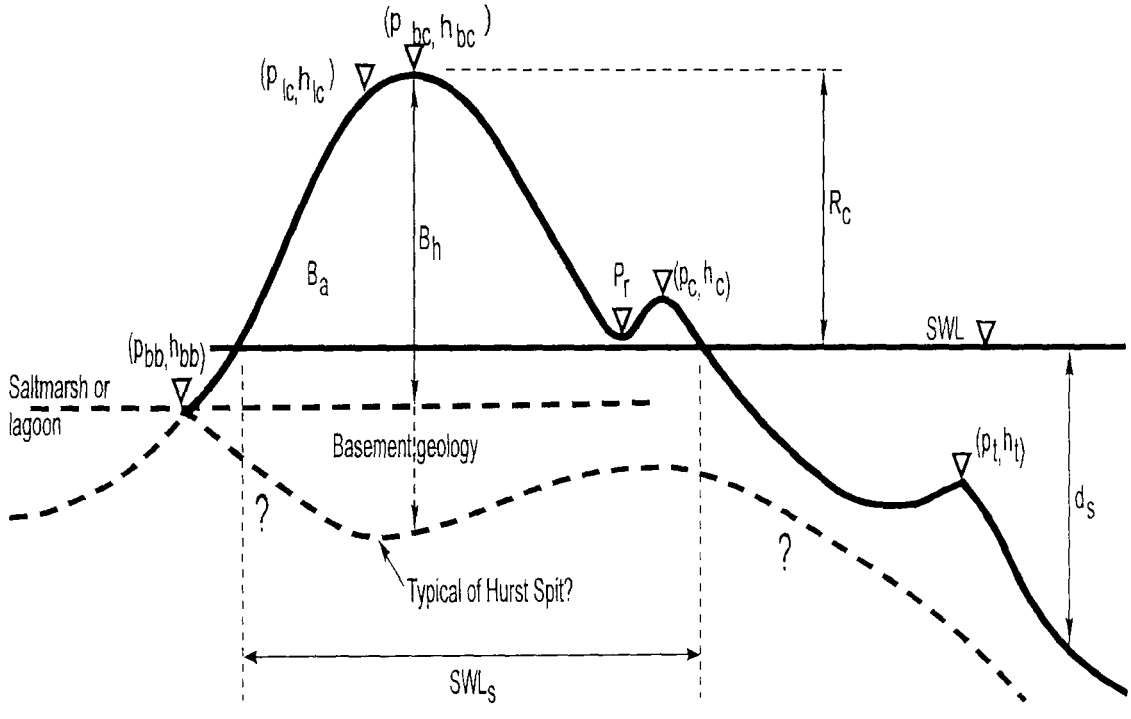

Figure 7.6 Schematic barrier beach profile, showing levels and definitions

The bed profiler data was reduced to a fixed datum; these were compared, graphed, and analysed, using functional profile response relationships (Powell, 1990). Over 3000 beach profiles were analysed, describing the beach elevation at 2m horizontal increments. A computer program was written to calculate beach width, and cross sectional-areas above defined levels; this provided input to the parametric analysis of the barrier crest development. The accuracy of the bed profiler was demonstrated, by comparison of beach profiles with profiles of the fixed bed sections of the model. Most profiles contained sections of the fixed bed, at both the start and end of the

profiles; these indicated that +/-0.05m full-scale (1.25mm model) could be achieved by the bed profiler. Attempts were made initially to define the key locations on each of the profiles: the curves were differentiated, to define the points of inflexion and the turning points in the profile. The large number inflexion points on the curve made this method impractical. However, eventually, the descriptor co-ordinates were extracted from the measured profiles, by visual analysis of a plotting program; these were combined for further analysis with the hydrodynamic variables.

The significance of the initial beach geometry, on the profile development of sand beaches, has been examined by a number of researchers (Dalrymple and Thompson, 1976; and Nicholson, 1968). These investigations have suggested that the initial beach slope had no effect on the final profiles. Elsewhere, van der Meer (1988) and van Hijum (1974) have found that the shape of the final profile of a shingle beach was unaffected by the initial profile, on (beach) slopes ranging from between 1:5 and 1:10. However, the initial profile was found to affect the direction of beach material movement and the method of profile formation. Other researchers have suggested that the initial beach slope does affect the formation of the final profile on sand beaches, (Chesnutt, 1975 and Sunumura and Horikawa, 1974).

A relationship was proposed between the initial beach slope and the prevailing wave steepness (King, 1972); this suggested that an increase in the initial beach slope angle changes the characteristics of the breaking wave. The critical steepness is higher for a steeper beach; at its most extreme, the beach slope will change the breaking wave type i.e. from plunging to surging. This relationship suggests that a critical wave steepness for a steep slope may result in spilling waves on a shallow slope. Such variations may explain the differences between the results of investigators (see above), with respect to the influence of profile formation on subsequent development.

The situation outlined in the preceding text is compounded when profile development on a barrier beach is considered. The results relating to a large proportion of the model data set concur, broadly, with conclusions of earlier studies (Powell, 1990); these have suggested that the initial profile does not influence the form of the final profile, but that it does affect the timing and the mode of formation of the profile. The data obtained as part of the present investigation included also conditions which were

dependant upon the initial profile; these occurred when the beach was subject to overwashing (Section 7.6.2).

Sediment grading has been recognised as a controlling geometric variable, in terms of profile response (Powell, 1990; van der Meer, 1988); however, such studies were limited to the examination of a single sediment size. Mass density of the beach material is another variable, to be considered; this can be combined with particle size to describe the effect of grain size and mass.

Spatial variation in the barrier crest geometry may be considerable, complicating the barrier crest response. For example, localised topographic lows can provide preferential sites for the formation of throats and washover fans. Such features may develop laterally, along the crest ridge, by expansion of throats into zones where the pre-storm crest may be significantly higher or wider. Field measurements have identified considerable spatial variability in the crest elevation (Section 6.5).

7.4.2 Hydrodynamic variables

The controlling variables, identified from earlier studies undertaken on shingle beaches, (van der Meer, 1988; Powell, 1990) are also applicable to the evolution of the barrier crest. The significance of each of the variables was examined, initially in isolation, and in a qualitative manner, in the present investigation. As such, profile response was plotted against the full range of conditions, for each of the variables. These relationships were assessed by comparison with the geometry of Hurst Spit, as surveyed in October 1990 (Appendix 2). Finally it should be noted that some variables were considered, but were not tested systematically.

The effects of environmental variables (see below) on crest evolution were examined, by comparison of pre- and post-storm profiles; this was based upon the response of a pre-storm profile of defined geometry (October 1990 survey of Hurst Spit). The conditions examined were typical of storm conditions at the experimental site, based upon numerical modelling of extreme events (Section 5.4). The influence of each of the variables was examined, retaining the others constant.

(a) Wave height

Wave heights relating to a random sea in deep water can be described by the Rayleigh probability distribution (Priestly, 1981). This approach allows the probability of exceedence of any values of wave height to be determined, if any particular significant value is known. The value used most frequently is the significant wave height, (H_s), defined by the mean of the highest one third of the waves in a time-series. H_s is often derived on the basis of spectral analysis, using the method of moments where ($H_s = 4m_o^{0.5}$, where m_o is the zeroth moment of the wave energy density spectrum). Other values used include: the root mean square wave height, H_{rms}; and the H_{10}, which is the mean of the highest 10 per cent of the waves in a time-series. Assuming a Rayleigh distribution, H_{10} can be described by $H_{10} = 1.27\ H_s = 1.79\ H_{rms}$ (Priestly, *op. cit*).

Whilst the assumption of a Rayleigh distribution is appropriate for deep water waves, shallow water conditions adjacent to the beach result in a different distribution of waves at the shoreline; here, maximum wave height is controlled by water depth. As the water depth to seaward of a beach (D_w) decreases, the largest waves in a train become depth-limited; consequently they begin to break offshore of the beach. Much energy is expended in breaking, reducing the subsequent impact of the waves on the adjacent beach. Eventually, so much energy is dissipated to seaward of the beach that its response to the incident wave conditions is significantly affected.

If it is assumed that offshore wave heights follow a Rayleigh distribution, then depth-limiting can be assumed to occur when $H_s/D_w>0.55$; this relationship has a dependence on foreshore slope (m). Hence, the breaking wave height at the toe of the beach, (Goda, 1985) and modified for application under random waves, is often a more suitable wave height variable, to use for the examination of shingle barrier response under extreme conditions.

$$H_{sb} = 0.12L_{mo}\,[1.0\text{-}\exp(\text{-}4.712D_w(1.0+15m^{1.33})L_{mo})] \qquad [7.1]$$

The location of the wave measurement point (selected for subsequent use in the parametric analyses of beach profile response) is of importance, although it has only rarely been identified in earlier investigations. Conditions measured in deep water are

unsuitable for use in the analyses, since potentially large changes can result from shallow water wave transformation processes. Waves measured above the active section of the beach are unsuitable for use, since they can be modified by the beach evolution process. The most suitable measurement point for waves is at the toe of the mobile beach, close to the point of beach profile closure; this was determined for the present investigation on the basis of the analysis of a time series of hydrographic survey profiles (Section 4.2). The wave heights used in analysis were measured in 7.9-9.3m of water. Conditions calibrated at the wave probes at the offshore model limit (Figures 4.12- 4.15) were in 10-12m of water, coinciding with the prediction points of the numerical modelling (Section 5.4).

A comparison of the test results, with variable significant wave height but effectively constant other (hydrodynamic) variables, has revealed a systematic lengthening of the beach profile with increasing H_s (under non-overtopping conditions). Such lengthening was most marked to seawards of the water line and beach intersection; this observation is consistent with that of Powell (1986). The response of the restrained beach profile, to wave attack (as outlined above), is not replicated, when overwashing or overtopping occurs on a barrier profile. The impact of wave height on a barrier profile, of finite width and elevation, is more complex than a restrained beach; it is partially dependent on a series of geometric variables. For example, crest elevation change is shown, as a function of H_s in Figure 7.7, for the range: H_s = 2.7 - 3.2m. A range of freeboard conditions is shown, with constant SWL, period, and a typical surface emergent CSA of $65m^2$.

Such geometric conditions were consistently below the crest evolution threshold, for H_s=2.7. An increase in wave height, to 3.0m, resulted in exceedence of the overtopping threshold for R_c<3.1m. A small increase in wave height, to H_s=3.2m, caused the overwashing threshold to be reached, for a range of freeboards. This response is inconsistent however, over a range of conditions; thus, it is possible for either overtopping or overwashing to occur for a range of R_c. This pattern indicates the influence of other variables, including small local and spatial variations in the crest geometry and CSA. The small change in H_s , between evolutionary states, demonstrates the sensitivity of the crest evolution to small changes in H_s or R_c. It can be concluded from Figure 7.7 that H_s and R_c have an important effect on the crest profile evolution.

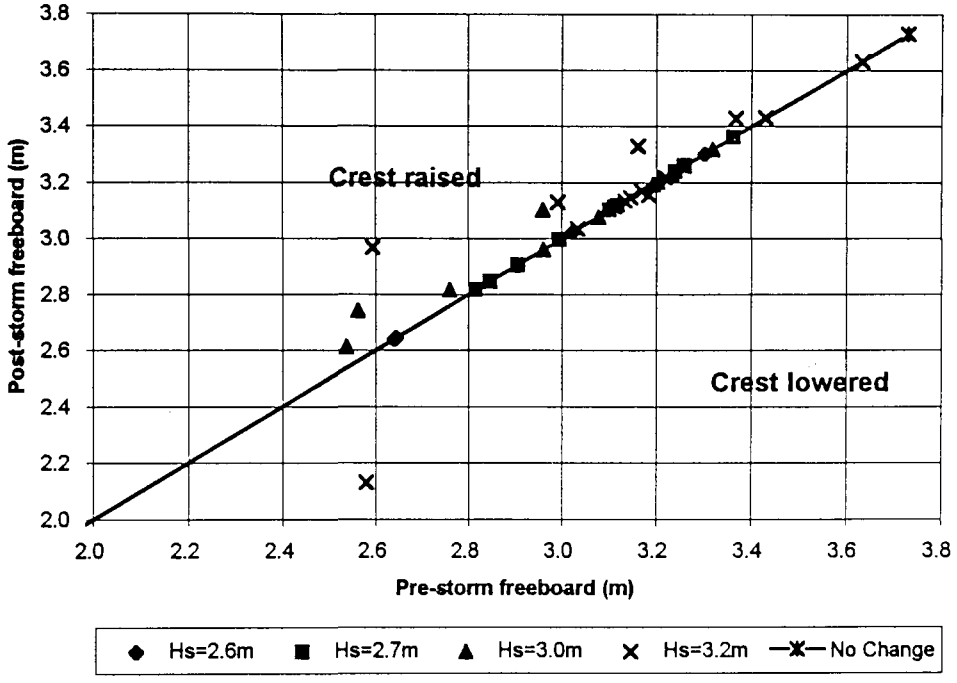

Figure 7.7 The effects of significant wave height on the barrier crest response, for a variable pre-storm freeboard (T_m=7.6s; SWL=2.27m ODN)

(b) Wave period

Random waves are characterised by a range in wave periods. However, the wave energy spectrum can be described in terms of three characteristic periods: the peak period of the spectrum (T_p); the significant period (T_s); and the average period of the zero crossings (T_m). T_m can also be calculated from the spectrum on the basis of $T_m = (m_o / m_2)^{1/2}$. The relationship between the three period descriptors is constant for a defined spectral shape, varying only with spectral type (Goda, 1976).

The test programme used generated waves with a constant spectral shape (JONSWAP). Provided that a consistent spectral shape is used, it is not necessary to

use each of the values of T_p, T_m and T_s in any analytical work. The relationships are linear and can be determined from a single value of wave period. The average zero up-crossing wave period (T_m) used in the present study, is consistent with that applied in other related research (van der Meer, 1988; and Powell, 1990).

A restrained beach responds to lengthening wave period, through increased wave run-up and the raising of the elevation of the foreshore crest. On exceeding the overwashing threshold, lengthening T_m causes more rapid changes to the barrier crest elevation. This trend can be demonstrated by reference to a sample data set, examined for a constant significant wave height of 3.2m, at a water level of 1.87m ODN and with an average surface emergent CSA of $60m^2$ (Figure 7.8)

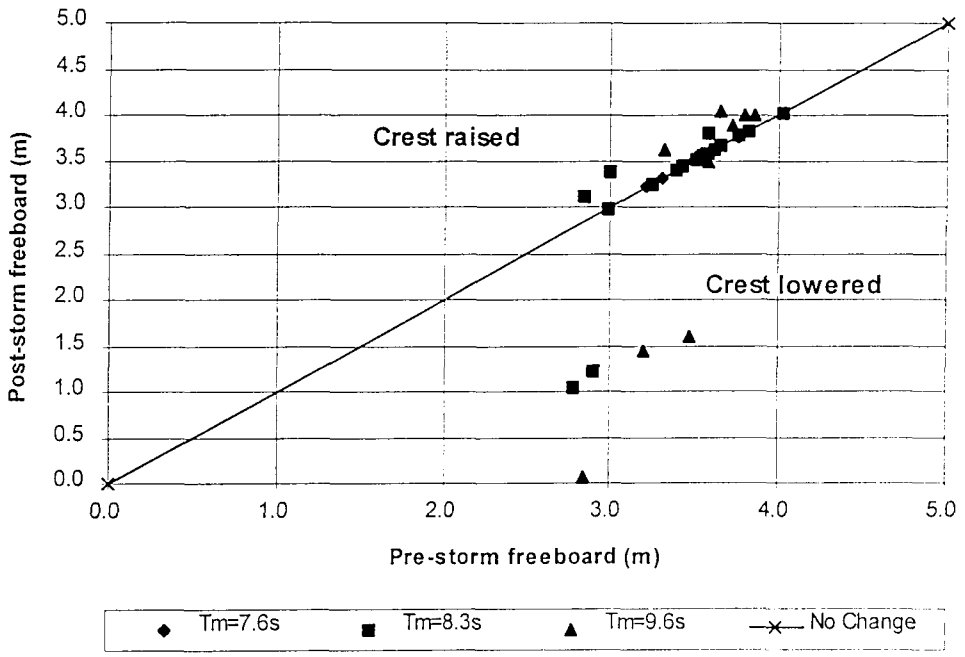

Figure 7.8 The effect of wave period on the profile development with variable freeboard (H_s=3.2m; SWL=1.87m ODN)

A "s-shape" response trend was observed similar to that relating to H_s, (Figure 7.7); this confirms the influence of wave period upon crest evolution. No change in the crest was observed with T_m=7.6s, but both overwashing and overtopping occurred with T_m=8.3s, when the range of freeboards spanned was close to the threshold

conditions. Crest elevation changes occurred for all the freeboards in the data set, when T_m=9.6s. The transition zone (containing both overwashing and overtopping) reflects, perhaps, the influence of solitary waves or groups of long period waves on the crest. The large volumes of water contained within a single wave can result in significant changes at the crest. The shortest wave period had minimal impact on the profile evolution, whilst the longer period waves resulted in overwashing of the crest. Elevation changes were generally <0.5m when overtopping resulted, whilst overwashing could result in crest elevation reductions of several metres.

(c) Water level

The influence of changing water level on a barrier beach is complex. For a barrier of particular geometry, the freeboard reduces between the water surface elevation and barrier crest as the water level increases. This effect impacts on the barrier, by reducing the surface emergent CSA and the span, at SWL; it affects nearshore depth-limited wave conditions. For similar offshore waves, the higher waves impinge higher up the profile. Tidal surges, in conjunction with storm wave conditions, are likely to be important in controlling sediment and profile response at mesotidal sites such as Hurst Spit (Section 3.2.1).

The effects of increasing water level are examined, in vertical step intervals for non-overtopping conditions in Figure 7.9. The wave conditions at the offshore boundary of the model are representative of a single set of deep water offshore conditions (H_s=6.6m, T_m=8.9s); these are typical of a 1:5 year return period storm at Hurst Spit. Such conditions show only small changes, resulting from nearshore wave transformations, at each water level. The predominant controlling variable is water level, which changes the point of attack on the beach; this results in a landward and upward migration of a profile, of nearly constant shape, with increasing water level.

The effects of water level are examined further in Figure 7.10, which illustrates similar profile development, leading to overtopping and overwashing at the highest water levels. The sequence (Tests B58-61) has demonstrated that the transition between overtopping and overwashing resulted from an increase in water level of 0.4m.

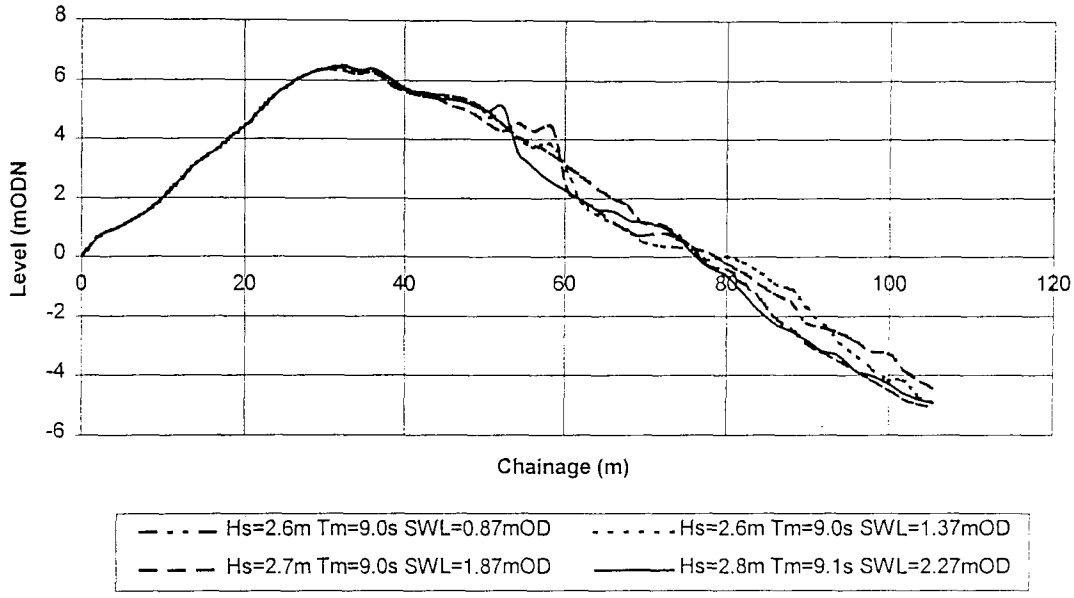

Figure 7.9 Effects of increasing water level on barrier profile development with no overtopping

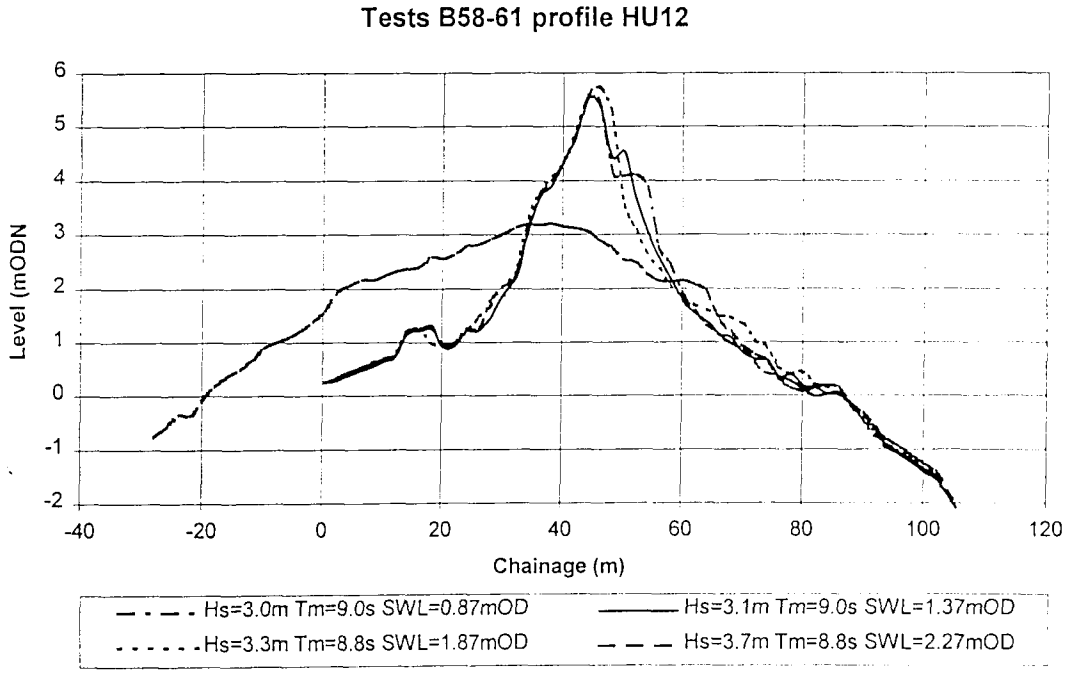

Figure 7.10 The effects of increasing water level on barrier crest development, under overtopping and overwashing conditions

The results shown on Figure 7.11 relate to four water levels, for constant offshore wave conditions, based upon the geometry of Hurst Spit in October 1990. These data identify a relationship between the barrier crest elevation change and barrier freeboard. The trend is masked partially, by the implicit changes in CSA and H_s, resulting from increasing water level. No changes occurred at either of the two lower water levels; this reflects a reduction in wave energy, resulting from the depth limitation on wave height. A distinct change in response can be identified at higher water levels, when the crest elevation changes occurred. Crest evolution was confined to overtopping at SWL=1.87m ODN, whilst both overtopping and overwashing were observed at SWL=2.27m ODN.

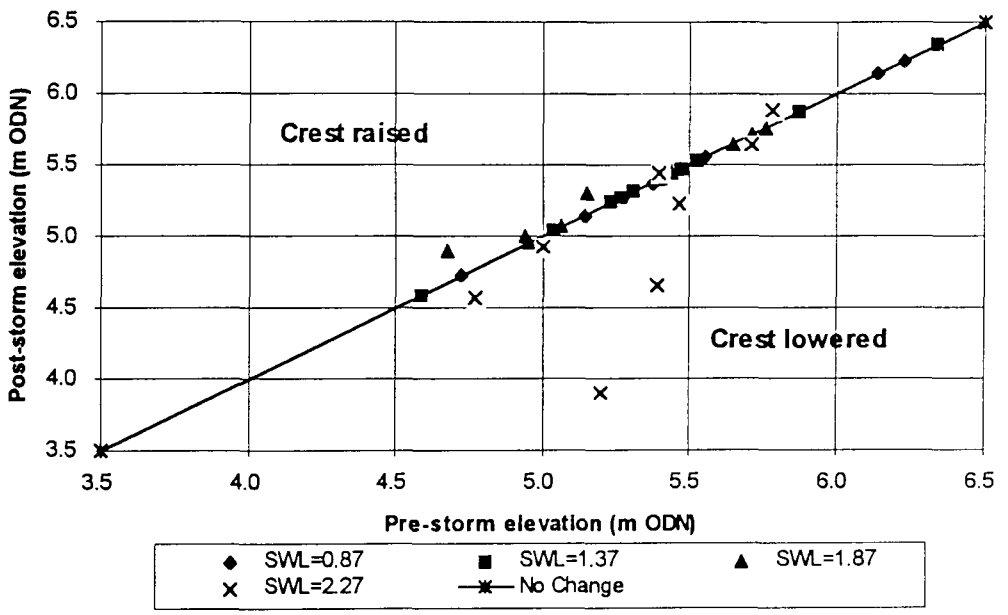

Figure 7.11 The effects of increasing water level, on barrier crest development (H_s=2.7m; T_m=7.6s)

The range in conditions presented are consistent with a range of thresholds, for both overtopping and overwashing. Changes in crest elevation of <0.5m resulted from overtopping; the response was less well-ordered, when overwashing and crest reduction occurred. This pattern suggests that crest evolution is sensitive to freeboard, CSA and spatial variation in the barrier geometry.

Incremental increases in the water level, on a barrier of constant geometry, progressively reduce the supratidal CSA of the barrier. The effects of such a sequence of water level were examined, by testing of beaches of differing CSA and constant freeboard, to isolate the relative impacts of freeboard and supratidal CSA. These effects are considered further in Section 7.5.

Hydraulic jumps were observed occasionally, when the transitional overtopping phase gave way directly to the overwashing phase (when stepping through a sequence of tests, over a range of water levels). This process occurred usually, when the crest ridge was very narrow.

(d) Wave grouping

The model observations have identified the apparent influence of wave grouping on crest evolution, for conditions close to the overtopping and overwashing thresholds. The instrumentation used and test procedures adopted did not permit the impacts of solitary waves, or groups of waves, to be monitored within context of profile response; however, this was noted qualitatively. The absence of such data may explain some of the scatter of results close to the overtopping and overwashing thresholds (see Section 7.6.2).

(e) Angle of wave approach

Although swash-aligned barriers are necessarily aligned normal to the predominant incident wave direction, waves often approach over a range of angles to the beach. The angle (ψ) impacts upon wave run-up and longshore transport directions and rates. Earlier research undertaken suggests that oblique wave approach results in a lower run-up, together with modification to the profile in proportion to the incident angle (Van der Meer, 1988; and van Hijum and Pilarczyk, 1982).

The effects of incident wave angle are not immediately obvious from the data collected during the present study, which is confined to the examination of incident waves approaching from the model offshore boundary at angles of between 0-20^{0}. This range

of approach angle represents subsequent refraction of waves and a minimal energy loss between the wave paddle and the test section; it results in virtually normally incident waves at the test section.

(f) Spectral shape of the prevailing waves

Previous studies undertaken on shingle beaches have suggested that the influence of spectral shape of the incoming waves is minimal (van der Meer, 1988). However, the results obtained from the current investigation have been confined to an examination of waves described by a JONSWAP spectrum. Field data (Section 6.4) has identified the occurrence of bi-model spectra, with a secondary spectral peak resulting from a swell wave component. Such spectral variations have not been considered, within previous investigations, in context with shingle beach profile response. Insufficient data is available to examine the effect of such spectral variability, within the present investigation. This particular variability of spectral shape is worthy of further investigation and is considered further (Section 8.6).

(g) Storm duration

Random waves lead to the generation of a wide range of hydrodynamic forces on a beach: the dynamic equilibrium profile will take longer to form, than if subjected solely to monochromatic waves. Investigations undertaken elsewhere, carried out using only monochromatic waves, have demonstrated rapid response to repeated forces on the beach; these resulted in the formation of an equilibrium profile (van Hijum and Pilarczyk, 1982). Subsequently Powell (1990) has examined the effects of storm duration on profile development. Considerable variability in the profile shape was noted, during the early stages of beach evolution.

Observations undertaken within the context of the present investigation have indicated that approx. 80% of the volumetric changes, towards the final dynamic equilibrium profile, occurred within 500 waves (when the beach was not subject to overwashing). Similarly, the influence of duration, on profile formation, depends also upon the shape of the initial profile, relative to the final dynamic equilibrium profile: when the final and

initial profiles are similar, the duration required to achieve the final profile is reduced (Powell, 1990).

The observations made within the present investigation concur, generally, with those made in earlier studies (Powell, *op cit*) for non-overwashing conditions. Certain profile variables appeared to be less sensitive to storm duration than others, within the present investigation. In particular, the location of the beach crest and the wave run-up limits took the longest to evolve, although these formed generally within a time scale of 500 waves. The beach step was formed more quickly, but its position was less well defined (than the beach crest); it was modified rapidly, often representing the last few waves in the time-series. Observations confirmed that the beach toe position shows no wave duration trend. This is not surprising, as this position lies at the limit of wave activity, where material movement should be at a minimum.

The influence of storm duration may be more significant, in the formation of profiles on barrier beaches. Waves exceeding the pre-storm beach crest may result in overwashing, crest reduction and lee slope deformation. A second stage of profile development follows, during which the overwashed roll-back profile evolves, to reach a new dynamic equilibrium; this is influenced by storm duration, at a defined water level. The inclusion of a time-dependent variable, into the analysis of profile development, is complicated by the initial beach geometry. Similarly, a constant test duration of 3 hr, used in the present investigation, may be insufficient to allow a dynamic equilibrium overwash profile to form under sluicing overwash conditions; however, it should be adequate to describe a restrained or overtopped profile, when water level conditions result in small quantities of overwashing. The tests undertaken here were designed to examine the profile response, based upon a SWL coinciding with a tidal stand over 3 hr. An equilibrium profile was not achieved, within the test duration, for some of the overwashing conditions; this occurred usually when the barrier CSA was small, relative to the prevailing hydrodynamic conditions.

The shape of the beach material has been considered in earlier studies (Van der Meer, 1988), but no influence on dynamic stability was identified. This particular control was not examined in this study, although further investigations may be justified to examine whether this variable may be of importance.

Summary of variables influencing barrier crest evolution

On the basis of the model results, wave height, period and water level have been identified the most significant of the controlling variables. Overtopping was generally confined to a narrow range of conditions; the maximum crest elevation increase observed, in response to this process, was 1m. However, most of the elevation changes were within the range 0.1-0.6m. In contrast, overwashing resulted in a wide variety of crestal changes; these ranged from minor reductions, to the lowering of the crest below SWL under extreme conditions.

Environmental variables		**Range**
Wave height, at beach toe	H_s	1.1-4.1m
Wave period	T_m	7.4-10.9s
Wave length	L_m	85.5-185.5m
Number of waves	N	990-1460
Angle of wave approach	ψ	$0\text{-}20^{O}$
Water depth, at beach toe	h	7.9-9.3m
Constants used in the model test programme		
Spectral shape		JONSWAP
Mass density of water	ρ	1
Acceleration of gravity	g	$9.81 ms^{-1}$
Structural variables		
Barrier crest freeboard	R_c	-0.37 to 7.8m
Supra-tidal CSA	CSA	$0.1 - 433m^2$
SWL span	SWL_s	2.9 - 110m
Nominal shingle grain diameter	D_{50}	0.020m
Foreshore slope angle	Cot α	5-20
Mass density of shingle	ρ_s	2.65

7.5 DEVELOPMENT OF DIMENSIONLESS GROUPINGS AND FUNCTIONAL RELATIONSHIPS

Site specific investigations, based upon Hurst Spit, have provided detailed information on the conditions which were likely to result in overtopping and overwashing of the barrier. The extensive data set incorporated also a wide range of barrier geometries and prevailing hydrodynamic conditions; these, if analysed in a dimensionless form, could provide an analytical framework for wider applicability. The dimensionless grouping of the controlling variables enables the parametric analysis of data, in the absence of any scale; this permits the application of results across the range of conditions tested, to many other similar locations. This approach is particularly useful, when multivariable groups are to be analysed; it assumes that for any pseudo-equilibrium state, there exists a functional relationship relating a response function to the determining variables. The form of function is unknown initially, but must be in the form of a power product; there must also be a dimensional balance on both sides of the equation. The analysis undertaken (Section 7.4) has indicated that the functional relationship, for barrier beach crest evolution thresholds, should be in the form of the following function:

$$\text{barrier response} = f\ (H_s, T_m, D_{50}, R_c, SWL_s, B_a, g, \rho, D_w, \cot\alpha, \psi)$$

Dimensionless groupings were determined by reference to earlier studies (van der Meer, 1988; Powell, 1990); these were supplemented by the examination of key variables (identified on the basis of the model results and the field observations), which affect evolution of shingle barriers. The variables can be used in isolation, or in combination, to determine parametric functional groupings to describe barrier crest responses. Some of the hydrodynamic groupings used in the present investigation are already well established; however, these have been refined, to determine the relative importance of governing variables in the parameter groupings, (particularly in relation to shallow water breaking wave conditions).

Although the above form of analysis permits the results to be applied to a wider range of locations, caution should be exercised in extrapolation beyond the framework of the test programme. Nonetheless, the extensive range of barrier geometries tested

were examined using dimensionless variables, in addition to the base conditions established for Hurst Spit.

7.5.1 Dimensionless response descriptors

Barrier evolution is characterised by changes to: crest elevation and position; lee toe position and elevation; and the surface emergent CSA of the barrier. Previously-defined responses, between the crest and wave base (Powell, 1990), have also been confirmed within the present investigation (Section 7.6). Linear profile descriptors can be non-dimensionalised, by reference to either of the linear hydrodynamic variables H_s or L_m, in relation to the SWL datum. Additional profile descriptors used to define barrier beaches include: barrier crest position and elevation, described by length descriptors p_{bc} and h_{bc}; the lee toe position and elevation, described by p_{bb} and h_{bb}; and the barrier width at SWL (SWL_s). These descriptors are illustrated in Figure 7.6. Response parameters can be related to functional groupings of dimensionless parameters, provided that all of the governing variables are considered within the empirical framework.

Although parametric profile descriptors provide a useful means of describing post-storm crest elevation and position in relation to a fixed datum, relative change of the barrier crest cannot be detected using this method. In such an analysis, no consideration is taken of the pre-storm barrier geometry, within the parametric framework. Determination of the overwashing threshold, together with the onset of migration of the beach crest, is of importance to barrier beach management. As qualitative comparison of profile response suggests that the pre-storm barrier geometry is a significant variable, the response function to be described by parametric analysis must include variables which describe barrier evolution in terms of pre- and post-storm variables; it must relate these responses to the combined hydrodynamic and structure parameter groupings. Such groupings can be used to predict the threshold at which barrier geometry becomes a governing variable.

A dimensionless grouping is required to identify the extent and the thresholds of modification to the barrier, in terms of change in the barrier freeboard. A relative barrier crest elevation factor can be expressed, either by reference to the basement of

the barrier, or by reference to SWL (Figure 7.12). The former method provides no indication of water level, whilst the latter method gives no indication of overall barrier size; nonetheless, both have their advantages. Although reference to the barrier basement provides a better indication of total barrier volume (than by reference to SWL), this may be difficult to quantify in practical terms. For instance, Hurst Spit has a variable basement level, which reflects differential loading and the compression of the underlying (saltmarsh) geology: this is a complex function of time, geological conditions, sediment loading and the prevailing hydrodynamic setting. Many barriers migrate across mudflat and channel systems, resulting in a variable basement elevation.

The test results indicated that, following the initial adjustment of the foreshore fronting the barrier, the surface emergent barrier has most control on the (barrier) crest evolution (Section 7.5.3). The most logical relationship is between freeboard and SWL; this provides a clearly-defined elevation, unaffected by basement geology, which can be applied to any barrier configuration.

The relative barrier freeboard factor (Figure 7.12) is defined on the basis of the comparison of pre- and post-storm barrier freeboards referenced to SWL.

$$R_{Bc} = R_{c(post)}/R_{c(pre)}$$

This descriptor adopts the same datum as an earlier parametric framework (Powell, 1990). The main problem with the use of the relative freeboard reduction factor is that it takes no account of the dissipative characteristics of the lower foreshore; it is, therefore, dependant (to some extent) on the foreshore geometry below SWL. Whilst such conditions may influence the duration of the dynamic equilibrium profile evolution, they will not have a significant effect on the final profile. The relative barrier width (R_{Bw}) provides a measure of change in the barrier width at SWL and is defined by :

$$R_{Bw} = SWL_{s(post)}/SWL_{s(pre)}$$

The relative barrier cross section (R_{Ba}) identifies changes to the barrier, above SWL, and is described by:

$$R_{Ba} = B_{a(post)} / B_{a(pre)}$$

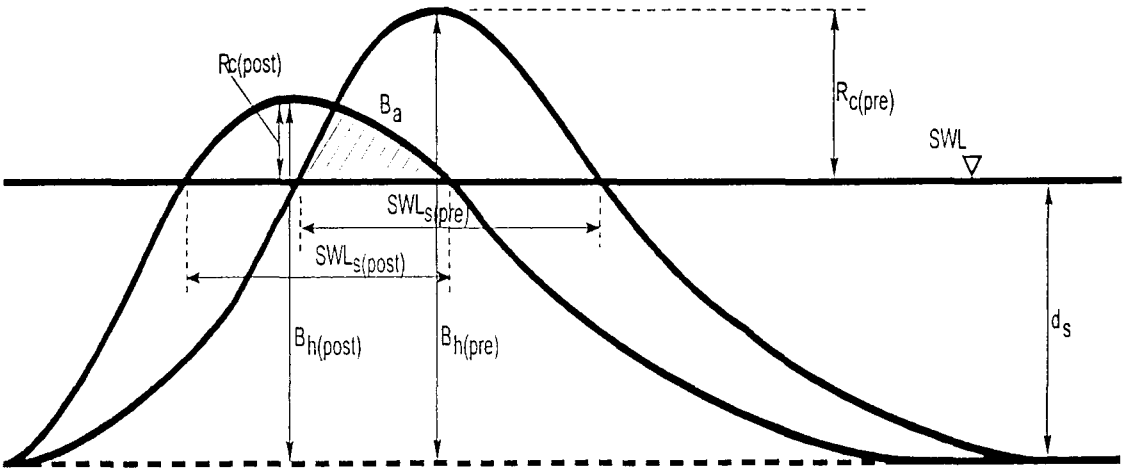

Figure 7.12 Parametric barrier evolution descriptors (for details see text)

7.5.2 Environmental variables

(a) Wave height

The wave height parameter used in previous analyses of shingle beach response is effectively a stability number, based upon the wave forces acting on a slope (Sigurdsson, 1962), derived from:

$$F=\rho g C D^2 H.$$

The parameter has been used in a variety of forms in stability-related formulae; it can be used to distinguish between dynamic and static structures. Earlier studies

(Powell,1990; and van der Meer, 1988) both used a derivative of this dimensionless wave height variable, relating sediment size to D_{50} grain size and shingle density:

$$H_s/\Delta D_{50}$$

Shingle beaches are characterised typically by this dimensionless parameter, lying within the range 15-500; this study covers the range 28-109. Whilst this grouping has been used previously in analytical work (Powell, 1990; and van der Meer, 1988), neither of the earlier investigators considered it to be a key grouping in the control of beach crest elevation. Whilst it may be useful to examine this grouping within the context of studies of barriers incorporating a range of sediment size and grading, this study considers only a single grain size grading.

The wave height parameter (h_c/H_s) provides a simple relationship between the response function and the wave height which is appropriate for the analysis of restrained beaches (Powell, *op. cit*). A more appropriate wave height parameter, for the assessment of barrier beaches, is considered within the context of structural variables (Section 7.5.3).

(b) Wave period

Wave steepness, (s), provides a measure of the combined deep water wave height and period, in a dimensionless form:

$$S = 2\pi H_s/gT_m^2$$

where:

$$L_m = gT_m^2/2\pi$$

Powell (1990) adopted a modified version of this expression, to provide the dimensionless steepness parameter grouping :

$$H_s/L_m$$

The influence of steepness, in shallow water conditions, is described by the surf similarity number (Irribarren, 1950). This descriptor relates the slope angle of the seabed to the wave steepness:

$$\xi = \tan\alpha / s^{(1/2)}$$

Battjes (1974) described breaker types in terms of this parameter, calling it the 'surf similarity parameter'; it is used to determine if, and how, the waves will break. Four types of breaking are discussed: surging; collapsing; plunging and spilling. The surf similarity parameter is related to a range of characteristic breaking criteria: breaker type; breaker height to depth ratio; the number of waves in the surf zone; the reflection coefficient; and the relative importance of set-up and run-up. Critical values are defined for the transition between each of the types of breaking. The parameter has been used by many authors to determine run-up and run-down (Gunbak, 1979; and Losada and Gimenez-Curto 1981). The main problem with the use of this parameter is, that dynamically-stable profiles are rapidly varying; these cannot be characterised by a single slope angle, and, consequently, its application to these studies is not appropriate.

(c) Time base

The duration of the tests was maintained constant during the experimental programme (in real-time). The dimensionless wave number (N) resulted in a range of time periods being tested, incorporating between 990-1460 waves: both are well above the time required (approx. 500 waves (Section 2.3)) to form a dynamic equilibrium profile (Powell, 1990). Either a dynamic equilibrium profile should form, or the overwashing threshold should be exceeded, within the test duration.

The influence of time is not considered further here, although it may be of significance for the formation of a dynamic equilibrium overwashed profile. Further work is required, to examine the influence of time on barrier profile evolution, following destruction of the pre-storm barrier crest by sluicing overwashing. Such a sequence of events may be a difficult process to model realistically, as: (a) changing water level appears to impact significantly on profile development; and (b) wave

models are usually run at discrete water levels. An approximation could be achieved, by testing through an incremental sequence of fixed water levels - on either side of the initial overwashing threshold.

Concluding remarks

The main environmental parameters are

Cot α	Foreshore slope angle
ψ	Incident wave angle, in relation to the beach normal
H_s/L_m	Wave steepness (wave period parameter)
$H_s/\Delta D_{50}$	Wave height parameter

7.5.3 Structure variables

The choice of dimensionless structure groupings for detailed examination is introduced here, by reference to the remaining group of dimensioned structure variables:

R_c	Barrier freeboard
B_a	Supra-tidal barrier cross section
SWL_s	SWL barrier span

Crest evolution trends are shown, as a function of freeboard and CSA, in Figure 7.13; these represent the whole of the test programme, but without reference to any hydrodynamic variables. Overtopping events which resulted in crest evolution were confined to a relatively narrow range of geometric configurations: on the basis of the analysis, freeboard and CSA are clearly very important. Linear structure variables were examined in parameter groupings, non-dimensionalised by H_s, to test for the most significant combination.

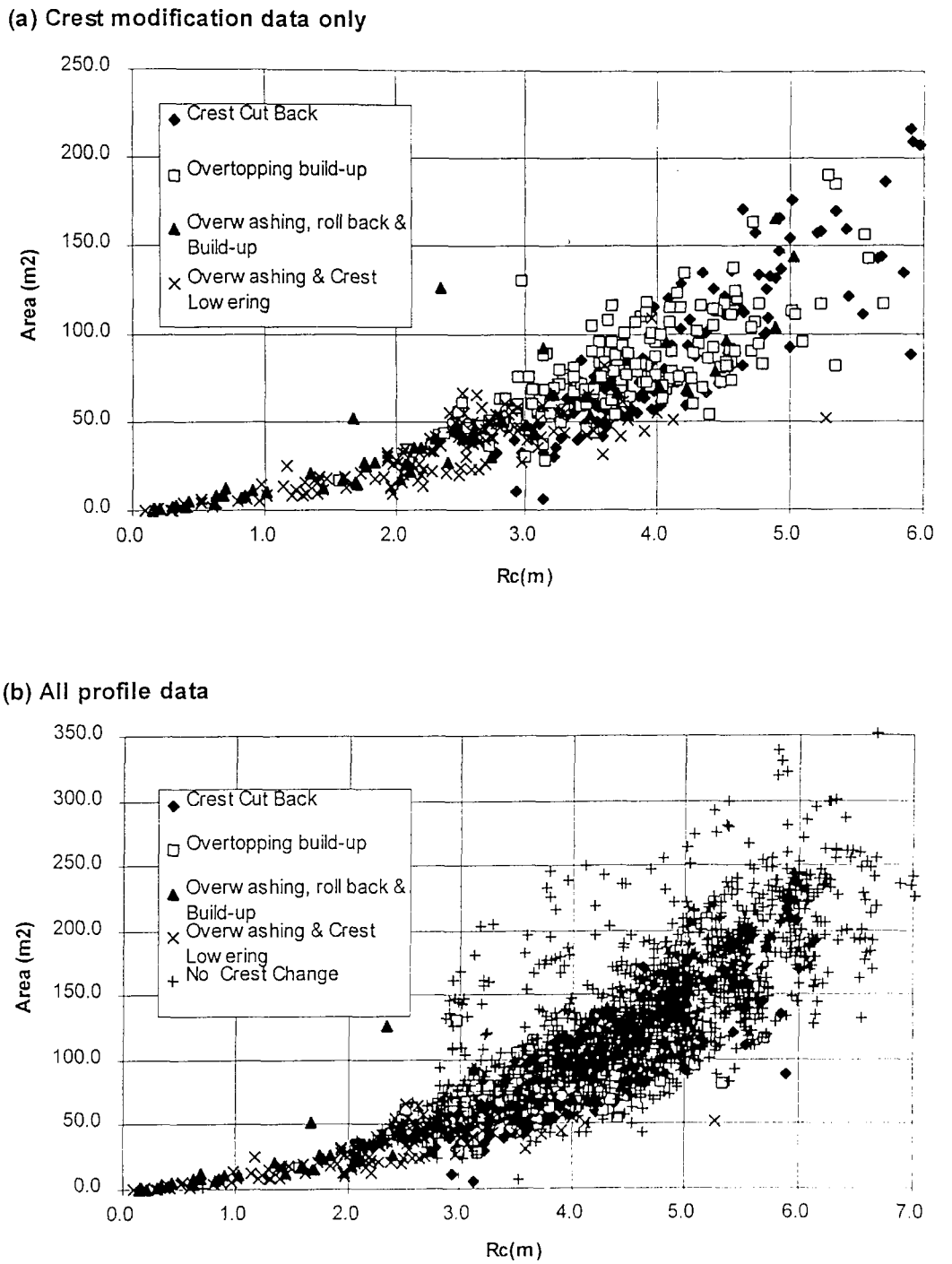

Figure 7.13 Barrier crest response as a function of freeboard and area: (a) crest modification data only; and (b) all profile data.

(a) Barrier freeboard

Dimensionless freeboard (R_c / H_s) is a commonly-used parameter, in studies of the wave overtopping of structures (Owen, 1980): it has a significant effect on the final form of the post-storm barrier profile. Figures 7.7-7.9 examine barrier response, as a function of freeboard and wave conditions: they demonstrate the significance of freeboard on overtopping in a qualitative manner. The barrier crest is sufficiently low to permit wave overtopping to occur (approx.) when R_c/H_s <1.1. The parameter can be used as an indicator for overtopping, but is insufficiently well-refined to examine whether overwashing will result. Although it is of limited value alone, freeboard is an important variable; as such it must form part of a final dimensionless structure grouping.

(b) Barrier width

The concept of a critical barrier width has been considered elsewhere by Jimenez and Sanchez-Arcilla (1998); whilst this may be appropriate for sand barriers, at a decadal time-scale, it does not appear to provide sufficient information to describe barrier inertia, in conjunction with the barrier height, for the short-term response of shingle barriers. This limitation may be due to the wider range of combinations of barrier shape on shingle barriers; these in turn are representative of the variable steepness of the upper barrier profile. A parameter grouping, comprising barrier span and freeboard, appears to be a logical combination to describe barrier shape or inertia. Such a combination is effective when the barrier approaches a triangular surface emergent form; this is often the case when the barrier is small. Such an approach does not always provide a good indication of the barrier shape, particularly when: (i) the crest is very low and the barrier very wide; (ii) the barrier is relatively high and narrow; or (iii) the barrier is both high and wide. The relationship between barrier span and freeboard is examined in Figure 7.14. A strong linear trend is shown for small barriers; this becomes much more widely scattered, as the barrier volume increases.

(a) Crest modification data only

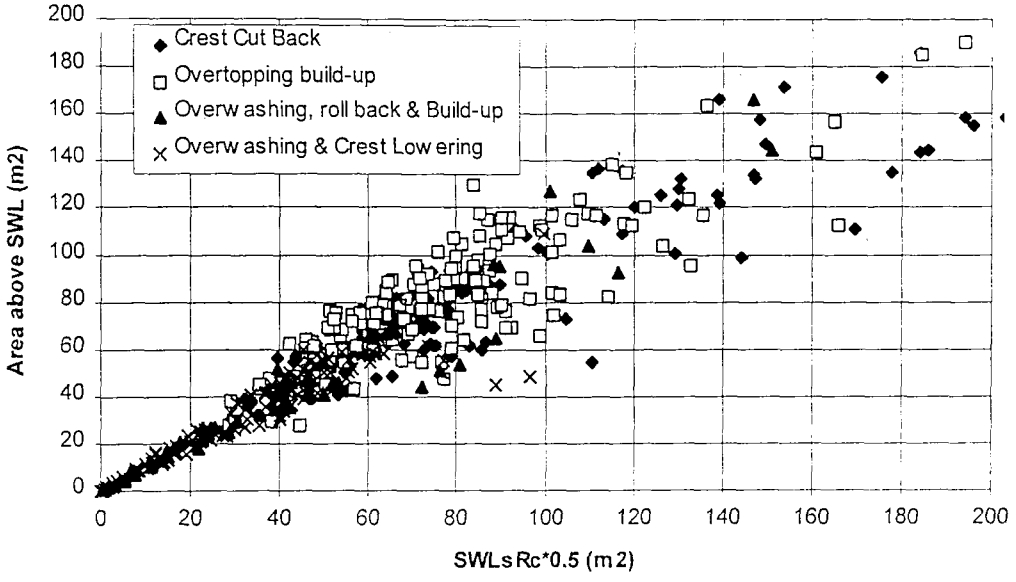

(b) All profile data

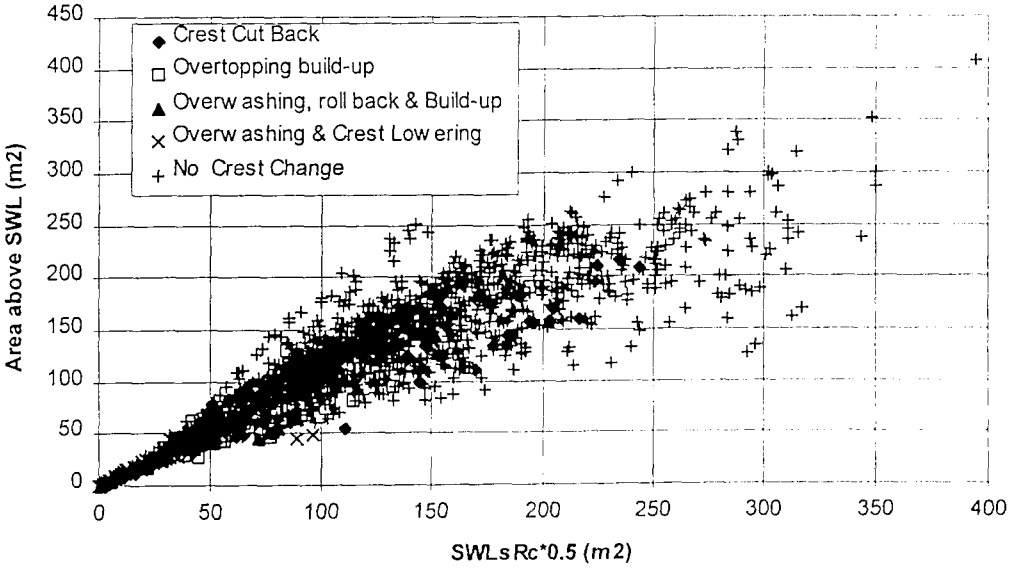

Figure 7.14 Barrier crest response as a function of freeboard and barrier span: (a) crest modification data only; and (b) all profile data.

(c) Supra-tidal barrier cross section

Whilst crest evolution is clearly linked with freeboard, the cross section of the barrier is also significant. The influence of the barrier cross section has been considered only rarely in studies of barrier evolution, although it has been suggested that sub-decadal evolution may be a function of CSA and barrier height (Orford *et al*, 1995). Barrier freeboard is often, although not necessarily, linked with barrier cross section; hence, these two variables must be considered separately, to analyse crest response. The barrier cross section determines the type of crest response under overtopping conditions. The effects of increasing surface emergent CSA, examined for common crest elevation, have indicated that a larger barrier is more likely to result in crest accretion than a narrow barrier, (under similar hydrodynamic conditions): smaller barriers are likely to undergo overwashing. CSA is an important variable, which must form part of a dimensionless parameter group; it can be used alone, but this provides no indication of the relative height or width of the barrier.

(d) Barrier inertia

The geometric relationship between barrier CSA, width and crest elevation has been investigated on the basis of field data, in the present study (Section 6.6) and, previously by Nicholls (1985). Barrier crest evolution responses are shown, without reference to hydrodynamic conditions, and for various combinations of freeboard, CSA, and barrier width, in Figures 7.13-7.14. Although the hydrodynamic conditions are not shown on the Figures, crest evolution data are concentrated where the barrier is low, and has a small volume. The overwashing threshold, for the most severe test conditions, occurred approx. when CSA<80m^2 and R_c<4m. The data were closely grouped about the mean line for events showing crest elevation change, particularly caused by overtopping; these became more widely scattered about the mean line trend for non-overtopping conditions. This pattern reflects the various evolutionary phases and movement between the various attractor states (Carter and Orford, 1993). The barrier is less likely to be affected by overtopping, when the volume is high: the scatter becomes less significant beyond the threshold limits of crest evolution, when profile response is no longer a function of barrier inertia. The barrier performs in the

same manner as a restrained beach under these latter circumstances, when the parametric framework (Powell, 1990) can be applied.

There is little to choose, in terms of predictive capability, between a combined freeboard and span parameter and a combined CSA freeboard parameter, although freeboard and CSA have provided a better description of shape: this combination is preferred for detailed analysis (see below). Barrier response was examined for common values of R_c and varying surface emergent CSA.

A barrier with a small CSA is found to be more likely to be subject to crest lowering by overwashing, than one with a larger CSA but with the same freeboard. Overwashing events do not necessarily result in crest lowering; this is essentially a function of CSA. The effects of a large CSA, but low freeboard, can result in overwashing and the formation of the crest at a higher level than the initial profile. However, for this to occur, the volume of the barrier must be sufficiently large to permit the dynamic equilibrium profile to form within the barrier. If the barrier is high and narrow, it will perform differently (in response to hydrodynamic forcing) than if it is wide and low. Freeboard can be used to determine the overtopping threshold, but CSA is found to be a better variable for the determination of overwashing. When combined, the two variables provide a barrier inertia grouping; this is a function of barrier freeboard and mass, which can describe evolution of the barrier in systematic manner. This relationship can be non-dimensionalised by wave height, to provide a proposed dimensionless barrier inertia parameter:

$$B_i = R_c B_a / H_s^3$$

This relationship is similar to the dimensioned barrier height and CSA relationship proposed for decadal evolution (Orford *et al*, 1995); it differs in terms of the absence of any reference to hydrodynamic variables; the use of mean sea level (as opposed to storm peak freeboard); and barrier height (as opposed to freeboard).

A significant proportion of the model tests resulted in non-overtopping conditions, with the dynamic equilibrium profile contained fully within the barrier. These are examined by reference to profile descriptor groupings (Powell, 1990) (see below).

7.6 ASSESSMENT OF THE VALIDITY OF PARAMETRIC RESPONSE DESCRIPTORS TO BARRIER BEACH RESPONSE.

Comparisons have been made (Figure 7.15) between the non-overtopping data obtained from the present study, with the functional relationship for the crest elevation parameter on restrained beaches (Powell, 1990). The latter expression equates with h_{bc}, when the beach evolution results in overtopping and accretion at the barrier crest. These earlier studies of shingle beach profile response arrived at conclusions which linked post-storm crest elevation with water level, wave steepness and significant wave height.

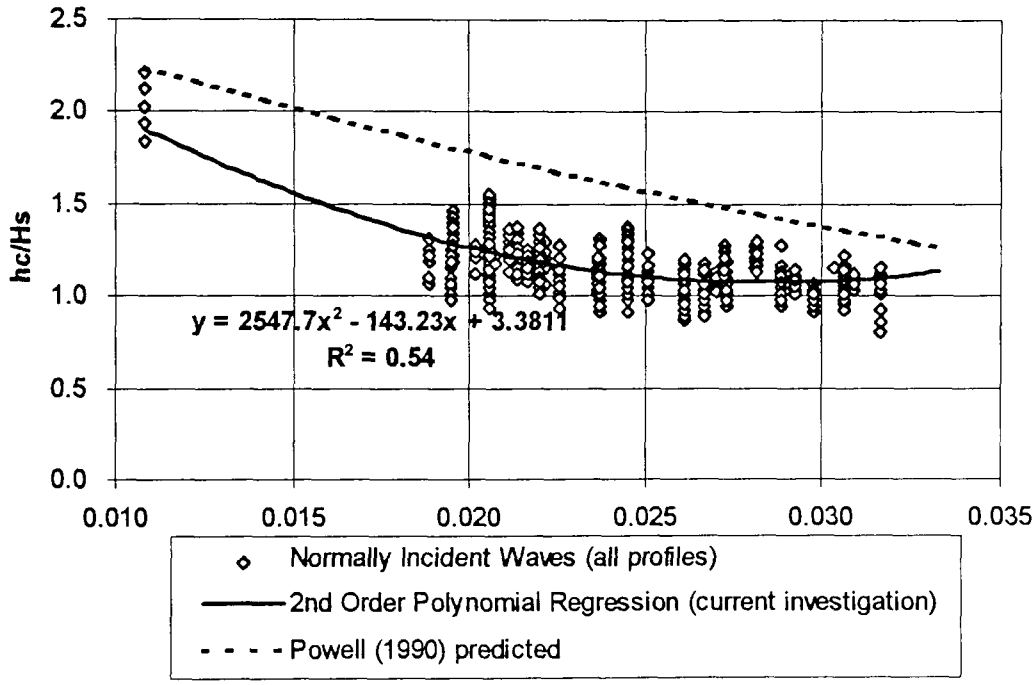

Figure 7.15 *h_c/H_s plotted against H_s/L_m (all profiles and no overtopping, with normally incident waves)*

The validity of the earlier parametric descriptors is examined now, for normally-incident breaking wave conditions measured at the toe of the beach: these relationships were supported previously, on the basis of only limited test results. The data here are found to be more widely scattered than the narrow range of confidence limits, suggested previously. Between 8-16 profiles were measured on each test section: crest elevations varied typically, by 0.3-0.7m, for each test section. This difference may

represent: spatial variations in the 3-dimensional model studies; the impacts of foreshore bathymetry; and breaking wave conditions. None of the aforementioned variables were considered originally, in the earlier flume studies. The data were reanalysed using mean values for each test (Figure 7.16); this demonstrates an improved correlation (R^2=0.67), but is still much more scattered than was suggested previously (Powell, 1990) (see Figure). The trend line for the regression analysis of the current study is lower than that predicted previously (Powell, *op.cit*); this suggests that crest elevation may form at a lower level. A revised prediction equation (equation 7.2) is provided for the conditions investigated as part of the present study; this utilises a similar 2nd order polynomial curve fitting function, to that used previously:

$$\frac{h_c}{H_s} = 3.2006 - 142.77\frac{H_s}{L_m} + 2367.6\frac{H_s}{L_m}^2 \qquad [7.2]$$

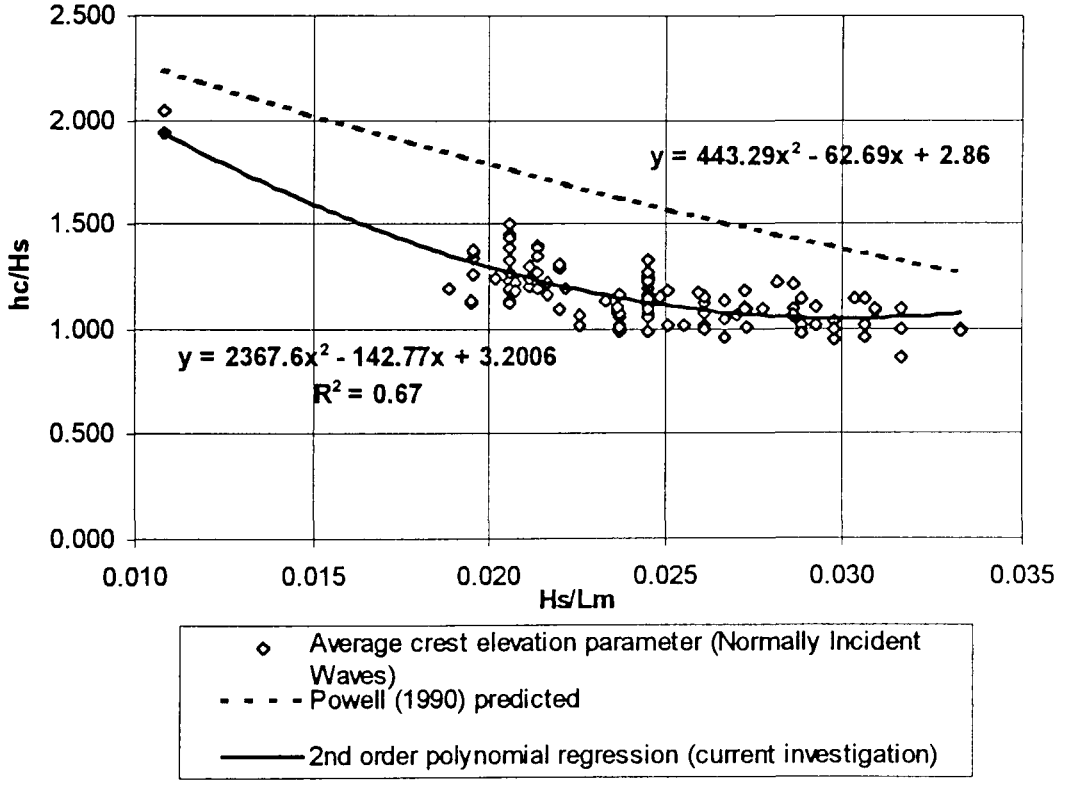

Figure 7.16 h_c/H_s plotted against H_s/L_m (average crest elevation and no overtopping, with normally-incident waves)

Figures 7.17-7.19 provide comparisons between data collected during the present study, with the theoretical relationships derived by Powell (*op.cit*) for p_c, p_t and h_t. These data provide further confirmation of the validity of the earlier analytical framework, but show similarly wide scatter; this may be due primarily to the prevailing breaking wave conditions, together with the localised spatial variability in wave conditions during the present investigation. The data for the step elevation parameter (Figure 7.18) have extended beyond the validity of the earlier investigations; this is the result of the combined influence of wave period and sediment grain size, as used here. A revised curve is shown for this descriptor; this is valid for the range of conditions tested within the context of the present study. The intersection of the 'best fit' curve for data from this study does not meet the predicted curve, with a smooth transition (see Figure).

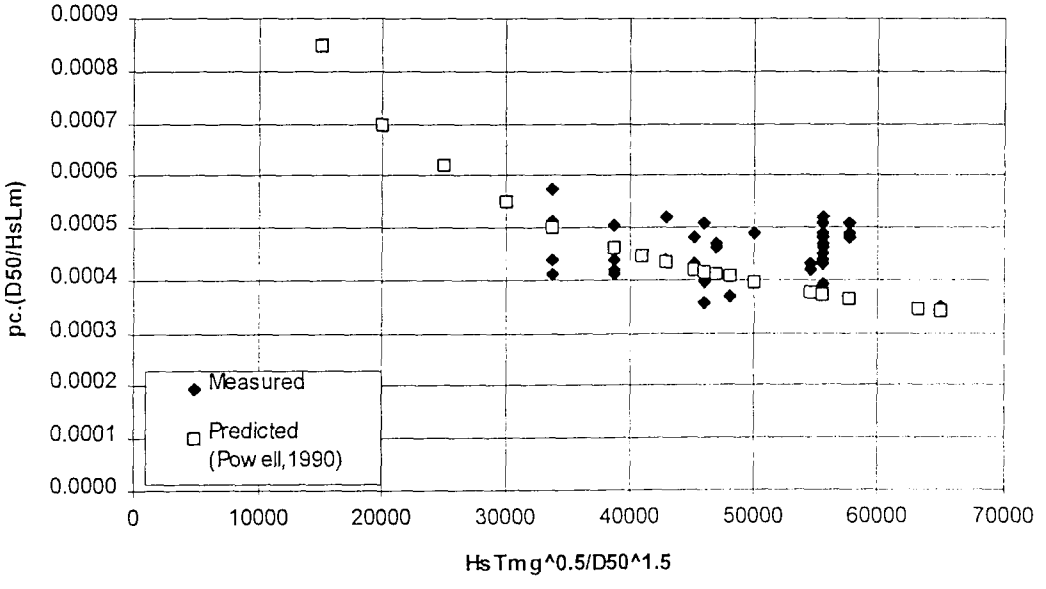

Figure 7.17 Comparison of the model results, with the predicted functional relationship (Powell, 1990) for crest position, under non-overtopping conditions.

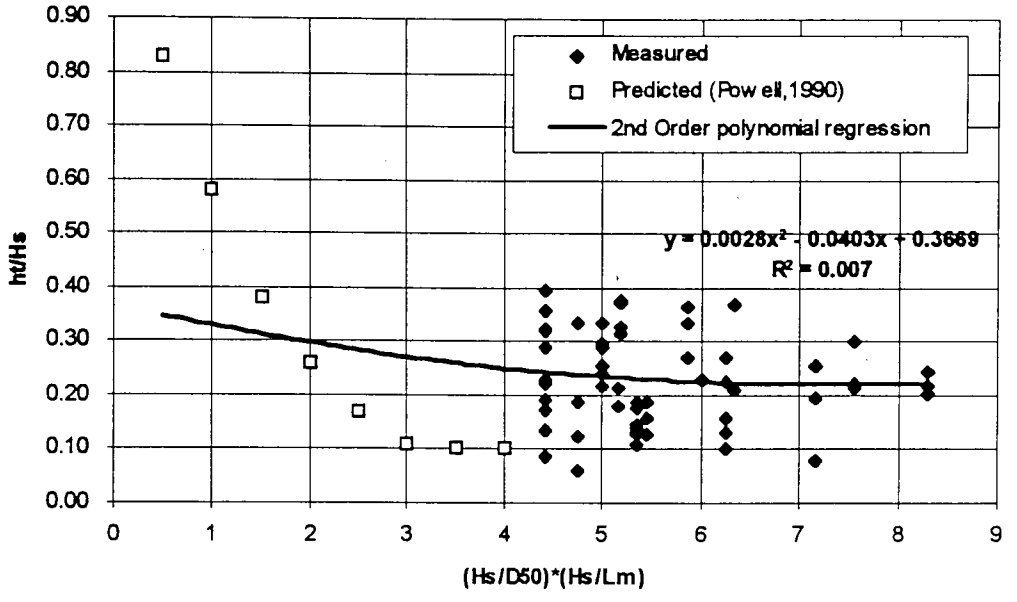

Figure 7.18 Comparison of the model results, with the predicted functional relationship (Powell, 1990) for step elevation, under non-overtopping conditions

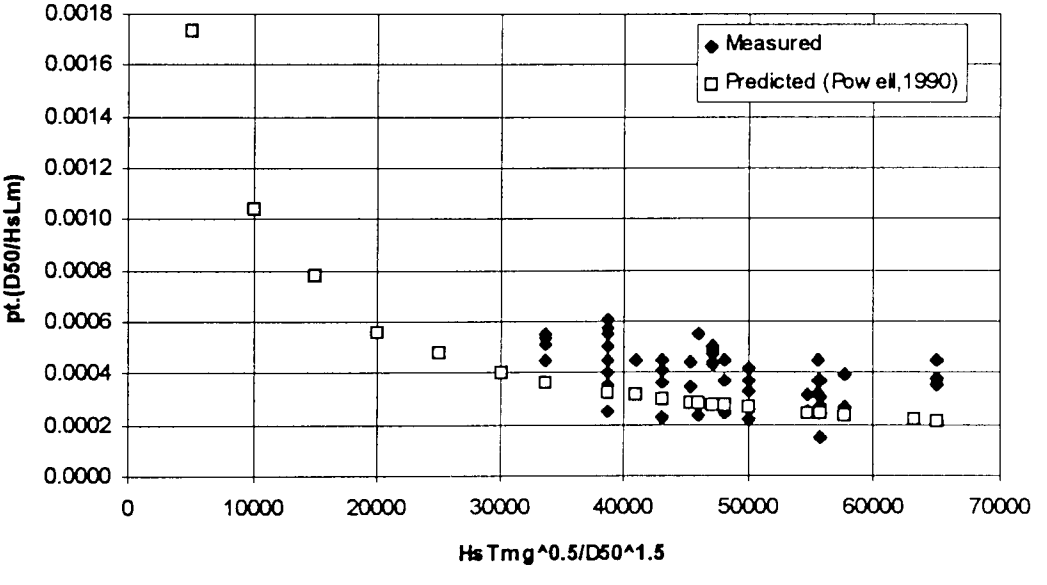

Figure 7.19 Comparison of the model results, with the predicted functional relationship (Powell, 1990) for step position, under non-overtopping conditions.

7.6.1 Oblique wave approach

The impacts of incident wave angle were examined on the crest elevation parameter, for the range 0-20^{O} (Figure 7.20). All the profile data are shown on the Figure, for non-overtopping conditions. The influence of incident wave angle is hidden largely, within the scatter of the data, for the range 0-20^{O}. The wave angle was measured in the model, between the wave paddle and the shoreline. The effects of wave transformations, between these locations, can modify further the angle of (wave) incidence on the beach; however, this was not measured accurately in the model. Video analysis of the incident wave angle suggests that long-crested waves, generated at angles between 0-15^{O} , generally approached the beach at an angle of less than 5^{O}; those generated at an angle of 20^{O}, approached at an angle of approximately 5-8^{O}. This observation explains the apparent lack of significance of wave angle, on the results for the range of offshore approach angles; likewise, more energy loss might be expected due to refraction.

The incident angle is complicated further by water depth, which is also variable: more refraction tended to occur at the lower water levels, although the difference is small over the range of water depths tested. The effects of wave angle are more marked for lower wave steepness. The longer period waves feel the bottom more rapidly than short period waves; likewise there is greater energy loss due to refraction.

The crest elevation should be reduced, theoretically, in response to increasing wave angle of approach (in relation to shore normal). A shortening of the profile parameters has been suggested, by $\sqrt{\cos\psi}$, under oblique wave attack (Van Hijum and Pilarcyzk, 1982); however, subsequent analysis (van der Meer,1988) has suggested a reduction factor of cos ψ. This latter functional relationship is plotted against measured data (Figure 7.20), for an offshore approach angle of 20^{O}; this overpredicts the crest elevation achieved. Regression analysis applied to the data obtained during the present investigation has identified a series of alternative relationships, for waves approaching from an angle of 20^{O}. Regrettably, this analysis does not appear to be statistically sound; the data were very scattered and a poor correlation (R^2=0.19) was observed.

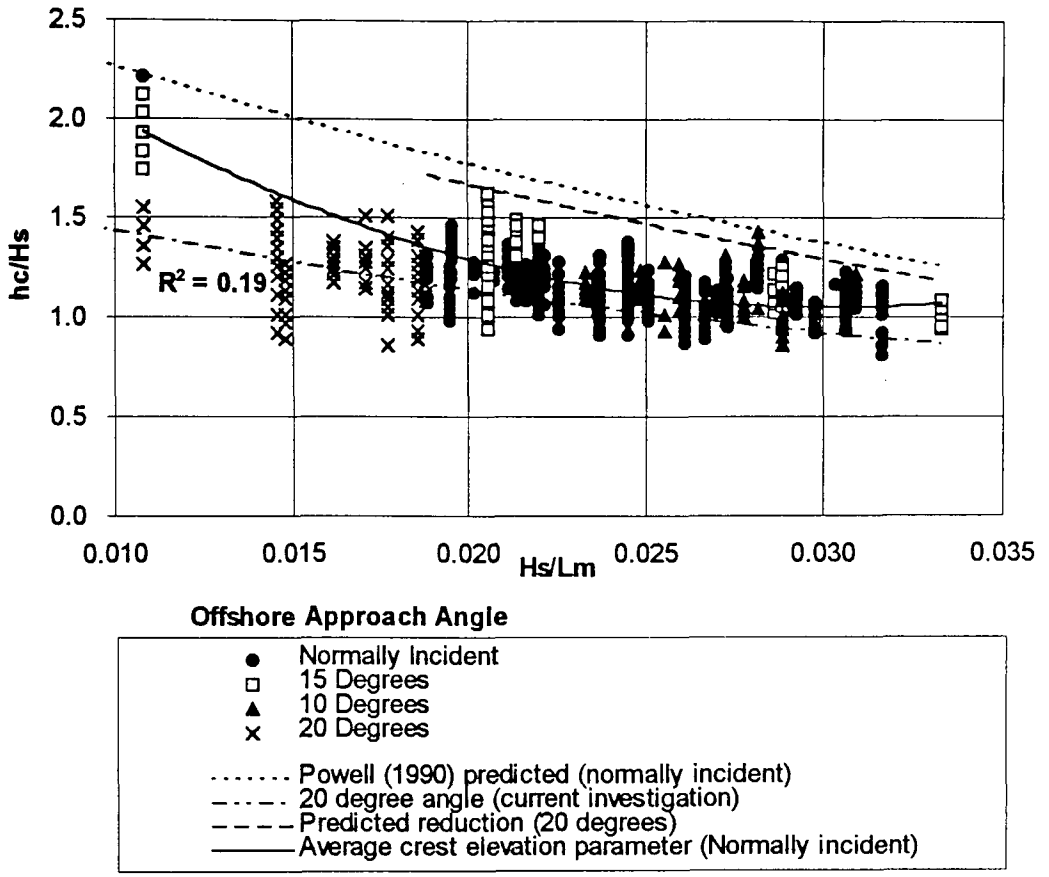

Figure 7.20 The influence of angle of wave approach on the crest elevation parameter (for details see text)

7.6.2 Overtopping and overwashing conditions

The combined data sets for overtopping and overwashing conditions were compared with the earlier theoretical relationship, for h_c/H_s, (Powell, 1990) and the revised relationship suggested for this study, for non-overtopping conditions (Figure 7.21). All the profile data are shown on the Figure. The results obtained for conditions resulting in overtopping and crest accretion followed the same pattern, as when the crest was not overtopped; the data generally fit well with the revised prediction curve, although they are more scattered. Further examination of some of the spurious data points, lying outside of the main trend, indicates that scatter may be a function of spatial variation of the pre-storm barrier geometry, or model end effects (Section 4.4.3(b)).

Averaged data sets are presented in Figure 7.22; this includes also non-overtopping data. Most of the data lying above the prediction curve lie close to the curve; this suggests that the peak run-up elevation is close to the maximum predicted previously (equation 7.2). However, most of the overwashing data lies below the prediction line; this in turn indicates overtopping and the formation of the post-storm crest at a lower level than predicted. The results imply that the functional relationship is invalid under overwashing conditions.

Although most of the data below the regression line represent overwashing conditions, there are also a significant number of data points within the overtopping category. These observations may represent conditions close to the overwashing threshold, where there was insufficient volume within the barrier to provide sediment for further crest accretion to occur - but insufficient energy for waves to overwash and reduce the crest elevation: this represents a narrow range of conditions. The two curves presented for the crest elevation parameter, for overtopping and non-overtopping conditions (Figure 7.22) follow similar trend lines. The small variation represents the limited and scattered overtopping data, at either end of the curve; this has, undoubtedly, skewed the derived relationship.

The profile response data (Figure 7.21) have demonstrated that overwashing events on barrier beaches generally lie outside of the limits of validity of the earlier parametric framework (Powell, 1990). The crest elevation response can be sub-divided into two sub-categories, under overwashing conditions (Section 7.2) (Figure 7.4). The crest will roll-back and reform, with a modified dynamic equilibrium profile, at a similar crest elevation to that suggested for restrained beaches (Section 7.6), if overwashing occurs and sufficient volume is available within the barrier. Alternatively, when the crest elevation was substantially lower, roll-back and crest elevation build-up occurred; this reflects either: (a) a lack of sediment availability; or (b) modification of a barrier which is associated with a low pre-storm freeboard. The pattern of crest elevation was not well described by the parametric framework, when the crest was lowered by overwashing: this suggests that an equilibrium profile is not established. This limitation may be a reflection of test duration, but is more likely to represent insufficient sediment available to allow the equilibrium profile to form. Factors other than those determined in earlier studies clearly influence barrier crest evolution. As the only other variables examined in the present investigation relate to barrier

geometry, the relationship must be a direct function, or derivative, of this particular control.

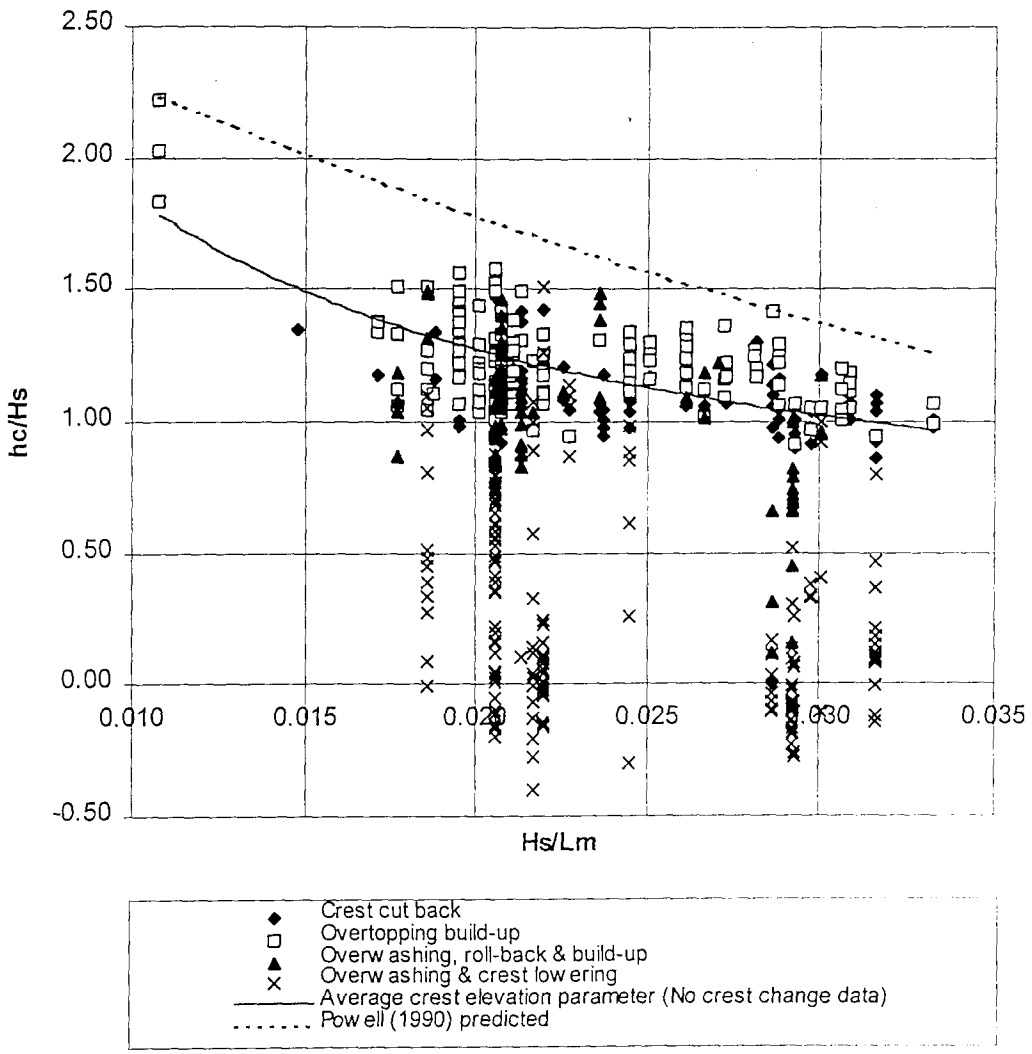

Figure 7.21 Variation in the crest elevation descriptor, in relation to overtopping and overwashing conditions (all data, see text)

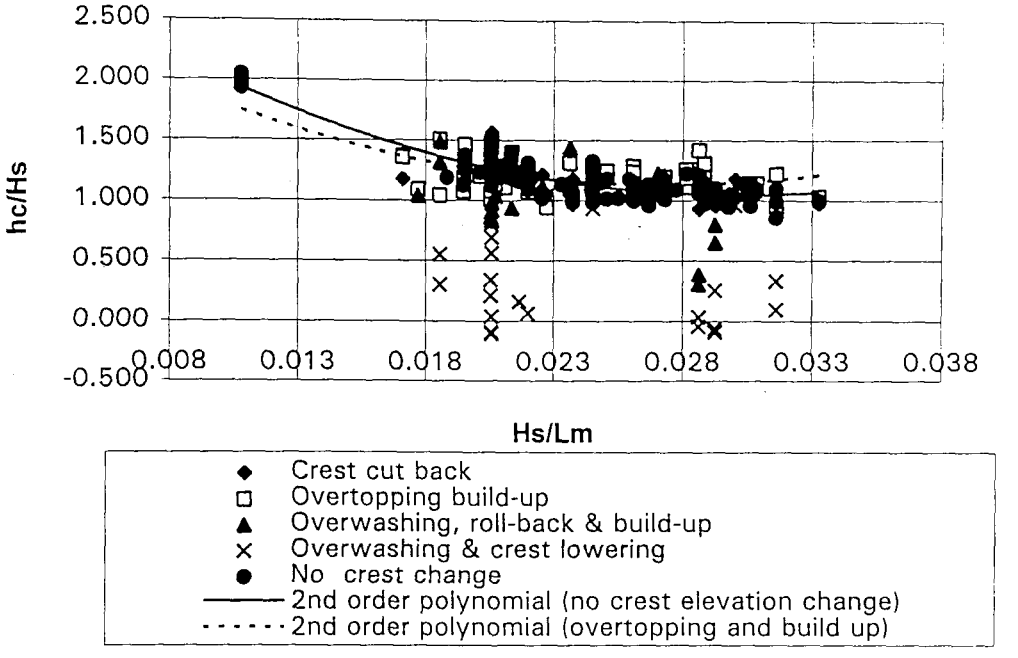

Figure 7.22 Variation in the crest elevation descriptor under overtopping and overwashing conditions (averages of the data sets)

7.6.3 Crest reduction, in response to foreshore widening

Crest elevation can be reduced also by non-overtopping conditions, resulting from widening of the active beach zone and cut-back of the profile into the barrier; this results in undermining and collapse of the barrier crest. Under these conditions, barrier response can be described by the earlier parametric framework (Powell, 1990). The dynamic equilibrium barrier crest elevation is a function of: pre-storm barrier elevation; the crest position parameter; and intersection of the natural angle of repose of the beach material, to landwards of the crest position, with the pre-storm barrier profile. Application of the parametric model (Powell, *op.cit*), modified by use of the revised predictors derived on the basis of results from the present study [equation 7.2], will predict the revised cut back elevation. Such an analysis takes into account the mass balance required to determine the equilibrium profile.

7.7 ASSESSMENT OF THE EFFECTS OF DIMENSIONLESS VARIABLES, ON BARRIER CREST RESPONSE

The impacts of parameter groupings which describe pre-storm barrier structure are examined here. A final list of functional relationships is produced; this provides response functions and determines threshold conditions for the barrier crest, under overtopping and overwashing conditions.

7.7.1 Relative exposure effects of barrier freeboard

The relative barrier elevation factor is a useful response function, for describing the type of crest response. The impacts of freeboard, on crest evolution, are examined in Figure 7.23; this shows R_c/H_s plotted against $R_{c(post)}/R_{c(pre)}$.

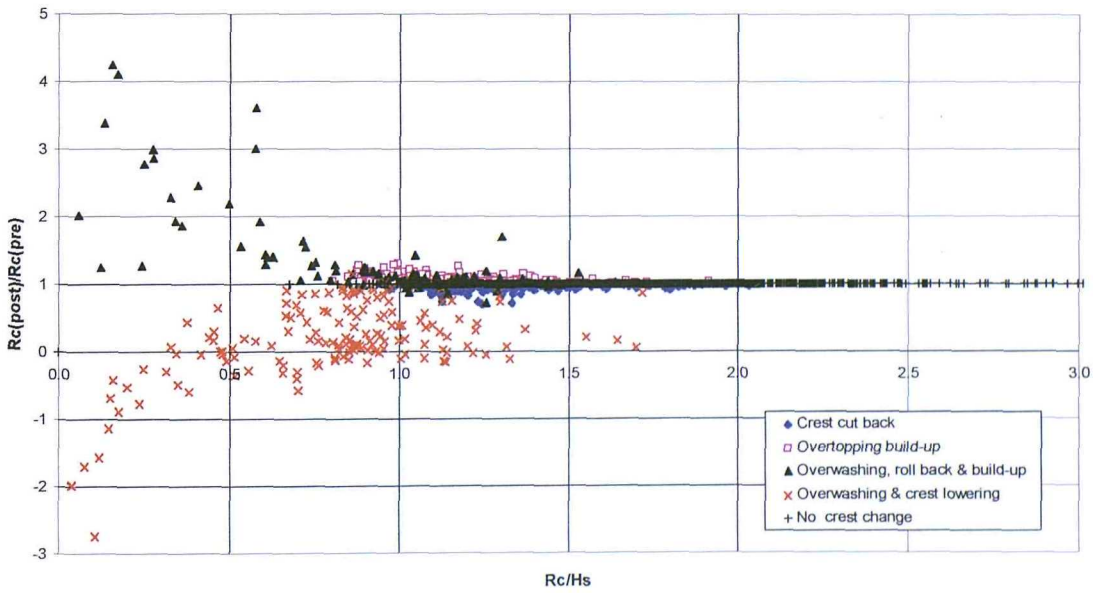

Figure 7.23 The influence of dimensionless freeboard, on the crest elevation change

Note: (a) measured data extends to Rc/Hs = 8

(b) all the crest elevation change data is shown on the Figure

A strong link has been observed between crest evolution, H_s and R_c (Figure 7.5). No change in the relative barrier elevation factor occurred, until the overtopping threshold was reached: at this point, the relative crest elevation ratio increased above 1. Further increases in wave energy resulted in the ratio falling below 1, indicating that the overwashing threshold had been passed. The relationship between overwashing and dimensionless freeboard was particularly strong for low crest elevations, but became less clear towards the overwashing threshold; this demonstrates the influence of the other variables on the relationship. These responses represent, partially, the range of barrier geometry examined in the test programme: the relationship between freeboard and barrier span follows a strong linear trend for the smaller barriers tested (R_c<1.8m); however, it is much more widely spread for the larger barriers, reflecting a wider range of relationships between the span and the freeboard.

An alternative dimensionless grouping was derived on the basis of the results of the present investigation; this relates freeboard to wave height and wave length: it is termed the critical freeboard factor (C_f)

$$C_f = \frac{R_c}{(H_s^2 L_m)^{1/3}} \qquad [7.3]$$

The influence of relative freeboard can be examined in relation to crest evolution. A barrier with its crest near to SWL is much more of a dissipative system, than one with a high crest (which is highly reflective). Taking this analysis to an extreme situation, water overlying the crest of a submerged barrier dampens the impact forces and attenuates the drag and lift forces on the shingle particles. This interpretation is illustrated most clearly in a dimensional plot of freeboard change, in m, against the dimensionless critical freeboard parameter (C_f) (Figure 7.24). The results obtained demonstrate that barriers with a low initial freeboard undergo less crestal elevation change, than those with a high initial freeboard, once the overwashing threshold has been reached.

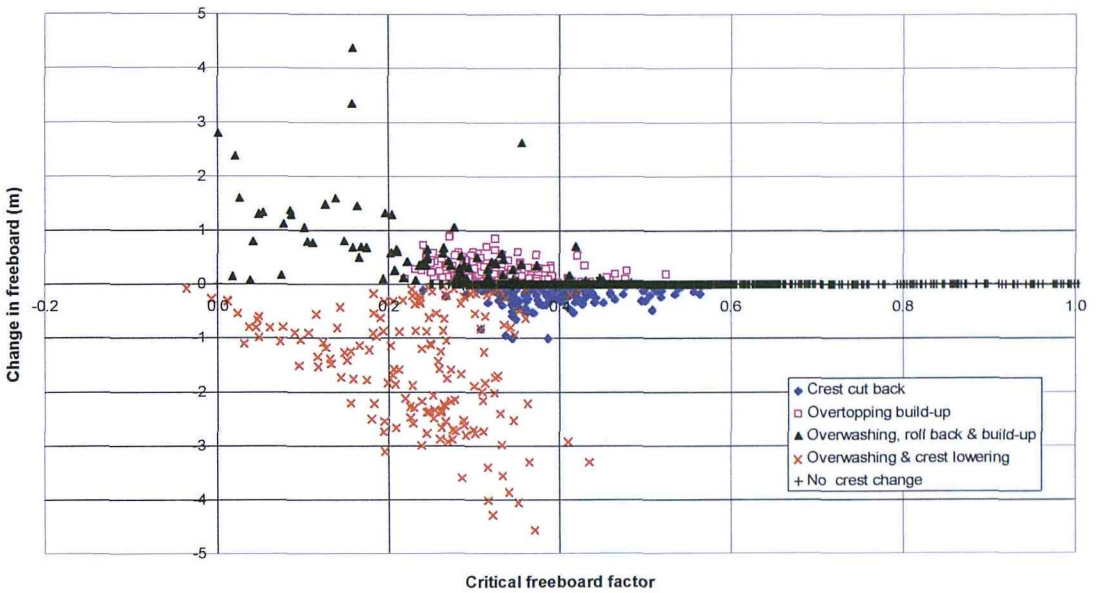

Figure 7.24 The relationship between crest reduction and a critical freeboard factor.

The crest elevation reductions reached a maximum of 4.5m, although changes at lower freeboards were much smaller (Figure 7.24); this demonstrates the significance of the overwashing threshold, on barrier evolution. The crest elevation may approach a limiting dynamic freeboard elevation under some overwashing conditions. A clear threshold was observed, at which no crest elevation changes occurred ($C_f > 0.53$).The data are grouped into a series of well-defined response bands (Figure 7.24). Overtopping predominated within the range $0.28 > C_f > 0.43$, with the data peaking at approximately $C_f = 0.31$, where a maximum crest elevation build up of 0.8m was observed. No overwashing was observed for $C_f < 0.43$, but overwashing always occurred for $C_f < 0.22$. A maximum elevation reduction of 1.1m was measured, resulting from foreshore widening; this response is not strictly a function of freeboard, but depends upon the barrier cross-sectional geometry. The critical freeboard factor can be presented as a dimensionless function, using the relative freeboard elevation factor (Figure 7.25). However, the trends discussed above are less easily observed using this method of presentation.

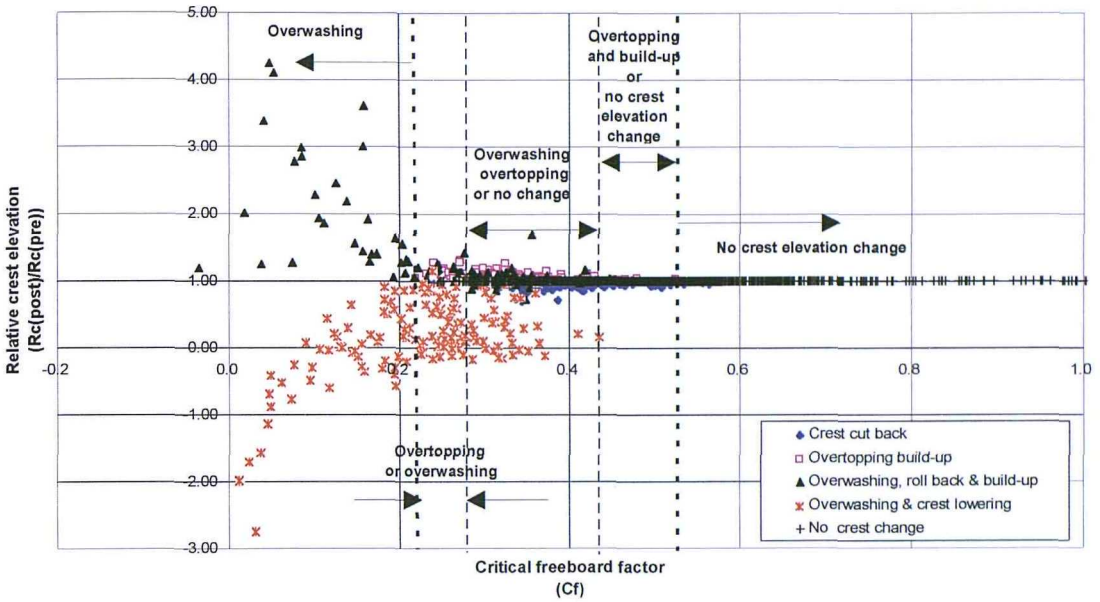

Figure 7.25 The relationship between relative crest elevation factor and a critical freeboard factor.

7.7.2 Effects of barrier inertia and wave steepness

The combined influence of freeboard (R_c) and surface emergent CSA are examined, by comparison of the dimensionless barrier inertia parameter B_i, with the wave steepness parameter H_s/L_m (Figure 7.26). The Figure shows data for all the profiles and all conditions below a barrier inertia parameter value of 50; additional results obtained for between 50-170 are not shown, but all data within this range were well above the overwashing threshold. There were two zones in the data presentation: (a) in which crest elevation was unaffected by wave action; and (b) where conditions always resulted in overwashing. Nonetheless, the data appear scattered around the overwashing threshold; this is a function, largely, of spatial variation of the barrier geometry.

The influence of any spatial variation in barrier geometry cannot be ignored, although the data do not permit a clear relationship to be determined between such variability and other controlling variables. The results can be expressed more usefully using

averaged barrier inertia data sets, for each test section; these have been combined with error bars, which reflect deviations of individual profiles; and provide an indication of the spatial spread of results (Figure 7.27). Presentation of the data in this manner provides a more tightly-controlled data set, which can be used to predict combinations of hydrodynamic and structure conditions, resulting in overwashing. Determination of the overwashing threshold was examined, using regression analysis of average dimensionless barrier inertia values, against wave steepness parameter values for each test condition. Confidence limits for the regression curves take into account the effects of spatial variation observed in the present investigation, but may not be representative of all shingle barriers. The data used were filtered from the whole overwashing data set to remove, selectively, those conditions which were well beyond the overwashing threshold. Curve fitting was carried out through the marginal data sets close to threshold conditions. Conditions resulting in overwashing can be predicted, on the basis of the functional relationship describing threshold conditions; this was determined by curve fitting of a power series regression.

$$\text{If} \quad \frac{R_c B_a}{H_s^3} < 0.0005\left(\frac{H_s}{L_m}\right)^{-2.55}, \qquad [7.4]$$

then overwashing will occur.

The R^2 value of 0.93 suggests that a valid relationship exists. Examination of the regression curve against the whole data set (Figure 7.26) provides further confidence in the functional relationship, but demonstrates a considerable spread of data above the regression curve. The regression curve provides a good indication of conditions where the overwashing threshold will (almost certainly) be exceeded. The upper bound confidence limits, fitted through the error band limits (Figure 7.27), should be used to predict the threshold at which overwashing is unlikely to occur. The upper limit confidence limit curve, for overwashing, is given by:

$$\frac{R_c B_a}{H_s^3} = 0.0006\left(\frac{H_s}{L_m}\right)^{-2.54} \qquad [7.5]$$

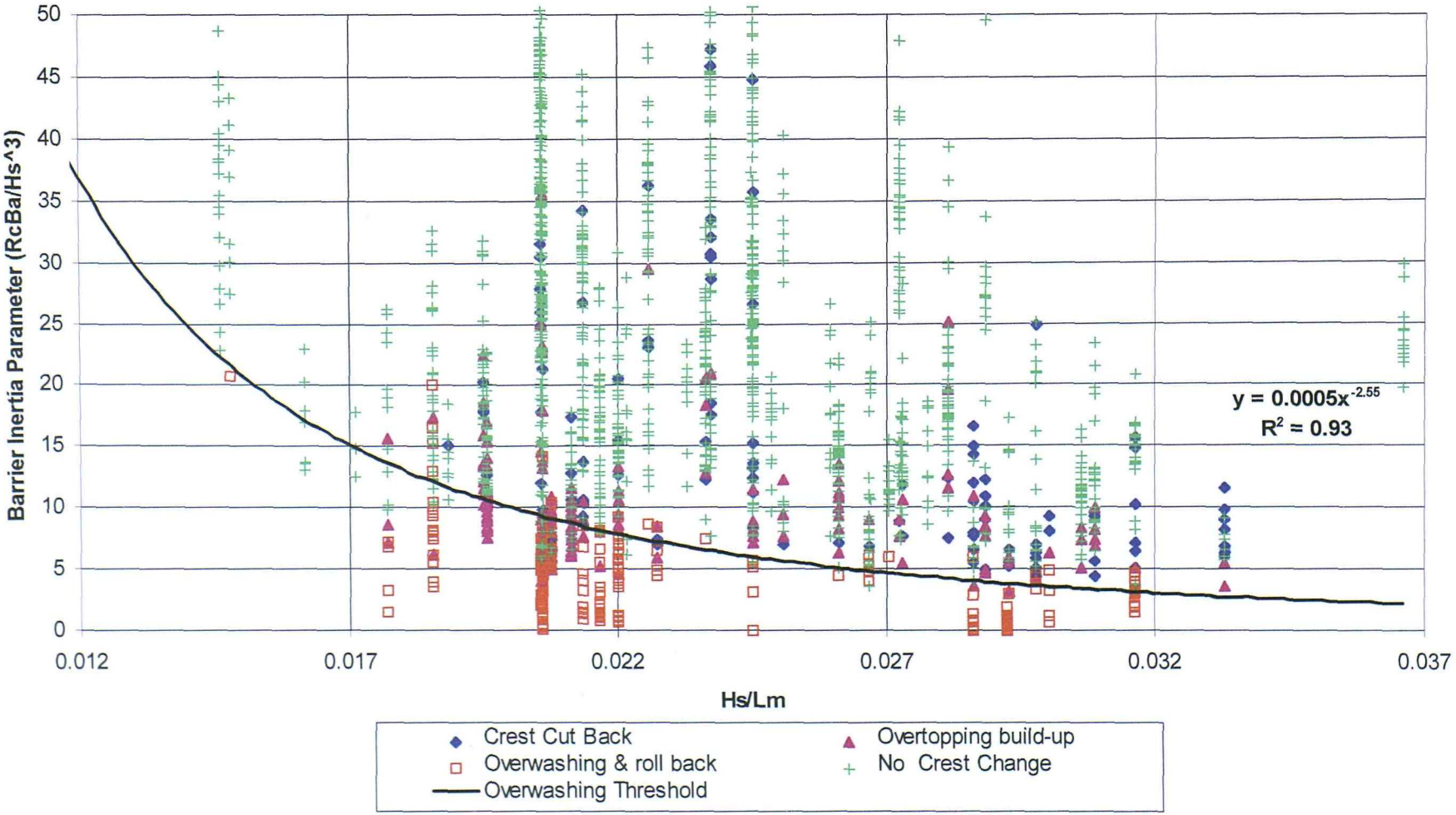

Figure 7.26 The barrier inertia parameter plotted against the steepness parameter - including all the data sets

Few non-overwashing data points occur below the 'best fit' curve; however, a swathe of overtopping data is observed in a narrow band immediately above the curve. Occasional spurious data points occurred above the prediction curve, but these reflect (largely), spatial variability in the barrier geometry. Scatter is more evident over the lower range of the wave steepness parameter (<0.018); this may be indicative of the effects of wave grouping, of a series of relatively long-period waves. Further data collection is necessary within this zone, to provide more confidence in the response of barrier beaches to swell conditions. Such conditions have been suggested to be the cause of overwashing on Chesil Beach (Babtie, 1997).

Although a swathe of data describing overtopping conditions lies immediately above the overwashing threshold curve (Figure 7.26), the barrier inertia parameter cannot be used in isolation to predict overtopping and build-up.This limitation is demonstrated by scattered data, well above the overwashing limits; these represent a large, but low, barrier. If the upper confidence limit of the overwashing threshold (determined by using the barrier inertia parameter) is not exceeded, the revised crest elevation parameter calculated for this study can be applied, to determine the elevation of the crest.

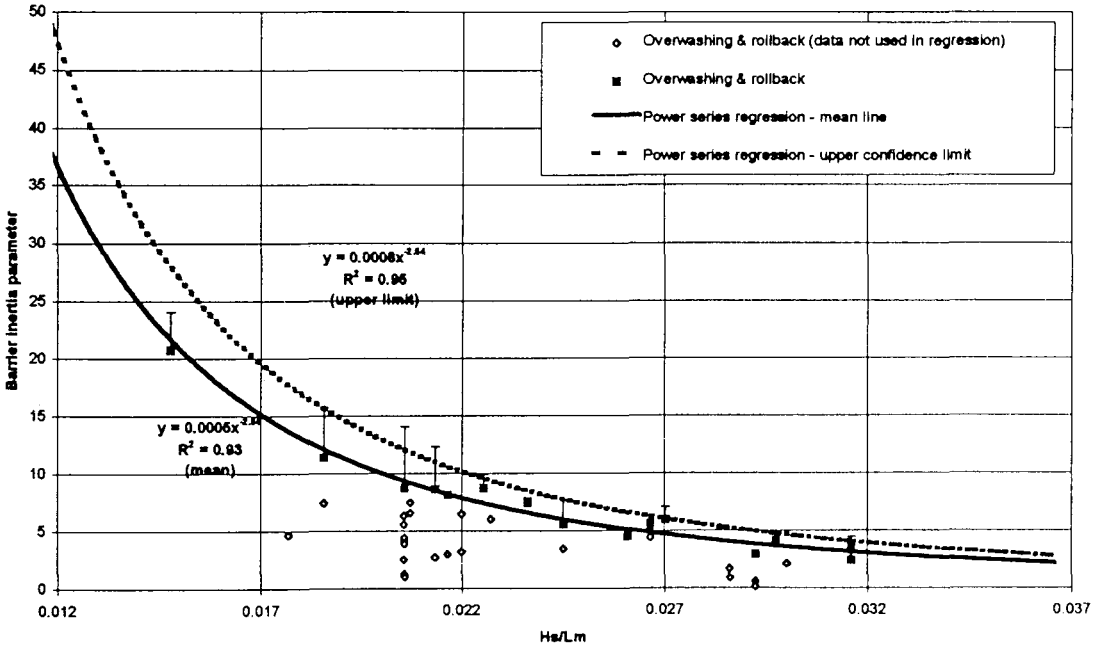

Figure 7.27 The determination of functional relationship between the barrier inertia parameter and steepness parameter, using averaged data sets.

Most data sets relate to a narrow range of geometric conditions, providing a high level of confidence in the results; others are more widespread, reflecting greater spatial variability. Error bands associated with each data set reflect this variability. It is suggested that the upper bound confidence limit is used for prediction purposes (Figure 7.27): this will provide a factor of safety, in order for the relationship to be used for management purposes. The range in validity of the relationship is controlled further, by the limitations of the test programme; these should be observed strictly, for predictive purposes.

Barrier elevation response factors suggest that hydrodynamic conditions become the more important governing variables (than barrier geometry) following the first overwashing event. However, initial changes to the crest elevation are likely to occur when the wave energy is at a maximum and the freeboard is at a minimum. This condition is indicated by higher relative barrier elevation changes, which tend to occur under conditions associated with higher overwashed pre-storm freeboards. Such a response indicates that a barrier with a large (overwashed) freeboard is likely to be lowered more, than one with an initially low freeboard. Once the overwashing threshold has been exceeded, the crest may evolve rapidly. Whilst structures with large grain size (i.e. >0.5m), such as dynamic reef breakwaters, are reported to undergo only erosion of the crest by overwashing (Ahrens, 1987), the barrier beach profile may undergo both erosion and accretion at the crest. Nevertheless, grain size is likely to become a significant variable, at some stage, between the conditions tested in this investigation ($H_s/\Delta D_{50}$= 15-500) and the studies of dynamic berm breakwaters; the latter typically have $H_s/\Delta D_{50}$= 6-20. The influence of this variable is recognised here, but is beyond the scope of the present investigation.

Shingle barriers undergo two alternative responses, following overwashing: (a) the beach may roll-back lowering the crest; or (b) the crest may roll-back and reform at a higher elevation than the pre-storm barrier. The response is strongly dependant upon the surface emergent CSA and the back barrier geometry. A two-stage conceptual model is proposed for overwashing. The beach will initially attempt to reach a dynamic equilibrium profile, as suggested by Powell (1990): if the critical barrier inertia (described by the upper confidence limit for equation 7.5) is exceeded, then the beach crest will be lowered by overwashing and a second-stage process begins. Provided that sufficient volume is available within the overwashed beach, the barrier

crest will reform farther to landwards; this may be to a higher elevation than the pre-storm profile, but generally to a lower elevation than predicted by the earlier functional relationship (Powell, 1990). The profile will form in a similar manner to the parametric model but the crest parameters will generally be unable to develop fully; this is due to the restricted barrier volume. The barrier may exceptionally reform to a profile described by these functional relationships; this will occur only when sufficient volume of material is made available, to reform a dynamic equilibrium profile. Such conditions may occur under the following circumstances: (a) where additional sediment is made available, in terms of longshore transport; (b) where pre-storm conditions are marginal to the overwashing threshold; or (c) as a result of spatial variability, when the overwashed profile forms as a result of outflanking of a topographic low, in a zone which is close to the overwashing threshold.

The predicted profile response and measured crest elevations are shown, for overwashing events when the barrier has subsequently reformed with the crest elevation above or at pre-test levels, in Figures 7.21 and 7.22. The influence of storm duration may be significant under these circumstances: a dynamic equilibrium profile may not have evolved fully by the end of the test, although the time required to achieve this (approximately 500 waves, (Powell, 1990)) was usually more than doubled in each of the tests. If the barrier volume is small, the dynamic equilibrium profile may not be able to reform and; a parabolic upwards convex curve will evolve at the crest; this is most likely to occur under sluicing overwash conditions, when the volume of water passing over the barrier is consistently high. The barrier will continue to roll-back until (storm) conditions recede, or energy is taken out by lengthening of the profile; this may also reflect the geometry and geology of the back barrier. In reality, tidal changes result in constantly changing water level and wave conditions: further, a fall in tidal elevation can influence the barrier evolution. Detailed examination of this process can be investigated properly, only under conditions which reflect changes in tidal elevation. The test sequence used in this study examined only the effects of incremental increases in water level on crest evolution, not incremental reductions.

A limited range of conditions were examined in the model tests, which resulted in the barrier forming with a negative freeboard; these indicate partial barrier breakdown and result only from extreme water level events, such as those at Hurst Spit on 17/12/89

(Section 6.5.2). Much of the sedimentary structure within the beach is destroyed by such events. The model test data have suggested that the crest will form, with a limiting maximum negative freeboard of -0.8m, under partial barrier breakdown; however, most of the data occurred in the range -0.3m to -0.5m. Overall the data should be viewed with some caution, due to the limited range of conditions tested. Insufficient data were available to confirm threshold conditions for this particular state of the system.

7.7.3 Limitations of the predictive framework

The data obtained generally fit the proposed dimensionless barrier inertia threshold parameter curve: there were only few apparently spurious data points, within a population of over 2200 data points. This encouraging grouping of the data is enhanced, when scattered individual data points are examined in isolation. The effects of spatial variability in the crest geometry are highlighted. The conditions which would not be expected to result in overwashing, when examined in a strictly 2-dimensional sense, show that this particular process has occurred on several occasions. Examination of the profiles which exhibited an unexpected response suggests that these are affected by the barrier geometry and response at adjacent profiles, where overwashing has occurred. Lateral expansion of washover throats can cause adjacent, and sometimes considerably higher, crest profiles to become outflanked.

Variability in the response function is dependant upon spatial variations in the pre-storm barrier geometry; the barrier geometry adjacent to the measured profile is also important in this respect. Analysis based upon the profiles, which lie within a zone of either irregular cross section or freeboard, may not represent the typical barrier response accurately. Instead, the processes are more likely to reflect the geometry of topographic lows, which may be subject to outflanking when overwashing occurs. If the barrier geometry is consistent spatially, with longshore transport in equilibrium along the whole of the barrier, spatial variability of the barrier crest response is less likely to occur. Further research could examine, usefully, strictly controlled 2-dimensional barrier response; this would refine the empirical framework, derived in the present investigation.

Numerical data were analysed, in conjunction with test observations and video analysis, from selected zones of interest. Possible explanations were sought for points scattered, on the graphical representation, beyond the normal limits of the threshold predictions. The most significant changes occurred when: either the barrier crest was narrow and waves extended the profile, cutting landwards across the test section; or where other features were located adjacent to the barrier (such as groynes or breakwaters) resulting in an 'end effect'. Despite the fact that long-crested waves were generated in the model, they did not always arrive at the test section with the same intensity. These differences are particularly noticeable when individual long-period waves break before reaching the structure, at some locations, they break at the structure in other locations.

The model results which identify overwashing or roll-back, do not differentiate between initial overwashing, resulting from profile widening, or from run-up exceeding the crest; this can be calculated using the profile predictor framework. Initial overwashing of the barrier resulted in many instances from foreshore widening and cut-back of the supratidal barrier, as opposed to run-up. It is not reasonable to assume that overwashing cannot occur, because the predicted run-up limit is below the barrier crest. In this case, the pre-storm profile and CSA is important. A large number of profiles were measured, which resulted in crest reduction due to widening of the profile - but no overtopping. This particular process does not seem to be recognised elsewhere, in the established literature; however, it is considered to be one of the most important processes leading to overwashing.

The pre-storm foreshore geometry may affect the rate of profile evolution. If the initial beach profile is similar to the dynamic equilibrium profile (for a particular storm), less profile evolution will be required to achieve the dynamic equilibrium profile. Most of the model tests were run on the 'as surveyed' profiles, or were stepped through a sequence (from low-to-high) of water levels; in this respect, the profiles were not dissimilar to the natural profiles. An artificially-graded beach, with a plain slope, may respond initially quite differently to a natural system. In such circumstances, the empirical framework proposed for the present investigation may not predict correctly, the barrier crest evolution.

7.8 CONCLUDING REMARKS

(a) Empirical calibration of the physical modelling methodology has demonstrated that such techniques are able to reproduce the response of a shingle barrier to extreme conditions, at an appropriate level, by direct comparison with measurements of full-scale storm events. A number of limitations to the modelling methodology have been identified, with recommendations being made for improvements to both the modelling methods and field validation techniques.

(b) The validity of a parametric framework (Powell, 1990) was examined, in 3-dimensional physical model studies. The results suggest that the beach crest will generally form at a lower level, than predicted previously, under breaking wave conditions. A revised crest elevation parameter equation has been proposed.

(c) Barrier evolution processes have been observed and described in the physical model studies; such evolution has been examined previously, primarily by inference of the processes (on the basis of examination of the change in sedimentary structure)(Orford *et al*, 1991a). The implications of overwashing, resulting from foreshore widening, are identified as an important process in barrier crest development; this is in addition to the run-up exceeding the barrier crest.

(d) An empirical framework has identified threshold conditions for overtopping and overwashing of Hurst Spit under extreme conditions; these can be related to extreme conditions identified in the numerical modelling phase of this study. A barrier crest evolution categorisation framework has been defined.

(e) A framework of governing variables has been examined, for shingle barrier crest evolution: overwashing of a shingle barrier is controlled primarily by wave height, wave steepness, freeboard and barrier CSA. A dimensionless barrier inertia parameter has been defined, which identifies the threshold conditions for overwashing of a shingle barrier. A predictive equation is presented, together with confidence limits and defined range of validity.

(f) The limits of validity of an earlier parametric framework (Powell, 1990) are examined, by reference to a two-stage conceptual model of barrier response.

(g) Overwashing will occur if the critical barrier inertia threshold is exceeded, when the parametric model is not valid for profile prediction. Overtopping or containment of the barrier crest will occur if the critical barrier threshold is not exceeded: the predictive model, as modified for breaking wave conditions, is valid under these conditions.

CHAPTER 8 DISCUSSION AND CONCLUSIONS - VALIDATION OF BARRIER BEACH CREST EVOLUTION FRAMEWORK

8.1 FIELD VALIDATION AT HURST SPIT

The predictive parametric framework for barrier crest evolution (developed in Chapter 7, on the basis of physical model test results) is examined here; it is tested by reference to field data gathered at Hurst Spit, both prior to and upon completion of the (1996) beach recharge scheme. Field data relating to extreme events (Section 6.5), are used to provide validation for the dimensionless barrier inertia, together with the critical freeboard parameters.

Profile response field data are illustrated, for the critical freeboard parameter, in Figure 8.1; this is comparable, directly, with Figure 7.25 (derived on the basis of the model data). Thresholds derived from the physical model studies are shown as dashed lines on the Figure.

Most of the field data results provide support for the suggested overwashing and overtopping thresholds, although several points lie outside of the expected response envelopes. Three data points lie to the left of the overwashing threshold on Figure 8.1 (within the 'overtopping and build-up' category). Closer examination of the survey data (e.g. Figure 6.19) shows that these particular profiles are located at the eastern end of Hurst Spit, where the wave climate prediction is most complicated (Section 5.4). Synthetic wave conditions were used to provide the data for the analysis of this event; these may be in error, due to the limitations of numerical modelling (see Section 5.4). Additionally, the same storm event resulted in longshore transport feeding this specific zone, due to the oblique wave attack; this is not represented by the predictive framework, which assumes longshore equilibrium. No overwashing data, collected in the field, are represented above the overwashing threshold (C_f=0.43). All of the remaining data lie within the appropriate response envelope, described by the relatively simple framework.

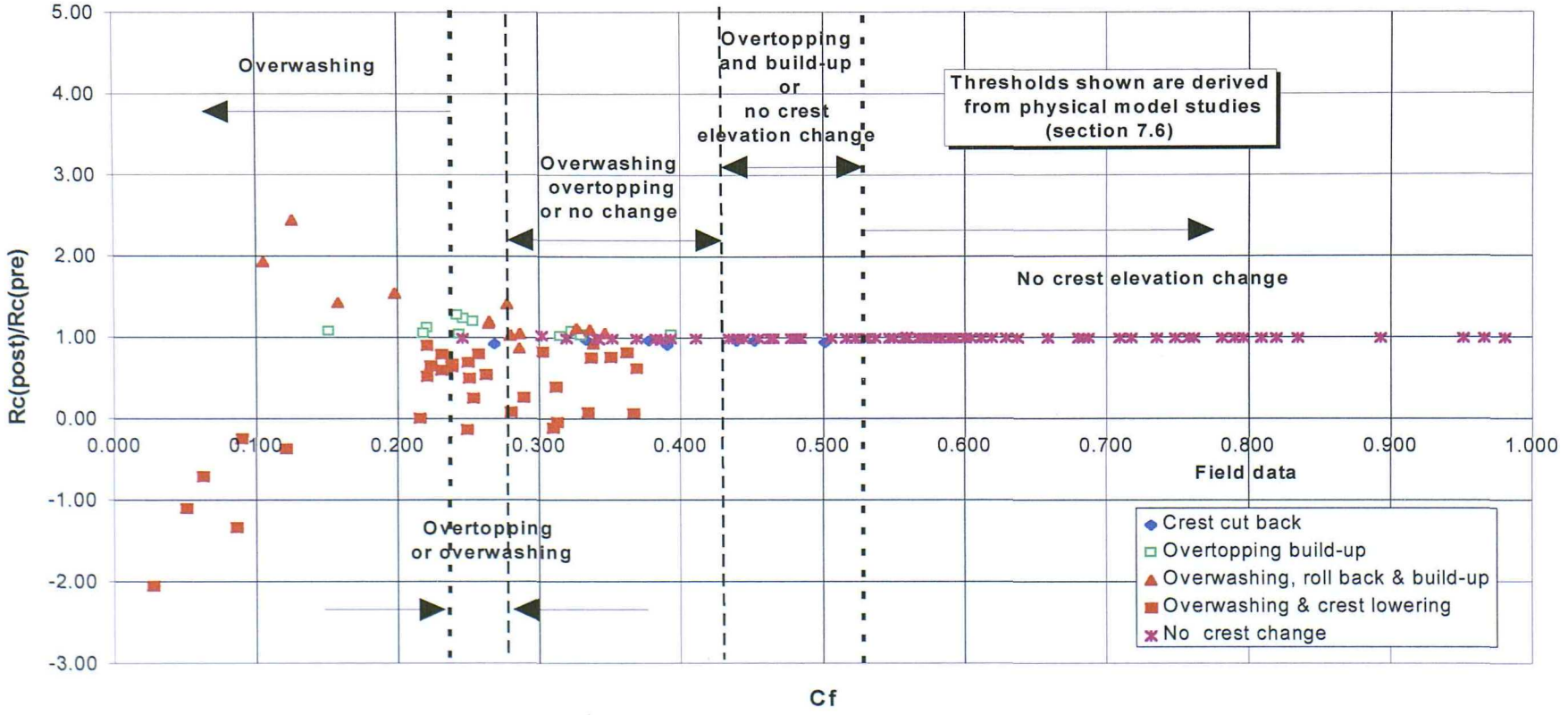

Figure 8.1 Application of the field data to the threshold conditions derived for the critical freeboard parameter on the basis of the physical model testing (see Section 7.7.1)

The field data are compared with the predicted barrier inertia threshold parameter in Figure 8.2; it is comparable directly with Figure 7.26, for the physical model data. The field data for the overwashing events are scattered, largely about the predicted overwashing threshold regression curve (within the predicted confidence limits). Regrettably, the model data are limited to within the range $H_s/L_m<0.032$; the regression curve has been extrapolated (to 0.055), to cover the full range of field data. The extrapolated curve may be defined inadequately over this range: predictions may be in error due to the lack of data. Notwithstanding this potential problem, the field data are largely consistent with the predicted response over the range of the extrapolated curve. Additional data are required to improve the validity of the framework; likewise, to define the overwashing threshold more precisely, for $H_s/L_m>0.032$.

Field data (for a steepness of 0.031) lie outside the confidence limits of the suggested overwashing threshold conditions (but are reasonably close to the threshold). Examination of the field data (Figure 6.40) suggests, also, that the conditions were close to the threshold for this particular event. Both cut-back and overwashing occurred within a narrow range of barrier inertia conditions: measured profiles demonstrate that the barrier crest had thinned to a narrow ridge, where cut-back occurred.

The events which were analysed upon completion of the (1996) Hurst Spit recharge scheme showed no crest evolution. All the data lay comfortably within the overwashing threshold limits (due to the relatively large recharge volume). The data presented are confined to barrier inertia parameter values of less than 50. Additional data were also recorded (to values as high as approx. 140); none of these exceed the threshold conditions.

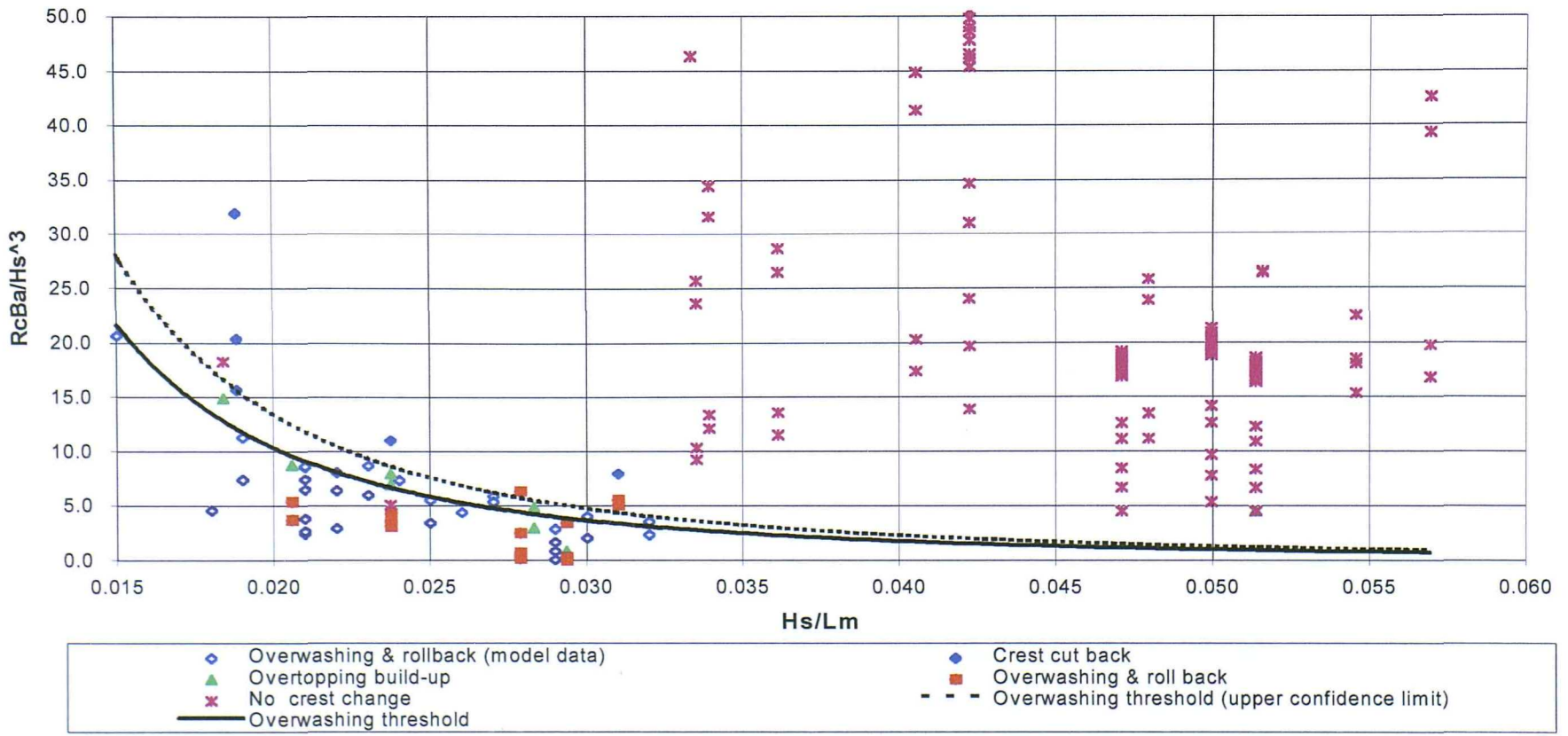

Figure 8.2 Application of the field data to the threshold conditions derived for the dimensionless barrier inertia parameter on the basis of physical model testing (see Section 7.7.2)

8.2 EFFECTS OF FORESHORE WIDENING ON BARRIER CREST DEVELOPMENT

The data presented in Chapters 6 and 7 demonstrate the validity of an earlier parametric framework (Powell, 1990), only when the dimensionless barrier inertia threshold has not been exceeded. This earlier method can be used to predict when crest lowering of the barrier will result from undermining and cut back, without overwashing: this has been identified as a significant barrier evolutionary process, both in the physical model (Section 7.2) and at full-scale in the field measurements (Section 6.5). The significance of the cut-back process is demonstrated, by examination of the cumulative effects of storms which lower the crest by undermining. This process is followed by storms, which can subsequently overwash the lowered profile; these are usually the result of events with long wave periods or at high water levels. Such combinations of events may result in migration and changes to the plan-shape position of the barrier. Applications of the predictive methods discussed, to predict overwashing conditions for beach management purposes, should include a sensitivity analysis of the various combinations of storm sequences. The earlier parametric model (Powell, 1990) and the critical barrier inertia threshold should be used together, on an iterative basis, to predict the influence of combinations of storm events.

8.3 USE OF THE PARAMETRIC FRAMEWORK, AT OTHER SITES

Although the proposed parametric framework appears to be valid for a range of conditions at Hurst Spit, it should be applied and tested at other sites under carefully-controlled measurement conditions. Beach profile measurements should identify all slope break points on the profile; they should include both typical profiles and topographic lows, in order to examine the possible influence of spatial variability in abrupt changes in (beach) crest elevation.

Tidal height measurements should be undertaken at, or very close to, the site: the effects of local wave set-up, or surges, can be missed when the tide gauge is located remotely from the site. Small errors in water level measurement can have significant

effects on the outcome of the results, in terms of: freeboard; surface emergent CSA; point of (wave) attack on the beach profile; and, finally, the breaking wave height.

The hydrodynamic conditions used in the empirical framework (T_m, H_s) are based upon measured wave conditions, in a 6-8m water depth. The influence of the foreshore slope angle, between the wave measurement point and the barrier, has not been examined within the present investigation; however, this may have a significant effect on the applicability of the formulae to some sites elsewhere.

Wave conditions derived for Hurst Spit have demonstrated significant longshore variability (Section 5.3), under extreme conditions, as a result of the complex offshore bathymetry. The location of the wave measurement points, together with wave transformation, should be considered carefully (either alongshore or cross-shore). Wave refraction models have been demonstrated by this study, to provide potentially misleading results; these are in terms of both angle and intensity of wave conditions, particularly where the bathymetry is complex (Section 5.3).

The range of geometric and hydrodynamic configurations, considered in the dimensionless testing framework, allows preliminary predictions to be made for other sites (subject to adherence to the measurement guidelines (outlined above)). A typical application of the predictive framework is illustrated in Figure 8.3; this shows predictions for the shingle barrier at Reculver (Kent). The data presented are based upon measured profiles and analysis of extremes for waves and water levels, provided by Canterbury City Council (Table 8.1).

Two contrasting barrier beach profiles are examined in the analysis, of variable CSA. The profile and hydrodynamic data presented (Figure 8.3) show an increasing likelihood of overwashing, with increasing severity of the prevailing storm conditions. The framework of the hydrodynamic conditions examined indicates that both the barrier profiles may be vulnerable to overwashing within the context of 1:100* year design storm. The profile with smaller cross section (BLS59) might be expected to undergo overwashing, during an event with a return period of 1 in 50 years. Qualitative assessment of the predictions, based upon the analysis of beach profile records (McFarland, *pers com*), suggest that the results are representative.

Return period (Yr)	SWL (mODN)	H_s (m)	T_m (s)
1	3.20	1.80	6.1
5	3.47	1.86	6.3
10	3.63	1.89	6.5
20	3.80	1.98	6.7
50	4.07	2.05	7.0
100	4.33	2.10	7.2
100*	4.74	2.15	7.5

Note: 100* refers to design conditions allowing for a factor of safety above the 100 yr return period event

Table 8.1 Design storm data for Reculver (data provided by Canterbury City Council).

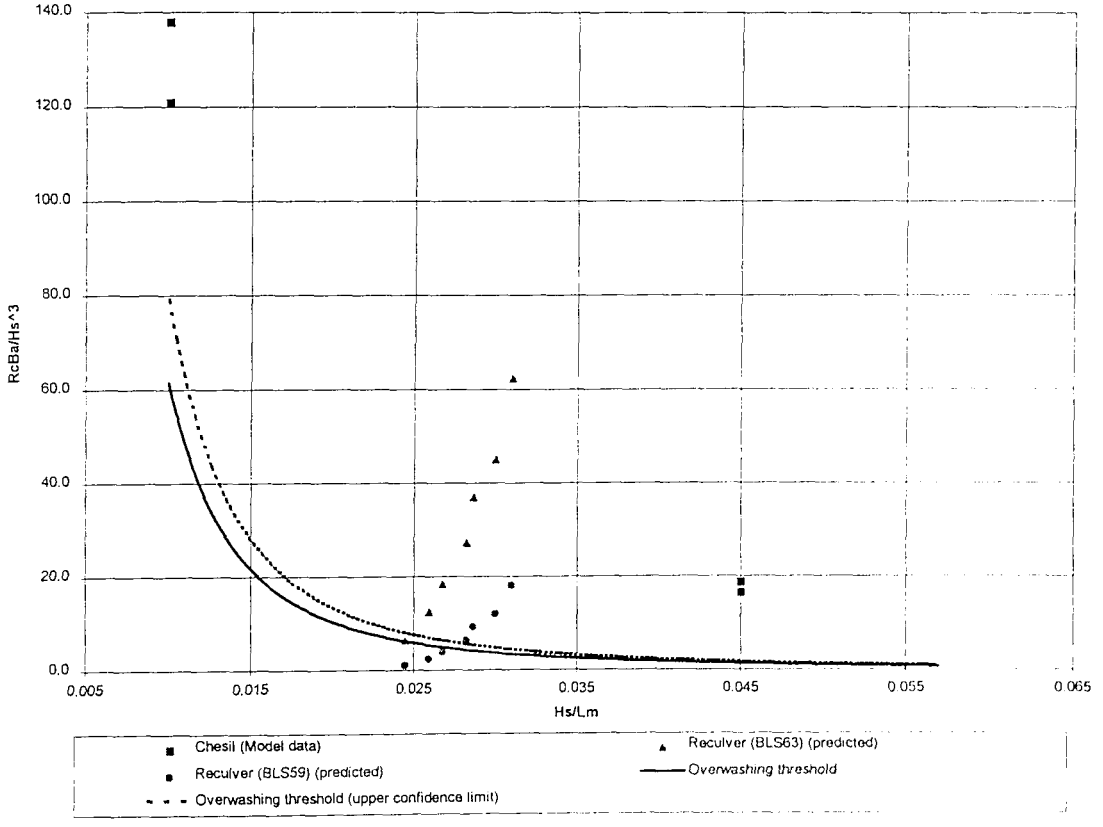

Figure 8.3 Application of threshold prediction, derived from physical model studies (Section 7.7.2), to Chesil Beach and Reculver (Northern Sea Wall) Shingle Bank

A further application of the parametric framework, based upon data relating to Chesil Beach (Dorset), is shown also in Figure 8.3. The data presented are derived from 2-dimensional physical model studies, designed to model water percolation through Chesil Beach (Hydraulics Research, 1984). Waves were measured in a water depth of approximately 14m; the beach profiles were based upon surveys undertaken of Chesil Beach. The conditions, for a wave steepness of 0.01 (H_s=3.6m; T_m=15.5s), resulted in occasional waves reaching the crest of the barrier (at a level of 14.7m ODN), but no overwashing; this suggests that conditions were close to the overwashing threshold, but did not exceed it. The data presented lie outside of the range of conditions examined within the present investigation. However, extrapolation of the predictive curve to a steepness of 0.01 suggests that the proposed relationship is also reasonable, for the above conditions. The curve becomes very steep over the lower range of wave steepness (<0.015); any inherent measurement errors may be accentuated by this trend. Although this interpretation of the data suggests that the results of the present investigation may be valid for lower wave steepnesses, this should be investigated further. No overwashing occurred for the other data set, shown for a wave steepness of 0.045 (H_s=7.0m; T_m=10.0s); this is consistent with the predicted response.

8.4 LIMITATIONS OF THE EXPERIMENTAL TEST PROGRAMME

Nearshore synthetic wave data have proven to be unreliable, in terms of both: (a) incident wave angle; and (b) the intensity of the conditions at the shoreline - in an area of complex offshore bathymetry, adjacent to Hurst Spit. Although the refraction modelling techniques appear to be valid in less complex areas, developments of modelling techniques are needed to improve predictions within such areas of complex bathymetry. The on-going programme of wave data collection (Section 4.2.4) should assist in the calibration of the numerical models (Chapter 5), providing better absolute estimates of nearshore wave conditions off Hurst Spit.

Physical modelling has been carried out in accordance with the scaling laws discussed in Section 4.4 which, whilst widely used, can provide only an approximation of real conditions; thus, some scaling effects are inevitable. Although the field data have demonstrated a good correlation between the model and full-scale performance, larger-scale testing would provide more confidence in the model results. A number of

local site-specific effects could not be reproduced in the model, particularly those relating to the basement geometry and geology of the cohesive sediments which lie beneath Hurst Spit; however, these are typical also of many other similar sites (Carter and Orford, 1993).

Although wave conditions were measured close to the shoreline, thereby minimising the effects of nearshore bathymetry on wave conditions, nearshore transformations may vary from site to site; these may influence sediment dynamic processes affecting the barrier.

Studies have been confined to the examination of a single wave energy spectral shape (JONSWAP) in the physical model studies (Figure 4.16), but the field data have demonstrated that local bi-modal spectra may occur (Figure 6.9). The influence of two clearly defined spectral peaks results in waves of two distinct period groupings, which are unlikely to be modelled well, by the empirical relationships discussed (Section 7.7). Although earlier model studies (van der Meer, 1988; Powell, 1990) have not identified an influence of spectral shape on profile development, these have been confined to the examination of single peaked-spectra. A long period wave component, in a bi-modal sea, may have a significant influence on the profile response. Analysis of wave data collected in the field, which is often confined to the determination of H_s and T_m, may be insufficient to describe the profile response of shingle barriers under such conditions. The frequency and magnitude of long-period waves within a storm is, perhaps, the most significant variable: observations obtained from model tests have demonstrated that relatively few long period individual waves are needed, to modify the barrier crest.

8.5 CONCLUSIONS

The overwashing threshold conditions for shingle barrier beaches can be predicted, using the dimensionless functional relationship derived for the barrier inertia and wave steepness parameters, within the range of conditions tested.

Overwashing will occur when:

$$\frac{R_c B_a}{H_s^3} < 0.0005\left(\frac{H_s}{L_m}\right)^{-2.55} \qquad [7.4]$$

The 95% upper confidence limits for the overwashing threshold are given by:

$$\frac{R_c B_a}{H_s^3} = 0.0006\left(\frac{H_s}{L_m}\right)^{-2.54} \qquad [7.5]$$

Field data gathered prior to, and upon completion of, the beach recharge (1996) at Hurst Spit provides limited confirmation of the validity of the relationship, (for a limited range of conditions).

The limits of validity of an earlier parametric framework (Powell, 1990) can be defined using the barrier inertia threshold parameter (as described above). Overtopping conditions and the crest elevation response of a shingle barrier can be described by these earlier functional groupings, when the hydrodynamic conditions do not exceed the critical barrier inertia threshold.

A revised functional relationship is proposed, for the crest elevation parameter:

$$\frac{h_c}{H_s} = 3.2006 - 142.77\frac{H_s}{L_m} + 2367.6\frac{H_s^{\,2}}{L_m} \qquad [7.2]$$

The significance of foreshore widening and beach crest undermining is highlighted as an important process, in the development of barrier overwashing conditions.

8.6 FUTURE RESEARCH

Validation and extension of the empirical framework

Further field validation should be carried out, to refine and validate the barrier inertia overwashing threshold parameter over a wide range of conditions, at a number of coastal locations. On-going data collection at Hurst Spit, as part of the NFDC coastal monitoring programme (Section 4.2), will provide appropriate site-specific data to assist in this particular research objective. The long-term deployment of a waverider buoy and tide gauge at the site will provide hydrodynamic input to this programme (Section 4.2.4). These data will also provide the opportunity to refine the analysis and understanding of extreme local wave and water level analysis.

The framework identified by the model studies and field data provides a first approximation for the prediction of overwashing threshold conditions; this can be refined further, by the selective testing of conditions close to the overwashing threshold, under more closely-controlled conditions, with minimal spatial variability (of the barrier profile). Near prototype-scale random wave flume studies would: (a) aid the development of confidence in the modelling methodology; (b) minimise the scale effects; and (c) provide confirmation of the functional relationships, over the lower part of the barrier profile (these cannot be measured, practicably, in the field). The influence of shingle grading on barrier crest evolution should also be examined.

The sensitivity of the barrier profile response, to spatial variation of the barrier geometry, should be examined in the systematic assessment of 3-dimensional response; this would require an extensive test programme, to provide statistically-valid data. The empirical framework could be extended usefully, through the examination of profile development, after the overwashing threshold has been exceeded. The influence of falling water level should be examined, on an overwashing barrier.

The results obtained within the present investigation are most widely-scattered for low wave steepness values (<0.015), although these seem to produce the most significant

changes to the barrier crest. The effects of swell waves should be examined further, to extend and validate the framework over this range of conditions. The effects of bi-modal wave spectra could be examined usefully, in studies designed to examine (barrier) crest response on a wave-by-wave basis, perhaps using video analysis. Direct comparison of the barrier response to JONSWAP and bi-modal (wave) spectra, consisting of a significant long period component could usefully extend the validity of the framework.

Measurements of the barrier profile have been limited to the upper segment of the profile. Similar studies at another site, with a larger tidal range, would allow the profiling to be undertaken lower on the profile.

The beach profiles should be measured, ideally, under the storm conditions: this would allow the response of the system to be measured at the peak of the storm. Development of remote sensing techniques to measure (through the water) offers the best possibility for this approach, (possibly using airborne techniques, such as LIDAR).

Regional wave climate studies

A wave-rider buoy was deployed for an indefinite period, in 1996, with a view to providing a high quality long-term wave data set; it remained in position upon completion of the current investigation. Statistical analysis of the data set will form part of an ongoing research programme, to revise extreme predictions for the region; this will be updated periodically, as part of the NFDC coastal research programme.

A statistical analysis of an extended time-series of extreme water levels would provide valuable management information for the site: an 'extremes analysis' based upon data from the present investigation would not be statistically valid. On-going data collection, together with regular calibration of the instrumentation, will provide a suitable time-series for an extreme tidal elevation analysis; this will form an extension of the present research programme.

A joint probability analysis should be undertaken on waves and tides based upon the simultaneous measurement of wave and water level conditions, upon completion of the analysis of extreme waves and tides.

Appendix 1: Survey methodology

Control surveys

The dynamic nature of the study area at Hurst Spit presents practical problems for the establishment of good survey control. The beach itself is mobile and has no fixed features, whilst the surrounding area is a soft mud flat and saltmarsh area which is liable to subsidence. Scaffold poles and timber piles have been installed as semi-permanent control markers; these have been maintained through the study period and have frequently been lost due to storm action or vandalism.

The plan position and elevation of the zero co-ordinates of each survey line was co-ordinated by static control surveys, carried out with a Trimble 4000SSe differential global positioning system. An extensive control network was established across the study area: a series of simultaneous observations of up to five control stations have been made to enable baseline vectors to be calculated for the whole network of control sites. A permanent differential base station, was installed at the NFDC depot in Hurst Road, Milford-on-Sea. This provides a well controlled fixed site for the broadcast of differential signals for use in the real time kinematic surveys, via a UHF radio link. Baseline vector measurements have subsequently been processed using GPSURVEY software and the TRIMNET network adjustment package.

The global positioning system provides data relative to the WGS84 ellipsoid using RTF89 co-ordinates; these have been transformed to OSGB36 datum and the Airy spheroid, using a series of datum transformations. The method used by the software is, essentially, a statistical method of fitting the data to the required projection, using defined parameters. The ellipsoid heights produced by the WGS84 GPS measurements are transformed to orthometric heights using a geoid model; this is supported by local orthometric control, derived from Ordnance Survey bench mark levels. There are small inherent errors in the transformation, due largely to the anomalies within the Ordnance Survey Transverse Mercator Projection and local

variability of the separation of the ellipsoid and geoid. These absolute positional errors are unimportant for the purposes of this study, as all subsequent measurements of profile response are made relative to a constant datum. Despite the small inaccuracies developed by the transformations, it was desirable to work within the OS co-ordinate system, as this enabled current data to be linked with historical data sets. The control surveys provided a plan position accuracy of +/- 2cm and vertical position of +/-3cm for each of the control stations.

Spot heighting

Detailed surveys of beach areas were carried out using spot heighting survey methods. These were undertaken either by theodolite or RTK GPS methods. Spot height point data were collected, over the whole of the area of interest, across a visually defined grid. Data points were recorded generally, at intervals of approximately 5 metres, or at clearly visible slope breaks - which ever was smaller. This survey method was adopted when the main purpose of the survey was to record plan shape and contour information: it was used also for: the determination of changes in beach volume; longshore transport rates; and for measuring the spatial distribution and geometry of features such as overwash fans following storms.

Topographic surveys were conducted with Real Time Kinematic DGPS (RTK), with pre selected horizontal and vertical tolerances of +/-20 millimetres, depending on conditions. The surveys were levelled to Ordnance Datum Newlyn (ODN) and co-ordinated to Ordnance Survey National Grid (OSGB36), using the control data discussed above. Surveys carried out using RTK GPS methods were pre-processed using TRIMMAP software to generate 3-dimensional co-ordinates to OSGB36. The co-ordinate data was processed using a combination of digital ground modelling (DGM3.9), and FASTCAD drawing software.

The DGM3.9 digital ground modelling programme provided a method of generating contours and profiles, by 3-dimensional analysis of the spot height data. Each data set was transformed into a regular grid of levels, at a defined interval, using a variety of methods of

linear interpolation. Data sets were compared and differenced at each node within the matrices; residual values were used to determine erosion or accretion. This approach was used extensively, both for the field data and also for the model data: it allowed volumetric calculations of changes to the beach to be made; it also allowed the precise location and quantification of discrete areas of erosion and accretion to be determined. The software also permited measured 3-dimensional point data to be exported to CAD packages without any modelling or interpolation. This technique was particularly useful, for the analysis of linear features and for mapping features with a clearly defined plan shape.

Appendix 2: SANDS DATBASE

A large quantity of field data was collected during the present investigation; this has been stored in a 'SANDS for Windows' database. The data is held by the Coastal Protection Group of the NFDC (at their Lymington office); it is used to inform the beach management programme for the beaches of Christchurch Bay. The principle data sets held within the database are listed below.

Beach profiles at 52 locations:	1987-1998
Wave data, for Milford-on-sea:	1996-1998
Tidal data, for Lymington River, Western Solent	1991-1998
Wind speed, and direction Lymington River, Western Solent	1991-1998
Barometric pressure, for and direction Lymington River, Western Solent	1991-1998
Tidal data, for Hurst Spit	1996-1998

Appendix 3: Physical model test programme

Test Number	Hs (m)	Tm (s)	SWL (mODN)	Incident Wave Angle	Test Type	Beach Profile Geometry
A01	2.50	8.4	0.87	230	Longshore Transport	1990
A02	3.60	10.7	0.87	230	Armour Stabilty	1990
A03	3.60	9.9	1.87	230	Armour Stabilty	1990
A04	3.80	9.7	2.27	230	Armour Stabilty	1990
A05	2.50	8.4	0.87	230	Longshore Transport	1990
A06	2.50	8.4	0.87	230	Groyne Layout	Proposed
A07	3.60	10.7	0.87	230	Armour Stabilty	Proposed
A08	3.60	9.7	1.87	230	Armour Stabilty	Proposed
A09	3.80	9.7	2.27	230	Armour Stabilty	Proposed
A10	2.50	8.4	0.87	230	Longshore Transport	Proposed
A11	2.80	8.4	0.87	230	Profile Response	Proposed
A12	2.90	8.4	1.37	230	Profile Response	Proposed
A13	3.00	8.4	1.87	230	Profile Response	Proposed
A14	2.80	8.4	0.87	230	Profile Response	Proposed
A15	2.90	8.4	1.37	230	Profile Response	Proposed
A16	3.00	8.4	1.87	230	Profile Response	Proposed
A17	3.1	8.4	2.27	230	Profile Response	Proposed
A18	2.90	8.4	0.87	220	Profile Response	Proposed
A19	3.1	8.4	1.37	220	Profile Response	Proposed
A20	3.3	8.4	1.87	220	Profile Response	Proposed
A21	3.6	8.4	2.27	220	Profile Response	Proposed
A22	3	9.7	0.87	220	Profile Response	Proposed
A23	3.66	9.6	1.37	220	Profile Response	Proposed
A24	3.65	9.6	1.87	220	Profile Response	Proposed
A25	3.84	9.6	2.27	220	Profile Response	Proposed
A26	4.12	8.4	0.87	220	Profile Response	Proposed
A27	4.39	8.4	1.87	220	Profile Response	Proposed
A28	2.90	8.4	0.87	220	Profile Response	Proposed
A29	3.1	8.4	1.37	220	Profile Response	Proposed
A30	3.3	8.4	1.87	220	Profile Response	Proposed
A31	3.6	8.4	2.27	220	Profile Response	Proposed
A32	3	9.7	0.87	220	Profile Response	Proposed
A33	3.66	9.6	1.37	220	Profile Response	Proposed

Table A3.1 Test Programme segment A - Summary of Test Variables

Note: Test duration is 3 hours for all tests

Test Number	Hs (m)	Tm (s)	SWL (mODN)	Incident Wave Angle	Test Type	Beach profile Geometry
B1	2.58	7.6	2.27	210	December 1989 Storm	October 1989
B2	2.58	7.6	2.27	210	December 1989 Storm	October 1989
B3	3.27	9.6	1.87	210	1:1 Year Storm	October 1990
B4	2.58	7.6	1.87	210	Profile Response	October 1990
B5	3.00	7.6	1.87	210	Profile Response	October 1990
B6	3.00	7.6	2.27	210	Profile Response	October 1990
B7	2.58	7.6	2.27	210	December 1989 Storm	October 1990
B8	2.70	8.4	0.87	225	1:1 Year Storm	October 1990
B9	3.00	9	0.87	225	1:5 Year Storm	October 1990
B10	3.20	8.3	1.87	225	1:1 Year Storm plus surge	October 1990
B11	3.40	8.3	2.27	225	1:1 Year Storm plus surge	October 1990
B12	3.00	8	2.27	225	Profile Response	October 1990
B13	2.60	7.6	2.27	225	Profile Response	October 1990
B14	2.70	8.4	0.87	225	Profile Response (1)	October 1990
B15	2.70	8.4	1.37	225	Profile Response	October 1990
B16	2.70	8.4	1.87	225	Profile Response	October 1990
B17	2.70	8.4	2.27	225	Profile Response	October 1990
B18	3.34	9.6	0.87	225	1:100 Year Storm	October 1990
B19	3.50	9.6	0.87	225	October 1989 Storm	October 1990
B20	2.7	8.4	1.87	225	Profile Response	October 1990
B21	3.40	8.3	2.27	225	Demonstration	October 1990
B22	2.7	8.4	0.87	225	Profile response(1)	October 1990
B23	3	8.4	1.37	225	Profile response	October 1990
B24	3.2	8.3	1.87	225	Profile response	October 1990
B25	3.00	9	0.87	225	Profile response	October 1990
B26	3.10	8.9	1.37	225	Profile response	October 1990
B27	2.7	8.4	0.87	225	Profile response(1)	12m crest 7mOD 7.0mODN
B28	3	8.4	1.37	225	Profile response	12m crest 7mOD 7.0mODN
B29	3.1	8.3	1.87	225	Profile response	12m crest 7mOD 7.0mODN
B30	3.40	8.3	2.27	225	Profile response	12m crest 7mOD 7.0mODN
B31	3.00	9	0.87	225	Profile response	12m Wide Crest @ 7.0mODN
B32	3.10	9	1.37	225	Profile response	12m Wide Crest @ 7.0mODN
B33	3.30	8.8	1.87	225	Profile response	12m Wide Crest @ 7.0mODN
B34	3.70	8.8	2.27	225	Profile response	12m Wide Crest @ 7.0mODN
B35	3.40	9.6	0.87	225	Profile response	12m Wide Crest @ 7.0mODN
B36	3.40	9.6	1.37	225	Profile response	12m Wide Crest @ 7.0mODN
B37	3.60	9.4	1.87	225	Profile response	12m Wide Crest @ 7.0mODN
B38	3.6	9.4	2.27	225	Profile response	12m Wide Crest @ 7.0mODN
B39	4.1	9.3	2.27	225	Profile response	12m Wide Crest @ 7.0mODN

Table A3.2 Test Programme Section B - Summary of Test Variables

Note: Test duration is 3 hours for all tests.

Table A3.2 Test Programme Section B - Summary of Test Variables (continued)

Test Number	Hs (m)	Tm (s)	SWL (mODN)	Incident Wave Angle	Test Type	Beach profile Geometry (Survey date)
B40	2.7	8.4	0.87	225	Profile response(1)	12m crest @ 7.0mODN + bastion modification 1
B41	2.7	8.4	1.37	225	Profile response	12m crest @ 7.0mODN + bastion modification 1
B42	2.7	8.4	0.87	225	Profile response(1)	12m crest @ 7.0mODN + bastion modification 2
B43	2.7	8.4	1.37	225	Profile response	12m crest @ 7.0mODN + bastion modification 2
B44	3.1	8.3	1.87	225	Profile response	12m crest @ 7.0mODN + bastion modification 2
B45	3.4	8.3	2.27	225	Profile response	12m crest @ 7.0mODN + bastion modification 2
B46	3.00	9	0.87	225	Profile response	12m crest @ 7.0mODN + bastion modification 2
B47	3.10	9	1.37	225	Profile response	12m crest @ 7.0mODN + bastion modification 2
B48	3.40	8.8	1.87	225	Profile response	12m crest @ 7.0mODN + bastion modification 2
B49	3.70	8.8	2.27	225	Profile response	12m crest @ 7.0mODN + bastion modification 2
B50	3.40	9.6	0.87	225	Profile response	12m crest @ 7.0mODN + bastion modification 2
B51	3.40	9.6	1.37	225	Profile response	12m crest @ 7.0mODN + bastion modification 2
B52	3.60	9.4	1.87	225	Profile response	12m crest @ 7.0mODN + bastion modification 2
B53	3.65	9.3	2.27	225	Profile response	12m crest @ 7.0mODN + bastion modification 2
B54	2.70	8.4	0.87	225	Profile response(1)	12m crest @ 6.1mODN + offshore breakwater
B55	3.00	8.4	1.37	225	Profile response	12m crest @ 6.1mODN + offshore breakwater
B56	3.10	8.4	1.87	225	Profile response	12m crest @ 6.1mODN + offshore breakwater
B57	3.40	8.4	2.27	225	Profile response	12m crest @ 6.1mODN + offshore breakwater
B58	3.00	9	0.87	225	Profile response	12m crest @ 6.1mODN + offshore breakwater

Table A3.2 Test Programme Section B - Summary of Test Variables (continued)

Test Number	Hs (m)	Tm (s)	SWL (mODN)	Incident Wave Angle	Test Type	Beach profile Geometry (Survey date)
B59	3.10	9	1.37	225	Profile response	12m crest @ 6.1mODN + offshore breakwater
B60	3.30	8.8	1.87	225	Profile response	12m crest @ 6.1mODN + offshore breakwater
B61	3.70	8.8	2.27	225	Profile response	12m crest @ 6.1mODN + offshore breakwater
B62	3.40	9.6	0.87	225	Profile response	12m crest @ 6.1mODN + offshore breakwater
B63	3.40	9.6	1.37	225	Profile response	12m crest @ 6.1mODN + offshore breakwater
B64	3.60	9.4	1.87	225	Profile response	12m crest @ 6.1mODN + offshore breakwater
B65	3.60	9.3	2.27	225	Profile response	12m crest @ 6.1mODN + offshore breakwater
B66	2.70	8.4	0.87	225	Profile response(1)	20m crest @ 6.1mODN + offshore bw mod b
B67	3.00	8.4	1.37	225	Profile response	20m crest @ 6.1mODN + offshore bw mod b
B68	3.10	8.4	1.87	225	Profile response	20m crest @ 6.1mODN + offshore bw mod b
B69	3.40	8.4	2.27	225	Profile response	20m crest @ 6.1mODN + offshore bw mod b
B70	3.00	9	0.87	225	Profile response	20m crest @ 6.1mODN + offshore bw mod b
B71	3.10	9	1.37	225	Profile response	20m crest @ 6.1mODN + offshore bw mod b
B72	3.30	8.8	1.87	225	Profile response	20m crest @ 6.1mODN + offshore bw mod b
B73	3.70	8.8	2.27	225	Profile response	20m crest @ 6.1mODN + offshore bw mod b
B74	3.40	9.6	0.87	225	Profile response	20m crest @ 6.1mODN + offshore bw mod b
B75	3.40	9.6	1.37	225	Profile response	20m crest @ 6.1mODN + offshore bw mod b
B76	3.60	9.4	1.87	225	Profile response	20m crest @ 6.1mODN + offshore bw mod b
B77	3.65	9.3	2.27	225	Profile response	20m crest @ 6.1mODN + offshore bw mod b

Table A3.2 Test Programme Section B - Summary of Test Variables (continued)

Test Number	Hs (m)	Tm (s)	SWL (mODN)	Incident Wave Angle	Test Type	Beach profile Geometry (Survey date)
B78					Breakwater Construction	12m crest @ 7.0mODN + offshore breakwater
B79	2.00	7.6	0.87	210	Profile response	12m crest @ 7.0mODN + offshore breakwater
B80	2.60	7.6	1.37	210	Profile response	12m crest @ 7.0mODN + offshore breakwater
B81	3.30	9.6	1.87	210	Profile response	12m crest @ 7.0mODN + offshore breakwater
B82	3.50	9.5	2.27	210	Profile response	12m crest @ 7.0mODN + offshore breakwater
B83	2.30	7.6	0.87	210	Profile response	12m crest @ 7.0mODN + offshore breakwater
B84	2.60	7.6	1.37	210	Profile response	12m crest @ 7.0mODN + offshore breakwater
B85	3.80	10.2	1.87	210	Profile response	12m crest @ 7.0mODN + offshore breakwater
B86	4.10	9.6	2.27	210	Profile response	12m crest @ 7.0mODN + offshore breakwater
B87	2.60	7.6	0.87	210	Profile response(1)	12m crest @ 7.0mODN + offshore breakwater
B88	3.45	9.5	1.37	210	Profile response	12m crest @ 7.0mODN + offshore breakwater
B89	4.00	9.6	1.87	210	Profile response	12m crest @ 7.0mODN + offshore breakwater
B90	4.10	9.6	2.27	210	Profile response	12m crest @ 7.0mODN + offshore breakwater
B91	3.70	8.8	2.27	235	Post drift profile	12m crest @ 7.0mODN + offshore breakwater
B92	2.70	8.4	0.87	235	Profile response(1)	12m crest @ 7.0mODN + offshore breakwater
B93	3.00	8.4	1.37	235	Profile response	12m crest @ 7.0mODN + offshore breakwater
B94	3.10	8.4	1.87	235	Profile response	12m crest @ 7.0mODN + offshore breakwater
B95	3.40	8.4	2.27	235	Profile response	12m crest @ 7.0mODN + offshore breakwater
B96	3.00	9	0.87	235	Profile response	12m crest @ 7.0mODN + offshore breakwater

Table A3.2 Test Programme Section B - Summary of Test Variables (continued)

Test Number	Hs (m)	Tm (s)	SWL (mODN)	Incident Wave Angle	Test Type	Beach profile Geometry (Survey date)
B97	3.10	9	1.37	235	Profile response	12m crest @ 7.0mODN + offshore breakwater
B98	3.32	9	1.87	235	Profile response	12m crest @ 7.0mODN + offshore breakwater
B99	3.70	9	2.27	235	Profile response	12m crest @ 7.0mODN + offshore breakwater
BD1	2.50	8.4	0.87	235	Littoral drift	12m crest @ 7.0mODN + offshore breakwater
BD2	2.50	8.4	0.87	235	Littoral drift	12m crest @ 7.0mODN + offshore breakwater
BD3	2.50	8.4	0.87	235	Littoral drift + currents	12m crest @ 7.0mODN + offshore breakwater
BD4	2.50	8.4	0.87	235	Littoral drift + currents	October 1990
BD5	2.50	8.4	0.87	235	Littoral drift	October 1990
BD6	2.50	8.4	0.87	235	Littoral drift + currents	October 1990
E01	2.7	8.4	0.87	225	Profile response(1)	12m crest @ 7.0mODN + offshore breakwater
E02	3	8.4	1.37	225	Profile response	12m crest @ 7.0mODN + offshore breakwater
E03	3.2	8.3	1.87	225	Profile response	12m crest @ 7.0mODN + offshore breakwater
E04	3.4	8.4	2.27	225	Profile response	12m crest @ 7.0mODN + offshore breakwater
E05	3	9	0.87	225	Profile response	12m crest @ 7.0mODN + offshore breakwater
E06	3.1	8.9	1.37	225	Profile response	12m crest @ 7.0mODN + offshore breakwater
E07	3.3	8.8	1.87	225	Profile response	12m crest @ 7.0mODN + offshore breakwater
E08	3.7	8.8	2.27	225	Profile response	12m crest @ 7.0mODN + offshore breakwater
E09	3.4	9.6	0.87	225	Profile response	12m crest @ 7.0mODN + offshore breakwater
E10	3.4	9.6	1.37	225	Profile response	12m crest @ 7.0mODN + offshore breakwater
E11	3.4	9.6	1.87	225	Profile response	12m crest @ 7.0mODN + offshore breakwater
E12	3.6	9.3	2.27	225	Profile response	12m crest @ 7.0mODN + offshore breakwater

Test Number	Hs (m)	Tm (s)	SWL (mODN)	Incident Wave Angle	Test Type	Beach profile Geometry (Survey date)
C01	2.90	9.5	0.87	210	October 1989 storm	September1989
C02	2.90	9.5	0.87	210	October 1989 storm	September1989
C03	2.5	7.4	2.1	210	December 1989 storm	October 1989
C04	2.6	9	0.87	210	1:1 Year Return Period	February 1991
C05	2.9	9.5	1.37	210	1:5 Year Return Period	February 1991
C06	2.6	9	0.87	210	1:1 Year Return Period	February 1991
C07	2.9	9.5	1.37	210	1:5 Year Return Period	February 1991
C08	2.9	9.5	1.37	210	1:5 Year Return Period	February 1991
C09	3.1	9.5	1.87	210	1:5 Year Return Period	February 1991
C10	1.05	7.9	0.87	210	Littoral Drift	February 1991
C11	1.05	7.9	0.87	210	Littoral Drift + Currents	February 1991
C12	2.6	9	0.87	210	Profile response	12m Wide Crest @ 7mODN
C13	2.6	9	1.37	210	Profile response	12m Wide Crest @ 7mODN
C14	2.7	9	1.87	210	Profile response	12m Wide Crest @ 7mODN
C15	2.7	9	2.27	210	Profile response	12m Wide Crest @ 7mODN
C16	2.9	9.5	0.87	210	Profile response	12m Wide Crest @ 7mODN
C17	2.9	9.5	1.37	210	Profile response	12m Wide Crest @ 7mODN
C18	3.1	9.5	1.87	210	Profile response	12m Wide Crest @ 7mODN
C19	2.90	9.5	0.87	225	October 1989 storm	September1989

Table A3.3 Test Programme Section C - Summary of Test Variables

Note: Test duration is 3 hours for all tests.

Test Number	Hs (m)	Tm (s)	SWL (mODN)	Incident Wave Angle	Test Type	Beach profile Geometry (Survey date)
C20	2.5	7.4	2.27	225	December 1989 storm	October 1989
C21	2.6	9	0.87	225	Profile response (1)	February 1991
C22	2.6	9	1.37	225	Profile response	February 1991
C23	2.7	9	1.87	225	Profile response(patched)	February 1991
C24	2.8	9.1	2.27	225	Profile response	February 1991
C25	2.6	9	0.87	225	Profile response(1)	Stepped crest @ 7mODN (Tapered profile to 6mODN)
C26	2.6	9	1.37	225	Profile response	Stepped crest @ 7mODN (Tapered profile to 6mODN)
C27	2.7	9	1.87	225	Profile response	Stepped crest @ 7mODN (Tapered profile to 6mODN)
C28	2.8	9.1	2.27	225	Profile response	Stepped crest @ 7mODN (Tapered profile to 6mODN)
C29	2.9	9.5	0.87	225	Profile response	Stepped crest @ 7mODN (Tapered profile to 6mODN)
C30	2.9	9.5	1.37	225	Profile response	Stepped crest @ 7mODN (Tapered profile to 6mODN)
C31	3.1	9.5	1.87	225	Profile response	Stepped crest @ 7mODN (Tapered profile to 6mODN)
C32	3.1	9.7	2.27	225	Profile response	Stepped crest @ 7mODN (Tapered profile to 6mODN)
C33	3.5	10.4	0.87	225	Profile response	Stepped crest @ 7mODN (Tapered profile to 6mODN)
C34	3.3	10.4	1.37	225	Profile response	Stepped crest @ 7mODN (Tapered profile to 6mODN)
C34	3.3	10.4	1.37	225	Profile response	Stepped crest @ 7mODN (Tapered to 6mODN))
C35	3.3	10.4	1.87	225	Profile response	Stepped crest @ 7mODN (Tapered to 6mODN))

Note: Test duration is 3 hours for all tests.

Table A3.3 Test Programme Section C - Summary of Test Variables (Continued)

Test Number	Hs (m)	Tm (s)	SWL (mODN)	Incident Wave Angle	Test Type	Beach profile Geometry (Survey date)
C36	3.5	10.4	2.27	225	Profile response	Stepped crest @ 7mODN (Tapered to 6mODN))
C37	2.6	9	0.87	225	Profile response(1)	Stepped crest @ 6.5mODN (Tapered to 5.5mODN))
C38	2.6	9	1.37	225	Profile response	Stepped crest @ 6.5mODN (Tapered to 5.5mODN))
C39	2.7	9	1.87	225	Profile response	Stepped crest @ 6.5mODN (Tapered to 5.5mODN))
C40	2.8	9.1	2.27	225	Profile response	Stepped crest @ 6.5mODN (Tapered to 5.5mODN))
C41	2.9	9.5	0.87	225	Profile response	Stepped crest @ 6.5mODN (Tapered to 5.5mODN))
C42	2.9	9.5	1.37	225	Profile response	Stepped crest @ 6.5mODN (Tapered to 5.5mODN))
C43	3.1	9.5	1.87	225	Profile response	Stepped crest @ 6.5mODN (Tapered to 5.5mODN))
C44	3.1	9.7	2.27	225	Profile response	Stepped crest @ 6.5mODN (Tapered to 5.5mODN))
C45	3.3	10.4	0.87	225	Profile response	Stepped crest @ 6.5mODN (Tapered to 5.5mODN))
C46	3.3	10.4	1.37	225	Profile response	Stepped crest @ 6.5mODN (Tapered to 5.5mODN))
C47	3.3	10.4	1.87	225	Profile response	Stepped crest @ 6.5mODN (Tapered to 5.5mODN))
C48	3.5	10.4	2.27	225	Profile response	Stepped crest @ 6.5mODN (Tapered to 5.5mODN))
C49	2.6	9	0.87	225	Profile response(1)	Stepped crest @ 6.0mODN (Tapered to 5mODN))
C50	2.6	9	1.37	225	Profile response	Stepped crest @ 6.0mODN (Tapered to 5mODN))
C51	2.7	9	1.87	225	Profile response	Stepped crest @ 6.0mODN (Tapered to 5mODN))
C52	2.8	9.1	2.27	225	Profile response	Stepped crest @ 6.0mODN (Tapered to 5mODN))
C53	2.9	9.5	0.87	225	Profile response	Stepped crest @ 6.0mODN (Tapered to 5mODN))

Note: Test duration is 3 hours for all tests.

Table A3.3 Test Programme Section C - Summary of Test Variables (Continued)

Test Number	Hs (m)	Tm (s)	SWL (mODN)	Incident Wave Angle	Test Type	Beach profile Geometry (Survey date)
C54	2.9	9.5	1.37	225	Profile response	Stepped crest @ 6.0mODN (Tapered to 5mODN))
C55	3.1	9.5	1.87	225	Profile response	Stepped crest @ 6.0mODN (Tapered to 5mODN))
C56	3.1	9.7	2.27	225	Profile response	Stepped crest @ 6.0mODN (Tapered to 5mODN))
C57	3.4	10.4	1.87	225	Profile response	Stepped crest @ 6.0mODN (Tapered to 5mODN))
C58	3.5	10.4	2.27	225	Profile response	Stepped crest @ 6.0mODN (Tapered to 5mODN))
C59	1.05	7.9	0.87	225	Littoral Drift	Proposed profiles
C60	1.05	7.9	0.87	225	Littoral Drift	Proposed profiles
C61	1.05	7.9	0.87	225	Littoral Drift	Existing Profile(February 1991)
Test C62	1.05	7.9	0.87	225	Littoral Drift	Existing Profile(February 1991)

Table A3.3 Test Programme Section C - Summary of Test Variables (continued)

Note: Test duration is 3 hours for all tests.

Test Number	Hs (m)	Tm (s)	SWL (mODN)	Incident Wave Angle	Test Type	Beach profile Geometry (Survey date)
D01	2.1	9.6	0.87	220	Profile response(1)	February 1991
D02	2.6	9.7	1.37	220	Profile response	February 1991
D03	3	10.6	1.87	220	Profile response	February 1991
D04	2.1	9.6	0.87	220	Profile response(1)	February 1991
D05	2.4	9.2	1.37	220	Profile response	February 1991
D06	2.4	9.1	1.87	220	Profile response	February 1991
D07	2.1	9.6	0.87	220	Profile response(1)	12m Wide Crest @ 5mODN
D08	2.4	9.1	1.37	220	Profile response	12m Wide Crest @ 5mODN
D09	2.4	9.1	1.87	220	Profile response	12m Wide Crest @ 5mODN
D10	2.4	9.1	2.27	220	Profile response	12m Wide Crest @ 5mODN
D11	2.1	9.6	0.87	220	Profile response(1)	12m Wide Crest @ 6mODN
D12	2.4	9.1	1.37	220	Profile response	12m Wide Crest @ 6mODN
D13	2.4	9.1	1.87	220	Profile response	12m Wide Crest @ 6mODN
D14	2.7	9.1	2.27	220	Profile response	12m Wide Crest @ 6mODN
D15	2.4	10.2	0.87	220	Profile response	12m Wide Crest @ 6mODN
D16	2.6	9.7	1.37	220	Profile response	12m Wide Crest @ 6mODN
D17	2.6	9.7	1.87	220	Profile response	12m Wide Crest @ 6mODN

Table A3.4 Test Programme Section D - Summary of Test Variables

Note: Test duration is 3 hours for all tests.

Test Number	Hs (m)	Tm (s)	SWL (mODN)	Incident Wave Angle	Test Type	Beach profile Geometry (Survey date)
D18	2.7	9.6	2.27	220	Profile response	12m Wide Crest @ 6mODN
D19	3.0	10.9	0.87	220	Profile response	12m Wide Crest @ 6mODN
D20	3.0	10.6	1.37	220	Profile response	12m Wide Crest @ 6mODN
D21	3.0	10.6	1.87	220	Profile response	12m Wide Crest @ 6mODN
D22	1.05	7.9	0.87	220	Littoral Drift	12m Wide Crest @ 6mODN
D23	1.05	7.9	0.87	220	Littoral Drift	12m Wide Crest @ 6mODN
D24	1.05	7.9	0.87	220	Littoral Drift	12m Crest @ 6mODN + groyne
D25	1.05	7.9	0.87	220	Littoral Drift	February 1991

Note: Test duration is 3 hours for all tests.

Appendix 4: Annual distribution of inshore wave conditions at Hurst Spit

H1 TO H2		P(H>H 1))	Wave angle in degrees North										
			175 185	185 195	195 205	205 215	215 225	225 235	235 245	245 255	255 265	265 275	275 285
0.0	0.2	0.8175	1161	4097	6197	3377	2574	4501	6670	2044	1762	0	0
0.2	0.4	0.4937	0	0	125	2451	2766	5717	827	0	0	0	0
0.4	0.6	0.3749	0	0	0	1360	6142	2039	0	0	0	0	0
0.6	0.8	0.2794	0	0	0	901	5132	341	0	0	0	0	0
0.8	1.0	0.2157	0	0	0	415	3054	3582	0	0	0	0	0
1.0	1.2	0.1452	0	0	0	198	1325	473	0	0	0	0	0
1.2	1.4	0.1252	0	0	0	266	1056	3334	0	0	0	0	0
1.4	1.6	0.0787	0	0	0	119	458	1645	0	0	0	0	0
1.6	1.8	0.0565	0	0	0	23	247	1870	0	0	0	0	0
1.8	2.0	0.0351	0	0	0	5	64	1543	0	0	0	0	0
2.0	2.2	0.0189	0	0	0	0	115	1045	0	0	0	0	0
2.2	2.4	0.0073	0	0	0	0	6	416	18	0	0	0	0
2.4	2.6	0.0029	0	0	0	0	4	115	1	0	0	0	0
2.6	2.8	0.0017	0	0	0	0	0	95	28	0	0	0	0
2.8	3.0	0.0005	0	0	0	0	0	13	1	0	0	0	0
3.0	3.2	0.0004	0	0	0	0	0	23	5	0	0	0	0
3.2	3.4	0.0001	0	0	0	0	0	0	8	0	0	0	0
3.4	3.6	0.0000	0	0	0	0	0	0	1	0	0	0	0
Parts per thousand for each direction			14	50	77	111	281	327	92	25	22	0	0

Table A4.1 Annual distribution of wave height and direction - Point 2
Location - Inshore Point 2, Christchurch Bay 1/1/74 - 28/2/90, data in parts per hundred thousand, significant wave height in metres

H1 TO H2		P(H>H1))	Wave angle in degrees North										
			175	185	195	205	215	225	235	245	255	265	275
			185	195	205	215	225	235	245	255	265	275	285
0.0	0.2	0.8175	0	4718	6275	4710	722	5466	4760	2473	2217	975	0
0.2	0.4	0.4944	0	6	18	3234	976	6504	1060	73	0	0	0
0.4	0.6	0.3757	0	0	0	1393	5852	2948	154	0	0	0	0
0.6	0.8	0.2722	0	0	0	682	5334	366	0	0	0	0	0
0.8	1.0	0.2084	0	0	0	327	6313	468	0	0	0	0	0
1.0	1.2	0.1373	0	0	0	421	3980	114	0	0	0	0	0
1.2	1.4	0.0922	0	0	0	222	1671	32	0	0	0	0	0
1.4	1.6	0.0729	0	0	0	215	2782	188	0	0	0	0	0
1.6	1.8	0.0411	0	0	0	13	1849	30	0	0	0	0	0
1.8	2.0	0.0221	0	0	0	0	799	11	0	0	0	0	0
2.0	2.2	0.0140	0	0	0	0	585	126	0	0	0	0	0
2.2	2.4	0.0069	0	0	0	0	176	111	0	0	0	0	0
2.4	2.6	0.0041	0	0	0	0	87	148	0	0	0	0	0
2.6	2.8	0.0017	0	0	0	0	11	109	0	0	0	0	0
2.8	3.0	0.0005	0	0	0	0	1	9	0	0	0	0	0
3.0	3.2	0.0004	0	0	0	0	4	28	0	0	0	0	0
3.2	3.4	0.0001	0	0	0	0	0	6	0	0	0	0	0
3.4	3.6	0.0000	0	0	0	0	0	4	0	0	0	0	0
3.6	3.8	0.0000	0	0	0	0	0	1	0	0	0	0	0
Parts per thousand for each direction													
			0	58	77	137	381	204	73	31	27	12	0

Table A4.2 Annual distribution of wave height and direction - Point 4
Location - Inshore point 4, Christchurch Bay 1/1/74 - 28/2/90, data in parts per hundred thousand, significant wave height in metres

H1	TO H2	P(H>H1))	Wave angle in degrees North										
			175	185	195	205	215	225	235	245	255	265	275
			185	195	205	215	225	235	245	255	265	275	285
0.0	0.2	0.8766	0	1965	9484	10087	2912	3685	2897	2990	1657	2067	1767
0.2	0.4	0.4815	0	0	0	4273	6466	6548	2288	821	4	0	0
0.4	0.6	0.2775	0	0	25	2925	4419	1316	156	2	0	0	0
0.6	0.8	0.1891	0	0	0	3234	4908	602	117	0	0	0	0
0.8	1.0	0.1005	0	0	0	2058	1875	71	23	0	0	0	0
1.0	1.2	0.0602	0	0	0	2612	1983	50	8	0	0	0	0
1.2	1.4	0.0137	0	0	0	513	556	6	0	0	0	0	0
1.4	1.6	0.0029	0	0	0	83	39	0	0	0	0	0	0
1.6	1.8	0.0017	0	0	0	23	124	0	0	0	0	0	0
1.8	2.0	0.0002	0	0	0	3	12	0	0	0	0	0	0
2.0	2.2	0.0001	0	0	0	0	10	0	0	0	0	0	0
Parts per thousand for each direction													
			0	22	108	294	266	140	63	43	19	24	20

Table A4.3 Annual distribution of wave height and direction - Point 6
Location - Inshore point 6, Christchurch Bay 1/1/74 - 28/2/90
data in parts per hundred thousand, significant wave height in metres

H1 TO H2		P(H>H1))	Wave angle in degrees North										
			175 185	185 195	195 205	205 215	215 225	225 235	235 245	245 255	255 265	265 275	275 285
0.0	0.2	0.7596	0	181	532	5367	8766	5818	4729	2343	2191	952	0
0.2	0.4	0.4508	0	10	69	2304	8792	4662	983	18	0	0	0
0.4	0.6	0.2824	0	0	0	4619	6074	421	0	0	0	0	0
0.6	0.8	0.1713	0	0	0	7378	1271	109	0	0	0	0	0
0.8	1.0	0.0837	0	0	0	4173	193	36	0	0	0	0	0
1.0	1.2	0.0397	0	0	0	2463	137	16	0	0	0	0	0
1.2	1.4	0.0135	0	0	0	1141	6	0	0	0	0	0	0
1.4	1.6	0.0021	0	0	0	186	0	0	0	0	0	0	0
1.6	1.8	0.0002	0	0	0	15	0	0	0	0	0	0	0
1.8	2.0	0.0001	0	0	0	6	0	0	0	0	0	0	0
2.0	2.2	0.0000	0	0	0	1	0	0	0	0	0	0	0
Parts per thousand for each direction			0	3	8	364	332	146	75	31	29	13	0

Table A4.4 Annual distribution of wave height and direction - Point 7

Location - Inshore point 7, Christchurch Bay 1/1/74 - 28/2/90, data in parts per hundred thousand, significant wave height in metres

REFERENCES

Ahrens, J.P., (1987). Characteristics of reef breakwaters. *Technical Report CERC-87-17, US Army Corps of Engineers, Coastal Engineering Research Centre, Vicksberg*

Allen, J., (1947). Scale models in hydraulic engineering. *Longmans Green* 232pp.

Allison, H.A., and Morley, J. (1989). Blakeney Point and Scolt Head Island. *Norwich National Trust.*

Andrews, P.B., (1970). Facies and genesis of a hurricane washover fan, St Joseph Island Central Texas Coast. *Report. Invest. 67 Bureau Econ. Geology, Univ. Texas, Austin. 147pp*

Arkell, W.J., (1955). The effects of storms on Chesil Beach *Proceedings. Dorset Natural. History Arch. Society, Vol. 76*: 141-145.

Babtie Group., (1997). Chesil Beach Investigation. Unpublished Report to the Environment Agency, South West Region.

Battjes, J. A., (1974). Surf similarity. *Proceedings of the 14th international Conference on Coastal Engineering, American Society of Civil Engineers; 466-479.*

Belknap, D.F., and Kraft, J.C., (1985). Influence of antecedent geology on stratigraphic preservation potential and evaluation of Delaware's barrier systems. *Marine Geology, Vol.63; 235-262.*

Blain, W.R., (1980). Tidal Hydraulics of the West Solent. Unpublished Ph.D. Thesis, Department of Civil Engineering, University of Southampton. 326pp.

Bluck, B.J., (1967). Sedimentation in beach gravels: examples from South Wales. *Journal of Sedimentary Petrology, Vol.* 37; 128-156.

Borrego, J., Morales, J.A. and Pendon, J.G., (1993). Holocene filling of an estuarine lagoon along the mesotidal coast of Huelva: the Piedras River mouth, SW Spain. *Journal of Coastal Research, Vol.9, 242-254.*

Bowen, A.J., (1969). *Journal of Geophysical Research, 74: 5467-5478.*

Boyd, R., Bowen, A.J., and Hall, R.K., (1987). An evolutionary model for transgressive sedimentation on the eastern shore of Nova Scotia. In D. Fitzgerald and P.Rosen: Glaciated coasts. Academic press, San Diego, 87-114.

Bradbury, A.P., Allsop, N.W.H., and Stephens, R.V., (1988). Hydraulic performance of breakwater crown walls. *Report No. SR146, Hydraulics Research Ltd. Wallingford.*

Bradbury, A.P., and Kidd, R., (1998). Hurst Spit stabilisation scheme - design of beach recharge. *Proceedings 33rd MAFF Conference of River and Coastal Engineers (in press).*

Bradbury, A.P., and Powell, K.A., (1992). The short-term profile response of shingle spits to storm wave action. *Proceedings of the 23rd International Conference on Coastal Engineering, 2694- 2707.*

Bray, M,J., (1997). Episodic shingle supply and modified development of Chesil Beach. *Journal of Coastal Research, Vol.13, No 4.*

Bray, M.J., Carter, D.J. and Hooke, J.M., (1991). Coastal Sediment Transport Study, Volume 4: Hurst Castle Spit to Swanage. Unpublished Technical Report, Department of Geography, Portsmouth Polytechnic. 76 pp.

Bristow, C.S., Raper, J.F. and Allison, H.M., (1992). Sedimentary architecture of a barrier island and recurved spits on a macrotidal coast. *Proceedings of Tidal Clastics '92, Third International Research Symposium on Modern and Ancient Clastic Tidal Deposits, Senckenberg Institute, Wilhelmshaven, Germany.*

Bristow., C.S., Horn, D.P., and Raper, J.F., (1993). Evolution of a barrier island and recurved spits on a macrotidal coast, *Proceedings. Large scale coastal behaviour 93, U.S Geological Survey Open file report 93-381, 238pp*

Bruun, P.M., (1962). Sea-Level Rise as a Cause of Shore Erosion. *Journal of the Waterways, Harbour and Coastal Engineering Division, ASCE, Vol.88, No. WWI, 17- 30*

Bruun., P.M., (1954).Coast erosion and the development of beach profiles. *US Army Corps of Engineers, BEB, TM-44.*

Carr, A.P., (1965). Shingle spit and river mouth: *short-term* dynamics. *Transactions of the Institute of British Geographers, Vol.36, 117-129.*

Carr, A.P., (1969), Size grading along a pebble beach: Chesil Beach, *Journal Sedimentary Petrology, Vol. 39, 297-311.*

Carr, A.P., (1970). The evolution of Orford Ness, Suffolk, before 1600 AD: geomorphological evidence. *Zeitschrift fur Geomorphologie, N.F. Vol.14, 289-300.*

Carr, A.P., (1974). Differential movement of coarse sediment particles, *Proceedings. 14th Conference. on Coastal Engineering, ASCE.*

Carr, A.P., (1982). Shingle beaches: aspects of their structure and stability. *Proceedings Symposium on shoreline Protection.*

Carr, A.P., and Blackley., N.W.L., (1969). Geological composition of the pebbles of Chesil Beach Dorset. *Proceedings. Dorset Natural History and Archaeological Society*

Carr, A.P., and Blackley., N.W.L., (1973). Investigations bearing on the age and development of Chesil Beach, Dorset and the associated area. *Transactions Institute British Geographers, Vol. 58, 99-111.*

Carr, A.P., and Blackley., N.W.L., (1974). Ideas on the origin and development of Chesil Beach, Dorset. *Proceedings. Dorset Natural History Archaeological. Society, Vol. 95, 9-17.*

Carr, A.P., and Hails, J.R., (1972). A process model for barrier evolution. *22nd International Geographical Congress , 11-12.*

Carter, R.W.G., (1988).Coastal Environments, Academic Press 617pp.

Carter, R.W.G., and Orford, J.D., (1981). Overwash Processes along a gravel beach in SE Ireland. *Earth surface Processes, Vol. 6, p413-426.*

Carter, R.W.G., and Orford, J.D., (1984). Coarse clastic barrier beaches : a discussion of the distinctive dynamic and morphosedimentary characteristics. *Marine Geology, Vol. 60, p377-389.*

Carter, R.W.G., and Orford, J.D., (1991). The sedimentary organisation and behaviour of drift-aligned gravel barriers. *Coastal Sediments '91, ASCE; 934-948.*

Carter, R.W.G., and Orford, J.D., (1993). The morphodynamics of coarse clastic beaches and barriers: a short- and long-term perspective. *Journal of Coastal Research, Special Issue 15, 158-179.*

Carter, R.W.G., and Wilson, P., (1992). Aeolian deposits and processes in northwest Ireland. *Special publications of the Geographical Society, London, 73, 173-191.*

Carter, R.W.G., Forbes, D.L., Orford, J.D., Jennings, S.C., Shaw, J., and Taylor, R.B., (1993a). Long-term morphodynamic evolution of beaches and barriers: examples from paraglacial coasts, *Proceedings. Large scale coastal behaviour 93, U.S Geological Survey Open file report 93-381, 238*

Carter, R.W.G., Johnston, T.W., and Orford, J.D., (1984). Stream outlets through mixed sand and gravel coastal barriers: examples from south east Ireland. *Zeitschrift. Geomorphologie. NF 28, Vol. 28 (4), 427-442.*

Carter, R.W.G., Orford, J.D., Forbes D.L., and Taylor, K.B., (1987). Gravel barriers headlands and lagoons: an evolutionary model. Coastal Sediments '87 ASCE, 2, 1776-1792.

Carter, R.W.G., Orford, J.D., Forbes D.L., and Taylor, K.B., (1990). Morphosedimentary development of drumlin-flank barriers with rapidly rising sea level, Story Head, Nova Scotia. *Sedimentary Geology, 69; 117-138.*

Chao, Y.Y., and Pierson, W.J., (1971). Experimental studies of the refraction of uniform wave trains and transient wave groups near a straight caustic. *Journal of Geophysical Research 7724, 4545-4554.*

Chesnutt, C.B., (1975). Laboratory effects in coastal movable bed models, *ASCE Proceedings Symposium on modelling Techniques.*

CIRIA., (1996). Beach Management Manual, (Eds) Simm, J.D., Brampton, A.H., Beech N.W., Brooke, J.S., Report 153, 447pp

Coates,T.T., and Bona, P.F.D., (1997). Recharged beach development, a field study at Highcliffe Beach, Dorset. *Report SR438, HR Wallingford.*.

Coates,T.T., and Lowe, J.P.,(1993). Three dimensional response of open and groyned beaches: physical model studies. *Report SR387, HR Wallingford.*

Dalrymple, R.A., and Thompson,W.W., (1976). Study of equilibrium beach profiles, *Proceedings 15th Conference on Coastal Engineering, 2, ASCE.*

Davis, P.G., (1991). Sand and gravel bar migration on the western end of Scolt Head Island, Norfolk, Unpublished Phd thesis, Birkbeck College, University of London.

De Boer, G., and Carr, A.P., (1969). Early maps as historical evidence for coastal change (Orford).(Spurn point). *Geographical Journal, Vol.135, 17-39.*

De Boer, G. (1981). Spurn Point: Erosion and protection after 1849. *In Neale, J. and Flenley, J., (Eds) The Quaternary in Britain, Oxford, Pergamon Press, 206-215.*

Dean,R.G.,(1977). Equilibrium beach profiles: US Atlantic and Gulf coasts. *University of Delaware, Department of Civil Engineering, Ocean Engineering, Report No 12.*

Dedow, H.R.A., Thompson,D.M.,and Fryer,D.K., (1976). The generation measurement and analysis of random seas. *HR Wallingford reprint L98*

Dillon, W.P., (1970). Submergence effects on a Rhode Island barrier and lagoon and influences on migration of barriers. *Journal of Geology, Vol. 78, 94-102.*

Dobbie, C.H., and partners, (1984). Breaching of Hurst Spit a desk study. Unpublished report to New Forest District Council.

Dyer, K.R., (1970). Sediment distribution in Christchurch Bay, S. England. *Journal of Marine Biological Association of U.K., Vol. 50, 673-682*

Eddison, J., (1983). The evolution of the barrier beaches between Fairlight and Hythe. *Geographical Journal, Vol.149, 39-53.*

Evans, O.F., (1942). The origins of spits bars and related structures. *Journal of Geology, Vol. 48, 476-511.*

Fisher, J.S., Leatherman, S.P., and Perry, F.C., (1974). Overwash Processes on Assateague Island, *Proceedings. 14th Conference. Coastal Engineering, ASCE 1194-1212.*

Fitzgerald, D.M., van Heteren, S., and Montello, T.M., (1994). Shoreline processes and damage resulting form the halloween eve storm of 1991 along the North and South shores of Massachusettes Bay U.S.A., *Journal of Coastal Research. 10 113-132.*

Fitzgerald, D.M.,(1976). Ebb tidal inlet of Price inlet S.C: geomorphology, physical processes and inlet shoreline changes. *Report 11-CRD, Coastal Research Division, Department of Geology, University of South Carolina, II-143-157.*

Folk, R.L., (1966). A review of grain size parameters. *Sedimentology 6.*

Folk, R.L., (1980). Petrology of the Sedimentary Rocks. (2nd Edition). *Hemphill Publishing Company, Austin, Texas, U.S.A. 182pp.*

Folk, R.L., and Ward, W.C., (1957). Brazos River bar: A study in the significance of grain-size parameters. *Journal of Sedimentary Petrology, 27: 3-26.*

Forbes, D.L., and Drapeau, G., (1989). Near bottom currents and sediment transport over the inner Scotian shelf; sea floor response to winter storms during CASP. *Atmosphere-Oceans, 27, 258-278.*

Forbes, D.L., and Taylor, R.B., (1987). Coarse grained beach sedimentation under paraglacial conditions, Canadian Atlantic coast. *In D. Fitzgerald and P.Rosen: Glaciated coasts. Academic press, San Diego, 51-86.*

Forbes, D.L., Orford, J.D., Carter, R.W.G., Shaw, J., and Jennings, S.C. (1995). Morphodynamic evolution, self-organisation and instability of coarse-clastic barriers on paraglacial coasts. *Marine Geology, Vol.126, 63-85.*

Forbes, D.L., Shaw, J., and Taylor, R.B., (1993). Mixed sand gravel barriers in eastern Canada: instability and differential preservation under rising sealevels, *IGCP UK working group final symposium: quaternary evolution : recent advances.*

Forbes, D.L., Taylor, R.B., Orford, J.D., Carter, R.W.G. and Shaw, J., (1991). Gravel-barrier migration and overstepping. *Marine Geology, Vol.97, 305-313.*

Froude, W., (1872) The mechanical properties of fluids. *British Association Report.*

Galichon, P., (1985). La formation des crochons sedimentaire: le cas de la Pointe d'Arcay, France. Revue de Geologie Dynamique de Geographie Physique, Vol. 26 (3), 163-171.

Galvin, C.J., (1968). Finite amplitude shallow water waves of periodically recurring form. *CERC reprint 5-72.*

Goda, Y., (1975). Irregular wave deformation in the surf zone. *Coastal engineering in Japan.Vol 18.*

Goda, Y., (1976). On wave groups. *Proceedings BOSS '76, 115-129.*

Goda, Y., (1985). Random seas and design of maritime structures. *University of Tokyo Press, Tokyo.*

Gourlay, M .R., (1980). Beaches: Profiles, Processes and Permeability. *Report No CE14, Dept. of Civil Engineering University of Queensland, Australia.*

Guilcher, A. and King, C.A.M., (1961). Spits, tombolos and tidal marshes in Connemara, west Kerry, Ireland. *Proceedings of the Royal Irish Academy, Vol.17, 283-338.*

Gunbak, A.R., (1979). Rubble mound breakwaters. *Norwegian Institute of Technology, Report No 1.*

Hague, R.C., (1992). UK South coast shingle study, joint probability assessment, *Report SR315, HR Wallingford.*

Halcrow, (1982). Hurst Castle Coastal Protection: Initial Design Report. Unpublished Technical Report, Halcrow and Partners. 32pp.

Halcrow, (1997). SANDS for WINDOWS, User Manual, 65pp.

Hardy, J.R., (1964). Sources of some beach shingles in England. *20th International Geographical Congress, Paper 1651*

Hasselmann, K.,(1973). Measurements of wind wave growth, swell and decay during the Joint North Sea Wave Project (JONSWAP) . *Deutsches Hydrographisches Institute , Hamburg.*

Hawkes, P.J., (1987). A wave hindcasting model. *Proceedings. Modelling the Offshore Environment, Society for Underwater Technology.*

Hayes, M.O., (1979). Barrier island morphology as a function of tidal and wave regime. In Leatherman, S.P. (Ed.) *Barrier Islands. New York, Academic Press, 1-28.*

Hayes, M.O., and Kana, T.W., (1976). Terrigenous Clastic Depositional Environments. *Univ. South Carolina, Columbia. Tech. Report No 11. 364pp.*

Henderson, G., (1979). A Study of the Wave Climate and Wave Energy in Poole and Christchurch Bays. Unpublished Ph.D. Thesis, Department of Civil Engineering, Southampton University. 475pp.

Henderson, G., and Webber, N.B., (1977). Storm surge in the U.K. South Coast. *Dock and Harbour Authority.1 57, 21-22.*

Henderson, G., and Webber, N.B., (1979). An application of the wave refraction diagrams to shoreline protection, with particular reference to Poole and Christchurch Bays. *Quarterly Journal of Engineering Geology, 12(4), 319-327.*

Hequette, A., and Ruz, M.H., (1991). Spit and barrier island migration in the south-eastern Canadian Beaufort Sea. *Journal of Coastal Research, Vol.7, 677-698.*

Hequette, A., Ruz, M.H., and Hill, P.R., (1995). The effects of the Holocene sea level rise on the evolution of the south-eastern coast of the Canadian Beaufort Sea. *Journal of Coastal Research, Vol.11, 494-507.*

Holland, K.T., Holman, R.A., and Sallenger A.H., (1991). Estimation of overwash bore velocities using video techniques. *Coastal Sediments '91, ASCE, 489-496.*

Horn, D.P., Raper, J.F., Bristow, C.S., Livingstone, D.L., Riddell, K.J., Fuller, T.W., and Morris, F.E., (1996). Spits and nesses: basic processes and effects

on long-term coastal morphodynamics, Unpublished Report, Birkbeck College, University of London.

HR Wallingford., (1991). Equipment guide.

Hudson, R., Herrman, F., Sager, R., Whalin, R., Keulegan,G., Chatham, C., and Hales, L., (1979). *Coastal hydraulic models. US Army Corps of Engineers, CERC Report No SR 5.*

Hughes, S.A., and Chiu, T.S., (1978). The variations in beach profiles when approximated by a theoretical curve. *University of Florida, Coastal and Oceanographic Department, Report No 78/010.*

Hughes, S.A., and Chiu, T.S., (1981). Beach and dune erosion during severe storms. *University of Florida, Coastal and Oceanographic Department, Report No TR/043.*

Hydraulics Research., (1984). Chesil Beach interceptor drain percolation studies. *Report EX1248 (Restricted).*

Hydraulics Research., (1985). HINDWAVE - A wave hindcasting method. *Report No IT288, 30pp.*

Hydraulics Research., (1985a). BBC Wave spectrum synthesiser - version 1A, Technical note.

Hydraulics Research., (1985b) Whitstable sea defences - mobile bed model studies. *Report No. EX1255, (Restricted).*

Hydraulics Research., (1986). Seaford frontage study - physical and numerical modelling. *Report no. EX1346 (Restricted).*

Hydraulics Research., (1987). OUTRAY - A Wave Refraction Model. *HR Report EX1979, 113pp.*

Hydraulics Research., (1988). Profile logging and control system used for breakwater, seawall and beach models - a user manual. *Report No IT320.*

Hydraulics Research., (1989a) Wind-wave data collection and analysis for Milford-on-Sea, *HR Report EX 1979. 20pp.*

Hydraulics Research., (1989b)., Christchurch Bay - Offshore Wave Climate and Extremes. *HR Report EX1934. 9pp.*

Hydraulics Research., (1989c). The JONSEY wave prediction model, training and user manual. Report EX1870, HR Wallingford.

Hydraulics Research., (1989d)., Wave study for Arun Coast .*Report No EX 1871.*

Hydraulics Research., (1989e) INRAY - A Wave Refraction Model including friction and breaking, training and user manual. *Report EX2020.*

Iribarren ,C.R., (1950). Generalizacion de la formula par calculo de los diques de escollera y combrobacion de sus coeficientes . (Generalistaion of the formula for calculation of rock fill dykes and verification of its coefficients). *Revista de Obras Publicas, Madrid, Translated by A.Haritos, WES Translation N. 51-4, 1951 U.S.A*

Jimenez and Sanchez-Arcilla., (1997). A conceptual model for barrier coastal behaviour at decadal scale: application to the Trabucador Bar. *Coastal Dynamics '97. ASCE, 913-922.*

Jol,H.M., Meyers, R.A., Lawton, D.C., and Smith, D.G., (1994). A detailed ground penetrating radar investigation of a coastal barrier spit, Long Beach, Washington, USA. *Proceedings ISAGEEP, Boston, 107-127.*

Kellerhalls, R., and Bray, D.I., (1971). Sampling procedures for coarse fluvial sediments, *Journal Hydraulic Div. ASCE, 97, 1165-1180.*

Kemp, P.H., (1963). A field study of wave action on natural beaches . *10^{th} IAHR Congress, London..*

Keulegan, G.H., and Krumbein, W.C., (1949). Stable configuration of bottom slope in shallow water and its bearing on geological processes. *Transactions America Geophysical union, 30, No 6,*

Kidson, C., (1963). The growth of sand and shingle spits across estuaries. *Zeitschrift fur Geomorphologie, Supplement bande 7, Vol.1, 1-22.*

King, C.A.M., (1972). Beaches and coasts. London, Edward Arnold.

King, C.A.M., (1973). Dynamics of beach accretion in south Lincolnshire, England. In coates, D.R., (Ed.) *Coastal Geomorphology, State University of New York, Binghamton, Publications in Geomorphology, 61-98.*

Kirk, R.M., (1980). Mixed sand and gravel beaches: morphology, processes and sediments. *Progress in Physical Geography, Vol.*4; 189-210

Komar, P.D., and Miller, M.C., (1973). The Threshold of Sediment Movement under oscillatory water waves, *Journal Sedimentary Petrology , Vol. 24, 109-121.*

Kraft, J.C., Allen, E.A., Belknap, D.F., John, C.J.,. and Maurmeyer, E.M., (1979). Process and morphologic evolution of an estuarine and coastal barrier system. *In Leatherman, S.P. (Ed.) Barrier Islands. New York, Academic Press, 149-184.*

Krumbein,W.C., (1934). Size frequency distribution of sediments. *Journal Sedimentary Petrology.*

Krumbein,W.C., (1954). Statistical significance of beach sampling methods. *Technical Memorandum No. 50. Beach Erosion Board, Corps of Engineers.*

Lacey S., (1985). Coastal Sediment Processes in Poole and Christchurch Bays and the Effects of the Coastal Protection Works. Unpublished Ph.D. Thesis, Department of Civil Engineering, Southampton University. 372pp.

Larcombe, P. and Jago, C.F. (1994). The Late Devensian and Holocene evolution of Barmouth Bay, Wales. *Sedimentary Geology, Vol.89, 163-180.*

Leatherman, S.P., (1976a). Quantification of Overwash Processes. Unpubl.PhD Thesis, Univ. Virginia.245pp.

Leatherman, S.P., (1976b). Barrier Island Dynamics: Overwash Processes and aeolian Transport. *Proceedings. 15th International Conference on Coastal Engineering, ASCE, 1958 - 1974.*

Leatherman, S.P., (1977). Overwash Hydraulics and Sediment Transport. *Coastal Sediments 77, ASCE 135-148.*

Leatherman, S.P., and Williams A T., (1977). Lateral Textural Grading in Overwash Sediments, *Earth Surface Processes. Vol. 2, 331-341.*

Leatherman, S.P., and Williams A.T., (1983).Vertical Sedimentation Units in a Barrier Island Washover Fan, *Earth Surface Processes. Landforms. Vol. 8, 141-150.*

Leatherman, S.P., Williams A.T., and Fisher, J.S., (1977). Overwash Sedimentation Associated With a Large Scale Northeaster, *Marine Geology. Vol. 24, 109-121.*

Lewis, W.V., (1931). The effect of wave incidence on the configuration of a shingle beach. *Geographical Journal, Vol. 78, 129-148.*

Lewis, W.V., (1938). The evolution of shoreline curves. *Proceedings of the Geologists Association, Vol. 49. 107-27.*

Longuet-Higgins, M.S., and Parkin, D.W., (1962). Sea waves and beach cusps , *Geographical Journal, Vol. 128.*

Losada, M,A., and Gimenez-Curto, L.A., (1981). Flow characteristics on rough, permeable slopes under wave action. *Coastal Engineering, 4, 187-206.*

Mason, T., (1997). Hydrodynamics and sediment transport on a macro-tidal mixed (sand and shingle) beach. Unpublished Phd Thesis, Oceanography, University of Southampton.

McClean, R,F., and Kirk, R.M., (1969). Relationships between grain size size-sorting and foreshore slope on mixed sand-shingle beaches. *New Zealand Journal of Geology and Geophysics, Vol. 12; 138-155.*

McFarland, S., Whitcombe, L.I., and Collins, M.B., (1996). Recent shingle beach renourishment schemes; some preliminary observations. *Ocean and Coastal Management Vol. 25, 143-149.*

McGammon, R.B., (1962). Efficiency of percentiles for describing the mean size and sorting of sediment particles. *Journal of Geology, Vol. 70, 435-465.*

McKay, P.J., and Terich, T.A., (1992). Gravel barrier morphology; Olympic National Park, Washington State, USA. *Journal of Coastal Research, Vol. 8; 813-829.*

McKenna, J., Carter, D.W.G., Orford, J.D., and Jennings, S.C., (1993). The impact of recent sea level and climatic changes on the west coast of Britain and Southeast Ireland. *Climate change, sea level rise and associated impacts in European Community, Final Report, EPOC-CT90-0015, 4, 12pp.*

McLean, R.F., and Kirk, R.V., (1969). Relationships between grain-size sorting and foreshore shape on mixed sand-shingle beaches. *New Zealand Journal of Geology and Geophysics, Vol. 12, 138-155.*

McManus, D.A., (1963). A criticism of certain usage of the phi notation. *Journal Sedimentary Petrology; Vol. 33, 670- 674.*

Muir-Wood A.M., (1970). Characteristics of shingle beaches; the solution to some practical problems, *Proceedings 12th Coastal Engineering Conference, Vol. 2, ASCE.*

Nicholls, R.J., (1983b). Beach Sediments between Milford -on-Sea and Hordle cliff. Unpubd Report CE/SED/83/2, Dept Of Civil Engineering, University Of Southampton.

Nicholls, R.J., (1983c). Beach Sediments between Hordle Cliff and Becton Bunny. Unpubd Report CE/SED/83/3 Dept Of Civil Engineering, University Of Southampton.

Nicholls, R.J., (1984). The formation and stability of Shingle spits. *Quaternary. Newsletter, 44.*

Nicholls, R.J., (1985). The Stability of the Shingle Beaches in the Eastern half of Christchurch Bay PhD Thesis Dept Of Civil Engineering, University Of Southampton.

Nicholls, R.J., (1985b). Beach Profiles from the eastern half of Christchurch Bay, Unpubd Report CE/PRO/85/1, Dept Of Civil Engineering, University Of Southampton.

Nicholls, R.J., 1990, Poole and Christchurch Bay. *In Carter, R.W.G., Allen, R.J.L., Carr, A.P., Nicholls, R.J., and Orford, J.D., (Eds) Coastal Sedimentary environments of southern England, S.Wales and SE Ireland (Field Guide 2), International Association of Sedimentologist, Field Trip Guide, 6-20.*

Nicholls, R.J., and Webber, N.B., (1987a). Coastal erosion in the eastern half of Christchurch Bay. *In Culshaw, M.G., Bell, F.G., Cripps, J.C. and O'Hara, M. (Eds) Planning and Engineering Geology (Geological Society of London, Engineering Geology Special Publication). 549-554.*

Nicholls, R.J., and Webber, N.B., (1987b). The past, present and future evolution of Hurst Castle spit, Hampshire. *Progress in Oceanography, Vol.18, 119-137.*

Nicholls, R.J.,(1983a). Beach Sediments of Hurst Castle Spit. unpubd. Report CE/SED/83/1 Dept Of Civil Engineering, University Of Southampton.

Nichollson, J.A., (1968). Laboratory study of the relationship between waves and beach profiles. *Institution Engineers Australia Conference on Hydraulics and Fluid mechanics.*

Nielsen, L.H., Johannsen, P.N., and Surlyk, F., (1988). A late Pleistocene coarse-grained spit platform sequence in northern Jylland, Denmark. *Sedimentology, Vol.35 (6). 915 938.*

Orford, J.D., (1975). Discrimination of particle size zonation on a pebble beach. *Sedimentology, Vol. 22; 441-463.*

Orford, J.D., (1977). A proposed mechanism for storm beach sedimentation. *Earth Surface Processes. Vol. 2, 381-400.*

Orford, J.D., (1979). Some aspects of beach ridge development on a fringing gravel beach, Dyfed West Wales. *Publications du CNEXO :Actes de Colloques No 9.33-44.*

Orford, J.D., and Carter, R.W.G., (1982). Crestal overtop and washover sedimentation on a fringing sandy gravel barrier coast, Carnsore Point, SE Ireland, *Journal of Sedimentary Petrology, Vol. 52, 265-278.*

Orford, J.D., and Carter, R.W.G., (1984). Mechanisms to account for the longshore spacing of overwash throats on a coarse clastic barrier. *Marine Geology, Vol. 56, 207-226.*

Orford, J.D., and Carter, R.W.G., (1985). Storm-generated dune armouring on a sand-gravel barrier system, south-eastern Ireland. *Sedimentary Geology, Vol. 42; 65-82.*

Orford, J.D., and Carter, R.W.G., (1991). The sedimentary organisation and behaviour of drift-aligned gravel barriers. *Coastal Sediments '91, A.S.C.E, 934-948.*

Orford, J.D., and Carter, R.W.G., (1993). Mesoscale forcing of a coastal gravel barrier, *IGCP UK working group final symposium: quaternary evolution : recent advances.*

Orford, J.D., Carter, R.W. G., and Jennings, S.C., (1991). Coarse clastic barrier environments evolution and implications for Quaternary sea-level interpretation. *Quaternary Int., Vol. 9: 87-104.*

Orford, J.D., Carter, R.W. G., McKenna, J., and Jennings, S.C., (1995). The relationship between the rate of mesoscale sea-level rise and the rate of retreat of swash-aligned gravel-dominated barriers. *Marine Geology, Vol. 124; 177-186.*

Orford, J.D., Carter, R.W.G., and Forbes, D.L., (1991a). Gravel barrier migration and sea level rise; some observations from Story Head, Nova Scotia, Canada. *Journal of Coastal Research, Vol. 7; 477-488.*

Orford, J.D., Carter, R.W.G., and McClosky, J., (1993). A method of establishing mesoscale (decadal to sub-decadal) domains in coastal gravel barrier retreat rate from tide gauge analysis, *Proceedings Large scale coastal behavior 93, U.S Geological Survey Open file report 93-381,155-158.*

Orford, J.D., Carter, R.W.G., McKenna.,J., and Jenkins, S.C., (1995). The relationship between the rate of mesoscale sea-level rise and the rate of retreat of swash aligned gravel - dominated barriers, *Marine Geology. Vol. 124 177-186.*

Owen, M.W., (1980). Design of seawalls allowing for wave overtopping. *Report No EX924, Hydraulics Research Wallingford.*

Palmer, H.R., (1834). Observations on the motion of shingle beaches. *Phil. Trans. Royal Society (London). Vol. 124, 567-576.*

Penland, S., and Suter, J.R., (1984). Low profile barrier island overwash and breaching in the Gulf of Mexico. *Coastal Engineering, ASCE, 2339-2345.*

Powell, K.A., (1986). The hydraulic behaviour of shingle beaches under regular waves of normal incidence. PhD Thesis, University of Southampton, Department of Civil Engineering,

Powell, K.A., (1990). Predicting short-term profile response for shingle beaches. *Hydraulics Research Report SR219.*

Powell, K.A., (1993). Dissimilar sediments: model tests of replenished beaches using widely graded sediment. *Report SR 350. HR Wallingford.*

Priestly, M.B., (1981). Spectral analysis and time series. Academic press, London

Raper, J.F., Bristow, C.S., Livingstone, D.L., and McCarthy, T., (1996). Evolution of the active spit complex on Scolt head Island North Norfolk: assessment of change from ground survey and aerial videography, (pers comm).

Rector, R.L., (1954). Laboratory study of the equilibrium profiles of beaches, *US Army BEB Tech memo 41.*

Regnauld, H., Carter, R.W.G., Monnier, O., and McKenna, J., (1993). Modelisation de l'evolution d'une fleche littorale et relation avec une elevation du nivau marin: exemple du Sillon du Talbert, Bretagne, France. *GAIA No 6, 59-64.*

Reynolds, O., (1887). On certain laws relating to the regime of rivers and estuaries, and on the possibility of experiments on a small scale, Brit. Assoc. Rept., 867.

Robinson, A.H.W., (1955). The harbour entrances of Poole Christchurch and Pagham. *Geographical Journal, Vol. 121, 33-50.*

Schwartz, R.K., (1975), Nature and genesis of some storm washover deposits. *Tech. Memo. 61, Coast. Eng. Res. Center, U S Army, Fort Belvoir, Va.*

Sevon, W.D., (1966). Sediment variation on Farewell Spit. *New Zealand Journal of Geology and Geophysics, Vol. 9, 60-175.*

Seymour, R.J., (1977). Estimating wave generation on restricted fetches. *Proceedings ASCE, vol 103.*

Sharp, J.J., (1981). Hydraulic modelling, *Butterworth 241pp*

Shennan, I., (1987). Holocene sea-level changes in the North Sea region. In Tooley, M.J. and Shennan, I. (Eds) Sea-level changes. *Institute of British Geographers Special Publication Vol. 20, 109-151.*

Short, A.D., (1979). Three dimensional beach-stage model. *Journal of Geology, Vol. 87, 553-571.*

Sigurdsson, G., (1962). Wave forces on breakwater capstones. *Proceedings ASCE, Journal of WHC and CED, Vol. 88, No WW3.*

Silvester, R., (1970). Growth of crenulate shaped bays to equilibrium. *Proceedings. A.S.C.E., Journal of Waterways Harbour Division, 96 (WW2): 275-287.*

Siringan, F.P., and Anderson J.B., (1993). Seismic facies, architecture and evolution of the Bolivar Roads, tidal inlet/delta complex, east Texas Gulf coast. *Journal of Sedimentary Petrology, Vol 63, 794-808.*

Smallman, J.V., (1987). The application of a computational model for the optimisation of harbour layout. *Proceedings COPDEC Conference, Beijing, China.*

Smith, D.G., and Jol, H.M., (1992). GPR results used to infer depositional processes of coastal spits in large lakes. *Proceedings Fourth International Conference on Ground Penetrating Radar. Rovaniemi, Finland. Geological Survey of Finland, Special Paper 16, 169-177.*

Southgate, H.N., (1984). Techniques of ray averaging. *International Journal for Numerical Methods in Fluids. Vol 4.*

Steers, J.A., (1948). The Coastline of England and Wales (Second edition 1964). Cambridge, Cambridge University Press.

Steers, J.A., (1960). Scolt Head Island. Cambridge, W. Heffer and Sons Ltd.

Stevens, C., (1992). The open coastline. *In Coastal Zone Management and Planning, I.C.E, 91-99.*

Sunamura, T., and Horikawa K., (1974). Two dimensional beach transformation due to waves. *Proceedings 14th Conference on coastal Engineering,ASCE.*

Suter, J.R., Nummedal, D., Maynard, A.K., and Kemp, P., (1982). *Proceedings 18th Conference Coastal Eng. ASCE 1459-1478.*

Swift, D.J.P., (1976). Barrier island genesis: evidence from the central Atlantic shelf, eastern U.S.A., *Sedimentary Geology, Vol. 14, 1-43.*

Thomas, R., (1996). Out on a limb. *Geographical magazine, Vol. 68 (6), 14-17*

Tyhurst, M.F., (1978). Tidal conditions in Poole Bay. *Journal of the Society of Civil Engineering Technicians, 5(6): 6-11.*

Van der Meer, J.W., (1988). Rock slopes and gravel beaches under wave attack. *Delft Hydraulics Communication No 396 152pp*

Van Hijum, E., and Pilarczyck, K.W., (1982). Equilibrium profile and longshore transport of coarse material under regular and irregular wave attack. *Delft Hydraulics Laboratory Publication No 274.*

Van Hijum, E., (1974). Equilibrium profiles of coarse material under wave attack. Proceedings. *14th Coastal engineering Conference, volume 2,ASCE.*

Van Vlymen, C.D., (1979). The natural history of Slapton Ley Nature Reserve. *The water balance of Slapton Ley. Field Studies, 5, 59-84.*

Velegrakis, A.F., (1994). Aspects of the morphology and sedimentology of a transgressional embayment system: Poole and Christchurch Bay, Southern England. Unpublished Phd Thesis, Department of Oceanography, University of Southampton.

Velegrakis, A.F., and Collins M.B., (1991). Coarse-grained Sediment Deposits in Eastern Christchurch Bay: A Preliminary Report. Unpublished Technical Report, SUDO/TECI9l/19C. Department of Oceanography, Southampton University. 15pp.

Velegrakis, A.F., and Collins, M.B., (1992). Marine Aggregate Evaluation of Shingles Bank, Christchurch Bay. Unpublished Technical Report, SUDO/TEC/92/14C 33pp.

Vellinga, P., (1984). A tentative description of a universal erosion profile for sandy beaches and rock beaches. *Coastal Engineering 8 177-188.*

Venkatamatharan, K., (1970). Formation of the barrier spit and other sand spit and other sand ridges near Chilka Lake on the east coast of India. *Marine Geology, Vol. 9, 101-116.*

Visocky, A.P., (1977). Groundwater surface relationships near the lake Michigen Shore. *Proceedings. Hydraulic. Coast. Zone, ASCE 195-222.*

Walker, J.R., Everts, C.H., Schmelly,S., and Demirel, D., (1991). Observations of a tidal inlet on a shingle beach. *Proceedings Coastal Sediments '91, ASCE, 975-989.*

Watts, G.M., and Dearduff, R.F., (1954). Laboratory study of effects of tidal action on wave formed beach profiles , *BEB Tech memo N0 52.*

Whitten, D.G.A. (1972). The Penguin dictionary of geology. Harmondsworth, Penguin.

Wright, L.D., and Short, A.D., (1984). Morphodynamic variability of surf zones and beaches: a synthesis. *Marine Geology, Vol. 56, 93-118.*

Wright, P., (1982). Aspects of the Coastal Dynamics of Poole and Christchurch Bays. Unpublished Ph.D. Thesis, Department of Civil Engineering, Southampton University. 20lpp.

Yalin, M.S., (1971). Theory of hydraulic models, *Macmillan, 259pp*

Yalin,M.S., (1963a). A model beach with permeability and drag forces reproduced. *10th Congress International Hydraulics Research.*

Yalin, M.S., (1963a). Method for selecting scales for models with movable bed involving wave motion and tidal currents. *Proceedings IAHR Congress, 221-229.*

Yasso, W.E., (1964). Geometry and development of spit-bar shorelines at Horseshoe Cove, Sandy Hook, N.J. *Technical report 5, Project NR 388-057, Office of Naval Research, Geography Branch.*

Zenkovich, V.P. (1967). Processes of coastal development. Edited by J.A. Steers and C.A.M. King and translated by D.G. Fry, Edinburgh, Oliver and Boyd.

Zenkovich, V.P., (1959). On the genesis of cuspate spits along lagoon shores. *Journal of Geology, Vol.67, 269-277.*